

Investigating Multistep Continuous Flow Processes Using Diazonium Salts

Christiane Schotten

This dissertation is submitted for the degree of Doctor of Philosophy (PhD) of Cardiff University



2018

Declaration

This work has not been submitted in substance for any other degree or award at this or any other university or place of learning, nor is being submitted concurrently in candidature for any degree or other award.

Signed (candidate)

Date

STATEMENT 1

This thesis is being submitted in partial fulfillment of the requirements for the degree of PhD.

Signed (candidate)

Date

STATEMENT 2

This thesis is the result of my own independent work/investigation, except where otherwise stated, and the thesis has not been edited by a third party beyond what is permitted by Cardiff University's Policy on the Use of Third Party Editors by Research Degree Students. Other sources are acknowledged by explicit references. The views expressed are my own.

Signed (candidate)

Date

STATEMENT 3

I hereby give consent for my thesis, if accepted, to be available online in the University's Open Access repository and for inter-library loan, and for the title and summary to be made available to outside organisations.

Signed (candidate)

Date

STATEMENT 4: PREVIOUSLY APPROVED BAR ON ACCESS

I hereby give consent for my thesis, if accepted, to be available online in the University's Open Access repository and for inter-library loans **after expiry of a bar on access previously approved by the Academic Standards & Quality Committee.**

Signed (candidate)

Date

Summary

This thesis describes the investigation of continuous flow processes that incorporate the generation and use of diazonium salts. In this manner, processes for the preparation of triazenes, indoles and acridones have been developed. Diazonium salts are potentially unstable and hazardous and have to be handled with care. The use of continuous flow processes enables the safe synthesis avoiding accumulation of large quantities. This is due to the possibility to intercept intermediates at a precise point in time within a closed system. Diazonium salts were prepared *via in situ* diazotization of anilines with isoamyl nitrite.

Triazenes were formed *via* the interception of diazonium salts with secondary amines. The process had to be carefully developed to avoid clogging and fouling of the reactor. 26 examples have been prepared. The thermal behavior of 13 triazenes has been compared to their corresponding tetrafluoroborate diazonium salts, which has shown they are significantly more stable. In addition, VT NMR analysis has been performed to explore restricted rotation around the triazene bond.

Further developments have found that indoles can be prepared *via* reduction of diazonium salts to their corresponding hydrazine with ascorbic acid and subsequent Fischer indole reaction in a microwave reactor. The use of such a hybrid, machine assisted approach has enabled the formation of a library of indoles. In this manner, 33 examples have been synthesised including the drug Zolmitriptan and nine of its analogues.

The formation of acridones from benzyne and anthranilates has been investigated. Benzyne was prepared *via* the thermal decomposition of benzenediazonium-2-carboxylate. The compound decomposes above ambient temperatures and is known to be explosive when dry. The formation of benzyne has been investigated using the Diels-Alder reaction with furan as a model reaction and then conditions were applied to a range of substrates to investigate the scope. Problems with solubility of starting materials, diazonium salts and products were encountered and partially solved through the screening of different solvents.

Finally, an exothermic reaction was investigated under continuous flow reactions. Commercially available thermocouples and *in line* NMR analysis were used to facilitate process optimisation. The exothermic reaction explored was the reduction of TMSCF_3 to TMSCF_2H with NaBH_4 . The exotherm was monitored using external, commercially available thermocouples to realise the development of a safe reaction regime. The incorporation of *in situ* NMR measurements has allowed realtime assessment of reaction conversion as a correlation to the exotherm. With the combined monitoring

Summary

approaches a safe scale up process has been established. A hybrid flow - batch approach was used to scale up the reaction and increase the space time yield compared to the previously reported batch reaction.

Acknowledgments

This thesis would not have been possible without the help and encouragement of others. Therefore, I would like to thank the people who made this work possible.

First of all, I would like to thank my supervisor Duncan for the opportunity to work in his group. It was a great honour to work in the DLB group as the first PhD student. Duncan taught me a lot during my time in Cardiff, not all of it being chemistry related. Thank you Duncan.

I owe my group great thanks for their support and everything else. They tolerated my bad moods, proof read my thesis (thank you Joey, Tom, Roddy, Yerbol and James), discussed problems (chemistry and personal), had BBQs with me and were just great. I need to especially mention Joey, who was my first friend in Cardiff (and luckily still is) and who helped (and argued with me) a lot in various situations.

In addition, I would like to thank the group members of the LCM, TW and DB groups. Especially I would like to mention Micol Santi and Alexandre Rossignon, who, amongst others, became dear friends.

I want to also thank all the students who worked with me. They all worked incredibly hard.

During my PhD I collaborated with a number of people. I would like to thank Joey, Bruker and the Pope group for their help.

A department is only as good as its technicians and supporting staff. My gratitude also goes to the technicians and other staff at Cardiff University. My special thanks go to the allrounder Rob Jenkins.

Finally, I need to thank my family and all my friends for their constant support, especially my parents Monika and Achim, my brother Andi and my boyfriend James. My father acknowledged very proudly just before I started in Cardiff, I would be the first Dr in my family. That gave me strength through the most difficult times.

I know it was sometimes not easy to tolerate me especially in stressful times and then hear me talking about chemistry all the other times. My family and friends still somehow managed to do so.

Special thanks go to James, who is always there for me and supported me in any way possible.

Abbreviations

BPR	back pressure regulator
DCE	dichloroethane
DCM	dichloromethane
DIBALH	diisobutylaluminium hydride
DIPEA	Diisopropylethylamine
DMAP	4-(dimethylamino) pyridine
DMF	dimethylformamide
DMSO	dimethylsulfoxide
DSC	differential scanning calorimetry
E_A	activation energy
EDG	electron donating group
EWG	electron withdrawing group
EtOAc	ethylacetate
FG	functional group
GC	gas chromatography
GCMS	gas chromatography coupled to mass spectrometry
HOMO	highest occupied molecular orbital
HPLC	high performance liquid chromatography
HRMS	high resolution mass spectrometry
IAN	isoamylnitrite
ID	inner diameter
IR	infrared
LCMS	liquid chromatography coupled with mass spectrometry
LUMO	lowest unoccupied molecular orbital
MeCN	acetonitrile
mp	melting point
MS	mass spectrometry
MW	microwave
NMP	<i>N</i> -Methyl-2-pyrrolidone
NMR	nuclear magnetic resonance
Nu	nucleophile
OD	outer diameter
P	productivity
PEG	polyethylene glycol
PFA	perfluoroalkoxy

SA:V	surface area to volume ratio
ScoP	safety cut-off point
S _E Ar	electrophilic aromatic substitution
S _N 1	unimolecular nucleophilic substitution
S _N 2	bimolecular nucleophilic substitution
S _N Ar	nucleophilic aromatic substitution
STY	space time yield
TBME	<i>t</i> butyl methyl ether
TiT	Tube in Tube
THF	tetrahydrofuran
TLC	thin layer chromatography
USB	universal serial bus
UV/Vis	ultraviolet/ visible light
Y	yield
VT	variable temperature

Table of Contents

Chapter 1 – Introduction.....	1
1 Enabling Technologies.....	2
1.1 Microwave Heating	2
1.2 Continuous Flow Processing.....	3
1.2.1 Heat Transfer.....	4
1.2.2 Mass Transfer.....	6
1.2.3 Generation and Use of Hazardous Material	10
1.2.4 Scale Up and Process Intensification.....	12
1.2.5 Library Preparation	15
1.2.6 Reaction Monitoring, Optimisation and Automation.....	17
1.2.7 Multistep Continuous Flow Processing	18
2 Diazonium Salts in Flow.....	25
3 Thesis Objectives.....	32
4 References	34
Chapter 2 – Investigating the Formation of Triazenes from Diazonium Salts.....	41
1 Introduction.....	42
1.1 Triazene Stability.....	44
1.2 Restricted Rotation in Triazenes.....	45
2 Results and Discussion.....	50
2.1 Flow Synthesis.....	50
2.2 Stability and DSC.....	54
2.3 Restricted Rotation and NMR Results.....	58
3 Conclusion and Outlook.....	65
4 References.....	68

Chapter 3 – Investigating the Formation of Indoles from Diazonium Salts.....	71
1 Introduction.....	72
2 Results and Discussion	78
2.1 Method Adaption for the Synthesis of a Series of Fluorinated Pyrazoles	89
3 Conclusions and Outlook.....	90
4 References	94
Chapter 4 – Investigating the Formation of Benzyne from Diazonium Salts.....	99
1 Introduction.....	100
1.1 Benzyne	100
1.2 Benzyne from Anthranilic Acid	102
1.3 Benzyne Reactions.....	104
1.4 Benzyne in Flow	105
1.5 Acridones	109
2 Results and Discussion	111
3 Conclusion and Outlook.....	121
4 References	124
Chapter 5 – Continuous Flow Reaction Monitoring for the Optimisation of Space Time Yield of an Exothermic Reaction.....	127
1 Introduction.....	128
2 Results and Discussion	133
2.1 Temperature Measurements.....	133
2.2 NMR Measurements.....	139
2.3 Hybrid Flow – Batch Large Scale Reaction.....	145
3 Conclusion and Outlook.....	151
4 References	152

Chapter 6 – Experimental.....	155
1 General Methods	157
2 Chapter 2 - Triazenes	159
3 Chapter 3 - Indoles	198
4 Chapter 4 - Benzyne	228
5 Chapter 5 – Exotherm Monitoring	238
6 References	246

Chapter 1: Introduction

Table of Contents

1	Enabling Technologies	2
1.1	Microwave Heating	2
1.2	Continuous Flow Processing	3
1.2.1	Heat Transfer	4
1.2.2	Mass Transfer	6
1.2.3	Generation and Use of Hazardous Material	10
1.2.4	Scale Up and Process Intensification.....	12
1.2.5	Library Preparation	15
1.2.6	Reaction Monitoring, Optimisation and Automation	17
1.2.7	Multistep Continuous Flow Processing	18
2	Diazonium Salts in Flow.....	25
3	Thesis Objectives	32
4	References	35

1 Enabling Technologies

Enabling Technologies such as continuous flow processing, mechanochemistry, electrochemistry, photochemistry and the use of microwave reactors have become of increasing interest in chemistry over the recent decades.^[1] The focus of this thesis is on the use and development of, and a desire to further understand continuous flow processing and its combination with microwave heating. Both technologies will be introduced here.

1.1 Microwave Heating

The use of microwaves in synthesis was originally introduced for chemical reactions in 1986 by Giguere and Majetich where they demonstrated the significant decrease in reaction time for both Diels Alder and Ene reactions.^[2] Since then, rapid heating by microwave irradiation has been applied to a wide range of reactions. This development started initially with modified kitchen microwaves and has since developed to the use of instruments dedicated to chemical synthesis.^[3] Microwaves, and especially those designed for use in chemical synthesis, offer the advantage of heating reactions very quickly in a simplified, safe and reproducible way. The use of sealed vials makes it possible to heat reactions above the atmospheric boiling point of the solvent which can result in a reduction of reaction times from days to minutes.

Microwave heating, or dielectric heating, is based on the ability of a particle to absorb the microwave energy and convert it into heat. These two processes are dependent on two properties of the particle, the dielectric constant and the dielectric loss. The ability to absorb the microwave energy is mostly dependent on the dielectric constant, the dipole moment of the particle. More polar particles absorb the energy more efficiently. The dipole of a molecule aligns with the alternating electric field of the applied electromagnetic microwave irradiation, which leads to an increase in rotational energy. This rotation can cause collision or friction between molecules and results in energy conversion into translational energy heating of the bulk reaction mixture. The dielectric loss describes the dissipation of the electromagnetic energy into this translational energy and heat. In addition to the dielectric constant and dielectric loss, microwave heating is also dependent on a number of other factors such as specific heat capacity and depth of microwave penetration. The heating performance or power absorption of a reaction mixture can be highly dependent on the solvent used as this is the most abundant type of molecule in a normal reaction mixture.

Nonthermal microwave effects have been discussed in the literature, where it has been noted that the use of microwaves influences the outcome of the reaction independent of

the heating properties.^[4] In addition, specific microwave effects, where the preferred energy absorption of molecules with a high dipole moment leads to different reaction outcomes, have been discussed.^[5] However, since then, investigations have shown that these effects are likely non-existent by the use of instruments that do not use microwaves but enable similar heating properties.^[6]

Microwaves for chemical synthesis can range from multimode to monomode devices. Multimode instruments are often larger and the microwaves move around the cavity reflecting off the walls and thus creating hot and cold spots. Therefore, reaction vessels are usually rotated within the cavity to average out these energy differences. In monomode instruments the cavity is the size of one wave which leads to more constant heating, especially on smaller scale (usually max 100 mL).

The introduction of microwave reactors for chemical synthesis included the development of a number of safety precautions. These include temperature, pressure and microwave power measurements and safety cut-off procedures. Even if a vessel bursts at elevated temperatures and pressures, the cavities are designed to protect the operator.

Applications of microwave reactors in organic chemistry range from metal-catalysed reactions, cycloaddition and rearrangement chemistry, carbonyl chemistry, organocatalysis to reactions involving gaseous reagents. Most of these are examples of endothermic reactions benefitting from high temperatures to reduce reaction times.^[3a]

Modern microwave reactors have the ability for process automation enabled by robotic arms. These arms can transfer vials from a rack into the microwave chamber and remove them automatically after the reaction is done. The robot arm can transfer the next vial into the chamber so that the next reaction is performed. This enables the user to program several reactions without manual interaction.

1.2 Continuous Flow Processing

Even though flow chemistry has been exploited on industrial scale for e.g. petrochemical industry for many years, it only recently has been discovered as an enabling tool in organic chemistry for the production of fine chemicals. Under continuous flow processing conditions reagents are delivered into a tubular reactor circuit by pumps (e.g. syringe or HPLC pumps). Most of the reactors in the circuit can be classified into microfluidic (10 to 500 μm inner diameter) and mini- or mesofluidic (500 μm to several mm inner diameter) scales dependent on the inner diameter of the tubing material. The reactants meet in these tubular reactors at mixing points and react along their length. The reaction time, which correlates directly to the residence time in the reactor, can be controlled *via* the volume of the reactor or the flow rate of the pumps. Stoichiometries of reactants are defined by the initial concentration in the reactor. This concentration can be either

controlled *via* the concentration of the reactant solutions or pump flow rates. The reactors can be heated or cooled. The system can be further modified, for example with *in line* monitoring, pressurising devices (Back Pressure Regulator, BPR) and *in line* downstream processing. At the outlet of the system the product solution is collected.

Each position along a reactor tube corresponds to a unique time point during the reaction, meaning the reaction progress is over the length of the tubing. Conversely, in a batch reaction the whole reaction mixture experiences the same composition in the reaction from start to finish, with the progress of the reaction being over time (Figure 1.1). This also means, that the scale of a continuous reaction is dependent on the time the reaction is run for, rather than reactor vessel volumes.

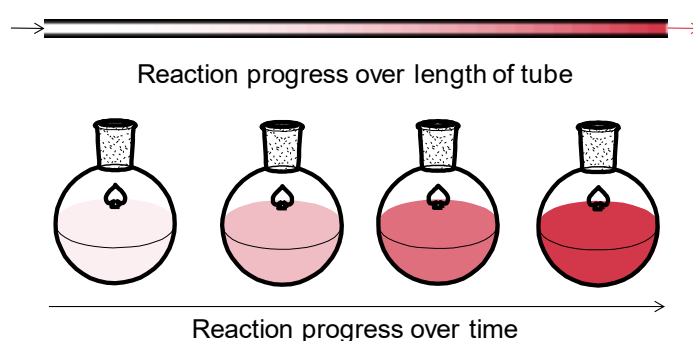


Figure 1.1: Reaction Progress in a Flow Reactor and Round Bottom Flask

Several advantages, such as efficient mass and heat transfer, increased safety, precise control of reaction parameters, the prospect of multistep procedures, automated processing and optimisation, characterise the popularity of continuous flow methods for small scale organic reactions.^[7] A few of the key differences to traditional batch chemistry will be discussed in this section giving examples where the use of flow has been demonstrated to improve the performance of a reaction.

Importantly, continuous flow processing is seen as an additional method to perform reactions.^[8] Whilst this method can have advantages over traditional batch chemistry, it is not proposed that it will replace it.

1.2.1 Heat Transfer

In a flow reactor the surface area to volume ratio (SA:V) is increased relative to the dimensions of a batch reactor (Figure 1.2). This leads to an improved heat transfer in a continuous flow process. This is advantageous for both endothermic and exothermic reactions. For endothermic reactions the heat has to be efficiently transferred into the reaction, whereas for exothermic reactions the heat has to be removed from the reaction. The heat transfer is directly proportional to the surface area, which means heating or

cooling the same volume under flow processing is more efficient compared to a batch reactor. The improved heat dissipation capacity, which is 1000 fold compared to a batch reactor, prevents hot spots and thermal runaways for exothermic reactions.^[9] In general, the heat transfer is dependent on the material of the tubing and its thermal properties. However, the use of thin tubing walls makes the impact negligible for most examples, especially at mesoscale.

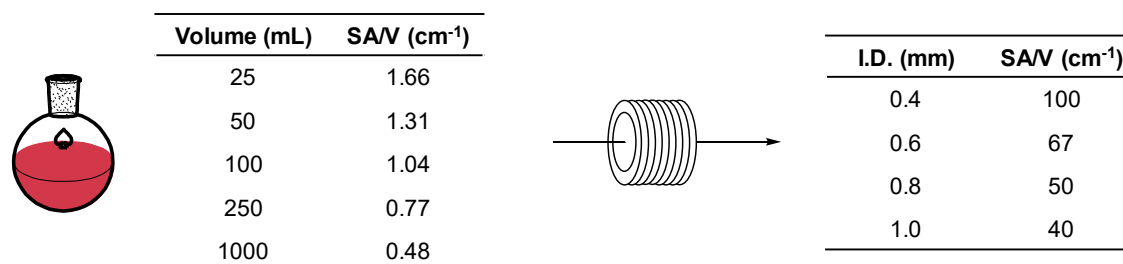


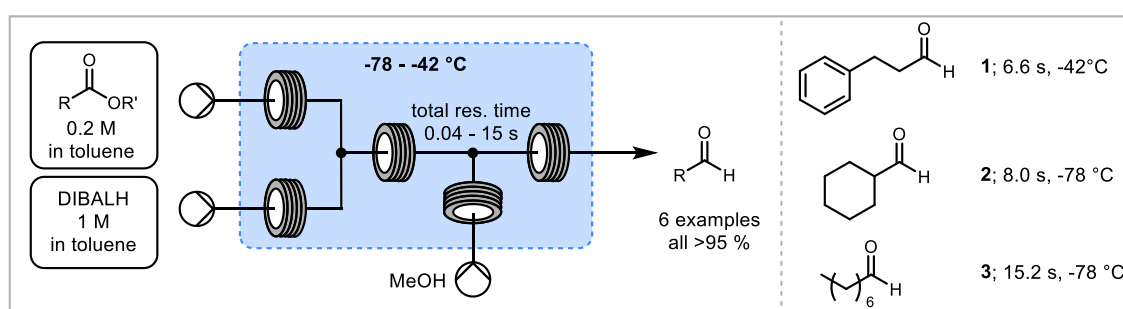
Figure 1.2: Comparison of SA/V for a Batch (left) and Flow (right) Reactor

In addition to improved heat transfer capacity, the use of backpressure regulators (BPRs) permits reactions to be performed under pressure thus providing the ability to superheat solvents past their atmospheric boiling point. Achieving elevated temperatures and pressures under continuous conditions has the prospect of scaling up a reaction easily that otherwise would require the use of autoclaves. This is opposed to a microwave reactor, where scale is dependent on the reaction vessel size and maximum pressures of 25 bar can be achieved. Additionally, the lack of a 'headspace' in a flow reactor can offer advantages for reactions involving volatile reactants. Notably, continuous microwave reactors and inductive heating have been investigated in addition to traditional heating methods.^[10]

Mostly, exothermic reactions have been investigated under continuous flow conditions due to the improved control over the temperature. Such reactions include for example nitrations and reactions with organometallic reagents. Exothermic reactions are particularly difficult to scale up in batch. This is due to the reduced SA:V in bigger reaction vessels, which limits the heat dissipation and thermal runaways become more likely. Usually such reactions are controlled by diluting, rapid mixing, low temperatures and long dosing times in batch. Due to the improved heat dissipation, exothermic reactions can be controlled under continuous conditions and thermal runaways avoided. In addition, increased selectivity can be observed due to the increased temperature control.

To highlight this control, Webb and Jamison reported the selective reduction of esters in flow to aldehydes with DIBALH (diisobutyl aluminium hydride) (Scheme 1.1).^[11] Crucial

for the process were cryogenic temperatures, fast mixing, short residence times and the ability to quench at a precise point during the reaction. This was achieved by intercepting the reaction mixture with methanol thus avoiding over reduction to the corresponding alcohols. Fast mixing was ensured by narrow tubing diameters (0.08 mm and 0.1 mm) and fast flow rates (2.5 mL/min – 30 mL/min). The solutions of DIBALH and the ester were pre-cooled before being combined in a residence coil that enabled both mixing and the reaction performance. This stream was then quenched with methanol, ensuring quenching was complete by passing the mixture through another residence coil for mixing purposes. In this manner, Webb and Jamison were able to produce six aldehydes from their corresponding esters greater than 95% yield.



Scheme 1.1: Selective Reduction with DIABLH under Continuous Flow Conditions^[11]

1.2.2 Mass Transfer

In addition to heat transfer, mass transfer can also be improved using by continuous flow methods. This includes both the transfer of reactants into the reaction solution and mixing of the reaction solution.

Mixing within a reaction is particularly important for very fast reactions where efficient mass transfer is critical to ensure high selectivities.^[12] Whether a reaction is mass transfer limited can be determined *via* the ratio of the rate of the reaction to the rate of the mass transfer by diffusion. This dimensionless ratio is called the Damköhler number and is used by chemical engineers to describe mass transfer limitations in reactions ($Da < 1$: no mass transfer limitation, $Da > 1$ mass transfer limitation). Batch reactions that are mass transfer limited are usually controlled through slow dosing, dilution or slowing the reaction down by cooling. Mixing is largely influenced by the flow regime within a reactor for both flow and batch processes. The Reynolds number is a way to predict flow patterns and is dependent on the viscosity and velocity of the fluid as well as the channel dimensions. Low Reynolds numbers (<2300) describe laminar flow patterns, whereas large Reynolds numbers (>2600) describe turbulent flow (Figure 1.3). Under laminar flow conditions, mixing is solely dependent on diffusion between sections that are orthogonal

to the direction of the flow. In continuous flow the small diameters ensure short diffusion paths. Mixing is highly increased in turbulent flow as sections orthogonal to the direction of the flow intermix. The flow regime can be changed *via* the flow rate. The Reynolds number increases with the flow rate, describing a turbulent flow.

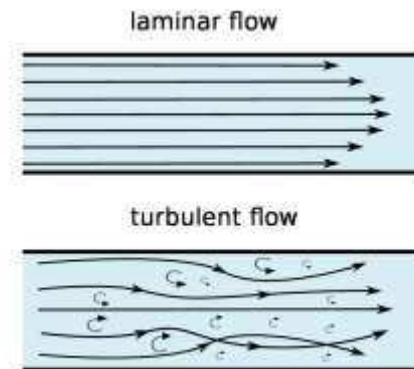


Figure 1.3: Laminar Flow (top) and Turbulent Flow (bottom)^[13]

To increase mixing in laminar flow, a variety of mixing devices has been developed that usually disturb the flow which leading to a turbulent flow regime (Figure 1.4).^[14] As these mixers only influence an existing flow and are not power driven, they are described as passive or static mixers. Mixers can be classified into devices that either combine streams in different ways and/ or disturb the original flow pattern. Active mixing can be achieved by mechanical agitation for example by the use of ultrasound, vibration or stirring.

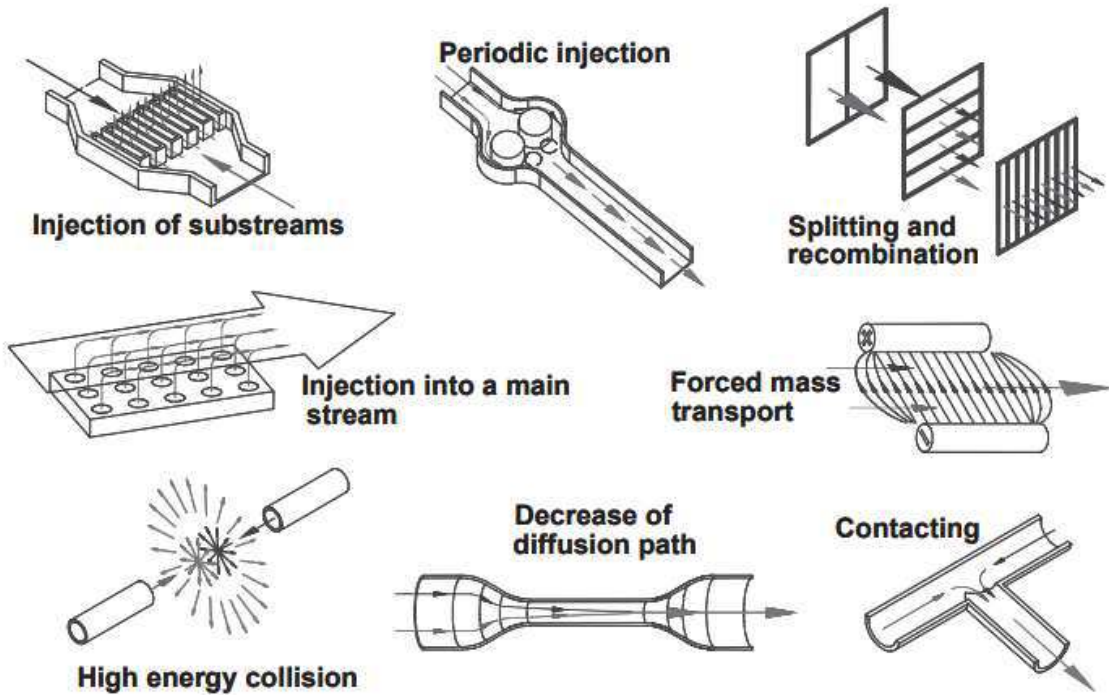


Figure 1.4: Passive Mixing Devices^[14]

In biphasic reactions, mass transfer is mostly dependent on surface area between phases. The small diameters within flow reactors increase the surface area between phases and thereby increase the mass transfer. This is important for multiphase systems such as liquid-liquid, gas-liquid, heterogeneous systems, liquid-solid and gas-solid processes as the interphasic area is proportional to mass transfer. Reactions that are mass transfer limited can therefore benefit from the increase in surface area afforded by mixers. In addition, gases can be accurately dosed into reactions by the incorporation of mass flow controllers or specially designed reactors such as the tube-in-tube^[15] or falling film reactor. In addition to the influence of flow patterns on mixing, the mass transfer in liquid-liquid and gas-liquid reactions also benefits from the small dimensions in a flow reactor as this enables Taylor flow (Figure 1.5).^[7f, 16] Taylor flow is a circular movement within droplets of one phase and increases the mixing within each droplet.

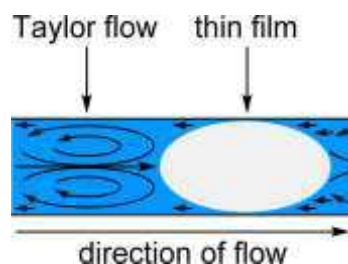
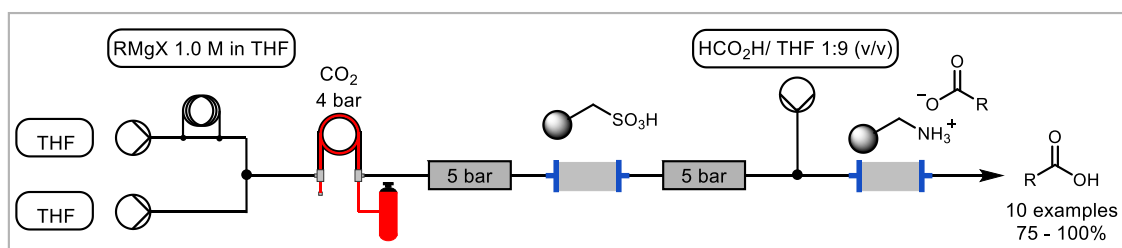


Figure 1.5: Taylor Flow^[11f]

For gas-liquid reactions, membranes can be incorporated into flow setups for the delivery of gases into a continuous flow reaction which ensures a homogeneous reaction mixture within a reactor. In 2010 Ley and co-workers reported the effective delivery of ozone using a ‘tube in a jar’ reactor.^[17] This was then further developed to the ‘tube-in-tube’ reactor for the delivery of gaseous carbon dioxide (Scheme 1.2).^[18] The tube-in-tube reactor consists of an inner tube, an AF-2400 semipermeable membrane, and an outer PTFE tubing. The reaction mixture passes through the inner tubing while the outer tube is pressurised with the desired gas. The membrane is permeable to some gases so that the reaction solution becomes enriched with gas while maintaining a homogenous mixture. The use of the tube-in-tube reactor was demonstrated in the conversion of carbon dioxide to carboxylic acids in a Grignard reaction. The reaction mixture was passed through a polymer supported sulfonic acid to protonate the product and remove magnesium salts. The product was then purified *via* the catch-and-release method. In this manner, the desired product is first caught on a polymer supported reagent (here ammonium hydroxide) while all other byproducts or unreacted starting materials pass through to waste collection. The product is then washed out with an appropriate solvent (here acetic acid/ THF, 1:9, v/v). The group prepared 10 examples in good yields (75-100%) and performed the reaction on a preparative scale (20 mmol). Since then this methodology has been used for the delivery of other gases such as hydrogen, NH₃, O₃, ethylene and diazomethane.^[15]



Scheme 1.2: First Report of the Tube-in-Tube Reactor for the Effective Delivery of Carbon Dioxide^[18]

Other reaction classes benefitting from the high SA:V are photochemical and electrochemical reactions. In photochemical reactions the light has to penetrate into the reaction. In batch processes the efficiency of the reaction is often limited by the penetration depth of the light into the bulk of the solution whereas in a flow reaction the dimensions are such, that enough light penetrates through the whole reaction solution thus increasing the photon efficiency.^[19] Similarly, in electrochemical reactions the contact with the electrodes and the transport of charged species is important for the reaction efficiency. The resistance of a reaction mixture is highly dependent on the distance between electrodes and the capacity of the reaction medium to transport

charged species. Often electrolytes are used to increase transport rates. In a flow reaction, the distance between electrodes is small, making transport of charged species easier.^[20]

1.2.3 Generation and Use of Hazardous Material

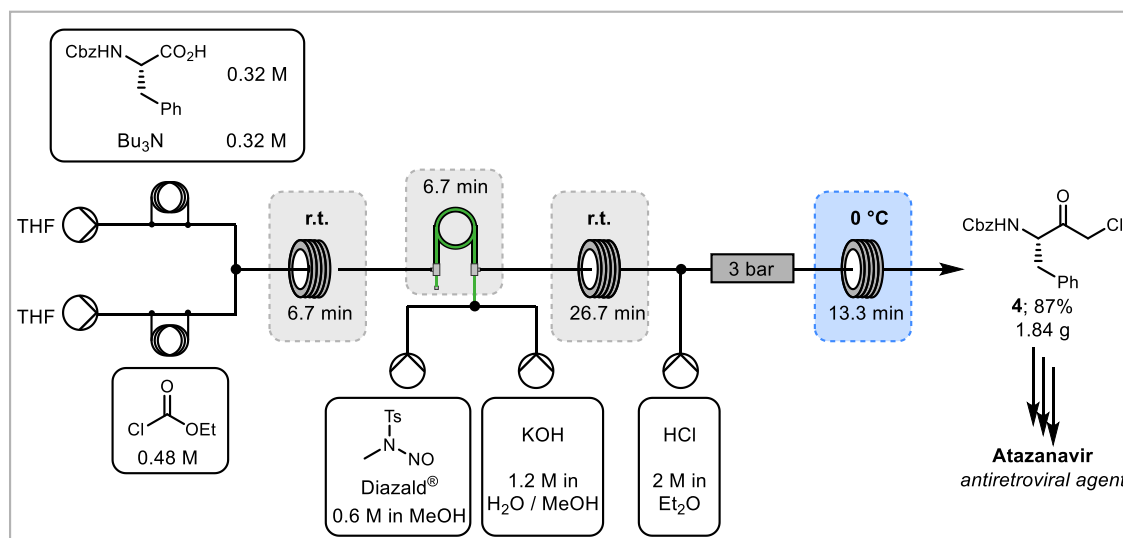
The increased heat and mass transfer in continuous flow processing results in accurate control of reaction parameters. This can make chemistry, that has been deemed as too dangerous become feasible under continuous flow conditions.^[21] Chemistry of that type is often called “forbidden”.^[22] Such chemistry often proceeds *via* the most time and atom efficient route but might require the intermediacy of highly reactive or potentially hazardous compounds (toxic, explosive etc.) as well as problematic reaction conditions (particularly high or low temperatures).

Continuous reactions are performed in a closed system so that highly reactive compounds can be made and consumed *in situ*. In any case, only small amounts of hazardous intermediates are present at any point in time due to the reaction progressing over the length of the tubing as opposed to the entire mixture being hazardous in batch. In addition, the direct use of such reactive compounds is possible as they can be accurately dosed.

Examples of those “forbidden” reactions are direct fluorinations^[23], nitrations^[24], halogenations, reductions^[25], organometallic reactions and reactions involving diazo-^[26], diazonium compounds^[27], azides^[28] or cyanides.

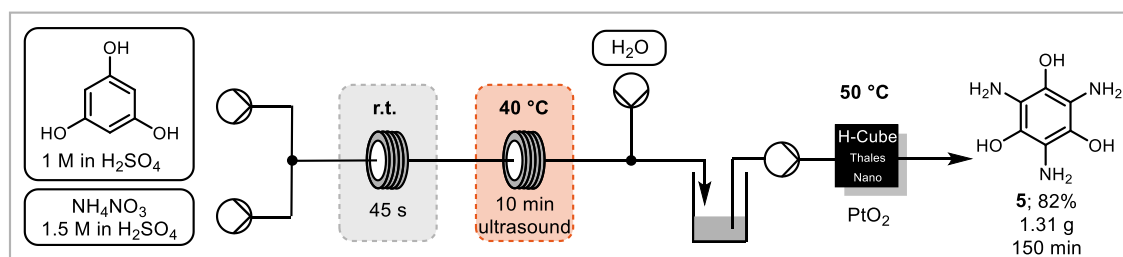
In addition to the increased control over potentially hazardous reactions, the small reactor volumes minimise the severity in case of an incident.^[9] For example, the power of an explosion is proportional to the total mass of explosive material to the power of 1/3 but also its propagation is suppressed in narrow tubing.^[9, 29] In addition, safety measures, such as pumps stopping at a pressure build up (for example due to a blockage), check valves or pressure release valves can be incorporated.

Kappe and co-workers used the tube-in-tube reactor to introduce diazomethane into a reaction (Scheme 1.3).^[30] Diazomethane is a useful C₁ building block but is usually avoided due to its toxicity and explosive nature and the difficulty to handle the gas. The group forms diazomethane *in situ* from Diazald® (*N*-methyl-*N*-nitroso-*p*-toluenesulfonamide) and potassium hydroxide which is fed into the inner tube of the tube-in-tube device. There it can permeate the membrane and react with the desired substrate. In the example shown in Scheme 6, diazomethane reacts with a Cbz protected phenylalanine, that is preactivated *via* the mixed anhydride, to form an α -diazo ketone which is transformed into the α -halo ketone with hydrochloric acid. The product is a key intermediate (**4**) for the antiretroviral agent Atazanarvir.



Scheme 1.3: *In Situ* Preparation and Consumption of Diazomethane Using a Tube-in-Tube Reactor^[30c]

Kappe and co-workers have also demonstrated the safe nitration of phloroglucinol and subsequent hydrogenation to triaminophloroglucinol using the H-Cube (Scheme 1.4).^[31] Nitration reactions are usually exothermic and some products are known to be explosive.^[24] Therefore, controlled, multiple nitrations can be problematic on scale up in batch. Under continuous flow conditions the exotherm can be more effectively controlled thus avoiding thermal runaways and making the process safer. Kappe and co-workers nitrated their starting material three times, incorporating an ultrasound bath to prevent clogging of the reactor. To prevent isolation of the highly explosive intermediate, the nitro groups were then reduced using the H-cube before isolation. The H-cube is a commercially available hydrogenation flow reactor that produces hydrogen from water by electrolysis and uses catalyst cartridges to perform the hydrogenation at elevated temperatures.^[32] The group was able to successfully demonstrate the scale up of their method, producing 1.31 g of their target compound in 150 min. The triaminophloroglucinol (**5**) is an important precursor for the chelating agent triaminotrioxoinositol (2,4,6-triaminocyclohexane-1,3,5-triol, which is found in applications in medicine and industry.



Scheme 1.4: Sequential Nitration and Hydrogenation in Flow^[31]

1.2.4 Scale Up and Process Intensification

The scale up of continuous flow reactions is attractive due to the improved performance regarding heat and mass transfer and safety. In comparison, batch processes often suffer from mixing or temperature control becoming inefficient when scaling up a reaction.

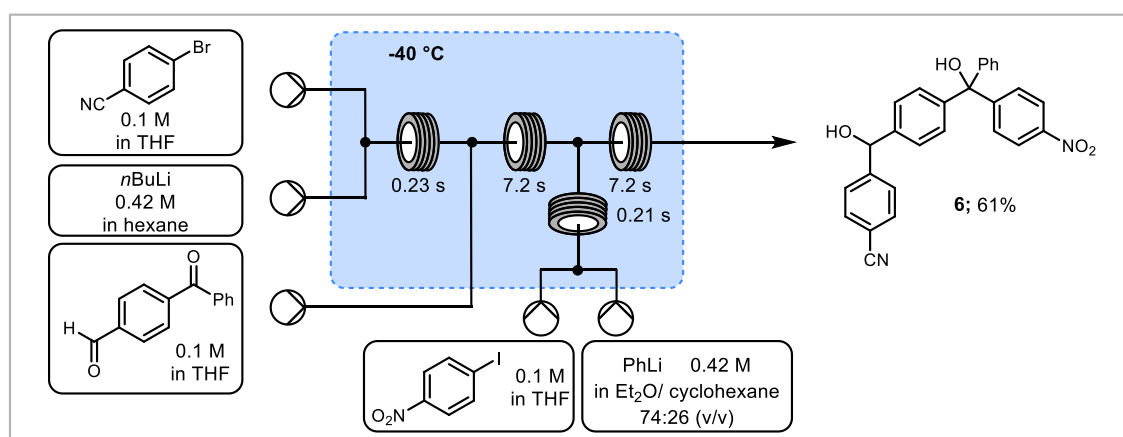
In flow, scale up can be achieved by running the reaction for a longer time, as scale is dependent on time rather than on the size of the reactor. To reduce further handling steps, the inclusion of downstream processing into the process or batch wise workup can be crucial avoiding decomposition of product in the crude mixture. Alternatively, several reactors can be run in parallel to enable a higher throughput. As each reaction tube is the same irrespective on the quantity of them, the scale can be increased without the need of further optimisation, known as numbering up. That means that parameters such as temperature, concentration and reaction time do not need to be changed in most cases. However, the increased number of pumps necessary for the numbering up approach makes it often less feasible for pilot plant scales and very cost intensive for even larger scales. In a third approach the diameter of the tubing can be increased to increase the throughput of each reactor. As the dimensions of the reactor are changed, some advantages of flow processing are diminished resulting from the decreased SA:V. This must be taken into consideration when scaling up a flow reaction and the process might have to be adjusted. For example, mixers are often incorporated into wider bore tubing.

Process intensification is a chemical engineering expression which describes the adjustment of a process to improve control of reactor kinetics (higher selectivity), higher energy efficiency, reduction of capital costs and improvement of safety. It is defined as the enhancement of transport rates to give each molecule in a process the same experience and a “development that leads to a substantially smaller, cleaner, safer and more efficient technology”.^[33] This means, a process is designed to be as efficient as possible whilst still ensuring high selectivity. The expression of process intensification is often interpreted in the chemistry community as described by Hessel *et al* in the use of “novel process windows” which is also described as “harsh conditions” by Kockmann and Roberge.^[34] These conditions are described as far from conventional methods involving, for example, high temperatures, high pressures and high concentrations. It also includes the use of explosive or highly exothermic conditions and thus the possible discovery of new chemical transformations in such reaction regimes. In small batch reactions harsh conditions might be feasible (sealed vessels, microwave heating etc.) but on large scale the required conditions are often not achievable. Exotherms on large scales must be controlled by high dilution and long dosing times which is against the

concept of process intensification. Continuous flow conditions enable a high measure of control of reaction parameters so that the incorporation of these “novel process windows” becomes possible.

One example of these “novel process windows” is described in Yoshida's flash chemistry.^[35] The concept demonstrated by Yoshida is based on high-resolution reaction time control, meaning very short residence times (milli second scale), enabling new chemical transformations. These transformations cannot be achieved in batch as the time resolution cannot be controlled accurately enough. The accurate time resolution is achieved by the addition of a quench in a precise point along the reactor, and therefore at a precise residence time. The use of flash chemistry prevents the decomposition of reactive intermediates and increases selectivity in the presence of a range of functional groups.

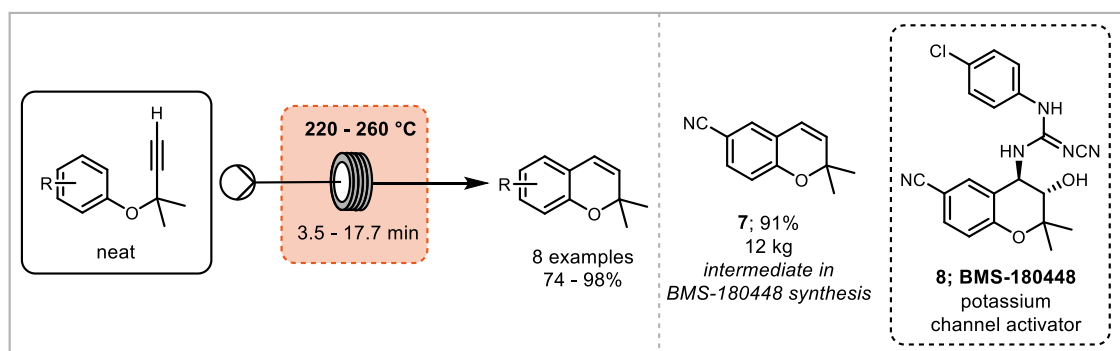
In this manner, Yoshida and co-workers showed how the increased fast mixing, accurate temperature control, and short reaction times enable formation of unstable aryllithiums bearing an electrophilic group. The group investigated the lithium-halogen exchange with *n*-BuLi whilst avoiding the aryllithium reacting with the electrophilic group in the starting material.^[36] These aryllithiums can then be quenched or trapped with a nucleophile. More recently, Yoshida and co-workers expanded on this work by trapping these unstable aryllithiums with difunctional nucleophiles (Scheme 1.5).^[37] The group was able to selectively react the aryllithiums with an aldehyde in the presence of a ketone without the use of protecting groups. In a subsequent reaction, the ketone was then reacted with another *in situ* produced aryllithium performing an overall three-component coupling.



Scheme 1.5: Chemoselective Lithium-Halogen Exchange and Trapping with Difunctional Electrophile^[37]

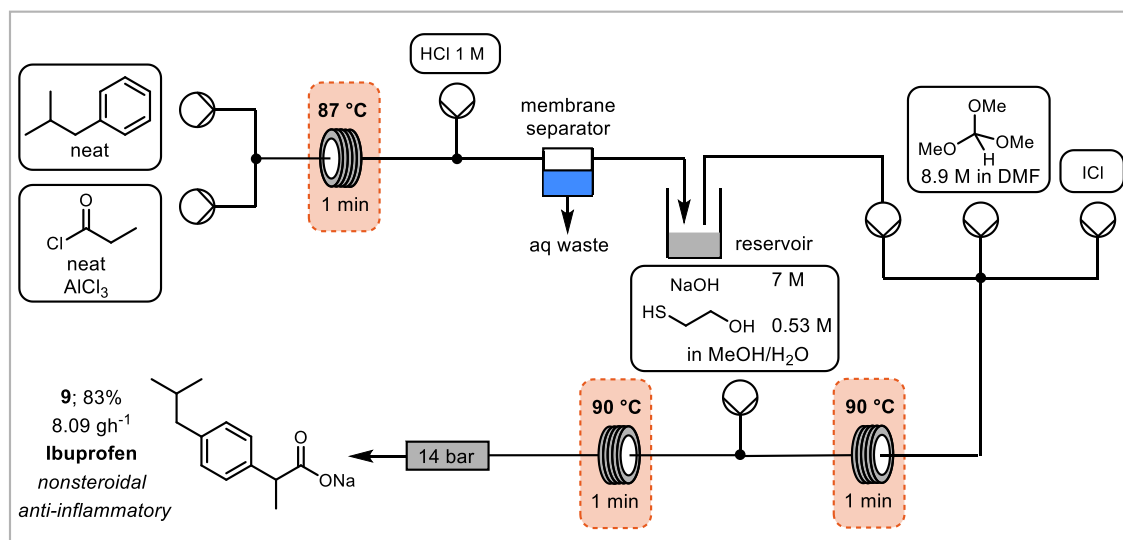
Bogaert-Alvarez *et al* demonstrated the use of the enhanced temperature control in a large-scale Claisen rearrangement under solvent-free conditions and high temperatures

(Scheme 1.6).^[38] Heat is required to initiate the reaction but the overall process is highly exothermic and can lead to thermal runaways and heat related product degradation. Therefore, batch reactions lead to low selectivity and scale up can be difficult. The group has been able to accurately control the temperature under continuous flow conditions and produce 12 kg of a key intermediate (**7**) in the synthesis of a potassium channel activator (**8**).



Scheme 1.6: Exotherm Control in a Large-Scale Claisen Rearrangement^[38]

Jamison and co-workers used the idea of process intensification in the synthesis of ibuprofen (**9**, Scheme 1.7).^[39] The authors “pushed the limits of continuous flow processing” by incorporating neat reagents and *in line* quenching and purification. The reaction could be performed with a total residence time of three minutes. The first step involves a Friedel-Crafts acylation under neat conditions followed by quenching of AlCl_3 and phase separation to collect the neat intermediate. The use of neat ICl as a 1,2-aryl migration promoter and trimethylorthoformate afforded the methyl ester of ibuprofen. Subsequent quenching of the remaining oxidant with a thiol and saponification of the ester product afforded ibuprofen as the sodium salt in 83% yield with a production rate of 8 gh^{-1} . The authors had to design the process to tolerate both neat, corrosive reagents and exotherms resulting from performing the process at high concentrations.



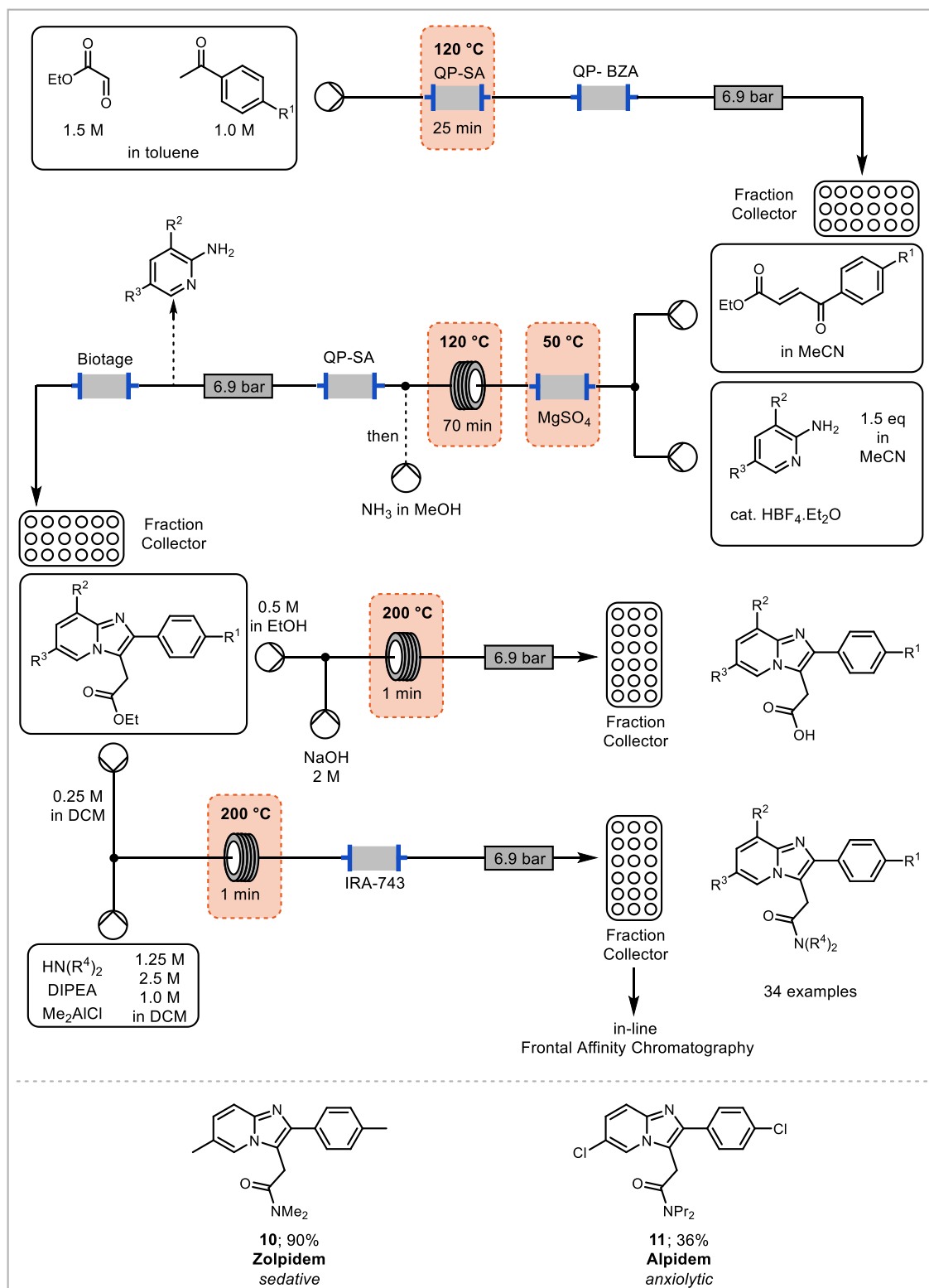
Scheme 1.7: Three Minute Synthesis of Ibuprofen^[39]

1.2.5 Library Preparation

Continuous flow processing can be used for the preparation of compound libraries, an important pursuit for industrial screening processes e.g. in the pharmaceutical industry.^[40] Once a flow process has been developed, many different substrates can be produced for screening purposes.

In a multistep synthesis, each step offers the prospect of introducing a range of differently substituted starting materials. With each such possible point for variation the diversity of potential products is increased. This is important especially in drug discovery where the ability to synthesise a range of analogues is necessary to find the most appropriate substitution of the pharmacophore.

Ley and co-workers demonstrated the synthesis of a library of potential GABA_A agonists using continuous flow methods (Scheme 1.8).^[41] Three reaction steps produced a range of analogues by collecting fractions of each substrate and then using it in a concurrent step. This process also included *in line* purification. In the first step the aldol condensation of ethyl 2-oxoacetate and an acetophenone introduced one point of variation in the intermediate. In the next step the formation of an imidazole through the condensation with a disubstituted aminopyridine installed two further points for structural variation. In a third step the ester moiety in the substrate could be hydrolysed to the acid or transformed into the amide. A total of 34 examples have been made using the author's method. Furthermore, *in line* frontal affinity chromatography was used to evaluate the biological activity of the prepared examples. These examples included the known drugs Zolpidem (**10**) and Alpidem (**11**).



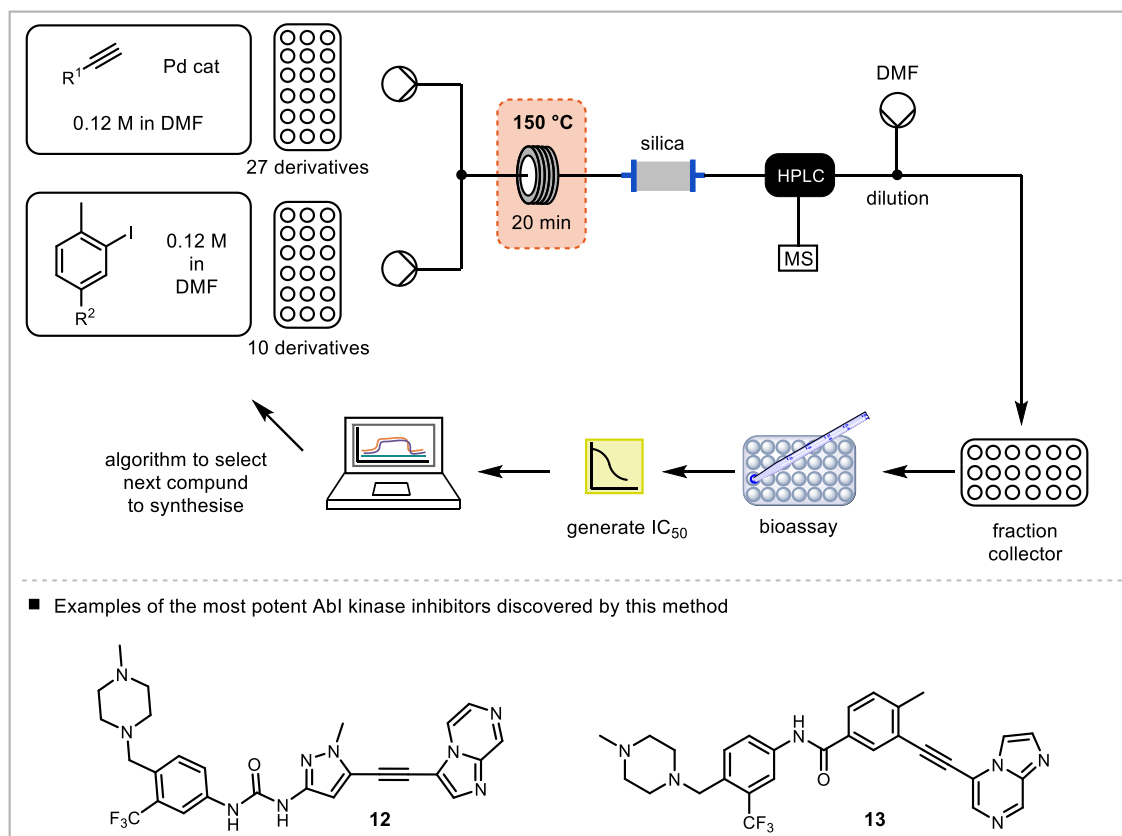
Scheme 1.8: Library Preparation of Potential GABA_A Agonists and Biological Activity Evaluation^[41]

1.2.6 Reaction Monitoring, Optimisation and Automation

The small reactor dimensions in continuous flow processing enable the fast and cost-efficient screening of reaction parameters, especially if monitoring is performed *in line*. When monitoring *in line*, devices are connected to the continuous setup and the whole reaction mixture flows through a measuring chamber. *In line* monitoring thereby makes the screening and optimisation without the change of a setup and sampling of solution possible. Devices such as UV/Vis, IR and NMR have been developed. In addition, on-line monitoring is possible with MS, GC, HPLC and Raman, where small samples are taken from the reaction mixtures. Digital cameras can be used for visual monitoring.^[42] These devices can be used to monitor starting materials, (hazardous) intermediates and products and help to identify optimised conditions. Algorithms such as DoE (Design of Experiment) can be used to plan experiment sets for optimization.

With the incorporation of analyses, automated systems become possible by the integration of software performing tasks (e.g. LabView, Matlab etc.). These automated systems include the monitoring of a reactant stream appearing and disappearing and permit control of downstream reagent streams, monitoring steady state operation and shutting down in case of deviation, but can also include algorithms for self-optimisation.^[42-43] These automated processes can reduce the workload of chemists avoiding repetitive tasks to free-up for more demanding tasks that cannot be undertaken by machines.^[44]

Cyclofluidic, Sandexis and Accelrys collaborated on the development of a closed-loop process for the rapid discovery of Abl kinase inhibitors (Scheme 1.9).^[45] The authors developed an algorithm that feedbacks the obtained information about their biological activity into the choice of new starting materials. In this manner a library of molecules was synthesised *via* a Sonogoshira coupling, purified and fed into a biological assay to determine the biological activity. Within 21 compounds, the authors were able to identify two novel templates for the Abl kinase inhibitors in this way (**12** and **13**). Key to realising this, was the use of a combination of activity prediction with a chemical space sampling algorithm for the construction of an activity model.



Scheme 1.9: Automated Synthesis and Screening of Compounds^[45]

1.2.7 Multistep Continuous Flow Processing

Multistep continuous flow processing combines several reaction steps into one uninterrupted reactor network by daisy-chaining these reactors and modules. Of further importance is that these steps are accomplished without isolating of intermediates. The compatibility of each step has to be taken into account when designing a multistep process in respect to solvent, side products and pH levels.

The process can include downstream processing such as *in line* purification (extractions with phase separators), distillation units for solvent switches and quenching units. Different methods have been developed to simplify purification such as the use of polymer supported reagents, catalysts and scavengers. One of these methods is the catch-and-release method mentioned previously.^[46] These purification steps can then improve the compatibility of downstream reactions.

Due to the use of additional reagent streams, the end flow rate increases with every step. The use of long reactor coils increases the pressure drop. Pressure drop describes the pressure with that a solution has to be pumped into a reactor to achieve a flowing output. Long, narrow paths increase the pressure drop and equipment needs to be compatible to achieve the necessary pressure. In some cases the collection of intermediate streams is necessary, to reset the flow rate and the pressure drop.

Modular, exchangeable systems for multistep synthesis can lead to greater diversity by changing the order of chemical steps and therefore affording different substrate classes. In the example from Seeberger and co-workers five different modules (module 1: oxidation, module 2: olefination, module 3: Michael addition, module 4: hydrogenation and module 5: saponification) were used for the synthesis of three compound classes: γ -lactams, γ -amino acids and β -amino acids (Figure 1.6, Scheme 1.10).^[47] Depending on the starting materials, the order of substrate addition and reagent choice in each module, different compounds could be targeted using the same equipment. In the first module primary or secondary alcohols were oxidized to the ketone or aldehyde. These could then either undergo a Knoevenagel olefination or a Horner-Wadsworth-Emmons homologation in the second module. The intermediate olefins could then either undergo hydrogenation in the fourth module followed by subsequent hydrolysis in the fifth module to lead to the β -amino acids or be further functionalized in a Michael Addition in the third module. The resulting γ -nitro esters could then either be hydrogenated to yield the γ -lactams after cyclisation or γ -amino acids after hydrolysis and subsequent hydrogenation.

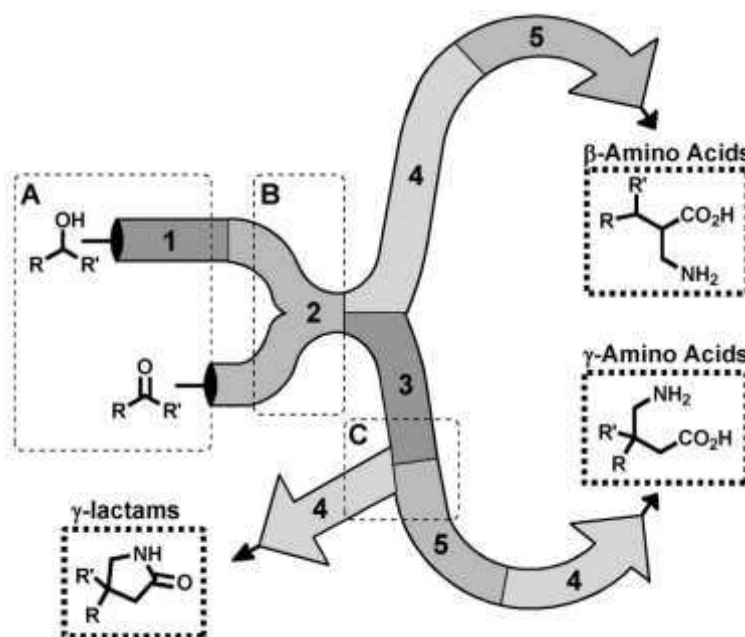
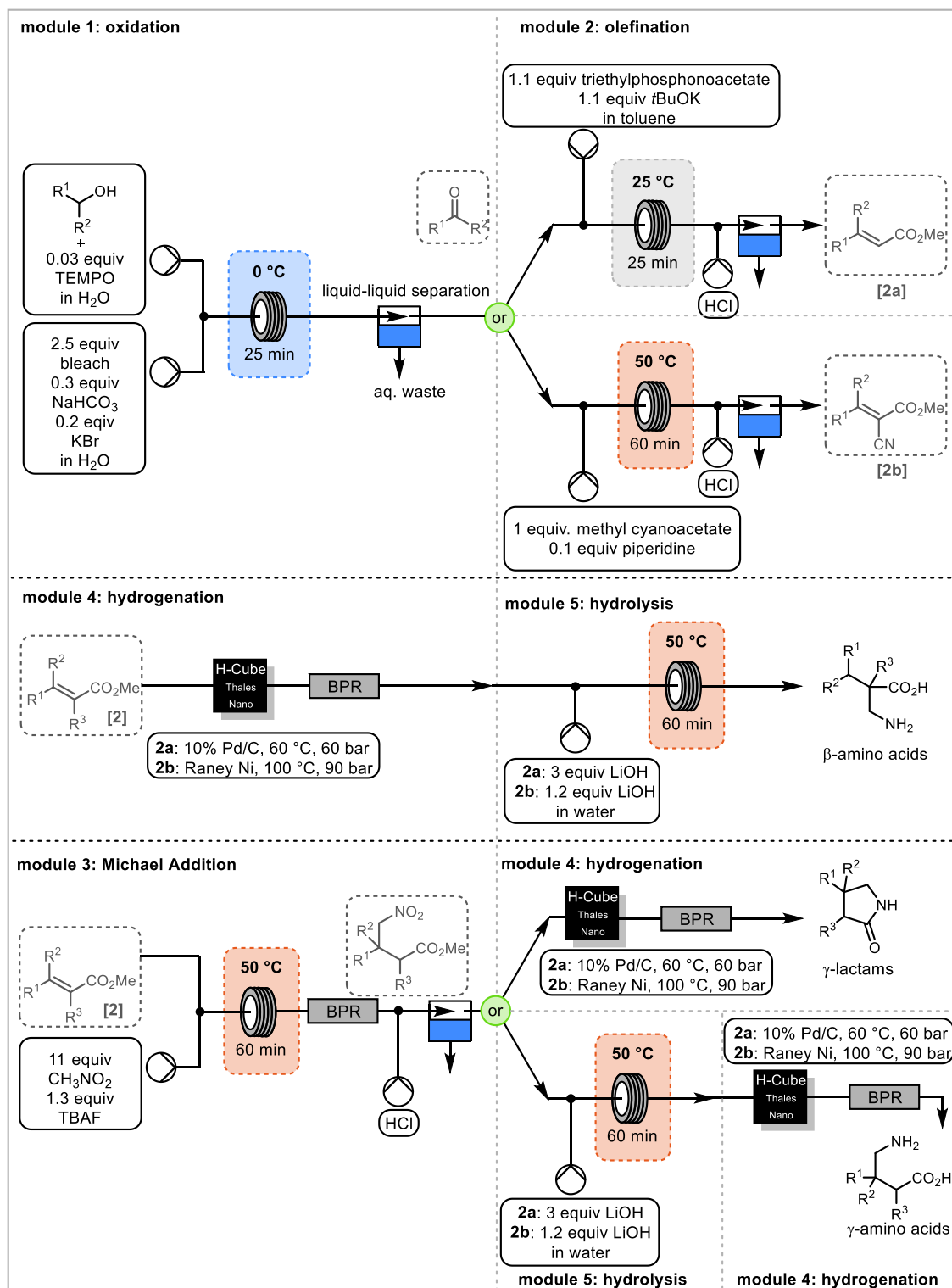


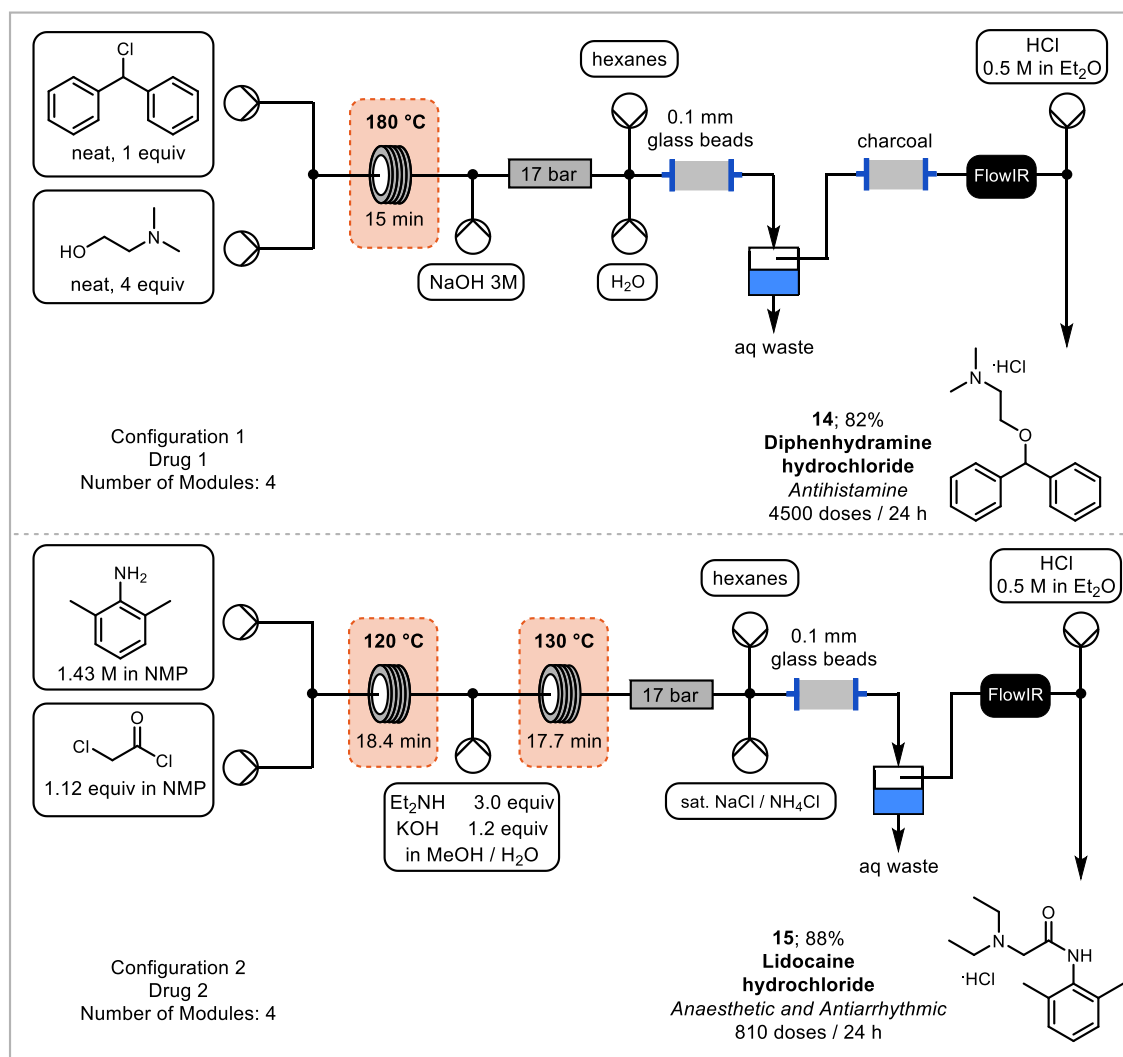
Figure 1.6: Schematic Overview of Divergent Synthesis to γ -Lactams, γ -Amino Acids and β -Amino Acids^[47]



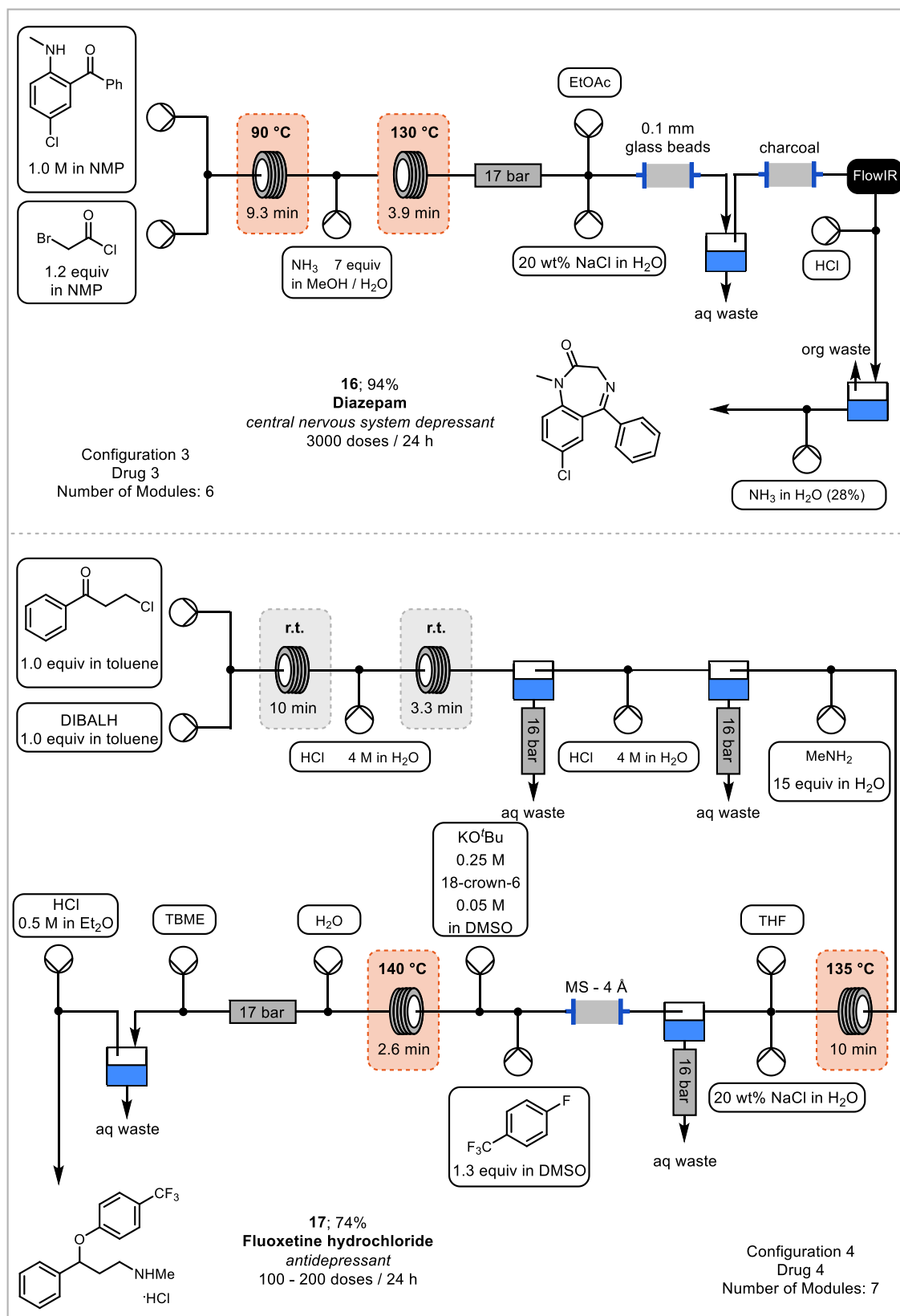
Scheme 1.10: Flow Scheme of Divergent Synthesis to γ -Lactams, γ -Amino Acids and β -Amino Acids^[47]

A Novartis-MIT collaboration demonstrated the modular multistep synthesis for the synthesis of drugs in a compact, reconfigurable manufacturing platform (Scheme 1.11 and 1.12).^[40b] The platform has the capacity to perform both upstream (reaction) and downstream (purification) processes and hosts the necessary equipment (upstream:

feeds, pumps, reactors, separators, pressure regulators; downstream: precipitation tanks, crystallisers, filters, formulation tanks) in a refrigerator sized platform (Picture 1.1). The authors demonstrated the power of such a modular approach by synthesising and purifying four different drugs in their system: diphenylhydramine hydrochloride (**14**), lidocaine hydrochloride (**15**), diazepam (**16**) and fluoxetine hydrochloride (**17**). Such a platform can be used for distributed manufacturing of drugs, which means the synthesis on demand where necessary, rather than large scale production in one factory.



Scheme 1.11: Modular Approach for the Synthesis of Diphenylhydramine (14**) and Lidocaine (**15**)^[40b]**



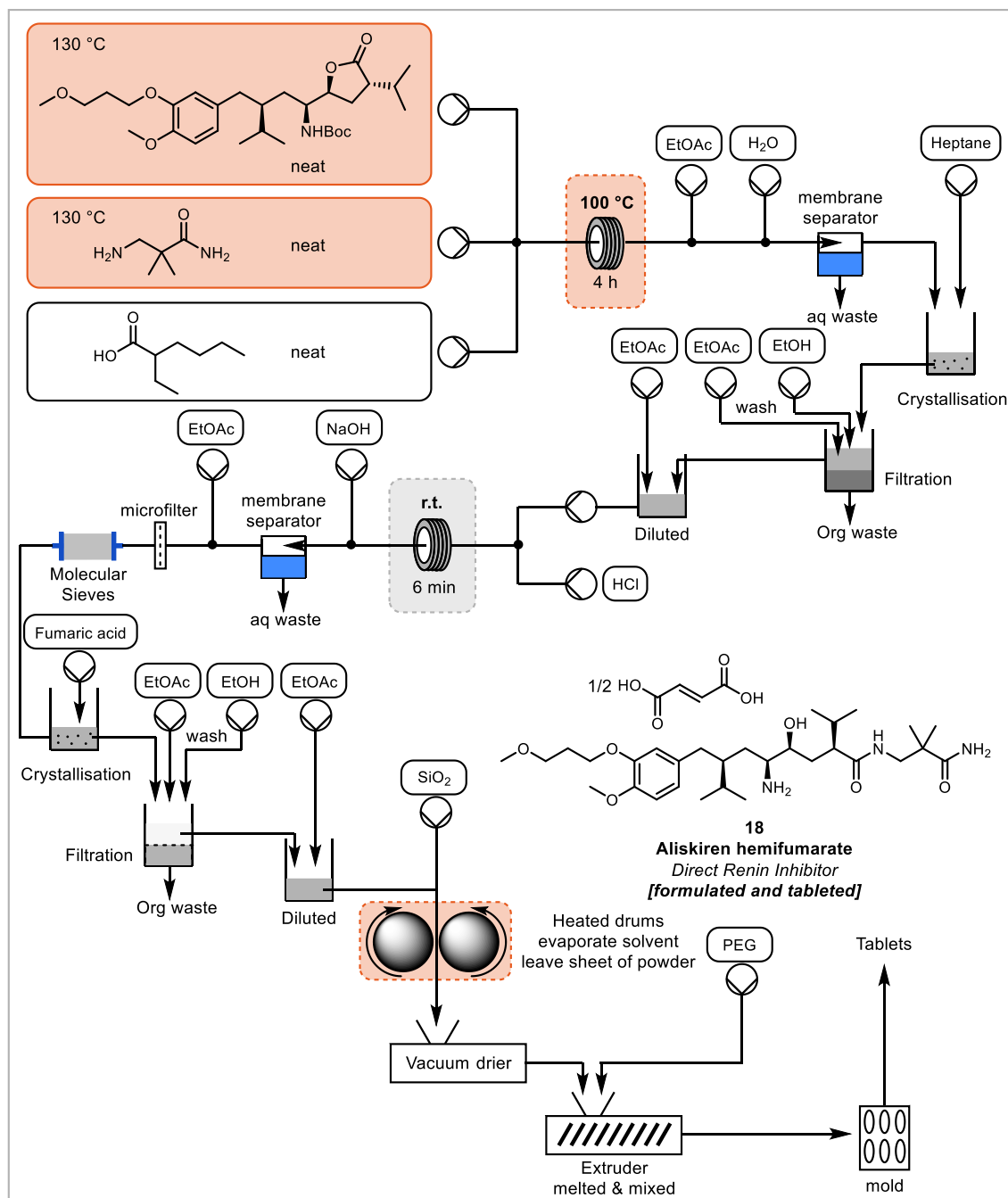
Scheme 1.12: Modular Approach for the Synthesis of Diazepam (16) and Fluoxetine (17)^[40b]



Picture 1.1: Refrigerator Sized Reconfigurable Manufacturing Platform^[40b]

Flow setups can be designed to also include formulation of the desired drug as demonstrated by the example of Aliskiren hemifumarate (**18**) as demonstrated in another collaboration by Novartis and MIT (Scheme 1.13).^[48] The neat starting materials were reacted at elevated temperatures before being diluted with ethyl acetate and water. The phases were separated and the product was precipitated with heptane. The obtained crystals were washed and taken up in ethyl acetate. The exact concentration of product going into the next reactor was measured to control the flow rate of the hydrochloric acid stream for the removal of the Boc protecting group. After quenching with sodium hydroxide the phases were separated and diluted to precipitate sodium chloride that was filtered off. Traces of water were removed by passing through a cartridge of molecular sieves. The product was precipitated with fumaric acid, filtered and washed. The wet filter cake was then diluted and SiO₂ was suspended into the solution as an excipient (formulation agent for long-term stability) before drying the mixture using two convection-heated drums producing a thin sheet of powder. Further drying under vacuum reduced the ethyl acetate content to under 5000 ppm. The resulting powder and polyethylene glycol powder (6000 Da) were fed into a twin screw extruder where the two materials

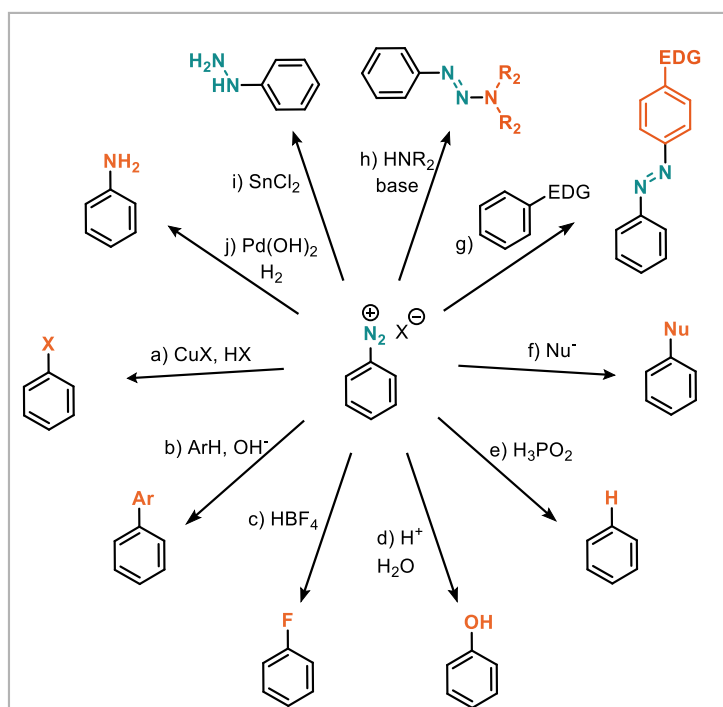
were continuously melted together and mixed. The outlet was passed into a tablet mold where the material is formed into tablets. This example demonstrates the ability of continuous flow processing assisting with the end-to-end manufacturing of drugs.



Scheme 1.13: End-to-End Manufacturing of Aliskiren Hemifumarate (18)^[48]

2 Diazonium Salts in Flow

Diazonium salts are important intermediates in organic synthesis and many transformations that use them have been developed (Scheme 1.14).^[49] One of the first reactions of diazonium salts was the Sandmeyer reaction, reported in 1884 where the treatment of diazonium salts with copper (I) chloride yielded chlorobenzene.^[50] Since then the reaction scope has been extended to other copper salts (CuBr, CuCN etc) (Scheme 15, a). The copper generates an aryl radical from the diazonium salt which is then intercepted by the (pseudo)halide. In 1896, Pschorr reported the copper initiated, intramolecular formation of biaryls, which was followed by the base initiated, intramolecular formation of biaryls (Gomberg-Bachmann reaction in 1924) (Scheme 15, b).^[51]



Scheme 1.14: Example Reactions of Diazonium Salts

The thermal decomposition of aromatic diazonium tetrafluoroborates results in a Balz-Schiemann reaction to form fluorobenzenes that cannot be accessed by the traditional Sandmeyer reaction (Scheme 15, c).^[52] Examples of further reactions include hydrolysis under acidic conditions (Scheme 15, d), reduction to benzene (Scheme 15, e), nucleophilic aromatic substitution losing nitrogen (Scheme 15, f), electrophilic aromatic substitution with electron-rich aromatics to form azo compounds important for the dye industry (Scheme 15, g), interception with nucleophiles such as secondary amines to form triazenes (Scheme 15, h), reduction to the hydrazine e.g. with SnCl₂ (Scheme 15,

i) reduction to the amine (Scheme 15, j), palladium-catalysed cross coupling reactions and Meerwein arylation.

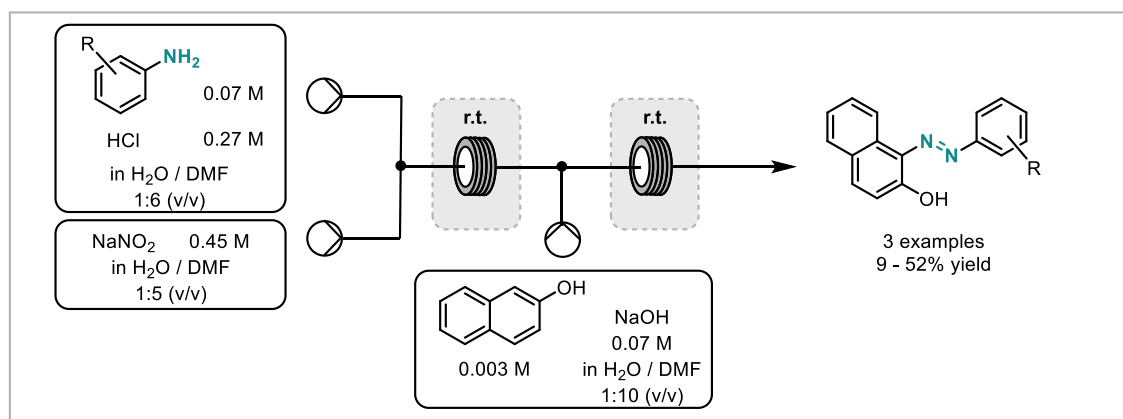
Diazonium salts are formed from the corresponding amine *via* a diazotisation with nitrites (Scheme 16). The reaction can be performed under aqueous conditions using sodium nitrite and acid to form nitrous acid (HONO) as the active diazotisation reagent. Alternatively, organic nitrites (RONO) can be used, which enables the reaction to be performed under non-aqueous and neutral conditions. The reaction proceeds *via* the nucleophilic attack of the amine lone pair onto the nitrogen of the nitrite. After proton transfer and loss of ROH (R= alkyl or H), the *N*-nitroso aniline is formed. Tautomerisation and protonation is necessary for the elimination of water to form the diazonium salt. Diazotisation reactions are thereby exothermic and occur instantly, even at low temperatures, which make thermal runaways likely.^[53]

Diazonium salts can generally be formed from both aromatic and aliphatic amines, however, aliphatic amines with α protons readily deprotonate to form the diazo compound. Therefore, usually only aromatic diazonium salts are discussed.

The stability of aromatic diazonium salts is highly dependent on the counter ion and the substitution of the aromatic ring.^[54] The dry salts can be especially hazardous to isolate as they are shock sensitive and decompose readily. Generally, diazonium salts are handled with care and under low temperatures (<0 °C) as most diazonium salts decompose at temperatures higher than 5 °C.^[53, 55] Aryl diazonium chlorides are even unstable above 0 °C and can explode.^[54b] More stable aryldiazonium salts are the tetrafluoroborate, tosylate, disulfonimide or carboxylate salts.^[54b, 56] Their thermal instability and the evolution of large volumes of gas upon decomposition or during the transformation has led to the development of continuous flow procedures, where mostly the diazonium salts are made and consumed *in situ*.^[21a, 27a, 27c] The increased temperature control and the fact that only small amounts of reactive diazonium salt are present at any time, makes the reaction inherently safer and more controlled. In addition to the safety aspect, performing diazotisations in flow can also increase the selectivity during the reaction. In batch, diazotisation reactions are usually controlled by dilution, long addition times, rapid mixing and low temperatures. These long addition times however, can lead to increased side reactions. This is because the product is in contact with the whole reaction mixture for a long time. By definition, the product is continuously formed and either isolated or consumed under flow conditions.

A few examples of developed continuous flow procedures for the safe preparation and consumption of diazonium salts will be discussed here and the benefit of flow highlighted. The first report of a diazotisation under continuous conditions was the *in situ* formation and consumption to yield azo dyes by deMello and co-workers in 2002 (Scheme 1.15).^[57]

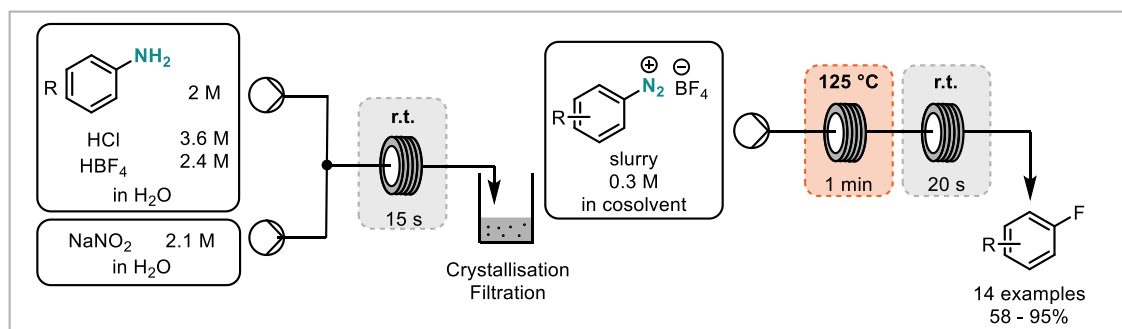
The authors initially formed the diazonium salt from the corresponding aniline and nitrous acid under aqueous conditions and intercepted it with naphthol in an electrophilic aromatic substitution to form the corresponding azo dye. The reaction was performed in a glass microchip reactor and the formation of the dye was monitored visually. The solvent system had to be carefully adjusted to ensure solubility of all reactants and avoid precipitation and thus a mixture of water and DMF was chosen. The authors isolated three examples (9-52%) as a proof-of-concept without further optimisation.



Scheme 1.15: Continuous Formation of Azo Dyes ^[57]

Since the first report of the synthesis of diazonium salts under continuous conditions, a lot of work has been undertaken in this area.^[27a, 27c] Shukla, Kulkarni and Ranade have developed a mathematical model for the mixing properties in a continuous flow reactor during the diazotisation reaction with nitrous and hydrochloric acid.^[53] The authors have validated their model through experimental data and have used it to predict reaction behaviour in a scaled up reactor (20 times). They proved that the reaction is restricted by mixing as the reaction itself is very fast. The authors demonstrated further, that initial concentration, inlet temperature, average heat capacity of the reaction mixture, residence time and heat transfer area were crucial parameters to be considered during scale up.

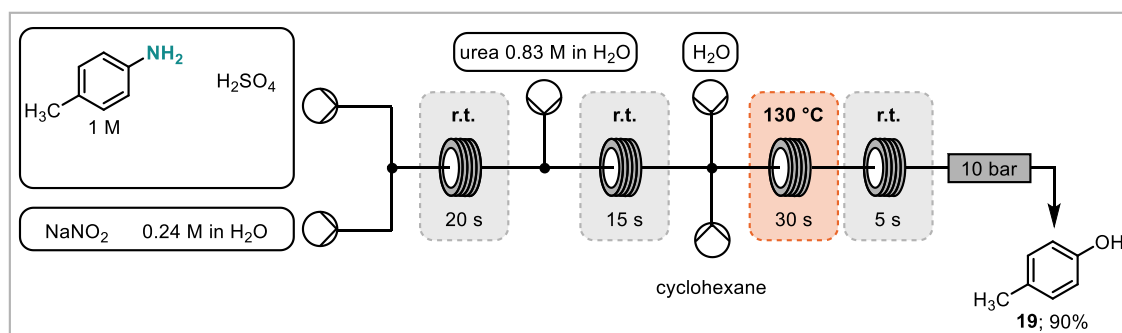
Yu *et al* reported the continuous Balz-Schiemann reaction for the formation of fluorobenzenes (Scheme 1.16).^[58] A range of anilines were diazotised and the products isolated as the tetrafluoroborate salts. The fluorodediazotisation was then performed in a separate step heating a slurry of the diazonium salt to elevated temperatures. As the cosolvent the target product was chosen to avoid further purification steps. The authors showed that the precise control of reaction parameters during the diazotisation enabled higher yields compared to the corresponding batch reaction.



Scheme 1.16: Continuous Balz-Schiemann Reaction^[58]

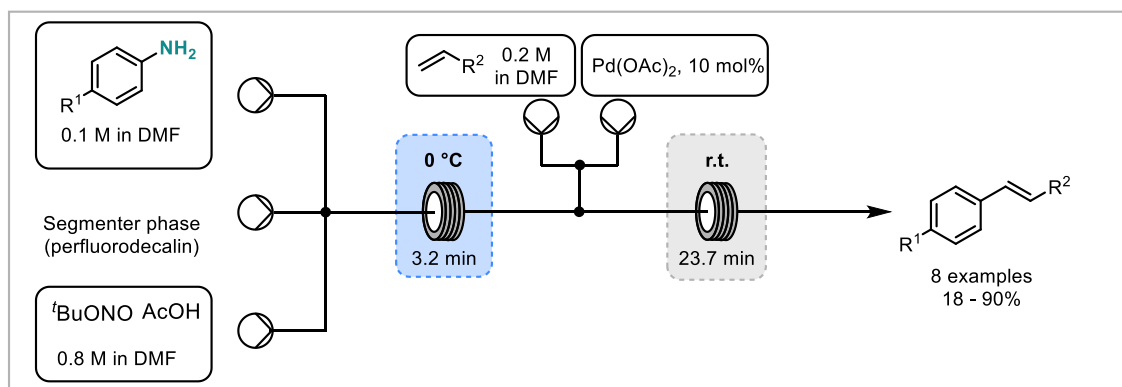
Buchwald and co-workers expanded on this work in 2016 avoiding the isolation of the diazonium salt.^[59] This could, however, lead to more side reactions due to by products still being present in the reaction mixture. Key was the development of reaction parameters to prevent side reactions and reactor clogging. This was achieved by the addition of LiBF_4 and the use of n -butyl acetate as solvent. The diazonium salt solution was then fed into a stirred batch reactor for the Balz-Schiemann reaction to occur under elevated temperatures.

The hydrolysis of a diazonium salt was demonstrated in the synthesis of *p*-cresol (**19**) by Yu *et al* (Scheme 1.17).^[60] The key achievement was the prevention of the coupling reaction of the hydrolysed product and the diazonium salt in an $\text{S}_{\text{N}}\text{Ar}$ reaction which is a problem in batch. Due to limited backmixing occurring under continuous flow conditions, this could be avoided. Other side reactions were prevented using urea for the quench of excess nitrous acid and the use of cyclohexane as a cosolvent.



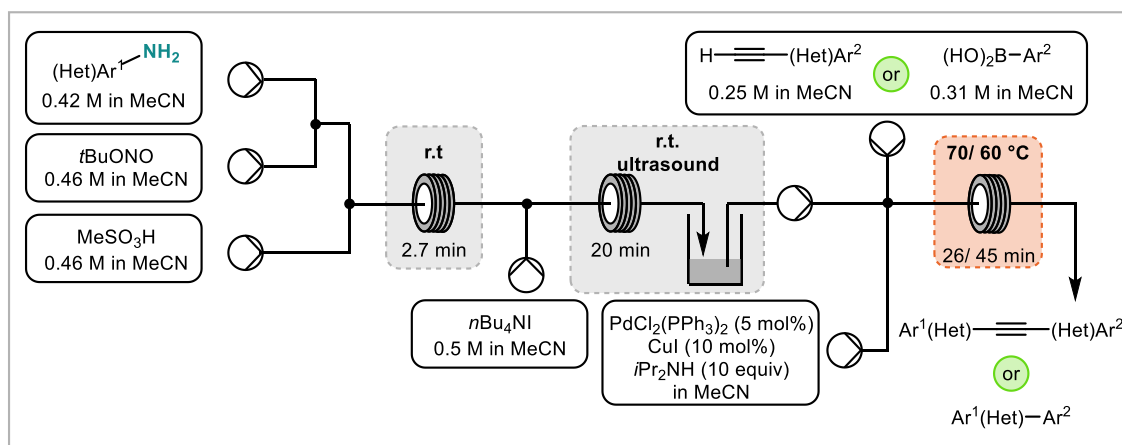
Scheme 1.17: Continuous Hydrolysis of a Diazonium Salt to form *p*-Cresol^[60]

Wirth and co-workers reported the use of segmented flow for the increased mixing in a Heck-Matsuda reaction (Scheme 1.18).^[61] This was achieved by the use of a segmenter phase. This segmenter phase consisted of a solvent immiscible with the reaction solvent and that no reactants were soluble in. The use of a segmenter phase insured increased reaction rates and also overcame the problem of reactor clogging.



Scheme 1.18: Segmented Flow Heck-Matsuda Reaction^[61]

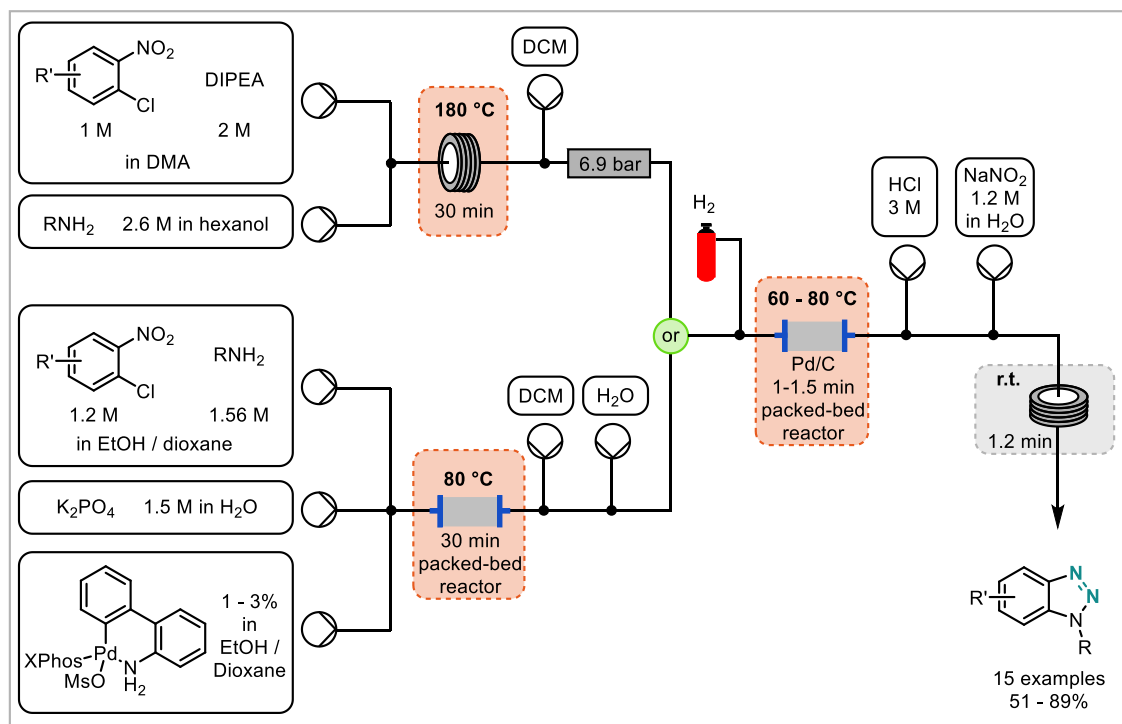
The use of diazonium salts in a Suzuki-Miyaura and Sonogoshira coupling *via* diazotisation of anilines was then later demonstrated by Organ and co-workers (Scheme 1.19).^[62] The reaction sequence proceeded *via* a diazotisation, Sandmeyer type iododediazotisation and then crosscoupling. The authors solved solubility problems by the adjustment of concentration and the type acid used. The iododediazotisation was performed in a reactor under ultrasound irradiation to help outgassing. The reaction mixture was then collected in a reservoir to release the gas before continuing with the crosscoupling reaction in the next step. The authors demonstrated this approach by preparing of 17 Sonogoshira and nine Suzuki-Miyaura products.



Scheme 1.19: Suzuki-Miyaura and Sonogoshira Coupling *via* Iododediazotisation^[62]

Buchwald and co-workers reported the formation of 1-substituted benzotriazoles *via* a C-N bond formation, hydrogenation, diazotisation, cyclisation sequence starting from an *o*-chloro nitrobenzene (Scheme 1.20).^[63] Traditional approaches (alkylation of benzotriazoles or the reaction of benzyne with azides) lack the regioselectivity this approach exhibits. The C-N bond formation was achieved by an S_NAr reaction of an electron-poor aromatic or *via* a Buchwald-Hartwig amination. The nitro group was then

reduced using hydrogen gas on a packed-bed reactor of Pd/C to the corresponding primary amine which was then diazotised. The secondary amine could then ring close by nucleophilic attack onto the diazonium salt to form the desired benzotriazole. Such a multistep approach would have been labour and time intensive in batch but could be accomplished under continuous conditions without the need of intermediate isolation.



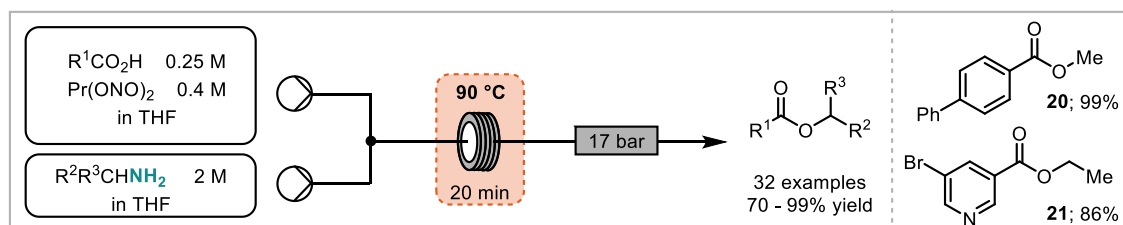
Scheme 1.20: Formation of Benzotriazoles via C-N Bond Formation, Hydrogenation, Diazotisation and Cyclisation Sequence^[63]

Baxendale and Baumann investigated the diazotisation reaction under continuous flow conditions concerning temperature, flow rate, interception with ascorbic acid, non-aqueous solution and the trapping of the aniline on a solid phase (immobilised sulfonic acid).^[64] Most importantly, the authors proved that dependent on the substituent, the chloride diazonium salts start decomposing at about 5 °C. 4-Nitro and 4-methoxy substituted diazonium salts only started to decompose over 25 °C due to the destabilisation of the formed cation.

Ley and co-workers demonstrated the continuous formation and interception of alkyl diazonium salts for the formation of hydroxyacids from amino acids without formation of the diazo compound.^[65] The key focus of this work was on the multiple *in line* liquid-liquid separation where hydrolysis of the diazonium salt took place. Cameras were used to monitor liquid levels precisely during the separation and enabled the step to be computer controlled for a triple extraction. The precise parameter control in each step

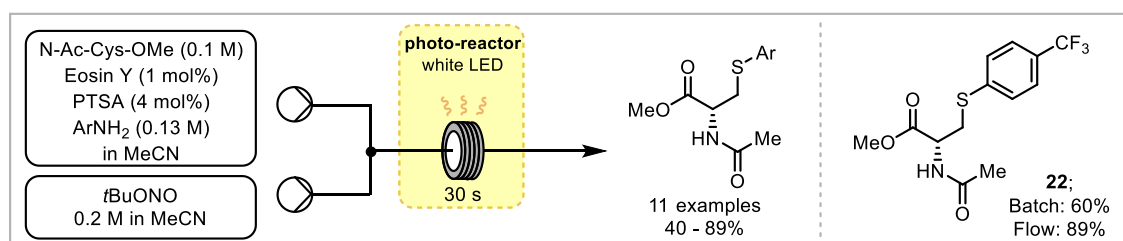
enabled the process to undergo hydrolysis to the desired product during the aqueous workup in spite of the hydrophobic nature of the product.

A recent example from Lebel and co-workers demonstrated the mild esterification of carboxylic acids using *in situ* formed diazonium salts as alkylating agents (Scheme 1.21).^[66] The authors highlight, that the carboxylic acid does not have to be further activated which is usually the case for other esterifications. Importantly, the authors demonstrated that the reaction does not proceed *via* the diazo compound. They also showed in a few mechanistic studies that the reaction proceeds *via* an S_N2 for primary amines and S_N1 with secondary amines due to the difference in stability. Interestingly, the authors used 1,3-propyldinitrite (Pr(ONO)₂) as the diazotisation agent and perform the diazotisation at elevated temperatures as this gave improved results.



Scheme 1.21: Mild Esterification of Carboxylic Acids^[66]

Noël and co-workers utilised diazonium salts in a photochemical reaction to arylate cysteine (Scheme 1.22).^[67] The use of eosin Y as an organic photocatalyst initiated the single electron transfer reaction to form an aryl radical from the diazonium salt in a Stadler-Ziegler type reaction. The use of visible-light enables mild conditions and the use of flow allowed the reaction times to be shortened from 2 h to 30 s. In addition to the arylation of cysteine, 4 dipeptides were arylated.



Scheme 1.22: Visible-Light mediated Arylation of Cysteine^[67]

3 Thesis Objectives

The use of continuous flow methods can have advantages over traditional batch methods in terms of reaction performance and safety as described in chapter 1.1. Especially in cases where reactions are particularly fast, the precise reaction control can benefit the outcome. In the event of hazardous intermediates, the use of continuous flow methods can increase the safety profile of a process due to a limited amount of intermediate present at any point in time.

The aim of this thesis is to explore the use of continuous flow methods for the development of processes using diazonium salts. Diazonium salts are known to be unstable and thus must be handled with care. This is especially the case if the exact properties are not known for an unreported compound. The use of continuous flow methods enables the use of diazonium salts in a safe way. Moreover, diazonium salts are known to be highly versatile and readily accessed intermediates. The development of continuous flow processes could lead to transformations or reactivity previously not available.

In this work continuous flow methodologies will be used for the development of processes for the synthesis of triazenes, indoles and acridones from diazonium salts. The processes must be carefully developed to avoid fouling and clogging of reactor systems. Particularly precipitation of diazonium salts and accumulation thereof could potentially be dangerous. In addition, the multistep procedure has to be designed so that each step is compatible with the next. Finally, the equipment has to be chosen to be appropriate for the process both in terms of performance and chemical compatibility.

Triazenes are prepared via the reaction of a diazonium salt with a secondary amine. There are examples of triazenes reported and in use as anti cancer agents. Triazenes are also interesting to the organic chemistry community due to their diverse reactivity and the ability to function as traceless directing groups. In addition, they can be viewed as protected diazonium salts as they mask the reactivity of a diazonium salt yet can be unmasked with the addition of an acid.

The multistep synthesis of triazenes is to be achieved starting from the corresponding aniline. After diazotisation the diazonium salt will be intercepted with a secondary amine to form a triazene. The direct comparison of the stability of a range of triazenes and diazonium salts is also an objective of this thesis. In addition, the use of triazenes as a traceless directing group for C-H activation is targeted.

Indoles are a moiety present in a range of drugs such as the triptan family. The most common synthesis is the Fischer indole synthesis where a hydrazine and a ketone react in the presence of acid at elevated temperatures to form the indole. Hydrazines however, are not always commercially available and are therefore often synthesised before use from the corresponding aniline *via* the diazonium salt. Usual syntheses reduce the diazonium salt with tin chloride. Recently, the use of ascorbic acid (Vitamin C) has been rediscovered as a metal free alternative for the reduction of diazonium salts.

In this project, the hydrazines are to be prepared *via* a multistep synthesis starting from commercially available anilines. In the first step the anilines are diazotised and then reduced with ascorbic acid to the hydrazine. Aliquots of this hydrazine solution are then transferred into microwave vials preloaded with the ketone to undergo the Fischer indole reaction under elevated temperatures in the microwave. Such a hybrid flow – microwave approach enables the rapid formation of a library of indoles which is particularly important in the area of drug discovery. In addition, the use of machine assisted synthesis offers the prospect of automation.

Acridones are precursors for acridiniums which are organic photoredox catalysts. In addition, they show antimalarial activity and are used as chemotherapeutic agents. Acridones can be prepared *via* the interception of benzyne with anthranilates. In this project, benzyne is to be prepared *via* the decomposition of benzenediazonium-2-carboxylate, which is the diazonium salt of anthranilic acid. The diazonium salt decomposes to form benzyne, nitrogen and carbon dioxide above ambient temperatures. In addition, explosions of the dry salt have been reported. The use of continuous flow methods enables the safe handling of this reactive intermediate and enables the precise interception to avoid side reactions. The prepared acridones can then be further functionalised to acridinium photoredox catalysts.

The last project in this thesis investigates an exothermic reaction under continuous flow conditions. The reaction investigated is the reduction of TMSCF_3 to TMSCF_2H with NaBH_4 . The reaction is highly exothermic and large scale batch reactions (above 20 g starting material) tend to be difficult to control. After the initial exotherm, the reaction continues and has to be stirred over night. The use of flow methods could enable the safe control of the initial exotherm to then finish the slow part of the reaction in a round bottom flask at elevated temperatures. The product is then obtained through distillation. A telescoped process where the first part of the reaction is controlled in flow and the second part is performed in a distillation flask is envisaged. The monitoring of the exotherm is key to realising the control of the reaction. Commercially available

thermocouples will be used to measure the temperature along the tubing. As the reaction still continuous after the flow part, the conversion is monitored using *in situ* NMR monitoring. For this the Bruker InsightMR flow tube is used. This enables the use of normal high field NMR machines and therefore high resolution spectra. The comparison of space time yields and a scale up of the reaction is targeted.

4 References

- [1] a) in *Comprehensive Organic Synthesis II Vol. 9*, 2 ed. (Eds.: P. Knochel, G. A. Molander), Elsevier, Amsterdam, **2014**; b) M. O'Brien, R. Denton, S. V. Ley, *Synthesis* **2011**, 2011, 1157-1192.
- [2] R. J. Giguere, T. L. Bray, S. M. Duncan, G. Majetich, *Tetrahedron Lett.* **1986**, 27, 4945-4948.
- [3] a) N. E. Leadbeater, in *Comprehensive Organic Synthesis II, Volume 9: Enabling Technologies for Organic Synthesis* (Eds.: P. Knochel, G. A. Molander), Elsevier, Amsterdam, **2014**, pp. 234-286; b) S. C. Ameta, P. B. Punjabi, R. Ameta, C. Ameta, *Microwave-assisted Organic Synthesis: A Green Chemical Approach*, CRC Press, **2014**; c) R. N. Baig, R. S. Varma, *Chem. Soc. Rev.* **2012**, 41, 1559-1584.
- [4] A. Loupy, D. Monteux, A. Petit, J. M. Aizpurua, E. Domínguez, C. Palomo, *Tetrahedron Lett.* **1996**, 37, 8177-8180.
- [5] a) M. R. Rosana, Y. Tao, A. E. Stiegman, G. B. Dudley, *Chem. Sci.* **2012**, 3, 1240-1244; b) G. B. Dudley, A. E. Stiegman, M. R. Rosana, *Angew. Chem. Int. Ed.* **2013**, 52, 7918-7923; c) R. Laurent, A. Laporterie, J. Dubac, J. Berlan, S. Lefeuvre, M. Audhuy, *J. Org. Chem.* **1992**, 57, 7099-7102.
- [6] a) T. Razzaq, J. M. Kremsner, C. O. Kappe, *J. Org. Chem.* **2008**, 73, 6321-6329; b) M. A. Herrero, J. M. Kremsner, C. O. Kappe, *J. Org. Chem.* **2008**, 73, 36-47; c) D. Obermayer, B. Gutmann, C. O. Kappe, *Angew. Chem. Int. Ed.* **2009**, 48, 8321-8324; d) C. O. Kappe, B. Pieber, D. Dallinger, *Angew. Chem. Int. Ed.* **2013**, 52, 1088-1094; e) N. Kuhnert, *Angew. Chem. Int. Ed.* **2002**, 41, 1863-1866.
- [7] a) J. C. Pastre, D. L. Browne, S. V. Ley, *Chem. Soc. Rev.* **2013**, 42, 8849-8869; b) T. Wirth, *ChemSusChem* **2012**, 5, 215-216; c) J. Wegner, S. Ceylan, A. Kirschning, *Chem. Commun.* **2011**, 47, 4583-4592; d) D. L. Browne, J. L. Howard, C. Schotten, in *Comprehensive Medicinal Chemistry III*, Elsevier, Oxford, **2017**, pp. 135-185; e) S. Born, E. O'Neal, K. F. Jensen, in *Comprehensive Organic Synthesis II, Volume 9: Enabling Technologies for Organic Synthesis* (Eds.: P. Knochel, G. A. Molander), Elsevier, Amsterdam, **2014**, pp. 54-93; f) M. B. Plutschack, B. Pieber, K. Gilmore, P. H. Seeberger, *Chem. Rev.* **2017**, 117, 11796-11893; g) R. L. Hartman, J. P. McMullen, K. F. Jensen, *Angew. Chem. Int. Ed.* **2011**, 50, 7502-7519; h) T. Noël, Y. Su, V. Hessel, in *Organometallic Flow Chemistry* (Ed.: T. Noël), Springer International Publishing, Cham, **2016**, pp. 1-41; i) D. T. McQuade, P. H. Seeberger, *J. Org. Chem.* **2013**, 78, 6384-6389; j) B. Gutmann, D. Cantillo, C. O. Kappe, *Angew. Chem. Int. Ed.* **2015**, 54, 6688-6728; k) D. Dallinger, C. O. Kappe,

- Current Opinion in Green and Sustainable Chemistry* **2017**, *7*, 6-12; l) J. Britton, C. L. Raston, *Chem. Soc. Rev.* **2017**, *46*, 1250-1271; m) D. Webb, T. F. Jamison, *Chem. Sci.* **2010**, *1*, 675-680; n) R. Porta, M. Benaglia, A. Puglisi, *Org. Process Res. Dev.* **2015**, *20*, 2-25; o) M. Baumann, I. R. Baxendale, *Beilstein J. Org. Chem.* **2015**, *11*, 1194-1219; p) T. Wirth, *Microreactors in organic chemistry and catalysis*, John Wiley & Sons, **2013**; q) J. Britton, T. F. Jamison, *Nat. Protoc.* **2017**, *12*, 2423.
- [8] D. E. Fitzpatrick, S. V. Ley, *React. Chem. Eng.* **2016**.
- [9] a) M. Gödde, C. Liebner, H. Hieronymus, *Chem. Ing. Tech.* **2009**, *81*, 73-78; b) H. P. Gemoets, Y. Su, M. Shang, V. Hessel, R. Luque, T. Noël, *Chem. Soc. Rev.* **2016**, *45*, 83-117.
- [10] a) T. N. Glasnov, C. O. Kappe, *Macromol. Rapid Commun.* **2007**, *28*, 395-410; b) S. Ceylan, C. Friese, C. Lammel, K. Mazac, A. Kirschning, *Angew. Chem. Int. Ed.* **2008**, *47*, 8950-8953.
- [11] D. Webb, T. F. Jamison, *Org. Lett.* **2011**, *14*, 568-571.
- [12] E. Mielke, P. Plouffe, N. Koushik, M. Eyholzer, M. Gottspöner, N. Kockmann, A. Macchi, D. M. Roberge, *React. Chem. Eng.* **2017**, *2*, 763-775.
- [13] T. L. Bergman, F. P. Incropera, *Fundamentals of heat and mass transfer*, John Wiley & Sons, **2011**.
- [14] V. Hessel, H. Löwe, F. Schönfeld, *Chem. Eng. Sci.* **2005**, *60*, 2479-2501.
- [15] M. Brzozowski, M. O'Brien, S. V. Ley, A. Polyzos, *Acc. Chem. Res.* **2015**, *48*, 349-362.
- [16] X. Tang, R. K. Allemann, T. Wirth, *Eur. J. Org. Chem.* **2017**, *2017*, 414-418.
- [17] M. O'Brien, I. R. Baxendale, S. V. Ley, *Org. Lett.* **2010**, *12*, 1596-1598.
- [18] A. Polyzos, M. O'Brien, T. P. Petersen, I. R. Baxendale, S. V. Ley, *Angew. Chem. Int. Ed.* **2011**, *50*, 1190-1193.
- [19] D. Cambié, C. Bottecchia, N. J. Straathof, V. Hessel, T. Noël, *Chem. Rev.* **2016**.
- [20] M. Atobe, H. Tateno, Y. Matsumura, *Chem. Rev.* **2017**.
- [21] a) M. Movsisyan, E. I. P. Delbeke, J. K. E. T. Berton, C. Battilocchio, S. V. Ley, C. V. Stevens, *Chem. Soc. Rev.* **2016**, *45*, 4892-4928; b) R. Singh, H.-J. Lee, A. K. Singh, D.-P. Kim, *Korean J. Chem. Eng.* **2016**, *33*, 2253-2267.
- [22] B. Gutmann, C. O. Kappe, *Chim. Oggi Chem. Today* **2015**, *33*, 3.
- [23] M. Baumann, I. R. Baxendale, L. J. Martin, S. V. Ley, *Tetrahedron* **2009**, *65*, 6611-6625.
- [24] A. A. Kulkarni, *Beilstein J. Org. Chem.* **2014**, *10*, 405-424.
- [25] M. Irfan, T. N. Glasnov, C. O. Kappe, *ChemSusChem* **2011**, *4*, 300-316.
- [26] S. T. R. Müller, T. Wirth, *ChemSusChem* **2015**, *8*, 245-250.

- [27] a) B. J. Deadman, S. G. Collins, A. R. Maguire, *Chem. Eur. J.* **2015**, *21*, 2298-2308; b) S. T. R. Mueller, T. Wirth, *ChemSusChem* **2015**, *8*, 245-250; c) N. Oger, E. Le Grogneq, F.-X. Felpin, *Organic Chemistry Frontiers* **2015**, *2*, 590-614.
- [28] M. Weber, G. Yilmaz, G. Wille, *Chimica Oggi* **2011**, *29*, 8-10.
- [29] N. Kockmann, P. Thenee, C. Fleischer-Trebes, G. Laudadio, T. Noel, *React. Chem. Eng.* **2017**, *2*, 258-280.
- [30] a) F. Mastronardi, B. Gutmann, C. O. Kappe, *Org. Lett.* **2013**, *15*, 5590-5593; b) E. Rossi, P. Woehl, M. Maggini, *Org. Process Res. Dev.* **2011**, *16*, 1146-1149; c) V. D. Pinho, B. Gutmann, L. S. M. Miranda, R. O. M. A. de Souza, C. O. Kappe, *J. Org. Chem.* **2014**, *79*, 1555-1562.
- [31] D. Cantillo, M. Damm, D. Dallinger, M. Bauser, M. Berger, C. O. Kappe, *Org. Process Res. Dev.* **2014**, *18*, 1360-1366.
- [32] http://thalesnano.com/products/h-cube-series/h_cube_pro, accessed 29.01.2018.
- [33] a) A. I. Stankiewicz, J. A. Moulijn, *Chem. Eng. Prog.* **2000**, *96*, 22-34; b) D. Reay, C. Ramshaw, A. Harvey, *Process Intensification*, Butterworth-Heinemann, Oxford, **2008**.
- [34] a) V. Hessel, D. Kralisch, N. Kockmann, T. Noël, Q. Wang, *ChemSusChem* **2013**, *6*, 746-789; b) N. Kockmann, D. M. Roberge, *Chem. Eng. Technol.* **2009**, *32*, 1682-1694.
- [35] a) J.-i. Yoshida, *Flash Chemistry: Fast Organic Synthesis in Microsystems*, Wiley, **2008**; b) J. I. Yoshida, *The Chemical Record* **2010**, *10*, 332-341; c) J. i. Yoshida, A. Nagaki, T. Yamada, *Chemistry—A European Journal* **2008**, *14*, 7450-7459; d) J.-i. Yoshida, Y. Takahashi, A. Nagaki, *Chem. Commun.* **2013**, *49*, 9896-9904; e) T. Wirth, *Angew. Chem. Int. Ed.* **2017**, *56*, 682-684.
- [36] H. Kim, A. Nagaki, J.-i. Yoshida, *Nat. Commun.* **2011**, *2*, 264.
- [37] A. Nagaki, S. Ishiuchi, K. Imai, K. Sasatsuki, Y. Nakahara, J.-i. Yoshida, *React. Chem. Eng.* **2017**, *2*, 862-870.
- [38] R. J. Bogaert-Alvarez, P. Demena, G. Kodersha, R. E. Polomski, N. Soundararajan, S. S. Wang, *Org. Process Res. Dev.* **2001**, *5*, 636-645.
- [39] D. R. Snead, T. F. Jamison, *Angew. Chem. Int. Ed.* **2015**, *54*, 983-987.
- [40] a) J. Li, S. G. Ballmer, E. P. Gillis, S. Fujii, M. J. Schmidt, A. M. E. Palazzolo, J. W. Lehmann, G. F. Morehouse, M. D. Burke, *Science* **2015**, *347*, 1221-1226; b) A. Adamo, R. L. Beingessner, M. Behnam, J. Chen, T. F. Jamison, K. F. Jensen, J.-C. M. Monbaliu, A. S. Myerson, E. M. Revalor, D. R. Snead, T. Stelzer, N. Weeranoppanant, S. Y. Wong, P. Zhang, *Science* **2016**, *352*, 61-67.
- [41] L. Guetzoyan, N. Nikbin, I. R. Baxendale, S. V. Ley, *Chem. Sci.* **2013**, *4*, 764-769.

- [42] S. V. Ley, R. J. Ingham, M. O'Brien, D. L. Browne, *Beilstein J. Org. Chem.* **2013**, *9*, 1051-1072.
- [43] a) D. C. Fabry, E. Sugiono, M. Rueping, *Isr. J. Chem.* **2014**, *54*, 341-350; b) D. C. Fabry, E. Sugiono, M. Rueping, *React. Chem. Eng.* **2016**, *1*, 129-133; c) N. Holmes, G. R. Akien, R. J. D. Savage, C. Stanetty, I. R. Baxendale, A. J. Blacker, B. A. Taylor, R. L. Woodward, R. E. Meadows, R. A. Bourne, *React. Chem. Eng.* **2016**, *1*, 96-100; d) N. Holmes, G. R. Akien, A. J. Blacker, R. L. Woodward, R. E. Meadows, R. A. Bourne, *React. Chem. Eng.* **2016**, *1*, 366-371; e) M. O'Brien, L. Konings, M. Martin, J. Heap, *Tetrahedron Lett.* **2017**, *58*, 2409-2413; f) M. O'Brien, D. A. Cooper, J. Dolan, *Tetrahedron Lett.* **2017**, *58*, 829-834; g) M. O'Brien, D. Cooper, *Synlett* **2016**, *27*, 164-168; h) M. O'Brien, P. Koos, D. L. Browne, S. V. Ley, *Org. Biomol. Chem.* **2012**, *10*, 7031-7036.
- [44] a) C. A. Shukla, A. A. Kulkarni, *Beilstein J. Org. Chem.* **2017**, *13*, 960-987; b) V. Sans, L. Cronin, *Chem. Soc. Rev.* **2016**, *45*, 2032-2043.
- [45] B. Desai, K. Dixon, E. Farrant, Q. Feng, K. R. Gibson, W. P. van Hoorn, J. Mills, T. Morgan, D. M. Parry, M. K. Ramjee, *J. Med. Chem.* **2013**, *56*, 3033-3047.
- [46] S. V. Ley, I. R. Baxendale, R. M. Myers, in *Comprehensive Medicinal Chemistry II, Volume 3: Drug Discovery Technologies* (Eds.: J. B. Taylor, D. J. Triggle), Elsevier, Oxford, **2007**, pp. 791-836.
- [47] D. Ghislieri, K. Gilmore, P. H. Seeberger, *Angew. Chem. Int. Ed.* **2015**, *54*, 678-682.
- [48] S. Mascia, P. L. Heider, H. Zhang, R. Lakerveld, B. Benyahia, P. I. Barton, R. D. Braatz, C. L. Cooney, J. Evans, T. F. Jamison, *Angew. Chem. Int. Ed.* **2013**, *52*, 12359-12363.
- [49] a) D. S. Wulfman, in *Diazonium and Diazo Groups, Part 1* (Ed.: S. Patai), John Wiley & Sons, Ltd., **1978**, pp. 247-339; b) A. F. Hegarty, in *Diazonium and Diazo Groups, Part 2* (Ed.: S. Patai), John Wiley & Sons, Ltd., **1978**, pp. 511-591; c) F. Mo, G. Dong, Y. Zhang, J. Wang, *Org. Biomol. Chem.* **2013**, *11*, 1582-1593.
- [50] a) T. Sandmeyer, *Ber. Dtsch. Chem. Ges.* **1884**, *17*, 1633-1635; b) T. Sandmeyer, *Ber. Dtsch. Chem. Ges.* **1884**, *17*, 2650-2653.
- [51] a) R. Pschorr, *Ber. Dtsch. Chem. Ges.* **1896**, *29*, 496-501; b) M. Gomberg, W. E. Bachmann, *J. Am. Chem. Soc.* **1924**, *46*, 2339-2343.
- [52] G. Balz, G. Schiemann, *Berichte der deutschen chemischen Gesellschaft (A and B Series)* **1927**, *60*, 1186-1190.
- [53] C. A. Shukla, A. A. Kulkarni, V. V. Ranade, *React. Chem. Eng.* **2016**, *1*, 387-396.

-
- [54] a) D. K. Kölmel, N. Jung, S. Bräse, *Aust. J. Chem.* **2014**, *67*, 328-336; b) A. Zarei, L. Khazdooz, H. Aghaei, G. Azizi, A. N. Chermahini, A. R. Hajipour, *Dyes Pigm.* **2014**, *101*, 295-302.
- [55] M. Sheng, D. Frurip, D. Gorman, *Journal of Loss Prevention in the Process Industries* **2015**, *38*, 114-118.
- [56] a) V. D. Filimonov, M. Trusova, P. Postnikov, E. A. Krasnokutskaya, Y. M. Lee, H. Y. Hwang, H. Kim, K.-W. Chi, *Org. Lett.* **2008**, *10*, 3961-3964; b) M. Barbero, M. Crisma, I. Degani, R. Fochi, P. Perracino, *Synthesis* **1998**, *1998*, 1171-1175.
- [57] R. C. R. Wootton, R. Fortt, A. J. de Mello, *Lab Chip* **2002**, *2*, 5-7.
- [58] Z. Yu, Y. Lv, C. Yu, W. Su, *Tetrahedron Lett.* **2013**, *54*, 1261-1263.
- [59] N. H. Park, T. J. Senter, S. L. Buchwald, *Angew. Chem. Int. Ed.* **2016**, *55*, 11907-11911.
- [60] Z. Yu, X. Ye, Q. Xu, X. Xie, H. Dong, W. Su, *Org. Process Res. Dev.* **2017**, *21*, 1644-1652.
- [61] B. Ahmed-Omer, D. A. Barrow, T. Wirth, *Tetrahedron Lett.* **2009**, *50*, 3352-3355.
- [62] M. Teci, M. Tilley, M. A. McGuire, M. G. Organ, *Chem. Eur. J.* **2016**, *22*, 17407-17415.
- [63] M. Chen, S. L. Buchwald, *Angew. Chem. Int. Ed.* **2013**, *52*, 4247-4250.
- [64] T. Hu, I. Baxendale, M. Baumann, *Molecules* **2016**, *21*, 918.
- [65] D. X. Hu, M. O'Brien, S. V. Ley, *Org. Lett.* **2012**, *14*, 4246-4249.
- [66] C. Audubert, H. Lebel, *Org. Lett.* **2017**, *19*, 4407-4410.
- [67] C. Bottecchia, M. Rubens, S. B. Gunnoo, V. Hessel, A. Madder, T. Noël, *Angew. Chem. Int. Ed.* **2017**, *56*, 12702-12707.

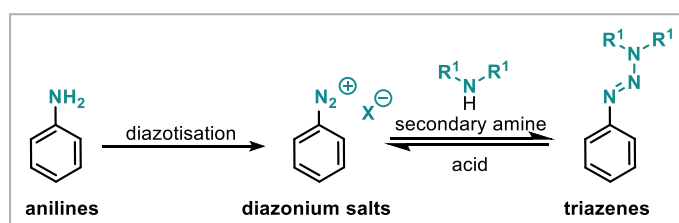
Chapter 2 – Investigating the Formation of Triazenes from Diazonium Salts

Table of Contents

1	Introduction	42
1.1	Triazene Stability	44
1.2	Restricted Rotation in Triazenes	45
2	Results and Discussion	50
2.1	Flow Synthesis	50
2.2	Stability and DSC	54
2.3	Restricted Rotation and VT NMR Results	58
3	Conclusion and Outlook	65
4	References	68

1 Introduction

The formation of C-N bonds for the construction of more complex molecules is often achieved through the formation of diazo- or diazonium compounds. However, safety hazards associated with the formation and isolation of those compounds make this route less popular. Thus, their preparation has been explored under continuous flow methods (see Chapter 1.2). Another alternative is the trapping of diazonium salts for example with a secondary amine to transform them into the corresponding triazene (Scheme 2.1). Triazenes can also be prepared from the corresponding azide^[1] in the presence of alkyl lithiums and alkylhalides or from Grignard reagents with nitrous oxide^[2] and lithium dialkylamides.



Scheme 2.1: Preparation of Triazenes

Triazenes are more stable than their diazonium salt congener and are therefore described as protected diazonium salts.^[3] Notably, also the protection of secondary and aromatic amines as the triazene using a diazonium salt as the protecting agent has been reported.^[4] This is due to triazenes being stable towards alkylating agents, strong bases, oxidation and reduction.

Triazenes are often described as the synthetic equivalent to the diazonium salt.^[5] This is due to the triazene being in equilibrium with the diazonium salt under acidic conditions. Therefore, triazenes have been used in a range of typical diazonium salt transformations in order to manipulate the functionality of the aromatic ring (Scheme 2.2). For success in these reactions a Brønsted or Lewis acid is required.

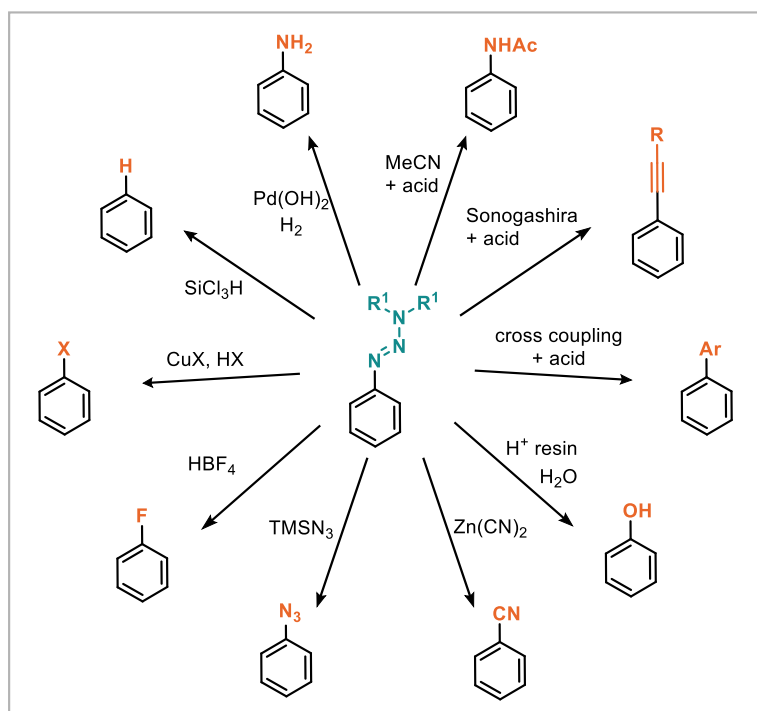
The formation of azides from triazenes has been demonstrated with trimethylsilyl azide by Knochel and co-workers where it undergoes a S_NAr reaction.^[5] Triazenes can be converted to aryl fluorides similar to the Balz-Schiemann reaction with diazonium salts in a Wallach reaction with HBF₄.^[19] The formation of other aryl halides has been extensively studied especially for iodinations.^[6] More generally, the use of trimethylsilyl halides^[7] or the halo acid with copper and HBF₄^[8] similar to the Sandmeyer reaction has been used for the formation of arylhalides. Similar to the transformation of diazonium salts, these transformations also occur *via* a radical mechanism. The triazene can be

removed to yield the unfunctionalised aromatic ring which is performed under reducing or acidic conditions with sodium borohydride or transition metal catalysis, phosphinic acid, HCl and acidic resin in water.^[9] This method is also used in deamination reactions of anilines *via* the diazonium salt. The diazonium salt decomposes to the aryl cation and subsequently to the aryl radical which is quenched by the acid. The triazene can be transformed into the corresponding aniline by a methanolic potassium hydroxide solution or reduction with Pd(OH)₂ with hydrogen gas.^[4b] The amide can be formed *via* the palladium catalysed CO capture.^[10] The diazonium salt is unmasked with an acid catalyst and undergoes oxidative addition onto the palladium catalyst. After nitrogen extrusion, CO is inserted and attack from the secondary amine leads to the formation of the amide and release of the palladium catalyst. In addition, the boron trifluoride-induced Suzuki coupling has been demonstrated, where the Lewis acid activates the triazene leaving group.^[11] Metal-free cross coupling reactions have been demonstrated to proceed *via* a radical mechanism where the triazene is cleaved to give the amine, aryl radical and nitrogen.^[12] The aryl radical can then react with another aromatic in a cross coupling reaction. The nitrile can be introduced using a mixture of Zn(CN)₂ and Zn(ClO₄)₂ *via* a radical mechanism.^[6a] In addition, triazenes can be transformed into the boranes with trifluoroborate to initiate the reaction.^[13] The perfluoroalkylation has both been demonstrated copper and silver mediated.^[14] The use of acids for the generation of the corresponding diazonium salt had to be avoided as this would lead to protonation of the perfluoroalkylate. Instead conversion to the iodide with methyl iodide and the subsequent metal mediated perfluoroalkylation proved successful.

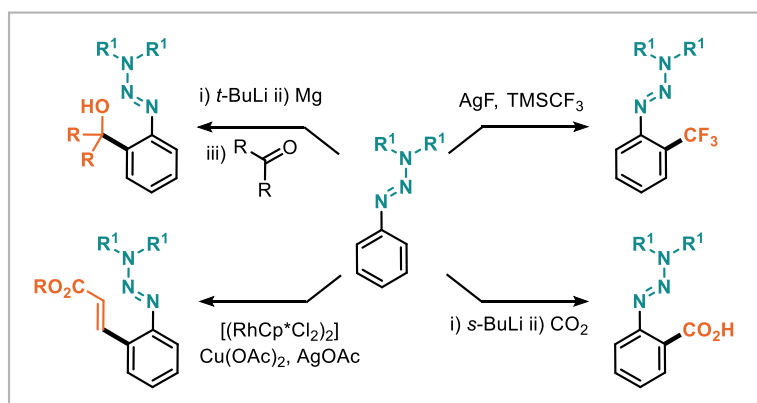
The wide variety of functional groups possible from triazene precursors, makes them attractive as linkers in solid-phase synthesis, for which most of these transformations have been established.^[15] The ability to remove the linker afterwards, makes them examples of traceless linkers. Especially the possibility to use triazene as precursors for cross coupling reactions has been exploited in syntheses such as the formation of macromolecules.^[15g, 16] In addition, triazenes have been used as precursors for drugs^[17], heterocyclic compounds^[18] and natural products.^[18b, 19] They have also been investigated as ligands for transition metal catalysis.^[20]

More recently, triazenes have found application as *ortho* directing groups (Scheme 2.3).^[21] Due to the possibility of transforming the triazene into a different functional group or completely remove it, the use of such a traceless directing group is attractive for synthesis and has been applied for the formation of the antibiotic Vancomycin.^{[22][29]}

Triazenes themselves are alkylating agents and therefore carcinogen. They have found use in cancer therapy and as antibiotics.^[5, 23]



Scheme 2.2: Example Reactions of Triazenes



Scheme 2.3: Example of Triazenes as Directing Groups in Metalation Reactions

1.1 Triazene Stability

Triazenes are described as protected diazonium salts due to their increased stability. Even though this is stressed in most publications using triazenes, proof of improved stability is scarce.

One method to determine the thermal stability of a compound is Differential Scanning Calorimetry (DSC).^[24] DSC consists of subjecting a small sample to a constant temperature ramp. The energy input to obtain this ramp is compared to a standard. From the difference in heat flow endothermic or exothermic processes can be identified as the energy input has to be increased or decreased respectively to maintain the constant change in temperature. The DSC results are presented in a graph as heat flow vs

temperature. The exact shape of the DSC curve is highly dependent on the heating rate and the amount of sample. This makes the shape of the DSC curve, including temperatures of the beginning or maximum of the curve, incomparable between different experiments. For comparison between experiments the onset temperature is used. The onset temperature is where the tangent of the highest slope of the DSC curve meets the interpolated baseline. The enthalpy of the endothermic or exothermic process can be calculated from the area under the curve.

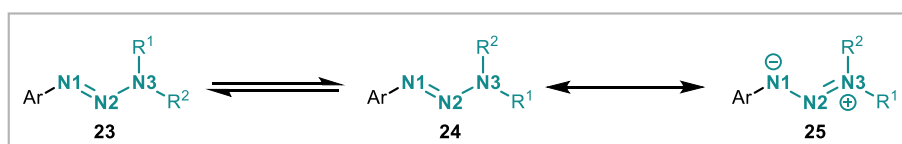
Lippert *et al.* have measured decomposition temperatures and the decomposition energy of six triazenes using a DSC.^[25] The authors showed that the decomposition temperature decreases with the electron withdrawing capacity of the substituents on the aromatic ring, whereas the sterics of the amine did not have a strong influence. The decomposition energy was calculated from the decomposition curve and showed that they are nearly twice as high as the energies for similar azo compounds.

Döbele *et al.* used triazenes for the formation of aryl fluorides via the Wallach reaction and measured the DSC for one of their triazene precursors to demonstrate the high stability of triazenes.^[15] The authors measured an onset temperature of 202.2 °C and decomposition ranged from 136 °C to 266 °C for a heating rate of 10 Kmin⁻¹. The enthalpy for the decomposition was determined to be 40 kJ g⁻¹.

Though the stability of triazenes compared to their diazonium salts is mentioned in most publications, no direct comparison of their stability has been made.

1.2 Restricted Rotation in Triazenes

Restricted rotation around the N2-N3 bond in triazenes can be observed due to a partial double bond character displayed in the resonance structure (Scheme 2.4). The partial double bond character is due to the delocalisation into the extended π system of aromatic triazenes. A double bond between N2 and N3 makes the substituents on N3 inequivalent. In the other extreme, a pure single bond, the substituents are equivalent as rotation makes them exchange rapidly.



Scheme 2.4: Restricted Rotation in Triazenes

The restricted rotation can be observed by NMR, as the exchange rate is of the scale of the NMR time scale. Depending on the strength of the double bond character and the

exchange rate, either only one sharp signal, one broad signal, two broad signals or two sharp signals can be observed (Figure 2.1).^[26]

Substituents on the N3 are equivalent if the exchange is fast and would give rise to one signal in the NMR spectrum (high limit). If the exchange is slow, the substituents are inequivalent, giving rise to two signals (low limit). In an intermediate exchange, the signals are broad. The point where the signals are not distinguishable any longer and are very broad is called coalescence. As the exchange rate can be changed with the temperature, variable temperature NMR (VT NMR) measurements can be used to influence the regime. The low limit, coalescence and high limit temperature are dependent on the field strength of the NMR machine. At lower field strengths the coalescence temperature is higher as the line width (in Hz) is dependent on the field strength.

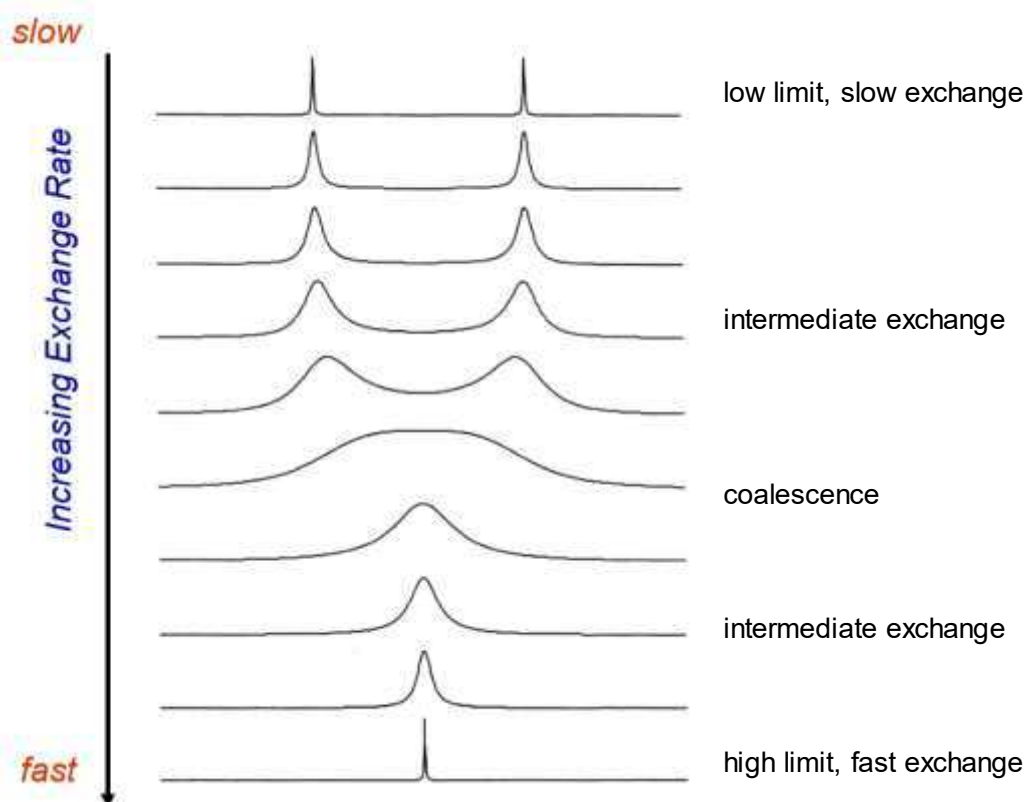


Figure 2.1: NMR Signal Dependency on Exchange Rate^[27]

NMR spectroscopy can be used to determine the exchange rate (k) at a known temperature. With exchange rates measured over a range of temperatures, the activation energy (E_A) can be calculated. For a symmetrical exchange, when both signals have the same intensity, the following equations can be used to calculate the exchange rates. It

is described as the line shape analysis as the additional line width $\Delta\nu$ of signals is taken into account.

fast exchange:

$$k = \frac{\pi \cdot (\delta_{A,0} - \delta_{B,0})^2}{2\Delta\nu}$$

at coalescence:

$$k = \frac{\pi \cdot (\delta_{A,0} - \delta_{B,0})^2}{\sqrt{2}}$$

intermediate exchange:

$$k = \frac{\pi \cdot \sqrt{(\delta_{A,0} - \delta_{B,0})^2 - (\delta_{A,c} - \delta_{B,c})^2}}{\sqrt{2}}$$

slow exchange:

$$k = \Delta\nu \cdot \pi$$

$\Delta\nu$: additional line width in Hz

$$\Delta\nu = \nu_{A,T} - \nu_{A,n}$$

$\delta_{A,0}$: position peak A in Hz at low limit

$\delta_{B,0}$: position peak B in Hz at low limit

$\delta_{A,c}$: position peak A in Hz at coalescence

$\delta_{B,c}$: position peak B in Hz at coalescence

$\nu_{A,T}$: line width of peak A at temperature T

$\nu_{A,n}$: natural line width of peak A (e.g. high or low limit)

From rate constants at different temperatures, the Arrhenius equation can be used to plot the Arrhenius plot ($\ln(k)$ vs $1/T$). From the slope the activation energy can be calculated.

$$k = Ae^{-\frac{E_A}{RT}}$$

$$\ln(k) = \ln(A) - \frac{E_A}{R} \frac{1}{T}$$

A: pre-exponential factor

E_A : activation energy

R: gas constant

As an alternative to the line shape analysis, the activation energy can be estimated from the peak positions at the low limit and the coalescence temperature only. To increase accuracy, the coalescence temperature can be determined on more than one field strength.

$$E_A = RT_C \left[22.96 + \ln \frac{T_C}{\delta_{A,0} - \delta_{B,0}} \right]$$

The restricted rotation of triazenes has first been mentioned and discussed in 1968 by Akhtar *et al.*^[28] The authors determined the coalescence temperatures for five *para* substituted 1-aryl-3,3-dimethyltriazenes (NO₂: +37 °C, Cl: -13 °C, H: -23.5 °C, CH₃: -31.5 °C, OMe: -44 °C) and calculated the rotational barriers. They demonstrated that electron withdrawing groups give rise to a higher double bond character. This means that triazenes with electron withdrawing groups on the aromatic ring rotate more slowly compared to triazenes with electron neutral or electron donating groups at the same temperature and are therefore in a slower exchange regime. The authors showed that the substituent influence on the rotational barrier follows a linear Hammett relationship. Marullo *et al.* confirmed this trend in the same year, giving similar coalescence temperatures (*p*-NO₂: +35.1 °C, *m*-CF₃: +5.3 °C, *p*-Cl -11.3 °C, H: -22.5 °C, *p*-CH₃ -33.9 °C).^[29] Axenrod and co-workers used ¹³C and ¹⁵N NMR studies to determine whether a non-aromatic resonance form, where the electron withdrawing group is charged, would contribute to the restricted rotation.^[30] They concluded, that the resonance form **25** (Scheme 2.4) would be the major contributor. Lunazzi *et al.* calculated rotational barriers for substituted piperidyl triazenes.^[31] They showed, that the bulk of the group is largely determined by the conformation of the ring and changes with increasing methyl substitution. The authors also demonstrated an NMR solvent effect on the exchange rate by using both CDCl₃ and CS₂. The non-polar solvent (CS₂) cannot interact with the charged resonance structures so that the double bond character is smaller.

Foster and co-workers determined the coalescence temperature and rotation rates and energies for *para*-substituted aryl triazenes derived pyrrolidine confirming a linear Hammett relationship for cyclic amines.^[32]

Nguyen *et al.* calculated rotational barriers and compared them to experimental data and confirmed the electronic effects of the aromatic portion computationally.^[33]

Lippert and co-workers determined coalescence temperatures and exchange rates for 1-aryl-3,3-alkyltriazenes with electron withdrawing substituents in different positions on

the aromatic ring. They confirmed the trend that the coalescence temperature increases with the electron withdrawing character of the substituent.^[25]

More recently, Zarei *et al.* demonstrated the synthesis of triazenes from stabilised diazonium salts and observed the restricted rotation for one of their products.^[34] The authors calculated the rate constant at the coalescence temperature to be 117 s^{-1} at 326 K.

Trialkyltriazenes have been found to exhibit a lower rotational barrier than aryltrialkyltriazenes. This is due to the aromatic ring in aryltrialkyltriazenes stabilising charges as demonstrated by Michejda and co-workers.^[1]

Bis-triazenes, with two triazene moieties in one molecule, are also reported to show restricted rotation.^[16a]

The partial double bond character in triazenes can also be displayed in crystal structures of triazenes, where the N2-N3 bond is, dependent on the substitution on the triazene, shorter than expected for an isolated N-N bond.^[20a]

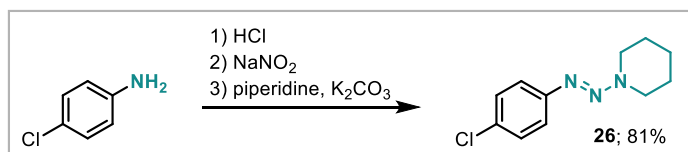
Even though restricted rotation in triazenes has been discussed in early literature, it is hardly acknowledged in recent literature.^[21] Reports show the broadened peaks in NMR spectra, but do not elaborate on this phenomenon. During the project this phenomenon was encountered and further investigated with the use of VT NMR.

2 Results and Discussion

The continuous flow synthesis of triazenes for the protection of diazonium salts was envisioned. The reaction was to be performed under continuous conditions to safely make and consume the diazonium salt. Then the stability of triazenes and their corresponding diazonium salts was to be compared.

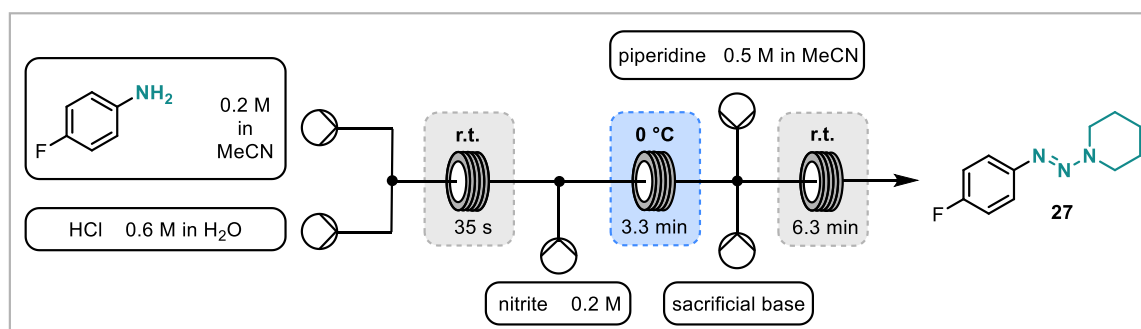
2.1 Flow Synthesis

Common syntheses of triazenes involve the diazotisation of an aniline and interception with a secondary amine in the presence of a sacrificial base. Following the procedure from Huang and co-workers 81% of the *p*-chloro substituted triazene **26** was obtained (Scheme 2.5).^[21b] In this procedure the diazotisation was performed under aqueous conditions with sodium nitrite and hydrochloric acid. The solution was then added to the sacrificial base, aqueous potassium carbonate, and the secondary amine, piperidine to yield the triazene.



Scheme 2.5: Initial Batch Reaction

After successful batch synthesis, a continuous flow setup was developed. The aniline was first mixed with the hydrochloric acid in a short room temperature reaction coil, then diazotised with a nitrite in a slightly longer 0 °C reaction coil, and then the interception with a secondary amine in the presence of a sacrificial base was envisioned (Scheme 2.6). As a model reaction the triazene **27** resulting from *p*-fluoroaniline and piperidine was investigated under continuous flow conditions.



Scheme 2.6: Envisioned Flow Setup

Upon adapting the aqueous diazotisation to a flow setup, a precipitate formed in the diazotisation coil due to the limited solubility of the diazonium salt in the aqueous solution (Table 2.1, entry 1). Changing the solvent to MeCN and using isoamyl nitrite as the diazotisation agent solved this problem and no precipitate was observed during the diazotisation (entry 2). When the diazonium salt was intercepted with piperidine and an aqueous potassium carbonate solution a precipitate was again observed (entry 3). This is probably due to the diazonium salt not being soluble enough in the aqueous solution. Investigation of different bases (entry 4-7) in a batch flask showed that organic bases in acetonitrile did afford a homogenous reaction mixture. The reaction was monitored using ^{19}F NMR and showed that the triazene was formed in all cases. However, when using triethylamine as a base, a complex reaction mixture was formed (entry 6). This is in congruence with the observation by Lazny *et al.* that triethylamine decomposes diazonium salts via the evolution of nitrogen.^[4a] The reaction proceeded well using excess piperidine (entry 7) so it was decided to use the secondary amine both as reagent and sacrificial base. The adaption to the flow process performed smoothly and triazene **27** was obtained in 48% yield (entry 8).

Table 2.1: Screening of Flow Compatible Conditions

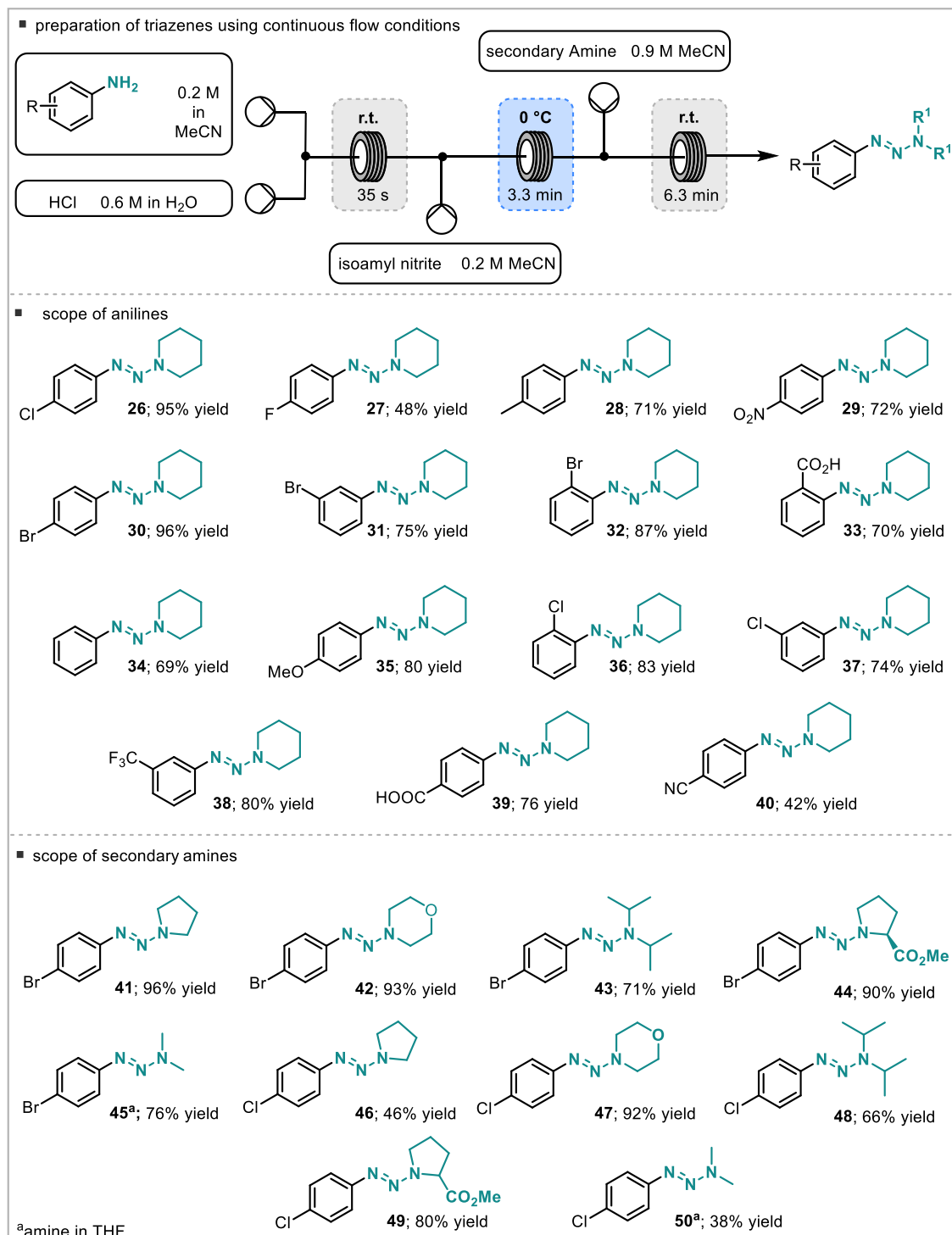
entry	setup	nitrite source / solvent	sacrificial base / solvent	observations
1	flow	NaNO ₂ in H ₂ O	-	precipitate in 2nd coil
2	flow	isoamyl nitrite in MeCN	-	no precipitate
3	flow	isoamyl nitrite in MeCN	K ₂ CO ₃ in H ₂ O	precipitate in 3rd coil
4	batch	isoamyl nitrite in MeCN	NaHCO ₃ in H ₂ O	no precipitate - triazene formed
5	batch	isoamyl nitrite in MeCN	Et ₃ N in MeCN	no precipitate - complex mixture
6	batch	isoamyl nitrite in MeCN	DMAP in MeCN	no precipitate - triazene formed
7	batch	isoamyl nitrite in MeCN	piperidine in MeCN	no precipitate - triazene formed
8	flow	isoamyl nitrite in MeCN	piperidine in MeCN	no precipitate - triazene formed - 48% yield

With working conditions in hand, the scope of the reaction was investigated for both the aniline and the secondary amine component (Scheme 2.7).

The reaction proceeded well giving good to excellent yields for a range of substituted anilines with piperidine as secondary amine. Halogens in *ortho*, *meta* and *para* position (**26**, **27**, **30-32**, **36**, **37**), electron rich (**28**, **35**) and electron poor aromatics (**29**, **33**, **38-40**) were tolerated. Electron poor aromatics such as *p*-F, *p*-NO₂, *p*-COOH and *p*-CN (**27**, **29**, **39**, **40**) gave slightly lower yields. This is probably due to a competing S_NAr reaction where the piperidine acts as a nucleophile on the aromatic ring of the diazonium salt, releasing nitrogen gas. In fact, for those examples small amounts of outgassing leading to segments of gas in the flow system could be observed. Notably, the triazene derived from anthranilic acid (**33**) could be isolated in 70% yield. The diazonium salt of anthranilic

acid is known to be particularly unstable due to the possibility of losing nitrogen and carbon dioxide to form benzyne (see Chapter 4).

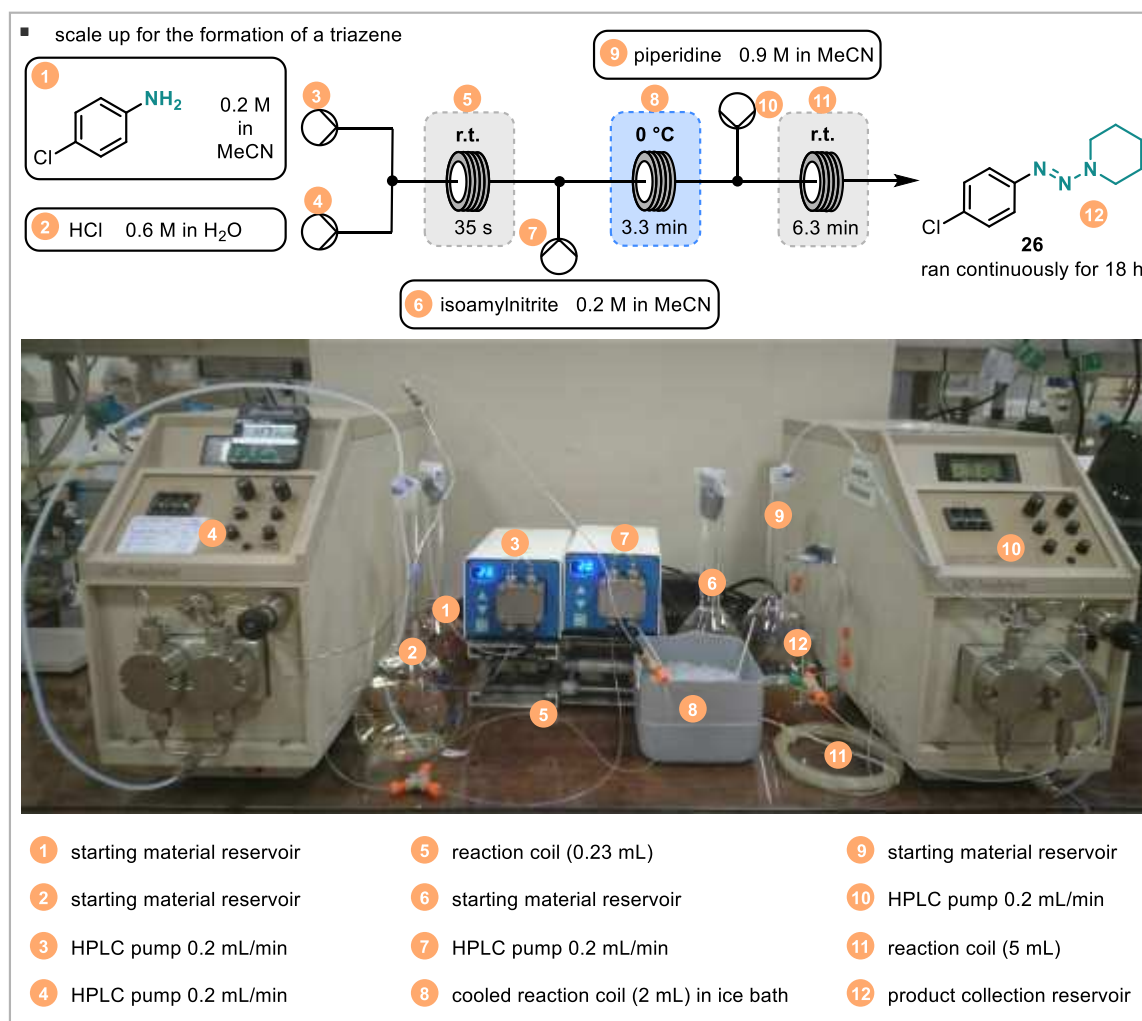
Importantly, none of these examples led to fouling or clogging proving that the developed conditions were widely applicable for the scale tested (1 mmol, 45 min run per experiment including steady state and collection).



Scheme 2.7: Substrate Scope of Triazenes in Flow

Next, the scope of secondary amines was investigated using both *p*-bromo and *p*-chloro aniline. Notably, again no fouling or clogging was observed across a variety of substrates. It was found, that piperidine (**26**, **30**), pyrrolidine (**41**, **46**), morpholine (**42**, **47**), diisopropylamine (**43**, **48**), *S*-proline methylester (**44**, **49**) and dimethylamine (**45**, **50**) could be incorporated. Importantly, dimethylamine was supplied as a solution in THF; the solvent change was compatible with the system.

Finally, the scale up of a triazene synthesis was performed (Scheme 2.8). Due to the limited stability of diazonium salts, the scale up of triazene syntheses in batch can be problematic. The increased reaction control and the fact that only limited amount of hazardous intermediate is present at any point in time makes the reaction inherently safer under continuous flow conditions. The reactants were pumped directly from solvent reservoirs using HPLC pumps. Example **26** with *p*-chloroaniline and piperidine as starting materials was chosen. The process was run continuously for 18 h without any problems. For the first hour, the output was collected and 92% of the triazene **26** was isolated. After that, the triazene was not isolated but the output was only regularly checked for quality due to increased downstream processing.



Scheme 2.8: Scale up for the Synthesis of Triazene 26

2.2 Stability and DSC

DSC measurements for a range of triazenes and their corresponding tetrafluoroborate diazonium salts were obtained for direct comparison of their stability (Scheme 2.9). The spectra were recorded from 40 °C to 200 °C with a gradient of 20 °C/min. A typical DSC spectrum is shown in Figure 2.3. Endothermic processes, such as melting, have a negative heat flow and exothermic processes, such as the decomposition have a positive heat flow. For each process the energy can be calculated from the sample mass and the area under the peak. The onset temperature is calculated from where the tangent of the highest slope meets the interpolated baseline. The onset temperature is independent of the method and sample mass and is used for comparison between experiments instead of the peak temperature or the start of a process temperature.

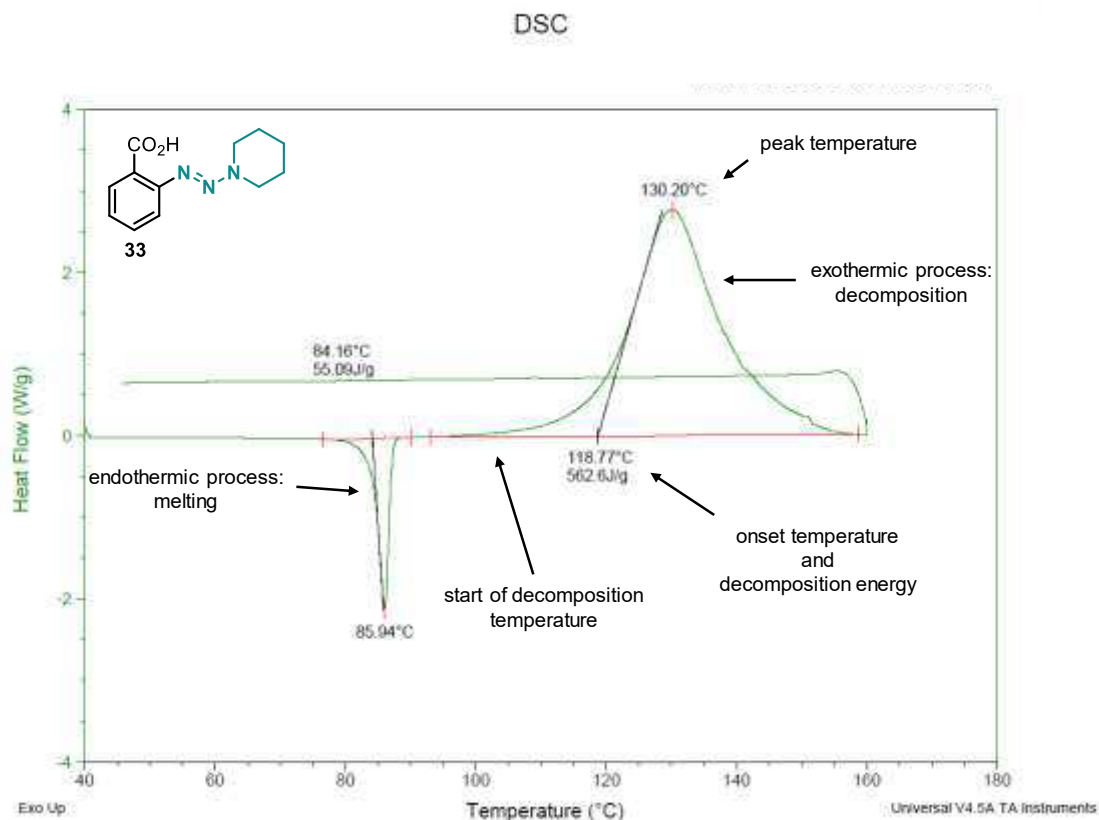


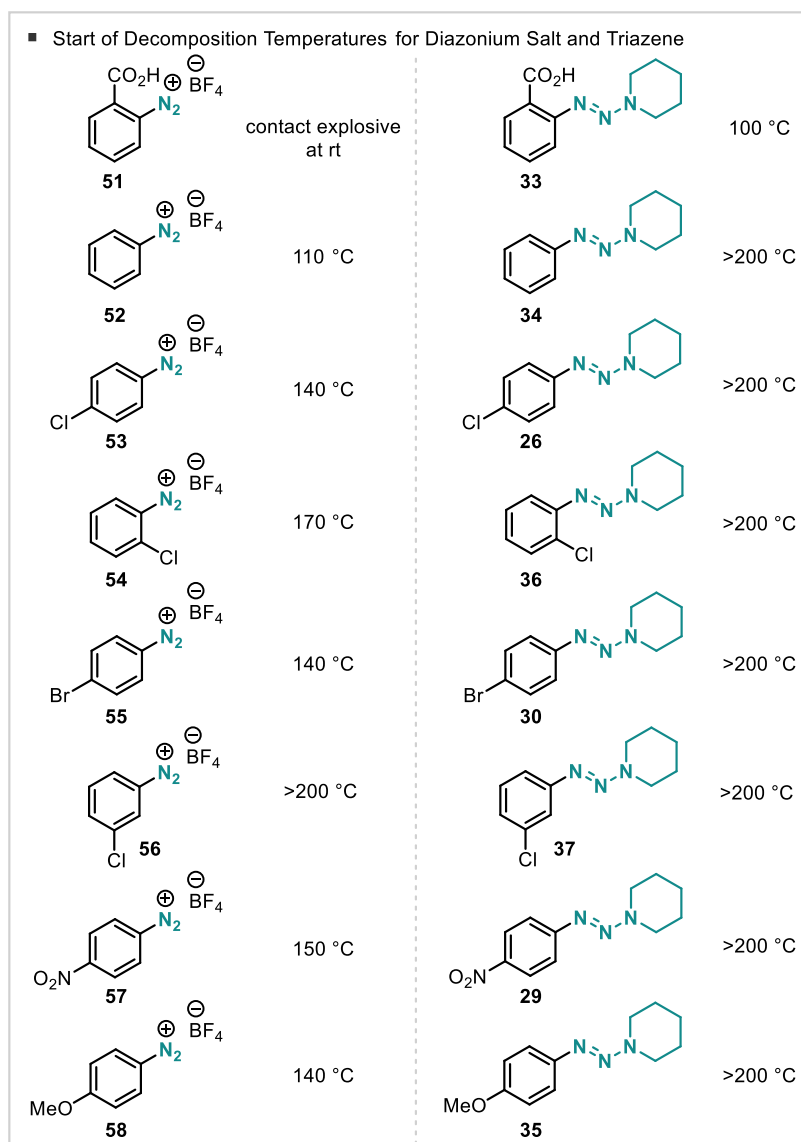
Figure 2.2: DSC of the Triazene 33 Derived from Anthranilic Acid

The diazonium salt **51** derived from anthranilic acid was not prepared as it is reported a contact explosive when dry (see Chapter 4). Notably, the corresponding triazene **33** could be readily isolated as a bench stable solid. The DSC (Figure 2.3) shows first an endothermic process (55 J/g) with an onset temperature of 84 °C and then a broad exothermic process (562 J/g) with an onset temperature of 119 °C and a peak temperature of 130 °C. The decomposition process starts at about 100 °C. The processes likely correspond to melting and decomposition of the sample. Despite the released energy during decomposition being 10 times bigger than the energy required for melting, the broad shape indicates that it is not a thermal runaway or sudden energy release as the heating rate does not accelerate.

For some of the compounds the melting range and the decomposition range overlapped which meant no accurate onset temperature or decomposition energy could be calculated. Instead the temperature where the decomposition starts is given for all compounds. This is valid as the spectra were all measured using the same heating rate and sample masses were approximately the same.

In addition to triazene **33**, unsubstituted triazene (**34**), triazenes with halogens in different positions (**26**, **30**, **37**, **38**), an electron poor-triazene (**29**) and an electron-rich triazene (**35**) were investigated. None of the other triazenes decomposed in the temperature

range tested (40 °C to 200 °C) whilst all the diazonium salts, except for *m*-chloro substituted one did. Notably, the *p*-nitro benzene diazonium tetrafluoroborate (**57**) decomposed with a particularly sudden energy release, that accelerated the heating rate of the DSC measurement showing a very sharp peak that is bent towards higher temperatures (Figure 2.3).



Scheme 2.9: Start of Decomposition Temperatures for Diazonium Salt and Corresponding Triazene

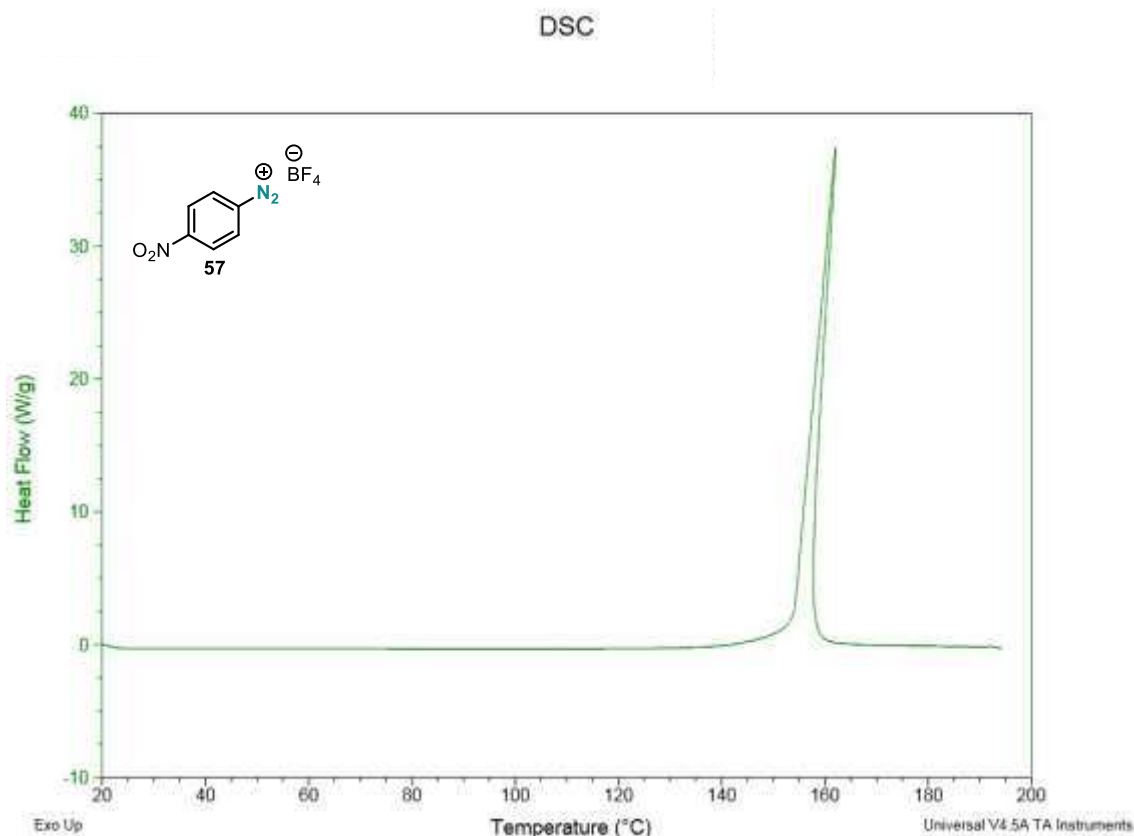
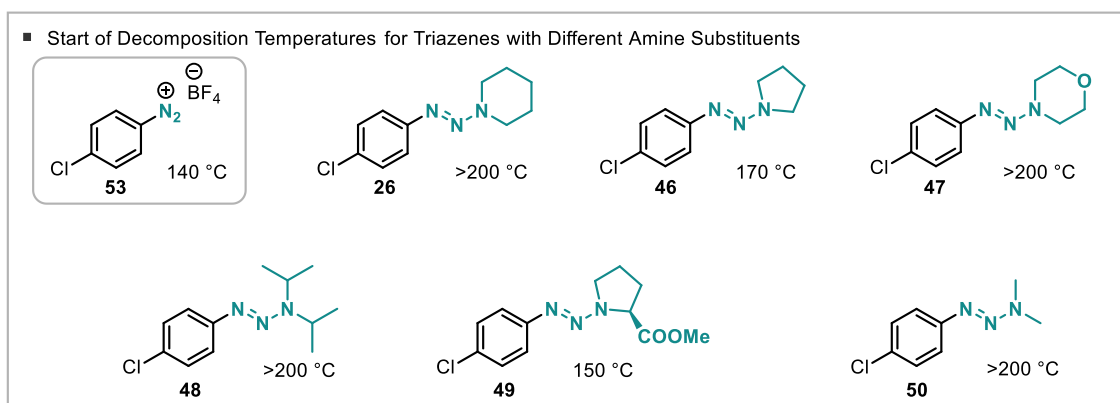


Figure 2.3: DSC of Diazonium Salt 57 with Sudden Energy Release

The DSCs for the triazenes of *p*-chloroaniline and a range of different secondary amines were compared (Scheme 2.10). The measurements show, that the secondary amine has an influence on the stability of the triazene. The triazenes from pyrrolidone **46** and proline methyl ester **49** decomposed at 170 and 150 °C, whereas all the other triazenes were stable within the temperature range. The triazene from proline methyl ester **49** exhibits a bulkier substituent which could influence the stability. However, the isopropyl-substituted triazene **48** does not decompose within the range measured. Triazenes **46** and **49** have the five-membered ring in common. This phenomenon will be investigated further.



Scheme 2.10: Start of Decomposition Temperatures for Triazenes with Different Amine Substituents

The comparison of DSC spectra for diazonium salts and their corresponding triazene clearly shows, that the triazenes are indeed more stable. The substitution on the aromatic ring can highly influence the stability, however for the triazenes tested only triazene **33** derived from anthranilic acid decomposed in the temperature range tested (40 – 200 °C). The nature of the secondary amine also has an influence on the stability, the two triazenes derived from the five-membered ring amines decomposed below 200 °C.

2.3 Restricted Rotation and VT NMR Results

Restricted rotation was observed in all NMR spectra for the prepared triazenes, spectra were obtained at -30, 20 and 50 °C. In ^1H spectra, the protons on the secondary amine usually gave only broad signals. In ^{13}C NMR the carbons on the secondary amine gave sharp, broad or no signal at all. In ^{13}C NMR the signals could be most effectively influenced by VT NMR thus ^{13}C NMR was used to display the restricted rotation. The linear Hammett trend could be confirmed, with electron poor aromatics giving high, electron neutral intermediate and electron rich aromatics giving low coalescence temperatures.

For the electron poor aromatic triazene **29** the piperidyl carbon peaks are all inequivalent at low temperatures and thus five peaks are visible in the spectrum at -30 °C. Upon heating, the signals broaden and coalesce until they are not visible in the spectra at 20 and 50 °C (Figure 2.4).

In the spectra for the electron neutral aromatic triazene **26** the peaks are broad at the low temperature (Figure 2.5). The peaks have coalesced and are not visible, whilst one broad peak appears at the high temperature. This indicates, that the coalescence temperature and rotational barrier energy is lower.

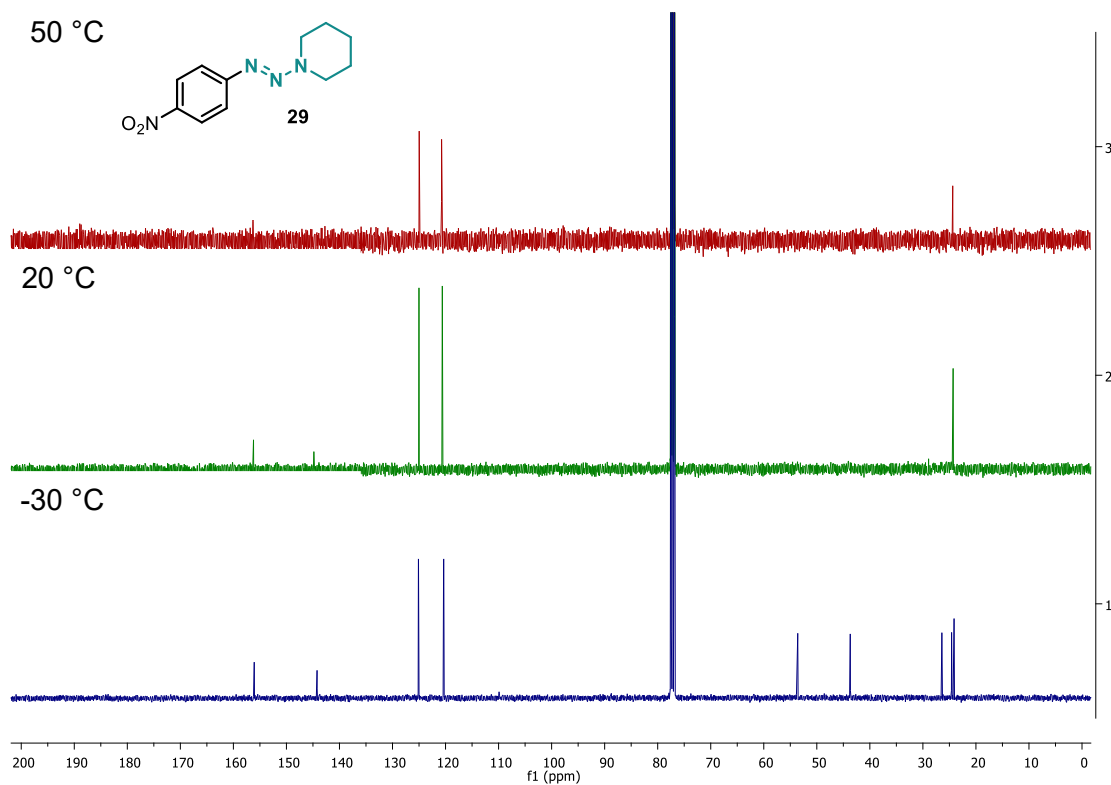


Figure 2.4: VT NMR for Electron Poor Triazene 29

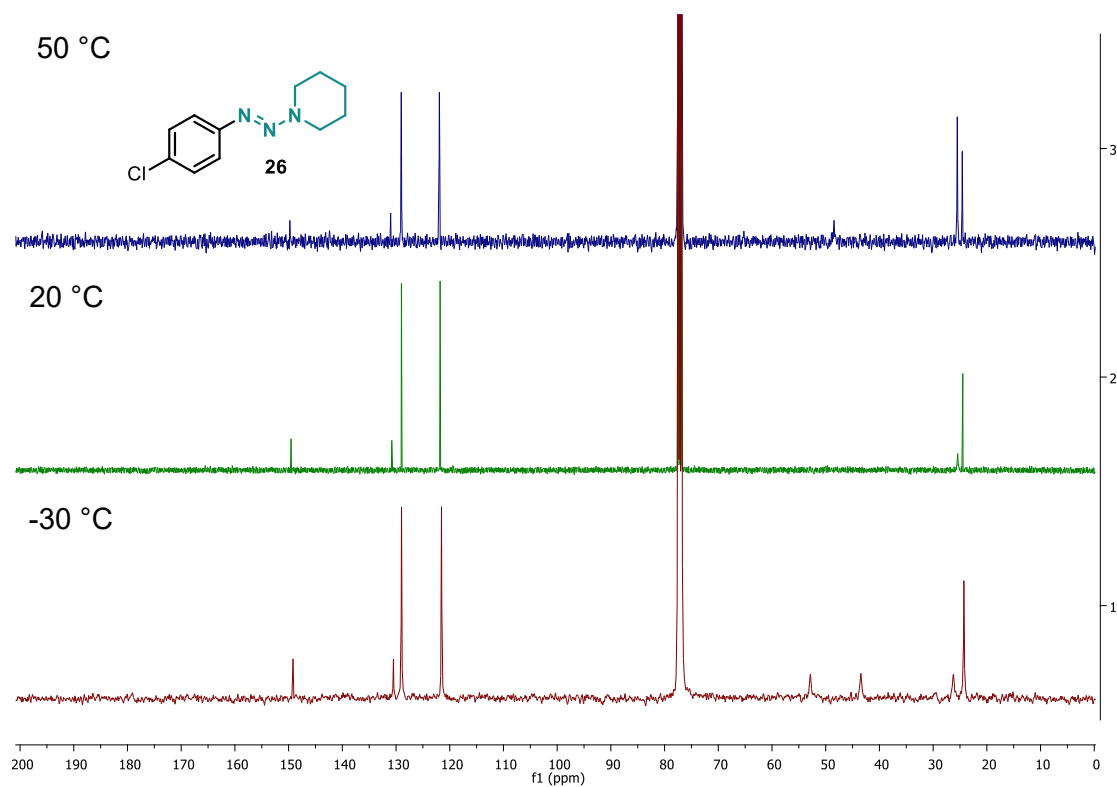


Figure 2.5: VT NMR for Electron Neutral Triazene 26

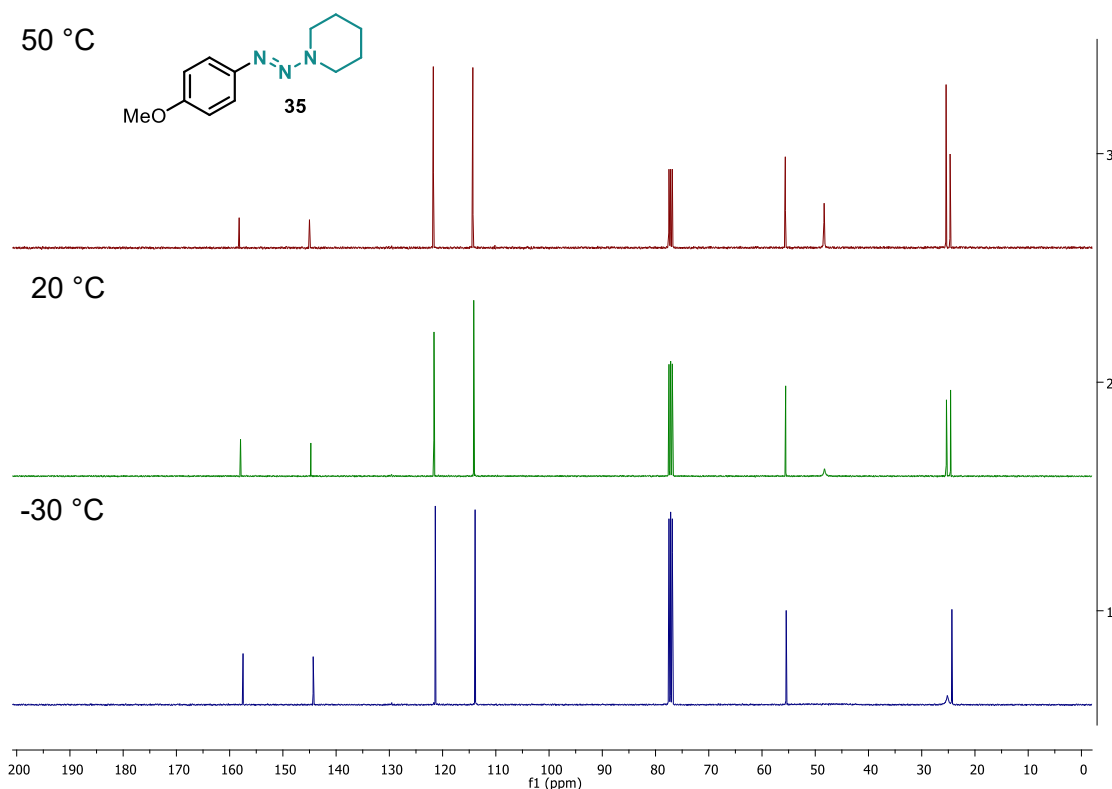
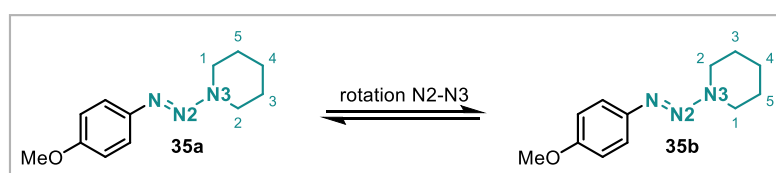


Figure 2.6: VT NMR for Electron Rich Triazene 35

The spectra for the electron rich aromatic triazene **35** show coalescence and non-visible piperidyl peaks at the lowest temperature (Figure 2.6). A broad peak then starts to be visible at room temperature which gets sharper upon heating to the higher temperature. Therefore, the coalescence temperature and rotational barrier are lowest for this example.

For one example a detailed analysis is performed in the temperature range from -60 to 50 °C, the maximum range for the solvent CDCl₃, taking NMR spectra at every 10 °C. The triazene **35**, 1-((4-methoxyphenyl)diazenyl) piperidine was chosen (Scheme 2.11, Figure 2.7) as it was to be expected to reach both the high and low limit within the temperature range possible with CDCl₃ (-60 °C to 50 °C).

The exchange rate regimes were determined (Figure 2.8) using the signals for C¹ (A) and C² (B) and the exchange rates calculated.



Scheme 2.11: Rotation around N2-N3 Bond for 1-((4-methoxyphenyl)diazenyl)piperidine (35)

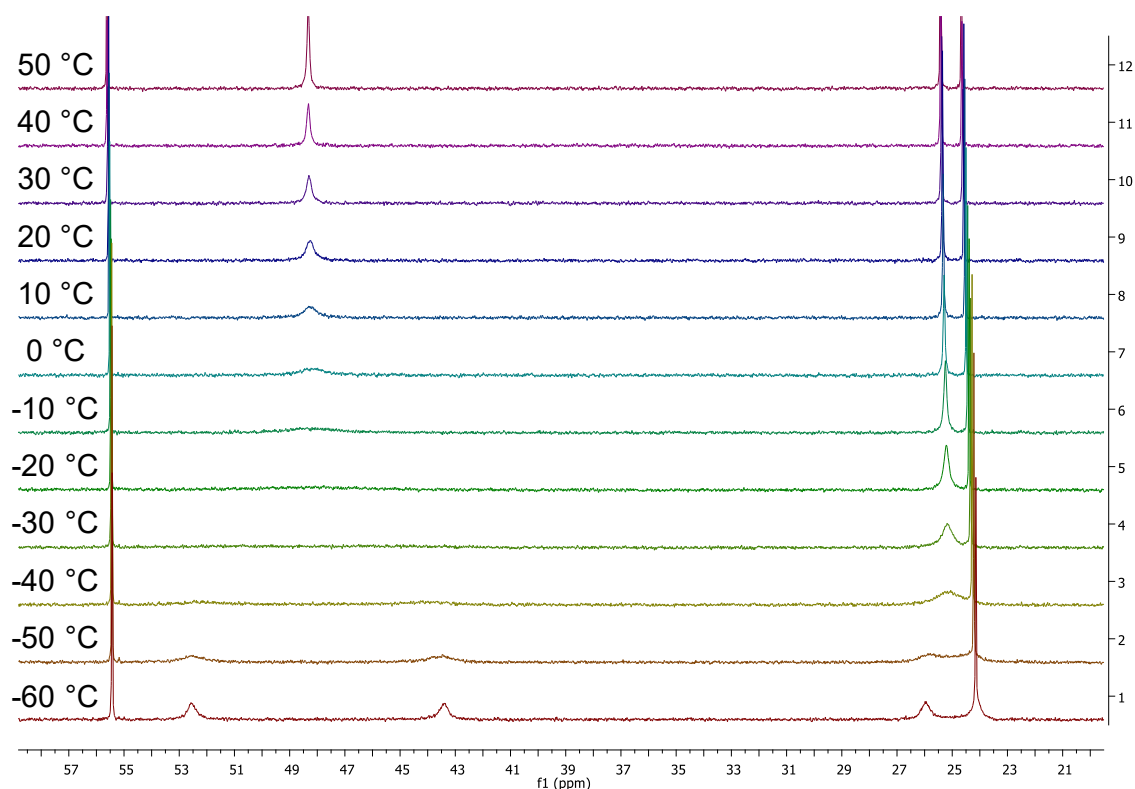


Figure 2.7: VT NMR for 1-((4-methoxyphenyl)diazenyl)piperidine (35), Zoom on Aliphatic Signals C¹-C⁵

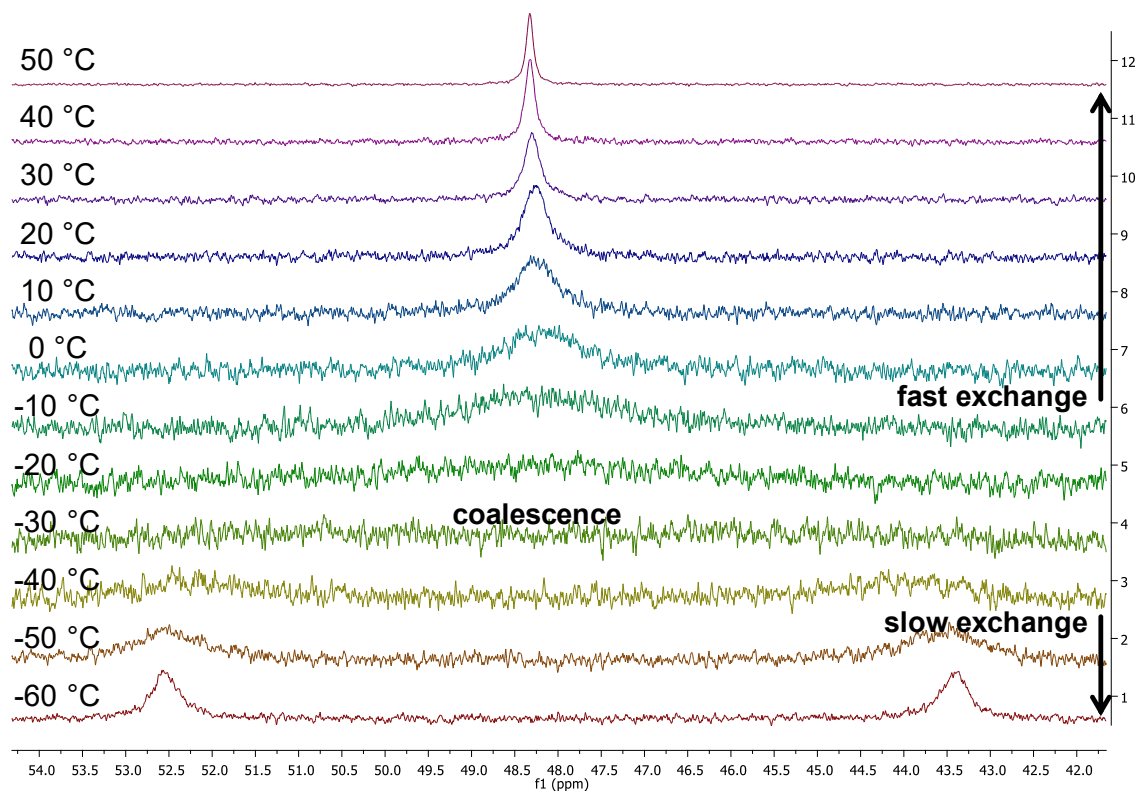


Figure 2.8: VT NMR for 1-((4-methoxyphenyl)diazenyl)piperidine (35), Zoom on Aliphatic Signals C¹ (A) and C² (B) with Exchange Rate Regimes

The exchange rate regimes were estimated to be: -60 °C - -40 °C slow exchange, -30 °C coalescence, -20 °C – 50 °C fast exchange. The line widths were calculated using the Bruker software topspin 3.5 (Table 2.2). Due to some peaks being poorly resolved, not all line widths could be determined.

Using the line width method (see Introduction, 1.2) the exchange rates were determined.

The positions of peak A and B in Hz at low limit were obtained from the spectrum at -60 °C:

$$\delta_{A,0} = 5310 \text{ Hz}$$

$$\delta_{B,0} = 4379 \text{ Hz}$$

The natural line width was determined from the highly resolved methoxy peak:

$$\Delta\nu_{A,n} = 2.02 \text{ Hz}$$

From the line width in each spectrum the rate constants could be calculated (Table 2.2). These were then used in an Arrhenius plot (Figure 2.9). The exchange rate at the point of coalescence is an outlier so that it was not taken into account for the trendline. From the slope (m) of the trendline the activation energy was calculated.

$$E_A = -m \cdot R$$

$$E_A = 46.8 \pm 2.4 \text{ kJmol}^{-1}$$

Table 2.2: Exchange Rate Calculations

temperature [°C]	exchange rate regime -	$\Delta\nu_{A,T}$ [Hz]	$\Delta\Delta\nu$ [Hz]	exchange rate [s ⁻¹]
-20	fast	825.815	823.80	1650
-10	fast	461.293	459.27	2959
0	fast	133.723	131.70	10320
10	fast	54.401	52.38	25948
20	fast	34.721	32.70	41564
30	fast	21.232	19.21	70747
40	fast	13.89	11.87	114507
50	fast	9.75	7.73	175834

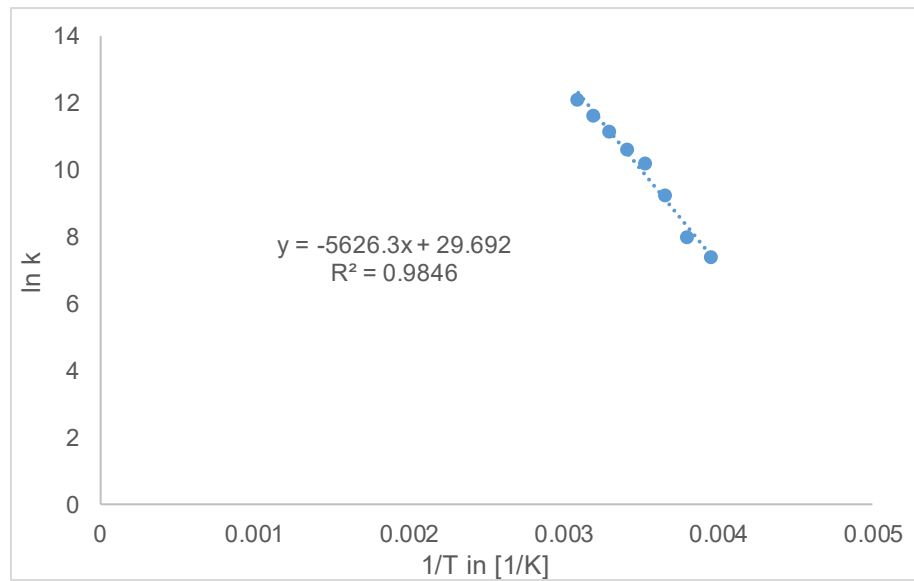


Figure 2.9: Arrhenius Plot

The coalescence temperature was estimated by plotting the activation energy vs coalescence temperature in the estimate (Figure 2.11).

$$E_A = RT_C \left[22.96 + \ln \frac{T_C}{\nu_{A,0} - \nu_{B,0}} \right]$$

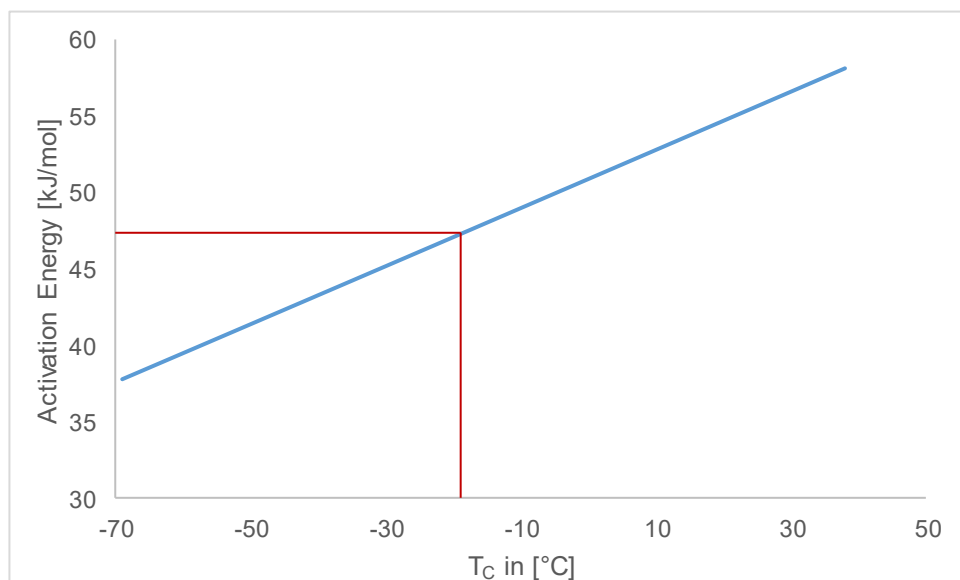


Figure 2.10: Determination of the Coalescence Temperature

The coalescence temperature was determined as $-22\text{ }^{\circ}\text{C}$. This is in congruence with the observations made in the spectra.

The coalescence temperature and the calculated activation energy are comparable to the values reported by Akhtar and co-workers for the dimethylamine triazene ($T_{\text{C}} = -44\text{ }^{\circ}\text{C}$, 31.0 kJmol^{-1})^[28] and by Foster and co-workers for the pyrrolidine triazene ($T_{\text{C}} = -19\text{ }^{\circ}\text{C}$, 50.2 kJmol^{-1}).^[32]

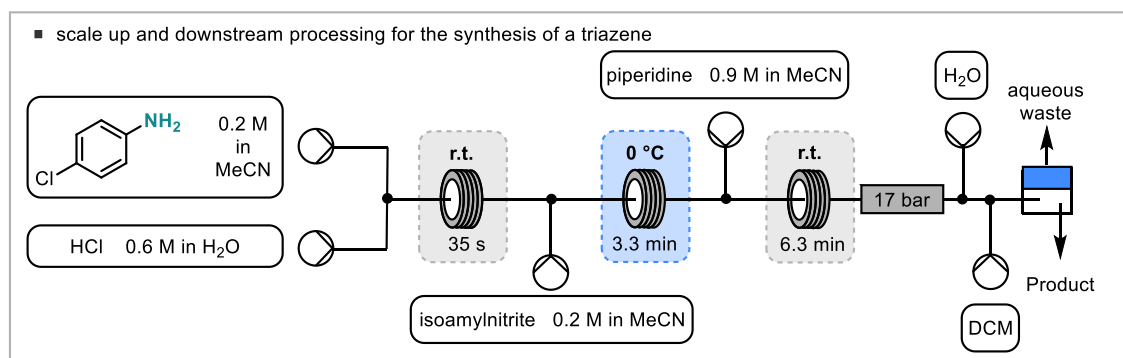
3 Conclusion and Outlook

The continuous flow synthesis of triazenes was developed and demonstrated in the synthesis of 26 examples. Both a range of anilines and secondary amines were tolerated in the reaction process. The scope of the process was further extended by the scale up of one reaction that was run continuously for 18 h without any problems due to fouling or clogging.

A range of triazenes were then investigated further for their stability. DSC spectra were recorded and compared to the DSC spectra of their corresponding diazonium salts. In all cases, the triazenes were significantly more stable. The direct comparison of triazenes and diazonium salts has not been demonstrated in the literature previously.

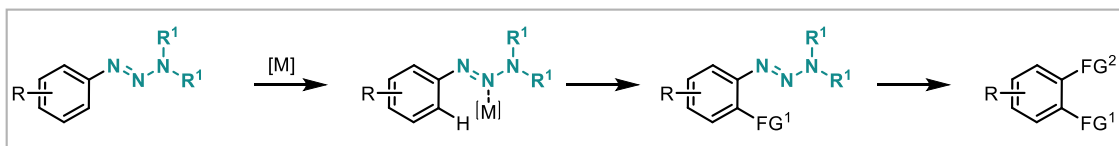
Finally, the restricted rotation around the N2-N3 bond in triazenes was investigated. The activation energy and the coalescence temperature for one example (**35**) was calculated using the line width method. The coalescence temperature and activation energy are in congruence with previously reported values for similar compounds.

Future work could include the incorporation of *in line* downstream processing in a scale up reaction (Scheme 2.12). This could then enable the continuous production of triazenes on large scale.



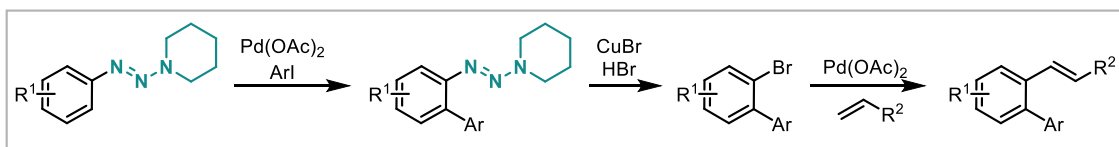
Scheme 2.12: Scale Up and Downstream Processing for the Synthesis of a Triazene

Synthesised triazenes could be used to investigate further reactions as traceless directing groups in C-H activation catalysis (Scheme 2.13). In the event, a metal catalysed C-H activation would install a first functional group (FG¹) and removal of the triazene moiety would install a second functional group (FG²).



Scheme 2.13: The Use of Triazenes for Metal Catalysed C-H Activation

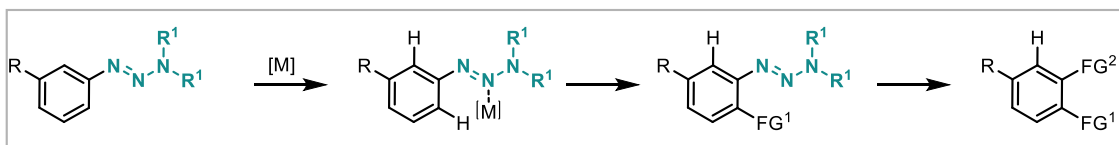
Yu and co-workers have recently demonstrated the use of hydrazones for the *ortho* C-H activation and have demonstrated palladium catalysed arylations, halogenations and iridium catalysed amidations.^[35] Similar to hydrazones, triazenes could be used as a traceless directing group for those reactions. A triazene could be arylated in the first step, the triazene moiety then removed to form the bromide, which could then be further functionalised in a Heck reaction to the aryl olefin (Scheme 2.14). This would afford *ortho* aryl olefins without a directing group remaining in the molecule.



Scheme 2.14: Synthesis of *ortho* Aryl Olefins Using Triazenes as Traceless Directing Groups

The stability of triazenes in correlation to their molecular structure could be further investigated. Key to realising this would be extended DSC measurements to higher temperatures. This would enable the determination of decomposition temperatures. The comparison of accurate decomposition temperatures could show structure relations. The effect of the secondary amine substituent could be further investigated. It was found in this thesis that the five-membered ring examples had a lower decomposition temperature. This observation could be further investigated by extending the scope to more five-membered ring amines.

The restricted rotation in triazenes could be used for the regioselective functionalisation in unsymmetric molecules (Scheme 2.15).



Scheme 2.15: Regioselective C-H Functionalisation due to Restricted Rotation in Triazenes

When using a triazine with a low rotational barrier the *ortho* positions are equivalent and no regioselectivity would be observed. The use of a triazine with a high rotational barrier would make the *ortho* positions inequivalent and regioselectivity possible.

4 References

- [1] D. H. Sieh, D. J. Wilbur, C. J. Michejda, *J. Am. Chem. Soc.* **1980**, *102*, 3883-3887.
- [2] G. Kiefer, T. Riedel, P. J. Dyson, R. Scopelliti, K. Severin, *Angew. Chem. Int. Ed.* **2015**, *54*, 302-305.
- [3] H. Jian, J. M. Tour, *J. Org. Chem.* **2005**, *70*, 3396-3424.
- [4] a) R. Lazny, M. Sienkiewicz, S. Bräse, *Tetrahedron* **2001**, *57*, 5825-5832; b) M. L. Gross, D. H. Blank, W. M. Welch, *J. Org. Chem.* **1993**, *58*, 2104-2109; c) R. Lazny, J. Poplawski, J. Köbberling, D. Enders, S. Bräse, *Synlett* **1999**, *8*, 1304-1306.
- [5] C.-Y. Liu, P. Knochel, *J. Org. Chem.* **2007**, *72*, 7106-7115.
- [6] a) T. B. Patrick, T. Juehne, E. Reeb, D. Hennessy, *Tetrahedron Lett.* **2001**, *42*, 3553-3554; b) Z. Wu, J. S. Moore, *Tetrahedron Lett.* **1994**, *35*, 5539-5542; c) J. S. Moore, E. J. Weinstein, Z. Wu, *Tetrahedron Lett.* **1991**, *32*, 2465-2466; d) N. D. Heindel, M. Van Dort, *J. Org. Chem.* **1985**, *50*, 1988-1990.
- [7] H. Ku, J. R. Barrio, *J. Org. Chem.* **1981**, *46*, 5239-5241.
- [8] M. Barbero, I. Degani, N. Diulgheroff, S. Dughera, R. Fochi, *Synthesis* **2001**, *14*, 2180-2190.
- [9] a) M. Lormann, S. Dahmen, S. Bräse, *Tetrahedron Lett.* **2000**, *41*, 3813-3816; b) N. Satyamurthy, J. R. Barrio, G. T. Bida, M. E. Phelps, *Tetrahedron Lett.* **1990**, *31*, 4409-4412.
- [10] W. Li, X.-F. Wu, *Org. Lett.* **2015**, *17*, 1910-1913.
- [11] a) T. Saeki, E.-C. Son, K. Tamao, *Org. Lett.* **2004**, *6*, 617-619; b) T. Saeki, T. Matsunaga, E.-C. Son, K. Tamao, *Adv. Synth. Catal.* **2004**, *346*, 1689-1692.
- [12] a) T. B. Patrick, R. P. Willaredt, D. J. DeGonia, *J. Org. Chem.* **1985**, *50*, 2232-2235; b) A. P. Colleville, R. A. J. Horan, S. Olazabal, N. C. O. Tomkinson, *Org. Process Res. Dev.* **2016**, *20*, 1283-1296.
- [13] C. Zhu, M. Yamane, *Org. Lett.* **2012**, *14*, 4560-4563.
- [14] a) A. Hafner, S. Bräse, *Adv. Synth. Catal.* **2013**, *355*, 996-1000; b) A. Hafner, T. J. Feuerstein, S. Bräse, *Org. Lett.* **2013**, *15*, 3468-3471; c) A. Hafner, A. Bihlmeier, M. Nieger, W. Klopper, S. Bräse, *J. Org. Chem.* **2013**, *78*, 7938-7948.
- [15] a) S. Bräse, S. Dahmen, M. Pfefferkorn, *J. Comb. Chem.* **2000**, *2*, 710-715; b) F. Avemaria, V. Zimmermann, S. Bräse, *Synlett* **2004**, *7*, 1163-1166; c) J. C. Nelson, J. K. Young, J. S. Moore, *J. Org. Chem.* **1996**, *61*, 8160-8168; d) S. Bräse, M. Schroen, *Angew. Chem. Int. Ed.* **1999**, *38*, 1071-1073; e) S. Bräse, D.

- Enders, J. Köbberling, F. Avemaria, *Angew. Chem. Int. Ed.* **1998**, *37*, 3413-3415; f) S. Bräse, J. Köbberling, D. Enders, R. Lazny, M. Wang, S. Brandtner, *Tetrahedron Lett.* **1999**, *40*, 2105-2108; g) L. Jones, J. S. Schumm, J. M. Tour, *J. Org. Chem.* **1997**, *62*, 1388-1410; h) J. L. Hudson, H. Jian, A. D. Leonard, J. J. Stephenson, J. M. Tour, *Chem. Mater.* **2006**, *18*, 2766-2770; i) B. Chen, A. K. Flatt, H. Jian, J. L. Hudson, J. M. Tour, *Chem. Mater.* **2005**, *17*, 4832-4836; j) M. Döbele, S. Vanderheiden, N. Jung, S. Bräse, *Angew. Chem. Int. Ed.* **2010**, *49*, 5986-5988; k) S. Bräse, S. Dahmen, *Chem. Eur. J.* **2000**, *6*, 1899-1905; l) S. Bräse, *Acc. Chem. Res.* **2004**, *37*, 805-816.
- [16] a) D. L. Hooper, I. R. Pottie, M. Vacheresse, K. Vaughan, *Can. J. Chem.* **1998**, *76*, 125-135; b) J. S. Moore, *Acc. Chem. Res.* **1997**, *30*, 402-413.
- [17] a) M. J. Wanner, M. Koch, G.-J. Koomen, *J. Med. Chem.* **2004**, *47*, 6875-6883; b) D. Farquhar, J. Benvenuto, *J. Med. Chem.* **1984**, *27*, 1723-1727.
- [18] a) C. Wang, H. Sun, Y. Fang, Y. Huang, *Angew. Chem. Int. Ed.* **2013**, *52*, 5795-5798; b) H. T. Dao, P. S. Baran, *Angew. Chem. Int. Ed.* **2014**, *53*, 14382-14386; c) C.-Y. Liu, P. Knochel, *Org. Lett.* **2005**, *7*, 2543-2546; d) M. E. P. Lormann, C. H. Walker, M. Es-Sayed, S. Bräse, *Chem. Commun.* **2002**, 1296-1297; e) A. Goeminne, P. J. Scammells, S. M. Devine, B. L. Flynn, *Tetrahedron Lett.* **2010**, *51*, 6882-6885; f) H. Sun, C. Wang, Y.-F. Yang, P. Chen, Y.-D. Wu, X. Zhang, Y. Huang, *J. Org. Chem.* **2014**, *79*, 11863-11872.
- [19] S. E. Reisman, J. M. Ready, M. M. Weiss, A. Hasuoka, M. Hirata, K. Tamaki, T. V. Ovaska, C. J. Smith, J. L. Wood, *J. Am. Chem. Soc.* **2008**, *130*, 2087-2100.
- [20] H. G. Ang, L. L. Koh, G. Y. Yang, *J. Chem. Soc., Dalton Trans.* **1996**, 1573-1581.
- [21] a) A. Hafner, S. Bräse, *Angew. Chem. Int. Ed.* **2012**, *51*, 3713-3715; b) C. Wang, H. Chen, Z. Wang, J. Chen, Y. Huang, *Angew. Chem. Int. Ed.* **2012**, *51*, 7242-7245.
- [22] F. Zhang, D. R. Spring, *Chem. Soc. Rev.* **2014**, *43*, 6906-6919.
- [23] a) C. A. Rouzer, M. Sabourin, T. L. Skinner, E. J. Thompson, T. O. Wood, G. N. Chmurny, J. R. Klose, J. M. Roman, R. H. Smith, C. J. Michejda, *Chem. Res. Toxicol.* **1996**, *9*, 172-178; b) C. Hejesen, L. K. Petersen, N. J. V. Hansen, K. V. Gothelf, *Org. Biomol. Chem.* **2013**, *11*, 2493-2497; c) F. Marchesi, M. Turriziani, G. Tortorelli, G. Avvisati, F. Torino, L. De Vecchis, *Pharmacol. Res.* **2007**, *56*, 275-287; d) T. Giraldi, T. Connors, G. Cartei, *Triazenes: Chemical, Biological, and Clinical Aspects*, Springer Science & Business Media, **2012**; e) C. S. Rondestvedt, S. J. Davis, *J. Org. Chem.* **1957**, *22*, 200-203; f) M. Julliard, G. Vernin, J. Metzger, *Synthesis* **1980**, *1980*, 116-117; g) A. Sonousi, D. Crich, *Org.*

- Lett.* **2015**, *17*, 4006-4009; h) C. May, C. J. Moody, *J. Chem. Soc., Chem. Commun.* **1984**, 926-927.
- [24] G. Höhne, W. F. Hemminger, H.-J. Flammersheim, *Differential Scanning Calorimetry*, 2 ed., Springer-Verlag Berlin Heidelberg, **2003**.
- [25] T. Lippert, A. Wokaun, J. Dauth, O. Nuyken, *Magn. Reson. Chem.* **1992**, *30*, 1178-1185.
- [26] S. A. Richards, J. C. Hollerton, *Essential practical NMR for organic chemistry*, John Wiley & Sons, **2010**.
- [27] O. Zerbe, S. Jurt, *Applied NMR spectroscopy for chemists and life scientists*, John Wiley & Sons, **2013**.
- [28] M. H. Akhtar, R. S. McDaniel, M. Feser, A. C. Oehlschlager, *Tetrahedron* **1968**, *24*, 3899-3906.
- [29] N. P. Marullo, C. B. Mayfield, E. H. Wagener, *J. Am. Chem. Soc.* **1968**, *90*, 510-511.
- [30] T. Axenrod, P. Mangiaracina, P. S. Pregosin, *Helv. Chim. Acta* **1976**, *59*, 1655-1660.
- [31] L. Lunazzi, G. Cerioni, E. Foresti, D. Macciantelli, *J. Chem. Soc., Perkin Trans. 2* 1978, 686-691.
- [32] N. Foster, B. Pestel, *Magn. Reson. Chem.* **1985**, *23*, 83-85.
- [33] M.-T. Nguyen, L. Hoesch, *Helv. Chim. Acta* **1986**, *69*, 1627-1637.
- [34] A. Zarei, L. Khazdooz, H. Aghaei, G. Azizi, A. N. Chermahini, A. R. Hajipour, *Dyes Pigm.* **2014**, *101*, 295-302.
- [35] X.-H. Liu, H. Park, J.-H. Hu, Y. Hu, Q.-L. Zhang, B.-L. Wang, B. Sun, K.-S. Yeung, F.-L. Zhang, J.-Q. Yu, *J. Am. Chem. Soc.* **2017**, *139*, 888-896.

Chapter 3 - Investigating the Formation of Indoles from Diazonium Salts

Table of Contents

1	Introduction.....	72
2	Results and Discussion	78
2.1	Method Adaption for the Synthesis of a Series of Fluorinated Pyrazoles	88
3	Conclusions and Outlook	90
4	References	94

1 Introduction

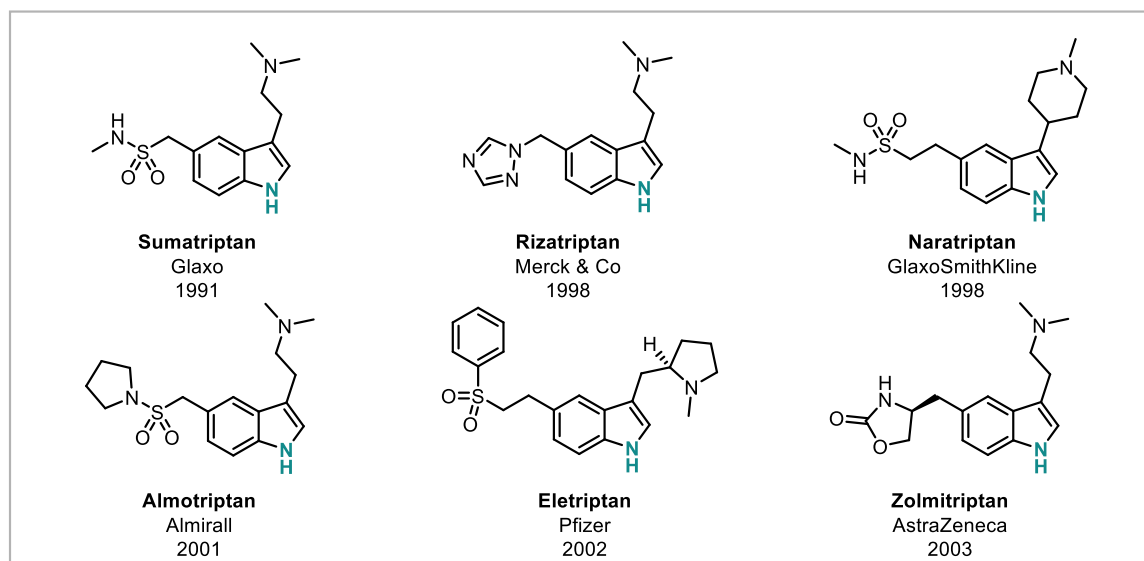
The automation of drug discovery is of particular interest for pharmaceutical industry and is a critical activity for the positive progression of our society and the improvement of the quality of life. Most new drugs can be classified as “follow-on” or “me-too” drugs as opposed to pioneer drugs. Pioneer drugs exhibit a new pharmacophore whereas “follow-on” or “me-too” drugs are analogues of the pioneer compound and are designed around the same pharmacophore.^[1] “Me-too” drugs are thereby developed in parallel to the pioneer drug but are marketed afterwards. They do not necessarily show improved properties. In contrast, “follow-on” drugs are always developed after the pioneer drug and show increased properties such as a lower dosing or weakened side effects.^[1] Their development is less risky for pharmaceutical companies opposed to the development of new pioneer drugs.^[2] In addition, pharmaceutical companies are interested in the ability to quickly introduce analogues of drugs to compete for a share of the market. Even though some experts see the development of those “follow-on” drugs as not driving forward innovation, this competition is raising the medical standard in society due to better availability (pricing) and improved properties of those drugs.^[3]

For the development of “follow-on” drugs, pharmaceutical companies have to be able to quickly make and screen analogues for their properties. Automation, computer control and the decreased handling operations that can be achieved under continuous flow conditions can benefit pharmaceutical companies in the discovery of those drugs.

In this work a hybrid machine (continuous flow – microwave) for the multistep synthesis (diazotisation, reduction, hydrolysis, cyclisation) of indoles was developed starting from commercially available anilines. Under continuous flow conditions, these anilines were converted into the diazonium salt and reduced to a masked hydrazine, an oxalyl hydrazide, with ascorbic acid and hydrolysed to the hydrazine. Fractions of the flow output were transferred into microwave vials preloaded with ketones to achieve the elevated temperatures necessary for the Fischer indole reaction in a robotic microwave. The machine enabled the safe synthesis and subsequent consumption (make and consume) of hazardous material within the continuous flow part and the automation of the diversification of a common stream of hydrazine into a library of indoles in a robotic microwave.

The Triptan drugs (5-HT agonists), which are used for migraine treatment and are an excellent example for a class of “follow-on” drugs (Scheme 3.1).^[4] Sumatriptan was the first triptan drug introduced in 1991 by Glaxo and is still in use for migraine treatment.^[5] Since then several other triptan drugs, with a few examples given here, have been introduced. Most triptan drugs are to date synthesised from the corresponding aniline via

a diazotisation, reduction, cyclisation sequence and they differ through the substituent on both the aromatic ring and the side chain of the ketone used.

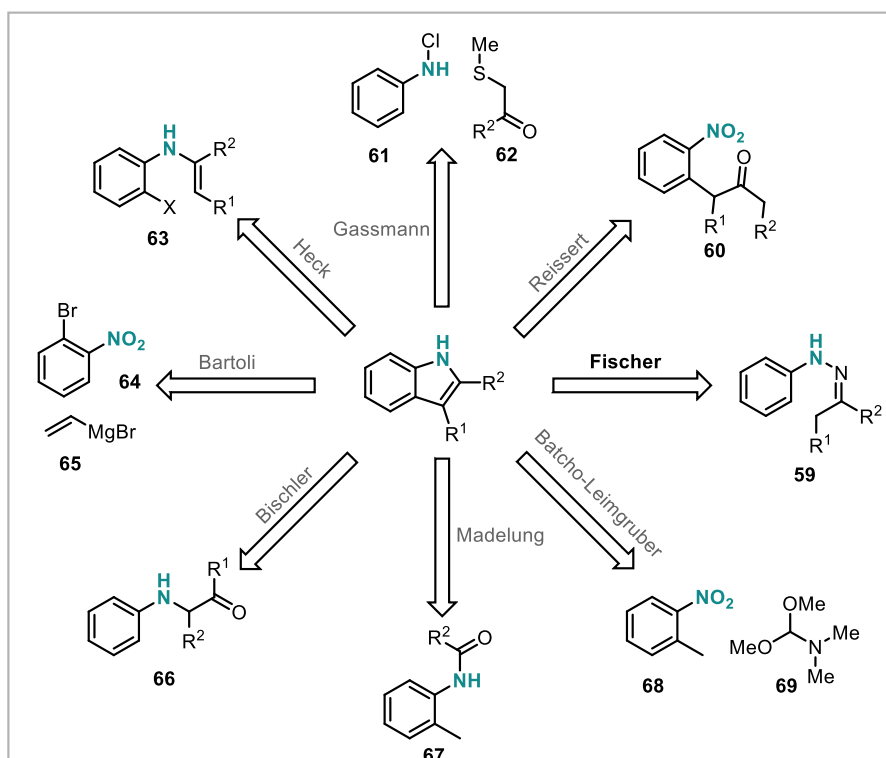


Scheme 3.1: Examples of Triptan Drugs

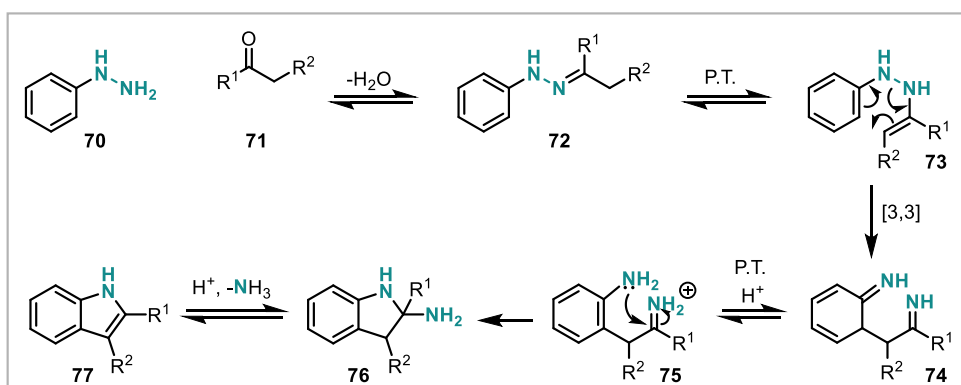
The synthesis of indoles in general, has been a subject of interest to the field of organic chemistry for many years due to their useful biological applications such as in agrochemical and pharmaceutical industry.^[6] Even though various syntheses are known, the Fischer indole reaction still remains one of the most important and is employed in various recent total syntheses, due its versatility.^[7] Other examples of named reactions for the formation of indoles are the Reissert, Gassmann, Heck, Bartoli, Bischler, Madelung and the Batcho-Leimgruber reaction (Scheme 3.2).^[8]

Other common syntheses involve transition-metals as catalysts that usually activate a C-H bond for the formation of pyrrole ring of the indole.^[9]

In the Fischer indole reaction a hydrazine (**70**) initially forms a hydrazine (**72**) with an enolizable ketone (**71**).^[10] After forming the enehydrazine (**73**), the new C-N bond is formed via a [3,3]-sigmatropic rearrangement. Rearomatisation and loss of ammonia as the byproduct forms the indole product (**77**). The Fischer indole reaction is usually performed by heating in the presence of an acid catalyst. Electron-donating substituents on the hydrazine increase the cyclisation rate, whereas electron-withdrawing substituents decrease the rate. The overall reaction rate can be increased by strongly acidic conditions as the reaction is acid catalysed (Scheme 3.3).



Scheme 3.2: Examples of Named Reactions to Form Indoles



Scheme 3.3: Fischer Indole Reaction

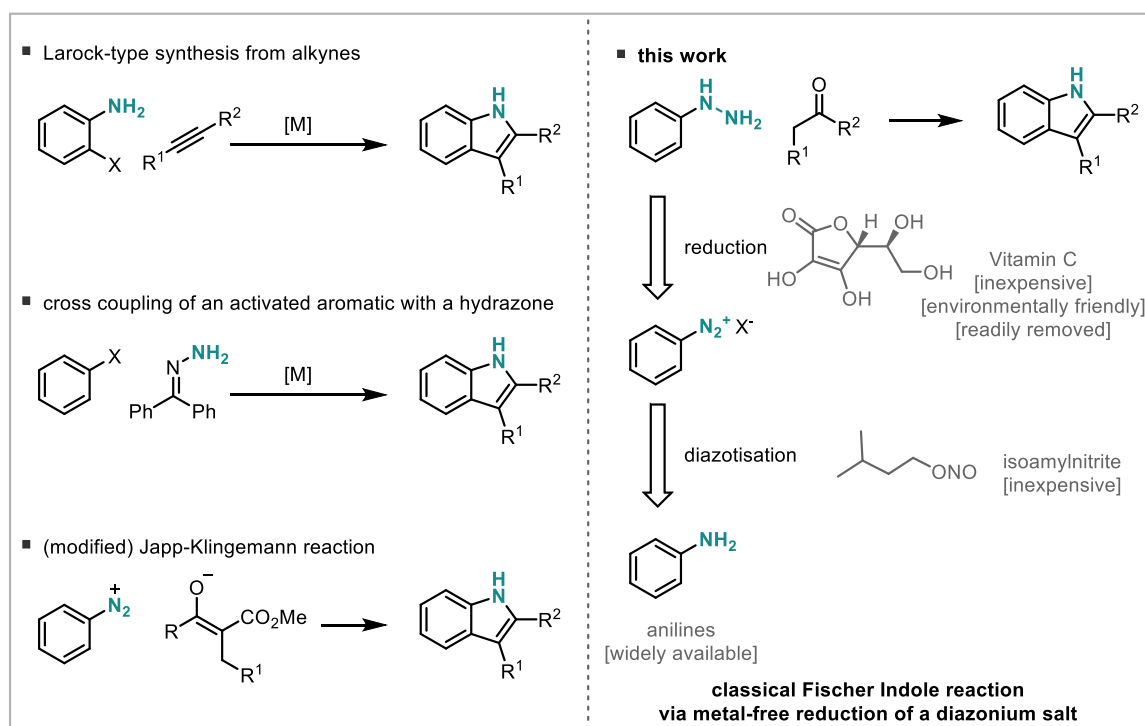
The Fischer indole synthesis is advantageous over other indole forming reactions, as the requisite starting materials are relatively trivial. In addition to the reaction with ketones, the reaction with cyclic enol ethers has been demonstrated.^[11]

However, the limited commercial availability of hydrazines limits the scope of the Fischer indole reaction. Therefore, other ways to access the key intermediate hydrazones and enehydrazines have been established (Scheme 3.4). These approaches are often referred to as ‘interrupted-Fischer’ syntheses.

The intermediate enehydrazines can be formed by a transition-metal catalysed hydroamination of alkynes in a Larock-type synthesis with different aromatic precursors such as anilines as starting materials.^[12]

Alternatively, the intermediate hydrazones can be formed by a transition-metal catalyzed cross coupling of activated aromatics and a different hydrazone such as benzophenone hydrazone.^[13] They can also be prepared in a modified Japp-Klingemann reaction.^[14] Alternatively the hydrazine can be formed prior to the Fischer indole reaction in an S_N2 reaction from hydrazine and an activated aromatic compound.

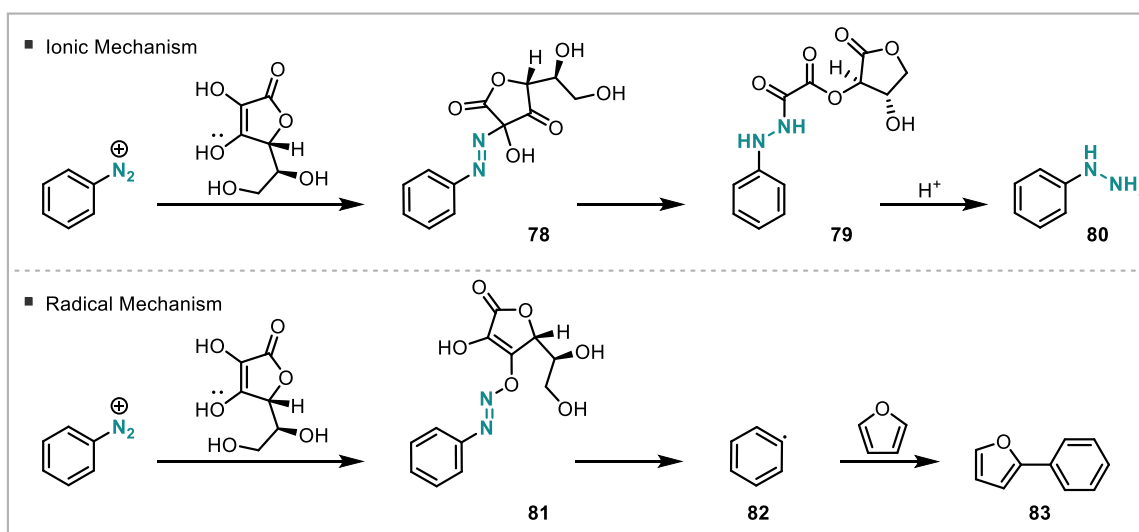
Hydrazines can also be prepared from the corresponding aniline via the reduction of the diazonium salt or, alternatively the *N*-nitroso derivative, with elemental tin, tin (II) chloride, or with elemental zinc, acetic acid, LiAlH₄ or sodium dithionite, respectively. The metal-free reduction of diazonium salts with ascorbic acid has recently been rediscovered.^[15]



Scheme 3.4: Access to the Starting Materials of the Fischer Indole Synthesis

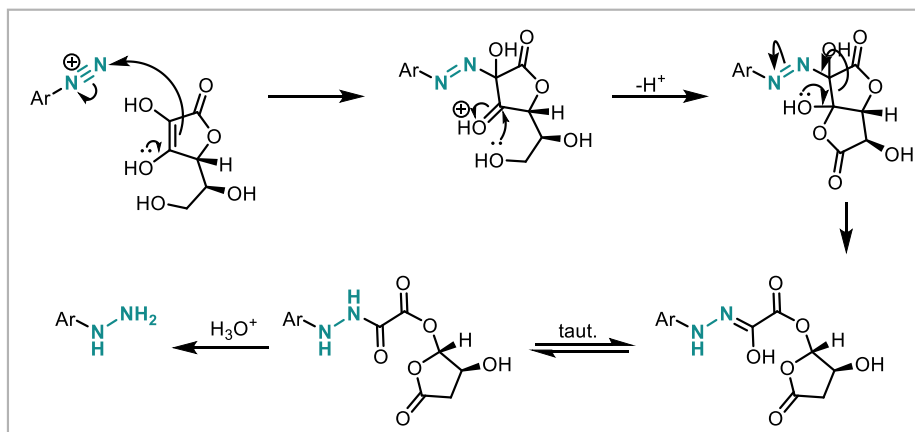
The reaction of diazonium salts with ascorbic acid was first reported by Doyle *et al.* in 1989.^[15a] Since then it has been studied in more detail and two main products have been reported: a diazoether (**81**) that can form aryl radicals and an oxalyl hydrazide (**79**) that can be hydrolysed to hydrazines (Scheme 3.5).^[15b-l] Backsheet *et al.* were the first who reported the oxalyl hydrazide (**79**) as a possible product in 1991 in the quantitative analysis of ascorbic acid in fruit juice.^[15c] Norris *et al.* were first to then use the oxalyl hydrazide (**79**) to isolate the corresponding hydrazines (**80**) after acidic treatment.^[15e]

In the case of the diazoether (**81**) the ascorbic acid functions as an *in situ* radical initiator at benign conditions. The diazonium salt is cleaved to give nitrogen, the ascorbate radical and an aryl radical (**82**) which can then undergo further reactions. This methodology has been employed in the cross coupling reaction with electron rich aromatics.^[15h] The literature suggests that both products are being formed. However, only the oxalyl hydrazide could be isolated by Browne *et al.*, who investigated the reaction of ascorbic acid and a diazonium salt to the oxalyl hydrazide who have reported a Japp-Klingemann type rearrangement (Scheme 3.6).^[15g] This investigation was further extended by Horan *et al.* who studied the radical initiated cross coupling reaction.^[15j] They confirmed the formation of the oxalyl hydrazide but also found the corresponding triazene to be an intermediate. They highlighted that the reaction mechanism of ascorbic acid with a diazonium salt needs further investigation due to its complexity.



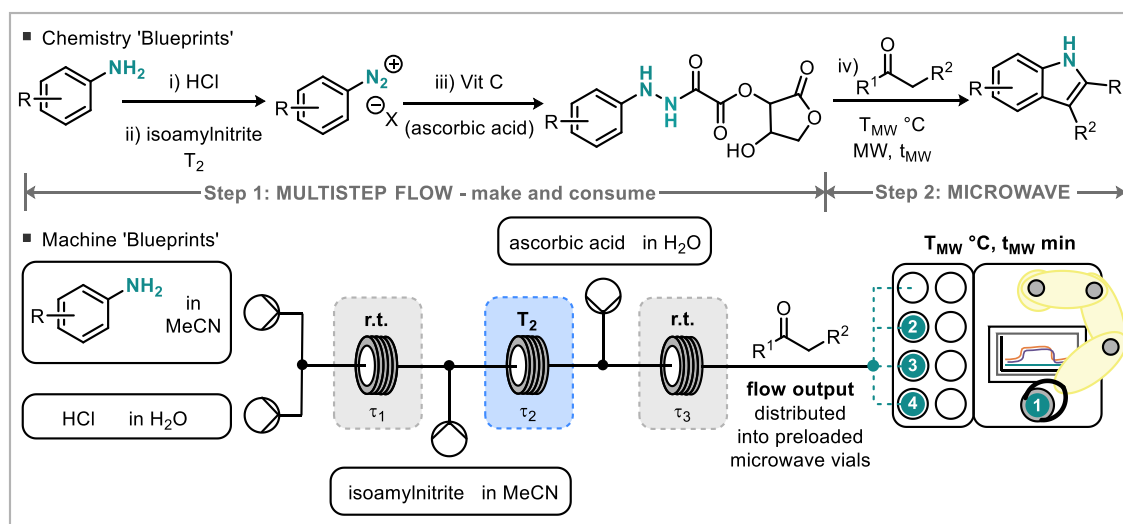
Scheme 3.5: Possible Products of the Reaction of Diazonium Salts with Ascorbic Acid

The oxalyl hydrazide (**79**) is acid labile and forms the hydrazine (**80**) under acidic conditions. This methodology has been used for the synthesis of Eletriptan (5-HT agonist, migraine treatment) by Ashcroft from Pfizer, who found an alternative to the current manufacturing route which uses tin chloride as the reducing agent.^[15f] The reaction with a 1,3-dicarbonyl to form the pyrazole has been reported by Poh *et al.*, where they monitored the formation of the oxalyl hydrazide in an *in line* IR spectrometer to optimise their flow setup.^[15k] Baxendale and co-workers have used the ascorbic acid reduction of diazonium salts to synthesise a key fragment of SR 142948A, a neurotensin modulator, adapting the method from Poh *et al.* to an aqueous diazotisation.^[16]



Scheme 3.6: Mechanism Suggested by Browne *et al.* [15g]

The aim of this project is to produce hydrazines *in situ* from anilines via the metal-free reduction of diazonium salts with ascorbic acid in flow (Step 1) and then convert the hydrazines directly into the indoles by a Fischer indole reaction in a microwave reactor (Step 2) (Scheme 3.7). This is approached in a modular hybrid setup, where a common stream of hydrazine from a flow setup (Step 1) is collected to then undergo the Fischer indole reaction in the microwave with an array of ketones (Step 2). The collection of the hydrazine could be automated using autosamplers and robotic microwaves. This enables the formation of a library of analogues important for drug discovery such as “follow-on” drugs. [1a, 1b]



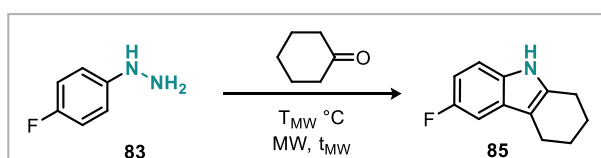
Scheme 3.7: General Idea

2 Results and Discussion

The reaction setup was broken down into the two envisioned steps: multistep flow and microwave to initially investigate the steps individually. The microwave step was chosen to be investigated first using *p*-fluorophenylhydrazine (**84**) and cyclohexanone as model substrates. The yield was determined via ^{19}F NMR with the use of trifluorotoluene as internal standard (Table 3.1). Pleasingly, the commercially available hydrochloride salt of *p*-fluorophenylhydrazine gave full conversion at 120 °C after 10 min and the clean indole was isolated quantitatively (entry 1). The complex reaction mixture deriving from the multistep flow setup was then simulated by preparing the hydrazine *in situ*. The yield decreased significantly to just 15 % (entry 2). Increasing the reaction temperature resulted in a 47% isolated yield at 160 °C (entry 4). This could be improved by increasing the equivalents of acid and isoamyl nitrite giving 73% of the desired indole **85**.

The discrepancy in yield for the commercial hydrazine and the *in situ* prepared hydrazine can be explained as the formation of the hydrazine is not quantitative and byproducts from previous steps could interfere with the Fischer indole reaction investigated in this step. This has been further investigated

Table 3.1: Optimisation of Microwave Parameters (Step 2)



entry	hydrazine source	T_{MW} [°C]	t_{MW} [min]	^{19}F yield [%]
1	commercial	120	10	98 (97)
2	<i>in situ</i> prepared	120	10	15
3	<i>in situ</i> prepared	140	10	30
4	<i>in situ</i> prepared	160	10	52 (47)
5	<i>in situ</i> prepared	180	10	46
6	<i>in situ</i> prepared	160	30	48
7 ^a	<i>in situ</i> prepared	160	10	67
8^{a,b}	<i>in situ</i> prepared	160	10	73

isolated yields in parenthesis; batch hydrazine formation: 1 mmol *p*-fluoroaniline, 1 mmol HCl, 1 mmol isoamyl nitrite, 1 mmol Vit C; a) 5 mmol of HCl; b) 1.2 mmol isoamyl nitrite

The formation of the oxalyl hydrazide in the first step was then first investigated using ^{19}F NMR with trifluorotoluene (**86**) as internal standard and each intermediate was monitored. An NMR was taken after the addition of each reagent to the *p*-fluoroaniline

(**87**) substrate (Figure 3.1). The aniline (**87**) (a) is first completely protonated (**88**) (b) and then completely converted into the diazonium salt (**89**) (c). Upon the addition of ascorbic acid, the diazonium salt is completely consumed and two new peaks are observed, one of which is expected to be the oxalyl hydrazone. Monitoring these two peaks over time showed that one of them (-109 ppm) decreases until only trace amounts remain, while the other one (-126 ppm) increases to approximately 100% (Figure 3.2) indicating that the first product is transformed into the second one.

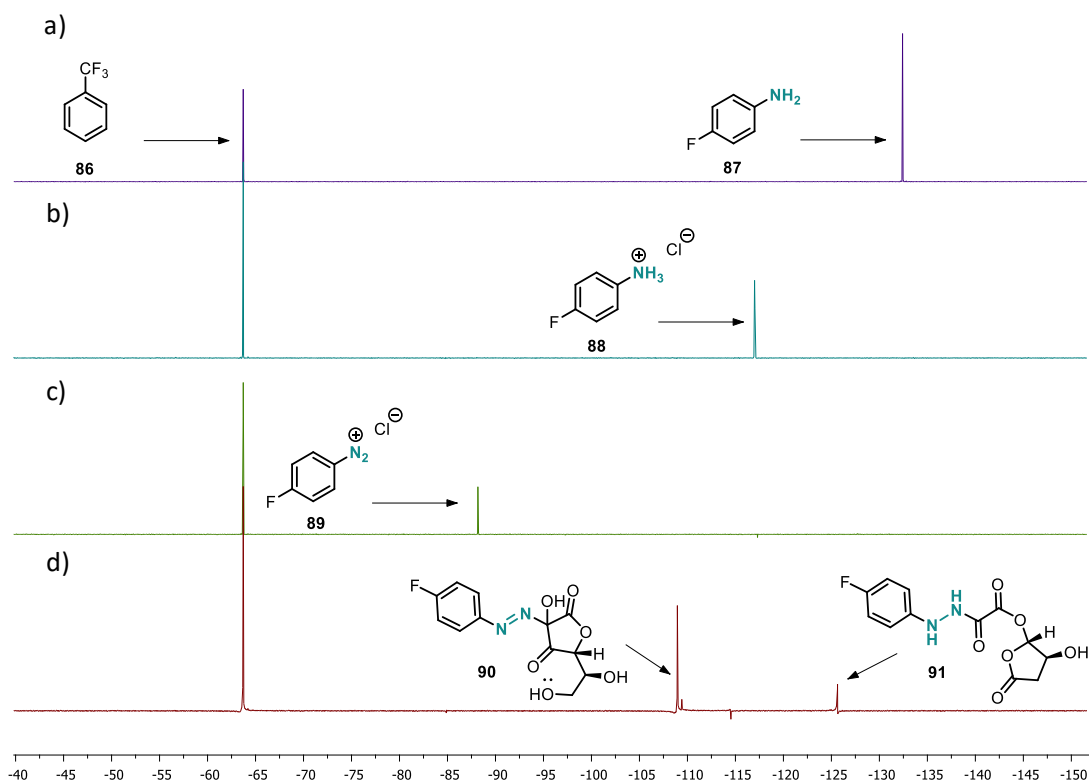


Figure 3.1: ^{19}F NMR Monitoring of the Reaction with Internal Standard; a) *p*-fluoroaniline (**87**) in MeCN; b) after addition of HCl; c) after addition of isoamyl nitrite, diazonium salt (**89**); d) after addition of ascorbic acid, two new peaks observed

The commercially available *p*-fluorophenylhydrazine hydrochloride (**84**) (-122 ppm) does not match the ^{19}F NMR shift of either of the peaks, suggesting that the second peak is not the hydrazine itself. In order to further investigate the nature of the two observed compounds, the reaction mixture was exposed to the cyclisation conditions in the microwave with cyclohexanone at three different times after the addition of vitamin C (0 min, 30 min and 180 min) and the yield increased over time (39%, 52% and 60% respectively). This indicates, that the second peak forming is not a degradation product but rather a second intermediate that undergoes the reaction with cyclohexanone.

The first peak could therefore be the adduct (**88**) of ascorbic acid and the diazonium salt before the rearrangement and the second peak the rearranged oxalyl hydrazide (**89**). This investigation of the intermediates from the aniline to the oxalyl hydrazide showed, that the protonation and diazotisation were faster than 7 min, which is the earliest an NMR spectra could be obtained.

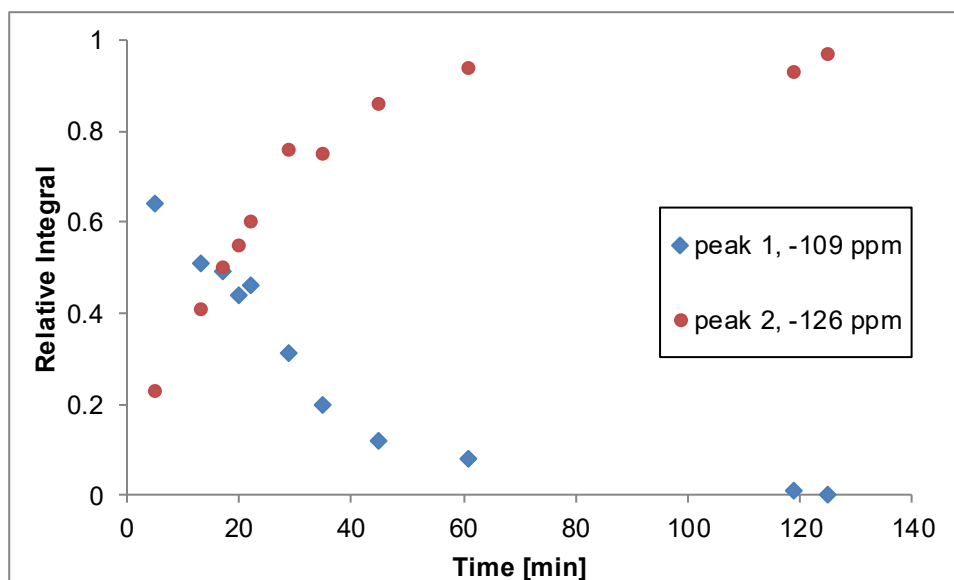
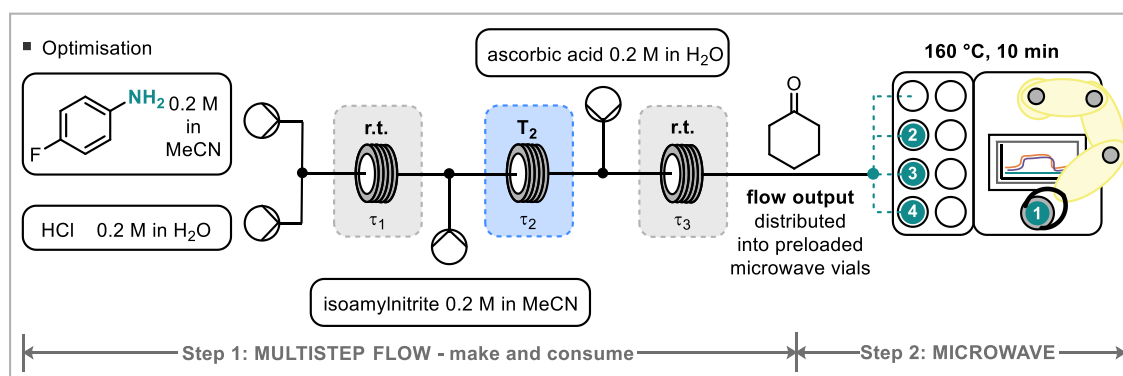


Figure 3.2: Products after Ascorbic Acid Addition Monitored over Time

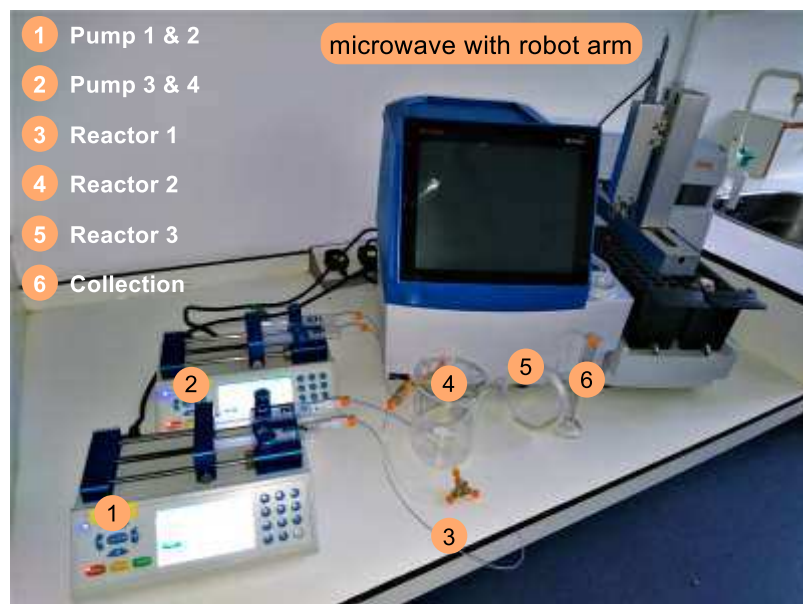
The envisaged setup for the multistep synthesis was therefore next investigated optimising the first step in flow with the concentrations identified from the previous step (Table 3.2). The initial yield of indole **85** in the telescoped process was 41% (entry 1). Increasing the concentration of hydrochloric acid and isoamyl nitrite resulted in an increase in yield to 72% (entry 2). An increase of the vitamin C concentration decreased the yield (entry 3). Performing the diazotisation step under room temperature instead of 0 °C decreased the yield (entry 4). The residence times in all reaction coils were screened (entries 6 - 9). Finally, optimised conditions for the first step proved to be 1 M hydrochloric acid in H₂O (5 equiv), 0.24 M isoamyl nitrite in MeCN (1.2 equiv), 0.2 M ascorbic acid in H₂O (1 equiv), 0 °C in the second reaction coil, residence times of 0.6 min (0.23 mL reaction coil), 3.3 min (2 mL reaction coil) and 3.3 min (5 mL reaction coil) at a flowrate of 0.2 mL/min for each pump giving 74% (68% isolated) of the desired indole **85** (entry 10) (Picture 3.1).

Table 3.2: Optimisation of the Telescoped Reaction



entry	c (HCl) [mol/L]	c (isoamyl nitrite) [mol/L]	c (Vit C) [mol/L]	T ₂ [°C]	T ₁ [min]	T ₂ [min]	T ₃ [min]	¹⁹ F yield [%]
1	0.2	0.24	0.2	0	0.6	3.3	3.3	41
2	1	0.2	0.2	0	0.6	3.3	3.3	72
3	1	0.24	0.24	0	0.6	3.3	3.3	62
4	1	0.24	0.2	rt	0.6	3.3	3.3	53
5	1	0.24	0.2	0	5	3.3	3.3	60
6	1	0.24	0.2	0	0.6	1.7	3.3	64
7	1	0.24	0.2	0	0.6	8.3	3.3	65
8	1	0.24	0.2	0	0.6	3.3	2.5	64
9	1	0.24	0.2	0	0.6	3.3	12.5	64
10	1	0.24	0.2	0	0.6	3.3	3.3	74 (68)

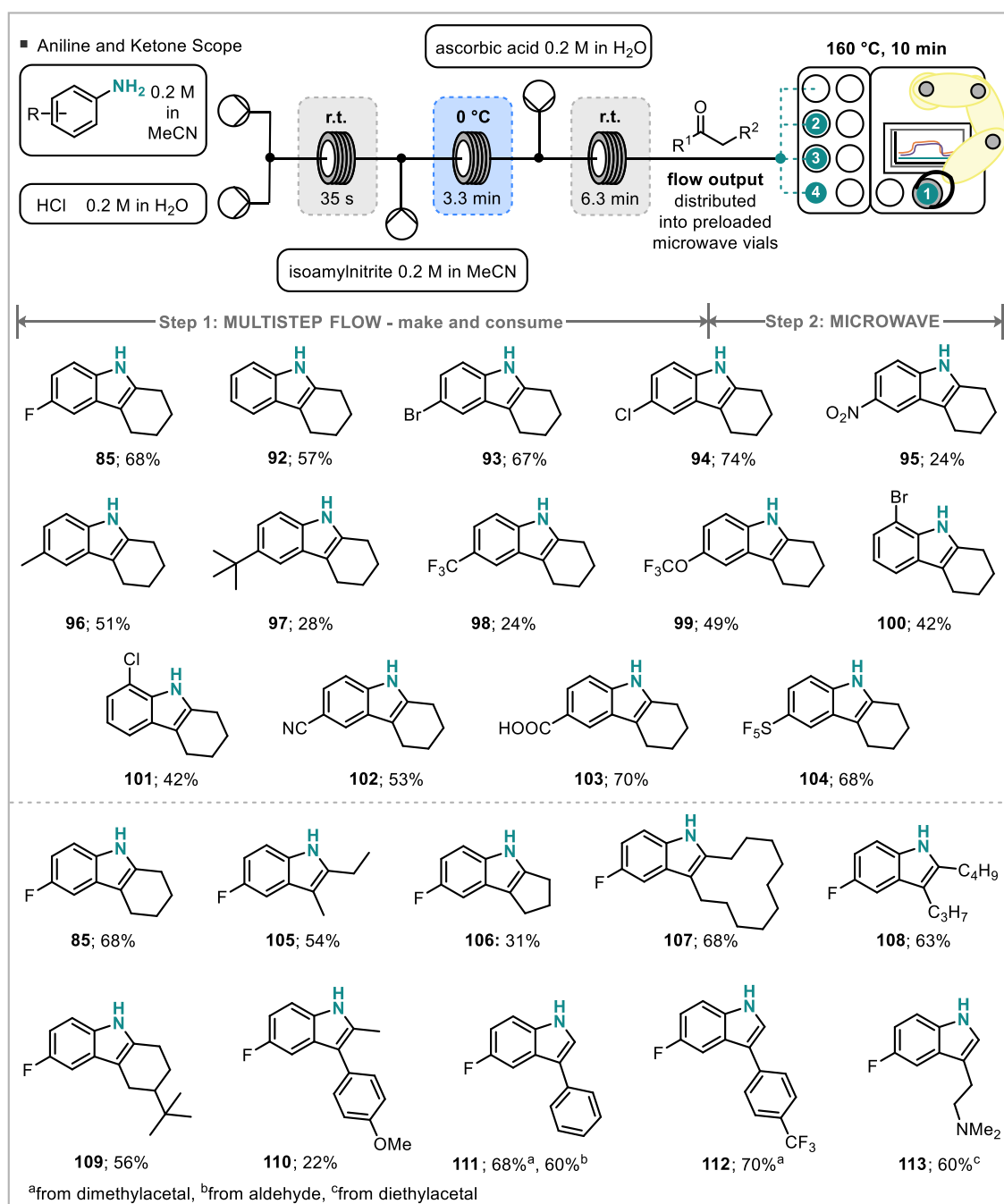
yields determined by ¹⁹F NMR with trifluorotoluene as internal standard



Picture 3.1: Picture of the Optimised Setup

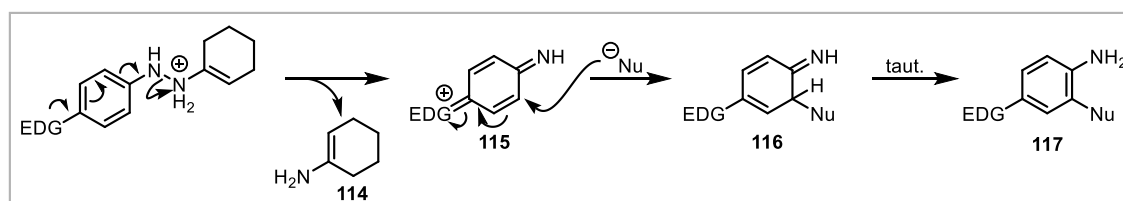
Following reaction optimisation, a substrate scope for a range of anilines and ketones was performed and 23 indoles were isolated (Scheme 3.8). For the aniline scope

cyclohexanone was chosen as the model ketone (14 examples). The reaction works well for most substrates screened with yields between 74 and 24%. The indole (**94**) derived from *p*-chloroaniline gave the highest yield (74%). Strongly electron-withdrawing groups such as *p*-nitro or *p*-CF₃ groups (**95**, **98**) produced lower yields (24%). This could be due to the competing aromatic radical formation with ascorbic acid, which is reportedly best with electron-poor aromatics.^[15h, 15i, 15j] Ortho substituted anilines give slightly lower yields of the indole (**100**, **101**) than their corresponding para-substituted anilines probably due to steric hindrance.



Scheme 3.8: Aniline Substrate Scope, isolated yields

However, no indoles from electron-rich anilines (*p*-OMe, *p*-OEt, *p*-SH, *p*-OH, pyridine derivatives) and *p*-iodoaniline could be obtained. *p*-Iodoaniline formed a precipitate upon mixing with hydrochloric acid that afforded clogging of the first reaction coil. Therefore, this reaction could not be performed. The reaction setup tolerated electron-rich anilines, but no indole product was observed. This is due to the Fischer indole reaction in step 2 not working efficiently. Brown *et al.* reported a side reaction for electron rich hydrazines occurring in the presence of acid and nucleophiles that results in a S_NAr at the position *ortho* to the hydrazine substituent (Scheme 3.9).^[17] The electron donating group enables the protonated enamine **114** to be released. Interception of the benzoquinone type intermediate **115** with a nucleophile (including chloride from hydrochloric acid in solution) and rearomatisation lead to the S_NAr product **117**.

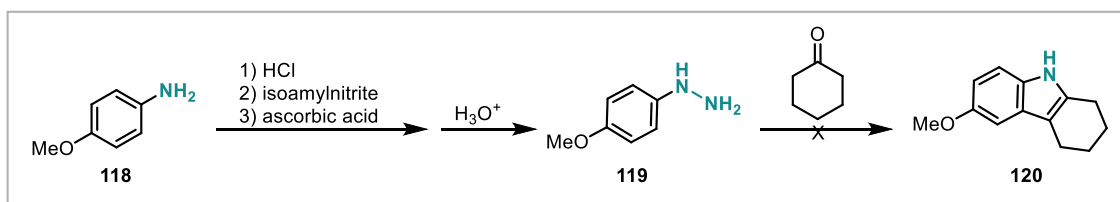


Scheme 3.9: Side Reaction in the Fischer Indole Reaction Reported by Brown *et al.*^[17]

The authors suggested avoiding acidic conditions (or instead use Lewis acids) and potential nucleophiles or to derivatise electron-donating groups to make them less electron-donating, which is in accordance with other literature.^[18] As avoiding acidic conditions and potential nucleophiles was not possible in the telescoped setup, other potential solutions were investigated. Buchwald and co-workers performed the Fischer indole reaction with hydrazones derived through cross coupling reactions and their scope included electron-rich aromatics.^[13a] The employed conditions were similar to the ones used in this work, aqueous solutions and heating under reflux, but they authors used TsOH instead of hydrochloric acid. Other reports decreased reaction times or temperatures to achieve the indolisation of electron-rich aromatics.

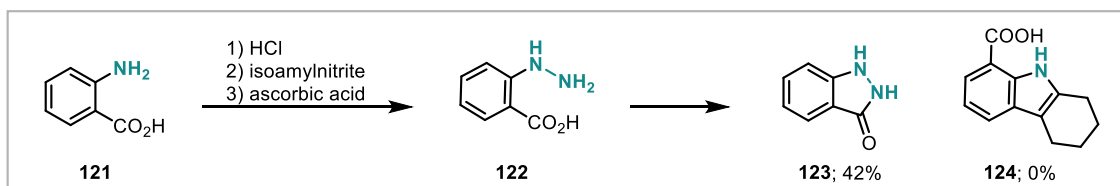
Conditions compatible with this work were screened for the example of the *p*-methoxyaniline **118** (Scheme 3.10). Different amounts of hydrochloric acid and changing the time of addition (in the beginning or with the ketone) which might influence the diazotisation and reduction did not show any success. TsOH was used as an alternative to hydrochloric acid, but again no indole was observed. Reducing the temperature to 120 °C showed traces of indole **120** in crude NMR spectra, but no indole could be isolated. No other major product, such as the S_NAr product suggested by Brown

et al. could be isolated either. The reaction mixtures generally showed a complex mixture of different compounds which could not be isolated.



Scheme 3.10: Reaction with *p*-Methoxyaniline

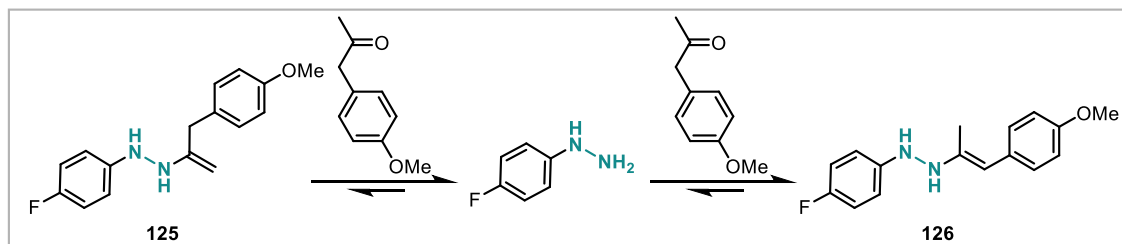
Anthranilic acid (**121**) could be successfully converted into the corresponding hydrazine (**122**) which is notable as the diazonium salt is highly unstable and can decompose to benzyne, carbon dioxide and nitrogen (see Chapter 4: Investigating the Formation of Benzyne from Diazonium Salts). However, under the elevated conditions in the microwave, the hydrazine cyclised intramolecularly to give the indazolone **123** instead of undergoing the Fisher indole reaction to the expected product **124** (Scheme 3.11). Under unoptimised conditions 42% of indazolone **123** were isolated.



Scheme 3.11: Reaction of Anthranilic Acid

A ketone substrate scope with *p*-fluoroaniline was performed preparing a range of different indoles (Scheme 3.8). A common stream from the flow setup with the *in situ* prepared oxalyl hydrazide (Step 1) was transferred into a microwave vial preloaded with the desired ketone as described in the concept. This enabled the quick synthesis of a library of different fluorinated indoles.

Indoles from cyclic, acyclic ketones and benzylic ketones could be isolated (**85**, **105-110**) in moderate to good yield (31-68%). Notably, for indole **110** two regioisomers could be expected but in the event only one could be isolated. The other regioisomer could however be observed in trace amounts in crude NMRs. This is most likely to be due to the higher stability of the formed enamine **126** that is in conjugation to the aromatic ring in comparison to the terminal enamine **125** (Scheme 3.12).



Scheme 3.12: Stability of Enamines Deciding Regioselectivity

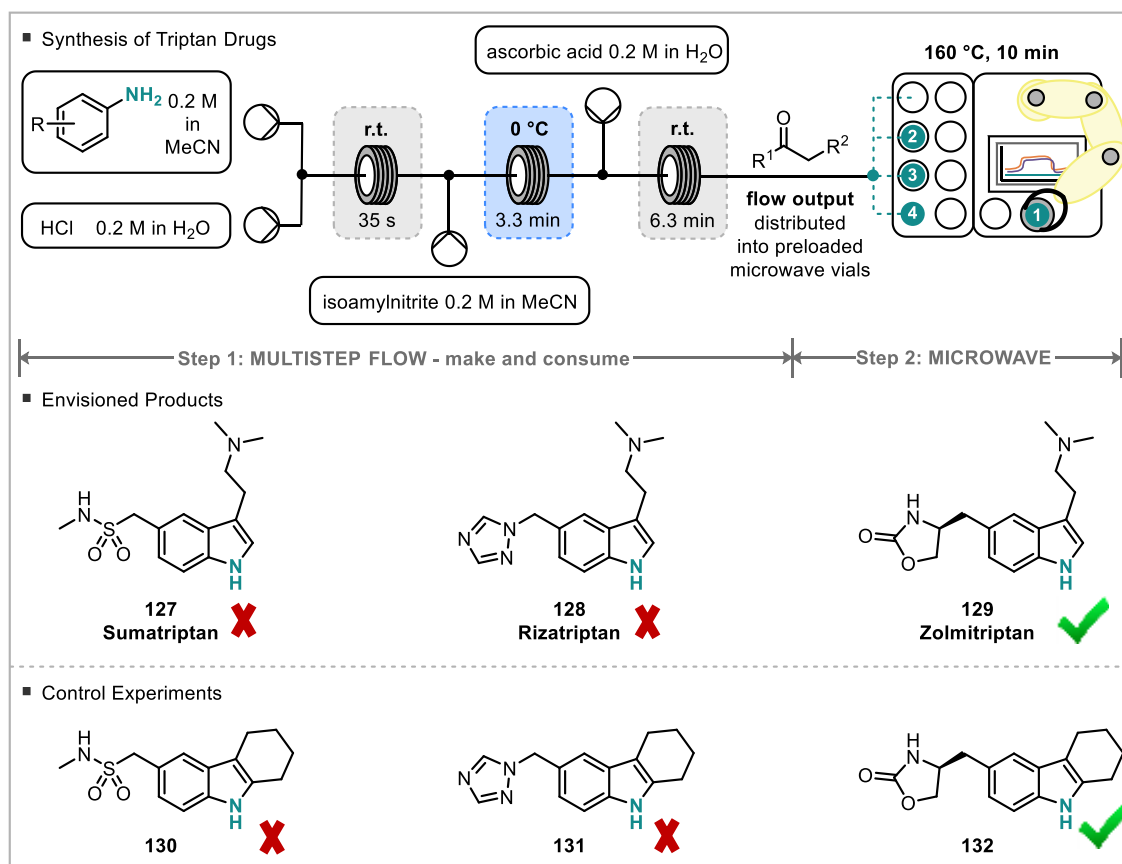
In addition to those examples, the substrate scope could be further extended to aldehydes and their acetals (**111**, **112**).

Finally, 4-dimethylaminobutyraldehyde diethyl acetal could be used to incorporate a tertiary amine in the indole C3 side chain (**113**) in 60% yield. This is particularly interesting for the synthesis of the triptan drugs, which all bear a tertiary amine and in some examples this exact side chain.

However, both acetone and acetophenone did not undergo the Fischer indole reaction. Acetophenone forms a relatively stable enamine with hydrazines, that can only undergo cyclisation to form the indole under strongly acidic conditions such as Lewis acids or polyphosphoric acid.^[7f, 19] However, these conditions are non-aqueous and are therefore not compatible in the multistep procedure envisioned so that they were not investigated further.

The reaction with acetone most likely does not give the desired indole as acetone is too volatile and is mostly present in the headspace of the microwave vial rather than in solution. This was addressed by increasing the equivalents of acetone (from 1 equiv under standard conditions to 2 equiv, 3 equiv and 19 equiv) but the indole could not be observed.

After demonstrating the feasibility of the method over a range of substrates the scope was to be further extended by the synthesis of the triptan drugs, Sumatriptan (**127**), Rizatriptan (**128**) and Zolmitriptan (**129**) from the corresponding anilines and 4-aminobutyraldehyde diethylacetal (Scheme 3.13). In the event, LCMS confirmed that only Zolmitriptan was formed under the applied general reaction conditions. To further investigate the reason, the reactions were performed with the model ketone cyclohexanone. Only the reaction with the Zolmitriptan aniline delivered the indole (**131**) (Scheme 3.13).

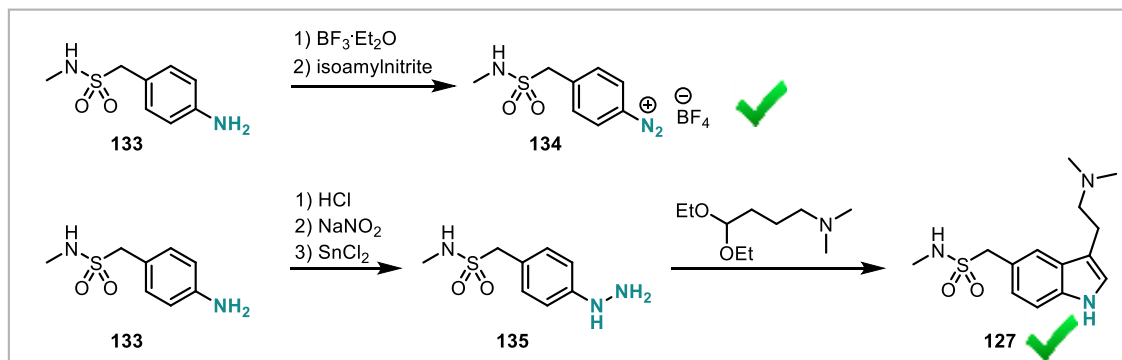


Scheme 3.13: Envisioned Synthesis of Triptan Drugs

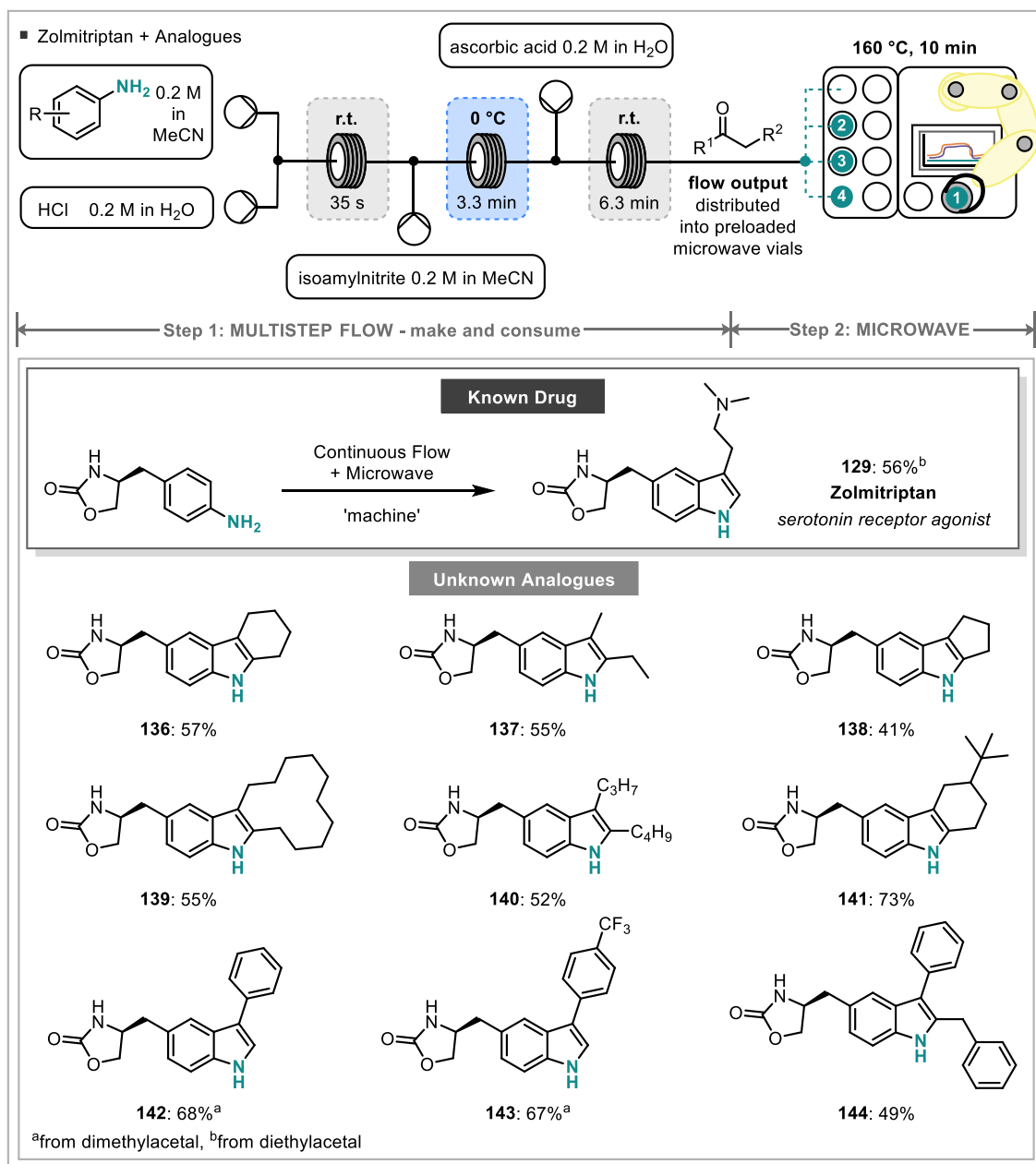
It was hypothesised that the formation of the hydrazine could be the problematic step. This was further investigated by performing the diazotisation and reduction for the Sumatriptan synthesis separately (Scheme 3.14).

The tetrafluoroborate diazonium salt **134** was produced and its formation confirmed by IR, but it degraded quickly before complete isolation. When reducing the diazonium salt *in situ* with SnCl₂, the hydrazine **135** could be obtained, but again it degraded quickly. The crude hydrazine was used to perform the Fischer indole reaction in the microwave with 4-aminobutyraldehyde diethylacetal and in the event, Sumatriptan (**127**) could be observed by LCMS but could not be isolated. The success in the synthesis of Sumatriptan when reducing the diazonium salt with tin chloride indicates that the reduction with ascorbic acid is not successful for this example. Sumatriptan is commercially produced via diazotisation and reduction with SnCl₂, also confirming the observations.^[6a]

Finally, attention was turned to the synthesis of Zolmitriptan analogues to demonstrate the ability to form a library using the developed setup (Scheme 3.15). In this manner, 9 analogues (**136 - 144**) and Zolmitriptan (**129**) were synthesised in moderate to good four step yields (41-73%).



Scheme 3.14: Reactions Towards Sumatriptan

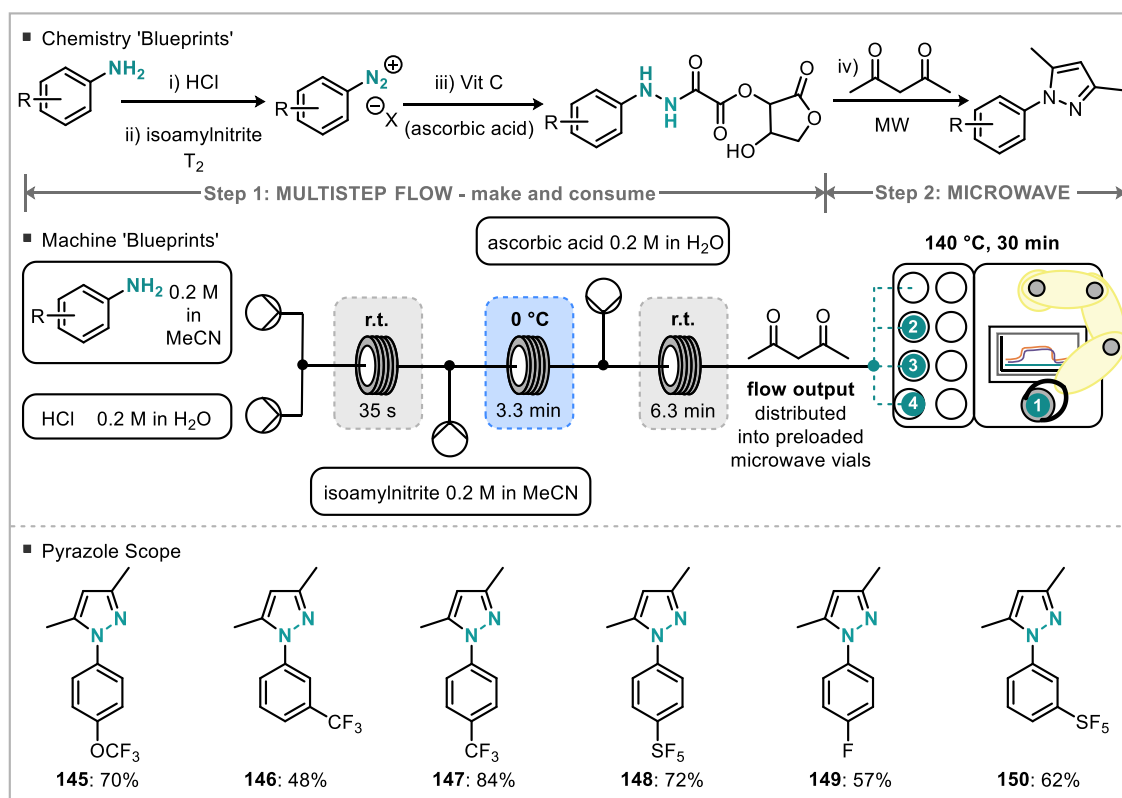


Scheme 3.15: Zolmitriptan Analogue Scope

2.1 Method Adaption for the Synthesis of a Series of Fluorinated Pyrazoles

The hybrid continuous flow – microwave multistep approach was adapted further for the synthesis of fluorinated pyrazoles. In a collaboration with the Pope group, these pyrazoles were then incorporated into novel iridium (III) complexes as ligands. These iridium complexes are interesting for applications in photoredox catalysis but also in organic light-emitting diodes (OLEDs) and oxygen sensors. Notably, these photoredox catalysts exhibit tunable photophysical properties depending on the electronic nature of the ligands.^[20]

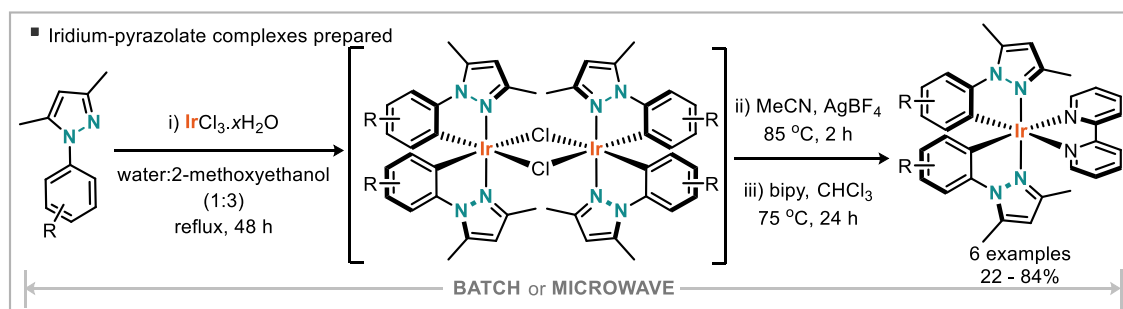
For the synthesis of a small series of fluorinated pyrazoles the corresponding anilines were transformed into hydrazines under continuous flow conditions and then added to a 1,3-diketone (acetyl acetone) for the microwave reaction (Scheme 3.16). This approach is similar to the one from Browne, Ley and co-workers who synthesised pyrazoles via the same route in a telescoped flow reaction.^[15k]



Scheme 3.16: Pyrazole Synthesis via Hybrid Continuous Flow – Microwave Approach

Small alterations to the setup were necessary to adjust the process for the condensation to pyrazoles. The acid and isoamyl nitrite concentration were decreased to 0.2 M, and

the second step was heated to 140 °C in the microwave for 10 min. In this manner six fluorinated pyrazoles were prepared in good to excellent four step yields (48 – 84%). The prepared pyrazoles were then used by the Pope group for the synthesis of iridium based photoredox catalysts (Scheme 3.17). The catalysts were prepared following a three step procedure, where first a chloro bridged dimer was isolated. This dimer was then split using AgBF_4 and then heated with bipyridine to give the desired complex as the tetrafluoroborate salt.^[20b]



Scheme 3.17: Iridium based Pyrazolate Photoredox Catalysts Prepared by the Pope Group

Stephenson and co-workers reported the synthesis of iridium complexes using the microwave to reduce the reaction times significantly.^[20a] Thus, the iridium complexes were also prepared using the microwave approach reducing the total reaction time for the formation of the complexes from 74 h to 1 h.

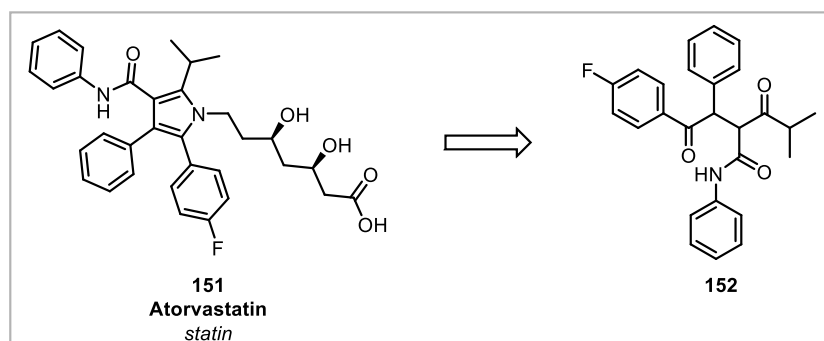
The work demonstrated in this collaboration reports the first generation approach towards a machine assisted preparation of iridium (III) photoredox catalysts which is the first step towards a fully automated process. In this manner, six pyrazoles have been synthesised which functioned as ligands in six novel iridium (III) complexes.

3 Conclusions and Outlook

A hybrid continuous flow – microwave machine for the multistep synthesis of indoles has been developed. The machine has been used to synthesise a library of 33 indoles, including Zolmitriptan and nine of its analogues. Notably, only ten of the examples had been characterised in the literature to date.

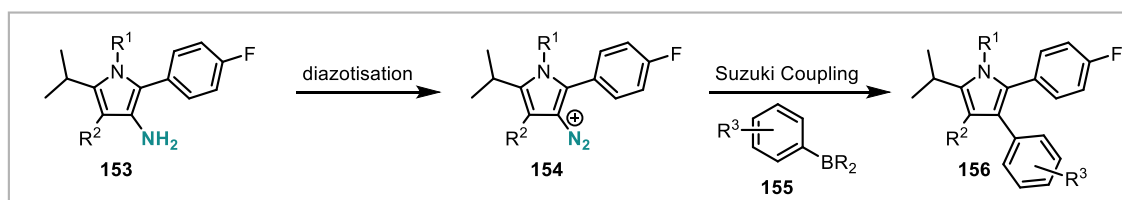
In addition, the machine has been used for the preparation of six fluorinated pyrazoles, which have been used for the formation of iridium complexes with the potential to be photoredox catalysts.

The machine could be used for the synthesis of other libraries. One example is described here. As an example, the synthesis of Atorvastatin (trade name Lipitor) is chosen. Atorvastatin (a statin) is a lipid lowering medicine used to reduce risk and development of cardiovascular disease. It is usually prepared in a Paal-Knorr condensation to form the pyrrole ring from the substituted diketone (**152**) and the corresponding amine (Scheme 3.18).^[21]



Scheme 3.18: Atorvastatin and its Diketone Precursor

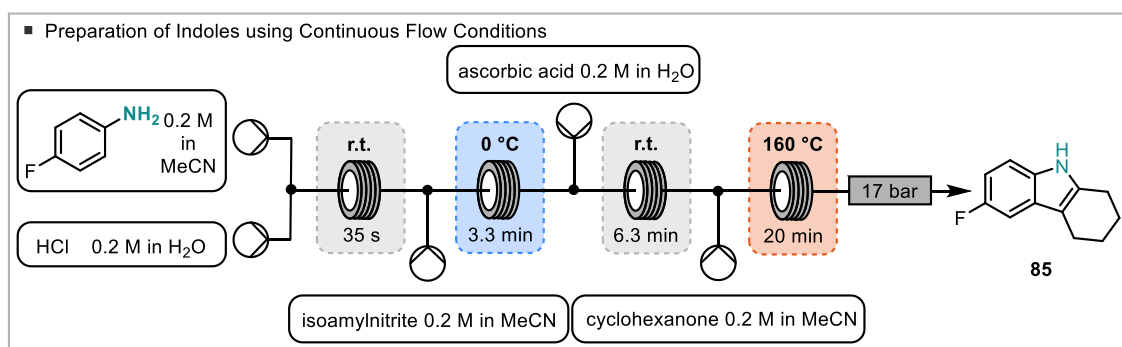
In the scope of this thesis, the use of diazonium salts for the preparation of Atorvastatin analogues is envisioned (Scheme 3.19). 3-Aminopyrroles (**153**) could be diazotised to form diazonium salts (**154**) under continuous flow conditions. These could then be functionalised in the microwave in a Suzuki coupling with boronic acids (**155**) to form Atorvastatin analogues (**156**). The starting 3-aminopyrroles could be prepared from the nitro-diketones in a Paal-Knorr condensation and subsequent reduction.



Scheme 3.19: Proposed Atorvastatin Analogue Synthesis

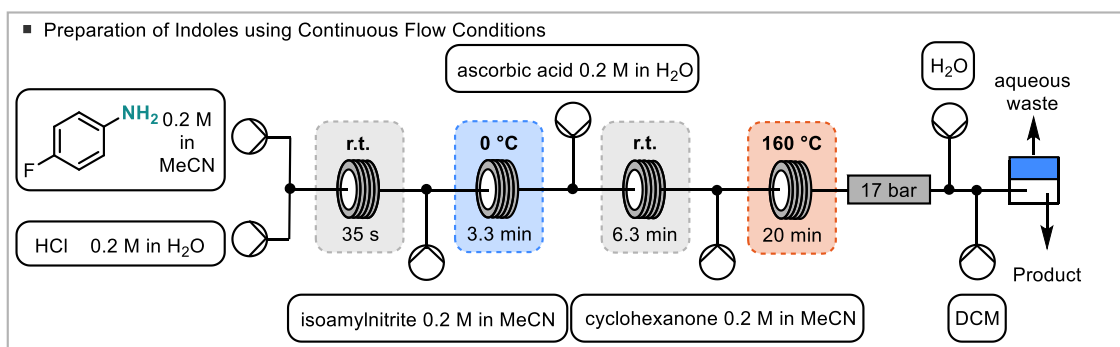
The complexity of the modular setup employed in this work is highly dependent on required capability and budget. The use of machine assisted approaches for the synthesis of compounds has been discussed and explored. These approaches can vary in complexity and include downstream processes, analysis and automated feedback systems for automisation.^[22] Many alterations are possible and three possible alterations will be described here.

Having used the described apparatus to create a range of analogues, the system could be modified by removing the microwave module and adding a fifth pump, high temperature reaction coil and back pressure regulator. This system would then permit scale-up of any one analogue of interest (Scheme 3.20). The material of the coil has to be carefully chosen to withstand both the temperature and the hydrochloric acid. A continuous setup like this should allow the production of tens of grams of material over a few days/ weeks without other alternations to the setup (7.4 g per day for the indole **85** assuming 68% yield).



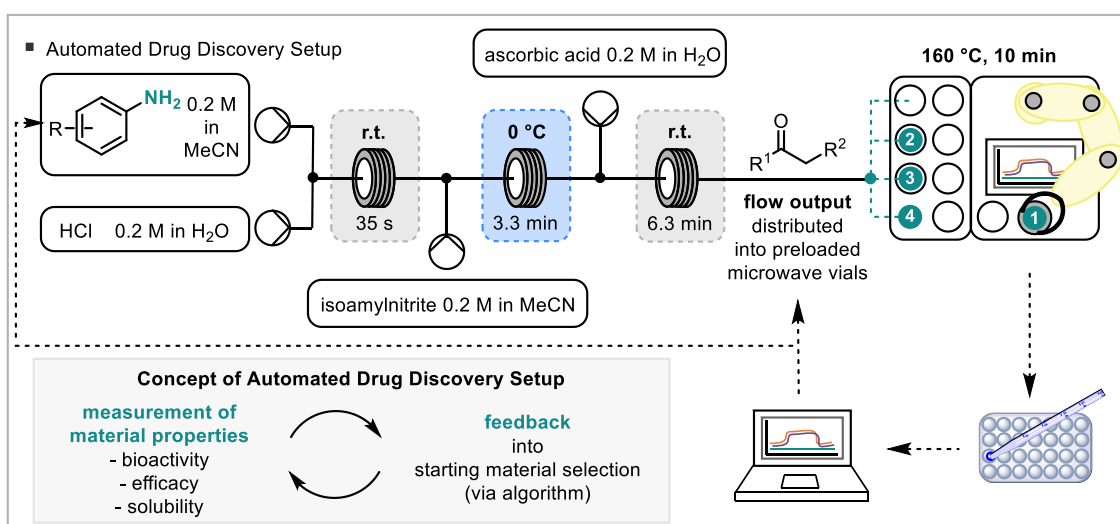
Scheme 3.20: Preparation of Indoles using Continuous Flow Conditions

The above-mentioned setup could incorporate an automated purification such as an *in line* liquid-liquid extraction by adding a module containing two pumps and an extraction device, such as a Biotage Universal Phase Separator, Syrris FLLEX or Zaiput device (Scheme 3.21).



Scheme 3.21: Preparation of Indoles using Continuous Flow Conditions Including Downstream Processing

The original setup could be further modified to also include downstream analysis and optimisation of performance properties (Scheme 3.22). This is in congruence with the envisioned automated synthesis machine in the synthesis of iridium pyrazolate photoredox catalysts. Such an ability would require a further liquid-handling robot to sample from the microwave reaction vial, a purification and analytical process (*in line* HPLC and MS) followed by a performance measuring assay. Such systems have been designed and reported already as a proof of concept.^[22k, 22l, 23] The assay would provide a data point to a computer algorithm that would then interpret the data and plan the next experiment/ molecule. The loop would be completed by adding a robotic device for picking and measuring substrate input feeds (for example a Mettler Toledo Quantos Dosing system).



Scheme 3.22: Automated Drug Discovery Setup

Similar to the formation of the indoles, the machine-assisted approach for the synthesis of iridium photoredox catalysts, has the prospect of automating the synthesis of a library

of different catalysts when autosamplers are used. The process can then be coupled to a screening device, in this case for the photochemical properties of the catalysts. These properties are for example the emission wavelength in a UV/Vis spectrum. The properties of photoredox catalysts are highly dependent on the electronic nature of the ligands and thus can be changed by changing the substituents on the ligands. The information measured in the screening device could be used to choose the next ligand to test in order to improve the properties. The use of an automated system allows a computer to control the starting material selection for the synthesis of ligands and then the catalyst formation step. In this manner, a range of complexes can be synthesised and screened in order to optimise the desired properties. This approach has been established for the screening of pharmaceuticals, but to date has not been used for the synthesis of metal based photoredox catalysts.^[22k, 22l]

4 References

- [1] a) E. Petrova, in *Innovation and marketing in the pharmaceutical industry*, Springer, **2014**, pp. 19-81; b) A. Hollis, *WHO report* **2004**; c) T. H. Lee *N. Engl. J. Med.* **2004**, *350*, 211-212.
- [2] H. Zhao, Z. Guo, *Drug Discovery Today* **2009**, *14*, 516-522.
- [3] F. Giordanetto, J. Boström, C. Tyrchan, *Drug Discovery Today* **2011**, *16*, 722-732.
- [4] a) J. J. Li, D. S. Johnson, D. R. Sliskovic, B. D. Roth, *Contemporary drug synthesis*, John Wiley & Sons, **2004**; b) P. P. A. Humphrey, *Headache: The Journal of Head and Face Pain* **2007**, *47*, S10-S19.
- [5] M. Baumann, I. R. Baxendale, *Beilstein J. Org. Chem.* **2015**, *11*, 1194-1219.
- [6] a) M. Baumann, I. R. Baxendale, S. V. Ley, N. Nikbin, *Beilstein J. Org. Chem.* **2011**, *7*, 442-495; b) N. K. Kaushik, N. Kaushik, P. Attri, N. Kumar, C. H. Kim, A. K. Verma, E. H. Choi, *Molecules* **2013**, *18*, 6620-6662; c) T. C. Barden, in *Heterocyclic Scaffolds II*, Springer, **2010**, pp. 31-43.
- [7] a) M. Inman, C. J. Moody, *Chem. Sci.* **2013**, *4*, 29-41; b) D. F. Taber, P. K. Tirunahari, *Tetrahedron* **2011**, *67*, 7195-7210; c) G. R. Humphrey, J. T. Kuethe, *Chem. Rev.* **2006**, *106*, 2875-2911; d) J. Park, D.-H. Kim, T. Das, C.-G. Cho, *Org. Lett.* **2016**, *18*, 5098-5101; e) P. A. Barsanti, W. Wang, Z.-J. Ni, D. Duhl, N. Brammeier, E. Martin, D. Bussiere, A. O. Walter, *Bioorg. Med. Chem. Lett.* **2010**, *20*, 157-160; f) N. Çelebi-Ölçüm, B. W. Boal, A. D. Hutters, N. K. Garg, K. N. Houk, *J. Am. Chem. Soc.* **2011**, *133*, 5752-5755.
- [8] J. A. Joule, K. Mills, *Heterocyclic Chemistry, 5th edition*, Wiley, **2010**.
- [9] a) T. Guo, F. Huang, L. Yu, Z. Yu, *Tetrahedron Lett.* **2015**, *56*, 296-302; b) C. Wang, H. Sun, Y. Fang, Y. Huang, *Angew. Chem.* **2013**, *125*, 5907-5910; c) J. Liu, W. Wei, T. Zhao, X. Liu, J. Wu, W. Yu, J. Chang, *J. Org. Chem.* **2016**, *81*, 9326-9336; d) J. Ghorai, A. C. S. Reddy, P. Anbarasan, *Chem. Eur. J.* **2016**, *22*, 16042-16046; e) M. Peña-López, H. Neumann, M. Beller, *Chem. Eur. J.* **2014**, *20*, 1818-1824.
- [10] B. Robinson, *Chem. Rev.* **1969**, *69*, 227-250.
- [11] K. R. Campos, J. C. S. Woo, S. Lee, R. D. Tillyer, *Org. Lett.* **2004**, *6*, 79-82.
- [12] a) K. Krüger, A. Tillack, M. Beller, *Adv. Synth. Catal.* **2008**, *350*, 2153-2167; b) Y. Liang, N. Jiao, *Angew. Chem.* **2016**, *128*, 4103-4107; c) T.-R. Li, B.-Y. Cheng, Y.-N. Wang, M.-M. Zhang, L.-Q. Lu, W.-J. Xiao, *Angew. Chem.* **2016**, *128*, 12610-12614; d) K. V. Chuang, M. E. Kieffer, S. E. Reisman, *Org. Lett.* **2016**, *18*,

- 4750-4753; e) S. Liang, L. Hammond, B. Xu, G. B. Hammond, *Adv. Synth. Catal.* **2016**, *358*, 3313-3318.
- [13] a) S. Wagaw, B. H. Yang, S. L. Buchwald, *J. Am. Chem. Soc.* **1999**, *121*, 10251-10263; b) J. F. Hartwig, *Angew. Chem. Int. Ed.* **1998**, *37*, 2090-2093; c) M. Wolter, A. Klapars, S. L. Buchwald, *Org. Lett.* **2001**, *3*, 3803-3805; d) A. DeAngelis, D. H. Wang, S. L. Buchwald, *Angew. Chem. Int. Ed.* **2013**, *52*, 3434-3437.
- [14] a) F. R. Japp, F. Klingemann, *Ber. Dtsch. Chem. Ges.* **1887**, *20*, 2942-2944; b) Z.-G. Zhang, B. A. Haag, J.-S. Li, P. Knochel, *Synthesis* **2011**, *2011*, 23-29; c) B. A. Haag, Z.-G. Zhang, J.-S. Li, P. Knochel, *Angew. Chem. Int. Ed.* **2010**, *49*, 9513-9516; d) S. Wagaw, B. H. Yang, S. L. Buchwald, *J. Am. Chem. Soc.* **1998**, *120*, 6621-6622.
- [15] a) M. P. Doyle, C. L. Nesloney, M. S. Shanklin, C. A. Marsh, K. C. Brown, *J. Org. Chem.* **1989**, *54*, 3785-3789; b) K. J. Reszka, C. F. Chignell, *Chem.-Biol. Interact.* **1995**, *96*, 223-234; c) E. Y. Backheet, K. M. Emara, H. F. Askal, G. A. Saleh, *Analyst* **1991**, *116*, 861-865; d) U. Costas-Costas, E. Gonzalez-Romero, C. Bravo-Diaz, *Helv. Chim. Acta* **2001**, *84*, 632-648; e) T. Norris, C. Bezze, S. Z. Franz, M. Stivanello, *Org. Process Res. Dev.* **2009**, *13*, 354-357; f) C. P. Ashcroft, P. Hellier, A. Pettman, S. Watkinson, *Org. Process Res. Dev.* **2011**, *15*, 98-103; g) D. L. Browne, I. R. Baxendale, S. V. Ley, *Tetrahedron* **2011**, *67*, 10296-10303; h) F. P. Crisóstomo, T. Martín, R. Carrillo, *Angew. Chem. Int. Ed.* **2014**, *53*, 2181-2185; i) B. Majhi, D. Kundu, B. C. Ranu, *J. Org. Chem.* **2015**, *80*, 7739-7745; j) M.-j. Bu, G.-p. Lu, C. Cai, *Synlett* **2015**, *26*, 1841-1846; k) J.-S. Poh, D. L. Browne, S. V. Ley, *React. Chem. Eng.* **2016**, *1*, 101-105; l) A. P. Colleville, R. A. J. Horan, S. Olazabal, N. C. O. Tomkinson, *Org. Process Res. Dev.* **2016**, *20*, 1283-1293.
- [16] M. O. Kitching, O. E. Dixon, M. Baumann, I. R. Baxendale, *Eur. J. Org. Chem.* **2017**, *2017*, 6540-6553.
- [17] D. W. Brown, M. F. Mahon, A. Ninan, M. Sainsbury, H. G. Shertzer, *Tetrahedron* **1993**, *49*, 8919-8932.
- [18] W. Marais, C. W. Holzapfel, *Synth. Commun.* **1998**, *28*, 3681-3691.
- [19] a) A. Dhakshinamoorthy, K. Pitchumani, *Applied Catalysis A: General* **2005**, *292*, 305-311; b) T. M. Lipińska, S. J. Czarnocki, *Org. Lett.* **2006**, *8*, 367-370.
- [20] a) T. M. Monos, A. C. Sun, R. C. McAtee, J. J. Devery, C. R. J. Stephenson, *J. Org. Chem.* **2016**, *81*, 6988-6994; b) E. C. Stokes, E. E. Langdon-Jones, L. M. Groves, J. A. Platts, P. N. Horton, I. A. Fallis, S. J. Coles, S. J. A. Pope, *Dalton Trans.* **2015**, *44*, 8488-8493.

- [21] a) B. D. Roth, in *Prog. Med. Chem.*, Vol. 40, Elsevier, **2002**, pp. 1-22; b) B. D. Roth, C. Blankley, A. Chucholowski, E. Ferguson, M. Hoefle, D. Ortwine, R. Newton, C. Sekerke, D. Sliskovic, M. Wilson, *J. Med. Chem.* **1991**, *34*, 357-363.
- [22] a) R. A. Skilton, A. J. Parrott, M. W. George, M. Poliakoff, R. A. Bourne, *Appl. Spectrosc.* **2013**, *67*, 1127-1131; b) R. A. Skilton, R. A. Bourne, Z. Amara, R. Horvath, J. Jin, M. J. Scully, E. Streng, S. L. Y. Tang, P. A. Summers, J. Wang, E. Perez, N. Asfaw, G. L. P. Aydos, J. Dupont, G. Comak, M. W. George, M. Poliakoff, *Nat Chem* **2015**, *7*, 1-5; c) A. J. Parrott, R. A. Bourne, G. R. Akien, D. J. Irvine, M. Poliakoff, *Angew. Chem. Int. Ed.* **2011**, *50*, 3788-3792; d) C. Dietze, S. Schulze, S. Ohla, K. Gilmore, P. H. Seeberger, D. Belder, *Analyst* **2016**, *141*, 5412-5416; e) A. Adamo, R. L. Beingessner, M. Behnam, J. Chen, T. F. Jamison, K. F. Jensen, J.-C. M. Monbaliu, A. S. Myerson, E. M. Revalor, D. R. Snead, T. Stelzer, N. Weeranoppanant, S. Y. Wong, P. Zhang, *Science* **2016**, *352*, 61-67; f) H. R. Sahoo, J. G. Kralj, K. F. Jensen, *Angew. Chem.* **2007**, *119*, 5806-5810; g) J. S. Moore, C. D. Smith, K. F. Jensen, *React. Chem. Eng.* **2016**; h) L. M. Groves, C. Schotten, J. Beames, J. A. Platts, S. J. Coles, P. N. Horton, D. L. Browne, S. J. A. Pope, *Chem. Eur. J.* **2017**, *23*, 9407-9418; i) D. Ghislieri, K. Gilmore, P. H. Seeberger, *Angew. Chem. Int. Ed.* **2015**, *54*, 678-682; j) F. Venturoni, N. Nikbin, S. V. Ley, I. R. Baxendale, *Org. Biomol. Chem.* **2010**, *8*, 1798-1806; k) L. Guetzoyan, N. Nikbin, I. R. Baxendale, S. V. Ley, *Chem. Sci.* **2013**, *4*, 764-769; l) B. Desai, K. Dixon, E. Farrant, Q. Feng, K. R. Gibson, W. P. van Hoorn, J. Mills, T. Morgan, D. M. Parry, M. K. Ramjee, *J. Med. Chem.* **2013**, *56*, 3033-3047; m) D. C. Fabry, E. Sugiono, M. Rueping, *Isr. J. Chem.* **2014**, *54*, 341-350; n) D. C. Fabry, E. Sugiono, M. Rueping, *React. Chem. Eng.* **2016**, *1*, 129-133; o) D. E. Fitzpatrick, S. V. Ley, *React. Chem. Eng.* **2016**; p) D. E. Fitzpatrick, C. Battilocchio, S. V. Ley, *Org. Process Res. Dev.* **2016**, *20*, 386-394; q) B. Desai, K. Dixon, E. Farrant, Q. Feng, K. R. Gibson, W. P. van Hoorn, J. Mills, T. Morgan, D. M. Parry, M. K. Ramjee, C. N. Selway, G. J. Tarver, G. Whitlock, A. G. Wright, *J. Med. Chem.* **2013**, *56*, 3033-3047; r) D. E. Fitzpatrick, C. Battilocchio, S. V. Ley, *ACS Central Science* **2016**, *2*, 131-138; s) R. J. Ingham, C. Battilocchio, D. E. Fitzpatrick, E. Sliwinski, J. M. Hawkins, S. V. Ley, *Angew. Chem. Int. Ed.* **2015**, *54*, 144-148; t) S. V. Ley, D. E. Fitzpatrick, R. J. Ingham, R. M. Myers, *Angew. Chem. Int. Ed.* **2015**, *54*, 3449-3464; u) S. V. Ley, D. E. Fitzpatrick, R. M. Myers, C. Battilocchio, R. J. Ingham, *Angew. Chem. Int. Ed.* **2015**, *54*, 10122-10136; v) N. Holmes, G. R. Akien, R. J. D. Savage, C. Stanetty, I. R. Baxendale, A. J. Blacker, B. A. Taylor, R. L. Woodward, R. E. Meadows, R. A. Bourne, *React. Chem. Eng.* **2016**, *1*, 96-100; w) J. Li, S. G.

- Ballmer, E. P. Gillis, S. Fujii, M. J. Schmidt, A. M. E. Palazzolo, J. W. Lehmann, G. F. Morehouse, M. D. Burke, *Science* **2015**, *347*, 1221-1226; x) M. O'Brien, D. Cooper, *Synlett* **2016**, *27*, 164-168; y) M. O'Brien, L. Konings, M. Martin, J. Heap, *Tetrahedron Lett.* **2017**, *58*, 2409-2413; z) M. O'Brien, D. A. Cooper, J. Dolan, *Tetrahedron Lett.* **2017**, *58*, 829-834.
- [23] W. Czechtizky, J. Dedio, B. Desai, K. Dixon, E. Farrant, Q. Feng, T. Morgan, D. M. Parry, M. K. Ramjee, C. N. Selway, T. Schmidt, G. J. Tarver, A. G. Wright, *ACS Med. Chem. Lett.* **2013**, *4*, 768-772.

Chapter 4 – Investigating the Formation of Benzyne from Diazonium Salts

Table of Contents

1	Introduction.....	100
1.1	Benzyne	100
1.2	Benzyne from Anthranilic Acid	102
1.3	Benzyne Reactions.....	104
1.4	Benzyne in Flow	105
1.5	Acridones	109
2	Results and Discussion	111
3	Conclusion and Outlook.....	121
4	References	124

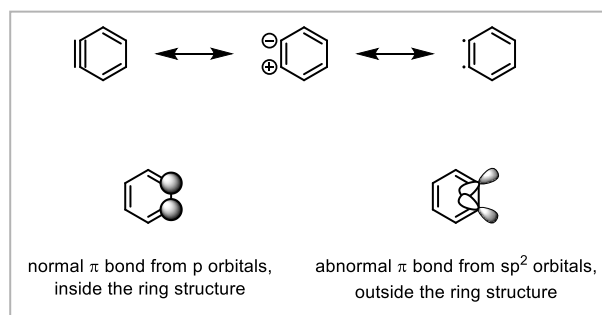
1 Introduction

This project aims to facilitate the safe handling of the benzyne precursor benzenediazonium-2-carboxylate in flow by making and consuming it *in situ*. Benzyne will then be used for the generation of valuable compounds in a multistep continuous flow process. Performing the reaction in flow allows the process to be inherently safer due to the small volume of reactive intermediate present at any time and the possibility to trap the reactive intermediate benzyne at a precise point in the reaction progress. Also, accurate temperature control allows the diazotisation step to be more controlled, avoiding exotherms leading to an uncontrolled decomposition of the diazonium salt. In addition, the good temperature control benefits the formation of benzyne under elevated temperatures.

1.1 Benzyne

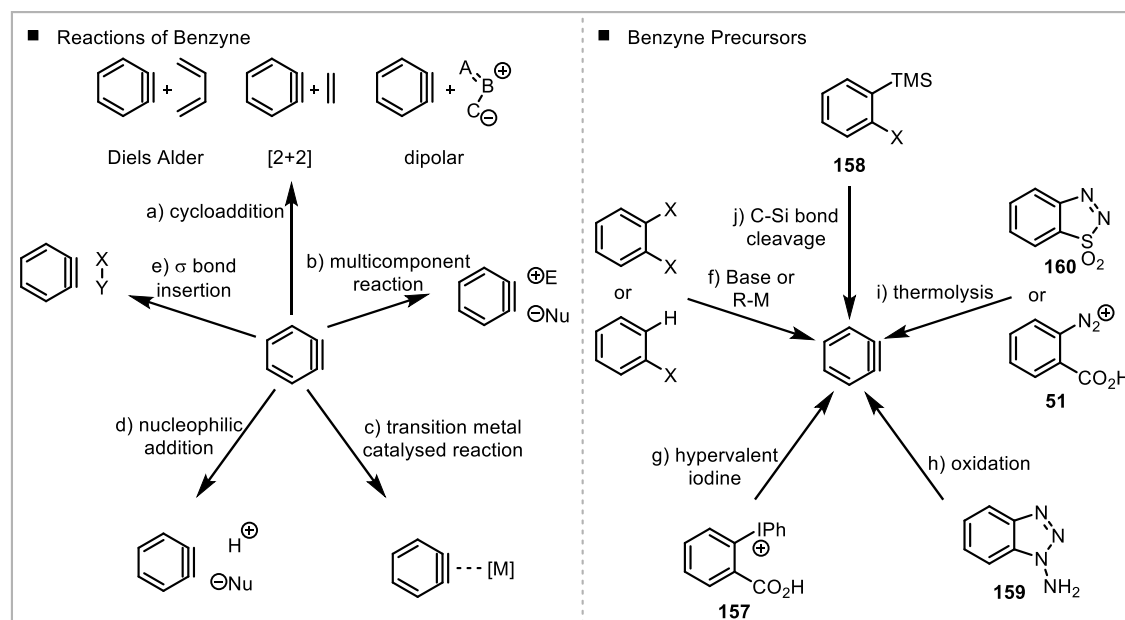
Benzyne is a useful building block for a number of transformations and has therefore been applied to a range of syntheses including natural products and heterocycles.^[1] Examples of transformations with benzyne include cycloadditions (Scheme 4.1, a), multicomponent reactions (b), transition metal catalysed reactions (c), nucleophilic additions (d) and σ bond insertions (e).

The reactivity of arynes is based on the bending of the triple bond to approximately 124° due to it being forced into a cyclic structure. This leads to mixing of the π^* and σ^* orbitals which lowers the LUMO considerably. In other words, the p orbital overlap is reduced, which makes arynes more reactive. This also results in arynes being primarily electrophilic, which is the opposite to alkynes.^[2] The reactivity can be displayed in the different resonance structures (Scheme 4.1) as the zwitterionic or the diradical structure. The triple bond is thereby formed by the overlap of sp^2 orbitals which are outside the ring.



Scheme 4.1: Benzyne Structure Representations

Benzynes can be synthesised from precursors, usually difunctionalised aromatic rings with a good leaving group and a group that can donate the electrons of the σ bond into the ring (Scheme 4.2, right).^[1a, 1c, 2-3]



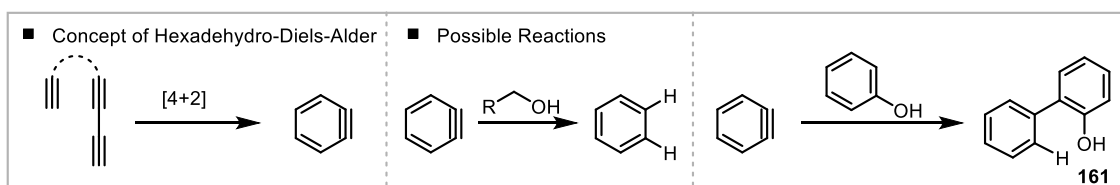
Scheme 4.2: Example Reactions of Benzyne and Methods for the Generation of Benzyne

The precursors can be classified into five different groups. The first example reported is the generation from an aryl halide via deprotonation or from a dihalide via halogen-metal exchange and subsequent elimination of the halide (Scheme 4.2, f). Examples include lithiates and Grignard compounds and the scope has been extended from just halides to other good leaving groups such as triflates. As strong bases must be used, harsh conditions limit the scope of that approach.

Other precursors usually utilise milder conditions as those precursors are highly activated themselves. Examples are the hypervalent iodine precursors (**157**) (Scheme 4.2, g) or precursors activated by a C-Si cleavage with a fluoride source such as the trimethylsilane aryl triflate (**158**) developed by Kobayashi in 1983 (Scheme 4.2, j).^[4] Another class can be activated by oxidation such as 1-aminobenzotriazole (**159**) which loses two nitrogen molecules upon activation (Scheme 4.2, h). However, the activation requires oxidants such as lead acetate which is not a desired route due to its toxicity. Two other examples, benzo azosulfone (**160**) and benzenediazonium-2-carboxylate (**51**) are derived from the diazotisation of the corresponding aniline (2-aminobenzenesulfonic acid and anthranilic acid) (Scheme 4.2, i). They decompose thermally to give sulfur dioxide or carbon dioxide, nitrogen and benzyne. Isolation of these compounds can be

dangerous as they can decompose violently upon impact. Indeed, the azosulfone (**160**) is rarely used as it decomposes at room temperature.

More recently tethered alkynes have been discussed as a route to arynes via a hexadehydro-Diels-Alder reaction as a mild route to form complex molecules (Scheme 4.3).^[5] Hoye and co-workers have thereby demonstrated the synthesis of benzyne both thermally and photochemically and applied their method to a range of trapping agents. Most importantly, they have shown that due to their mild and neutral conditions, different products can be observed compared to more traditional methods. Typical products observed under traditional methods are the adducts with alcohols. The authors could synthesise benzene with an alcohol as a proton source in one example and observed the S_{EAr} product (**161**) in the reaction with phenol in another example.



Scheme 4.3: Hexadehydro-Diels-Alder Reaction to Form Benzyne, Products Observed^[5]

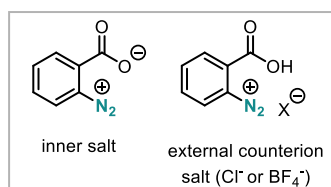
Most of these precursors are relatively expensive and substituted ones are often not commercially available. That means that a multistep synthesis for the precursors has to be applied prior to the actual synthesis.

The use of benzenediazonium-2-carboxylate offers the advantage of a simple one step procedure from commercially available anthranilic acids.

1.2 Benzyne from Anthranilic Acid

The advantages of the use of benzenediazonium-2-carboxylate, such as its easy preparation from readily available starting materials and mild conditions necessary for the formation of benzyne, are leading to its reinvestigation as a benzyne precursor.

Benzenediazonium-2-carboxylate has first been reported by Hantzsch and Davidson in 1896 where they reported the explosive nature of the dry compound.^[6] In addition to it existing as the inner salt, it can be isolated as the tetrafluoroborate or the chloride salt (Scheme 4.4) (both referred to as **51**).

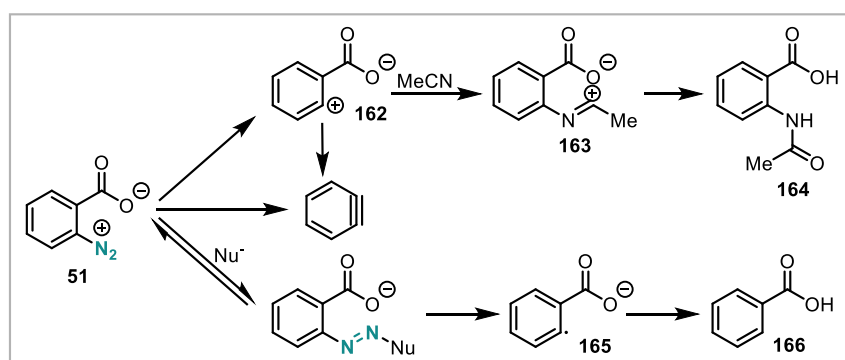


Scheme 4.4: Forms of Benzenediazonium-2-carboxylate

The decomposition of benzenediazonium-2-carboxylate was then further investigated by Stiles and Miller in 1960 and they proved the existence of benzyne by trapping benzyne with furan and anthracene in a Diels-Alder reaction and a nucleophilic addition with carboxylic acids.^[7]

Stiles and Miller then investigated the use of benzenediazonium-2-carboxylate as a benzyne precursor in parallel with Friedman and Logullo in 1963 in the search for milder conditions as opposed to the only method available at this time, which is the use of strong bases on arylhalide precursors.^[8] Notably, they isolated benzenediazonium-2-carboxylate in spite of its unstable nature and crystallised it as nearly colourless needles. However, they also mention that especially the dry benzenediazonium carboxylate is explosive when heated or scraped against a hard surface, which is also confirmed by accidents reported with these compounds and resulting warnings in the preparation.^[9]

Buxton *et al.* conducted mechanistic studies and showed that dependent on the solvent and ring substitution, different byproducts can be observed during the preparation and decomposition (Scheme 4.5).^[10] These byproducts can be derived by the stepwise loss of nitrogen and carbon dioxide and the authors have been able to trap the 2-carboxyphenyl cation (**162**) with acetonitrile (**163**) leading to the 2-carboxybenzimidazole (**164**) after aqueous workup. The diazonium salt can also be trapped with a nucleophile and the adduct can then homolytically decompose to form the 2-carboxyphenyl radical (**165**) which leads to benzoic acid (**166**) after aqueous workup.



Scheme 4.5: Decomposition Pathways of Benzenediazonium-2-carboxylate^[10]

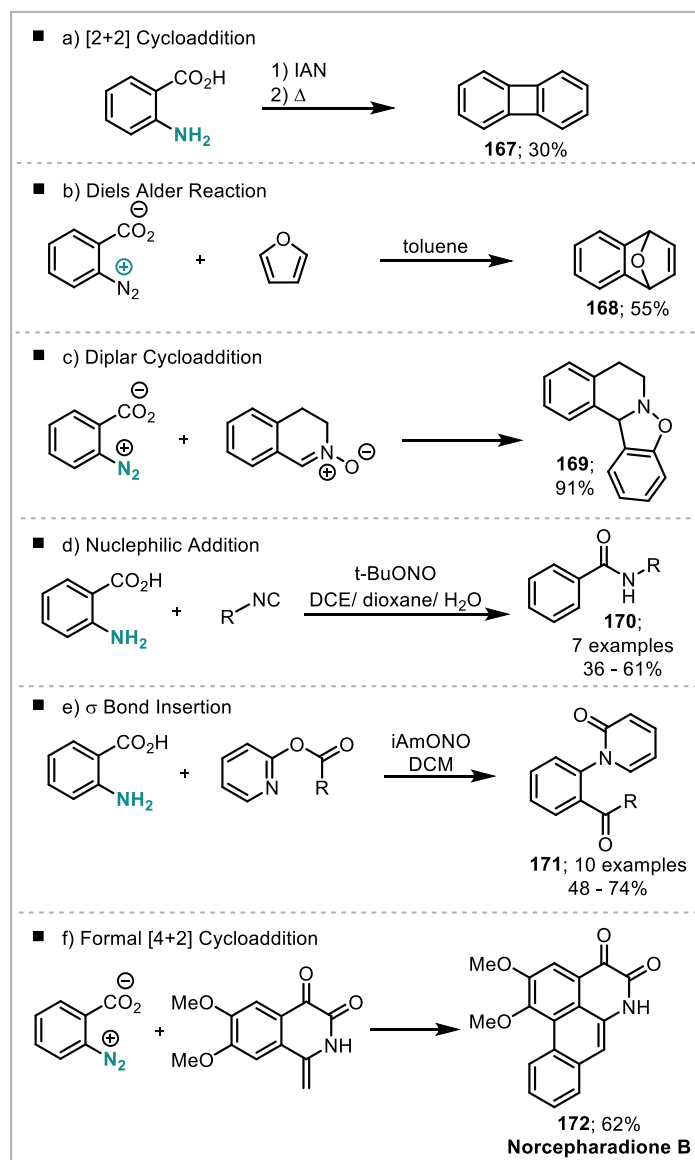
Since then benzenediazonium-2-carboxylate has been used as a benzyne precursor in a range of reactions including natural product synthesis with a lot of work having been published by Castedo in the 1980s and 90s for the preparation of isoquinoline derived alkaloids.^[11] Also the preparation from the dimethylamine triazene of benzenediazonium-2-carboxylate has been demonstrated by Moody in 1984 for the synthesis of the alkaloid ellipticine.^[12]

The isolation of the precursor is usually avoided and typical procedures drop the diazotisation agent into a hot solution of anthranilic acid and the trapping agent to make and consume the diazonium salt and benzyne immediately.

1.3 Benzyne Reactions

A range of different reactions with benzyne are known so the focus in this work will be on examples with benzyne derived from benzenediazonium-2-carboxylate (Scheme 4.6). Since the first proposal of the benzyne structure by J.D. Roberts in 1953,^[13] cycloaddition reactions with benzyne have been one of the most frequently employed class of reactions as the complexity of molecules can be quickly increased (Scheme 4.6a).^[14] The [2+2] cycloaddition of benzyne with itself, leads to the formation of biphenylene (**167**) that can often be seen as a side product in benzyne reactions.^[9c] The [2+2] addition of benzyne is thermally allowed due to the orthogonal π bonds comparable to a ketene. The Diels-Alder reaction with benzyne is employed in a lot of examples such as natural product synthesis (Scheme 4.6b).^[1a-e] Usual dienes are electron rich such as furan or anthracene and procedures in the literature to form these type of products, e.g. dihydroepoxynaphthalenes (**168**) from furan, are commonly *via* benzyne.^[7, 15] Seidl *et al.* investigated the formation of isoxazoles from *N*-oxides in dipolar cycloadditions (Scheme 4.6c). The authors were able to isolate stabilised isoxazoles such as benzisoxazoles (**169**) from the reaction with benzyne.^[16] For the nucleophilic additions on benzyne a lot of examples are known both inter- and intramolecularly (Scheme 4.6d).^[2] The example reported here uses isocyanides as nucleophiles to form the corresponding amide (**170**) after aqueous workup.^[17] Rayabarapu *et al.* reported the σ bond insertion of benzyne into pyridyl carboxylates (Scheme 4.6e).^[18] The reaction proceeds via the nucleophilic attack of the pyridine nitrogen and the back attack of the resulting anion onto the ester with resulting cleavage to form the acylphenyl pyridine (**171**) product. The last example shown is a formal [4+2] cycloaddition that proceeds stepwise (Scheme 4.6f).^[19] Castedo and co-workers developed a protocol with isoquinoline derivatives to generate aporphinoid alkaloids via this method. The enamine attacks the benzyne and the resulting anion can

then perform a conjugate addition into the iminium. Formal dehydrogenation then forms the alkaloid Norcepharadione B (**172**).

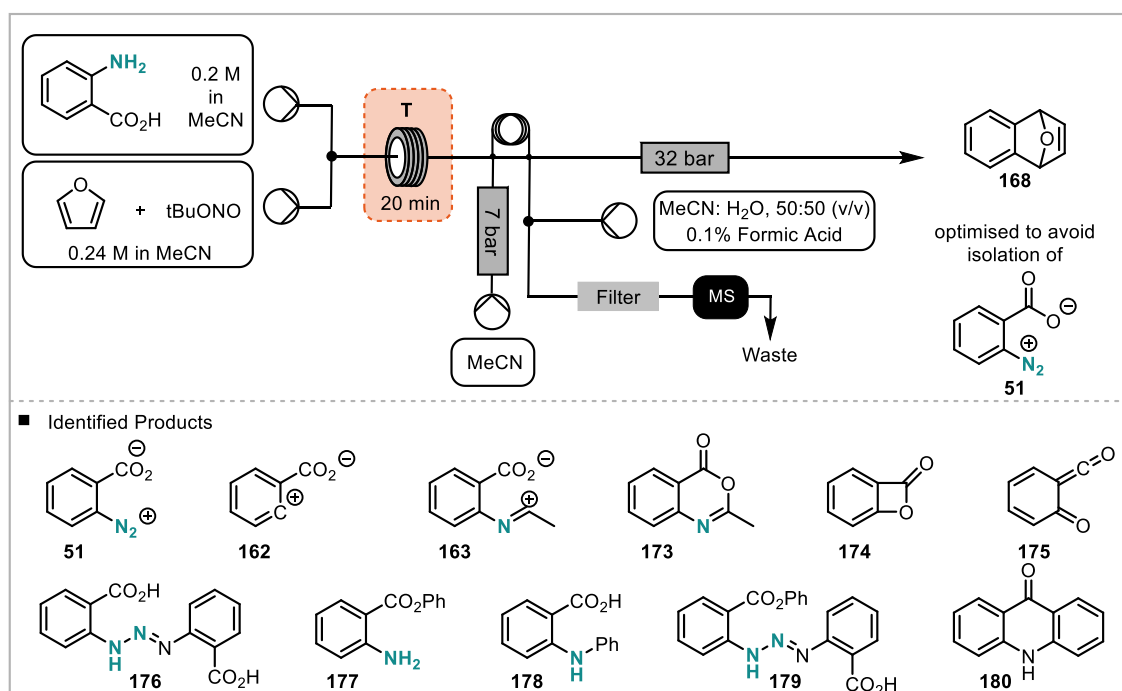


Scheme 4.6: Reactions with Benzyne

1.4 Benzyne in Flow

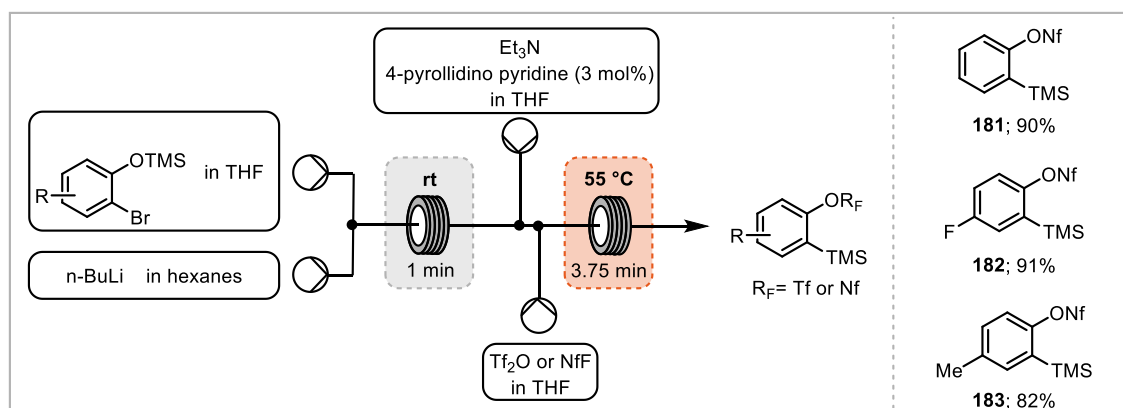
Due to the unstable nature of the benzenediazonium-2-carboxylate, flow procedures have been developed for its safe production and consumption. However, to date only a few investigations have been undertaken under continuous flow conditions. In addition, the use of benzyne from other precursors under continuous flow conditions is underrepresented. The reports in the literature make use of improved reaction parameter control for safety or selectivity reasons.

The diazotisation of anthranilic acid, decomposition of the diazonium salt and subsequent benzyne trapping with furan to the dihydroepoxynaphthalene (**168**) has been investigated by Ley and co-workers for the demonstration of an on-line mass spectrometer in flow (Scheme 4.7).^[20] The authors optimised the reaction to fully convert the benzenediazonium-2-carboxylate (**51**) for safety reasons. The setup consisted of merging a stream of anthranilic acid and a stream of furan and *t*-butylnitrite into a reactor coil at elevated temperatures. The outlet was passed through a sampling loop with a two-way-six-ports valve. At this point samples of the reaction stream could be taken for the on-line MS analysis. The stream was further diluted and filtered before passing through the spectrometer. The bulk reaction solution was collected for waste after passing through a back pressure regulator. With the aid of the mass spectrometer the authors have been able to optimise the process for the full consumption of the benzenediazonium-2-carboxylate (**51**). In addition, they could identify some intermediates and byproducts such as the carbocation (**162**) and acetonitrile adduct (**163**) confirming some of the observations made by Buxton *et al.*. They also observed the triazene (**176**) resulting from anthranilic acid attacking benzenediazonium-2-carboxylate and products resulting from benzyne reacting with starting materials and intermediates. They have also observed the acridone (**180**) which is the product of the reaction of anthranilic acid and benzyne.



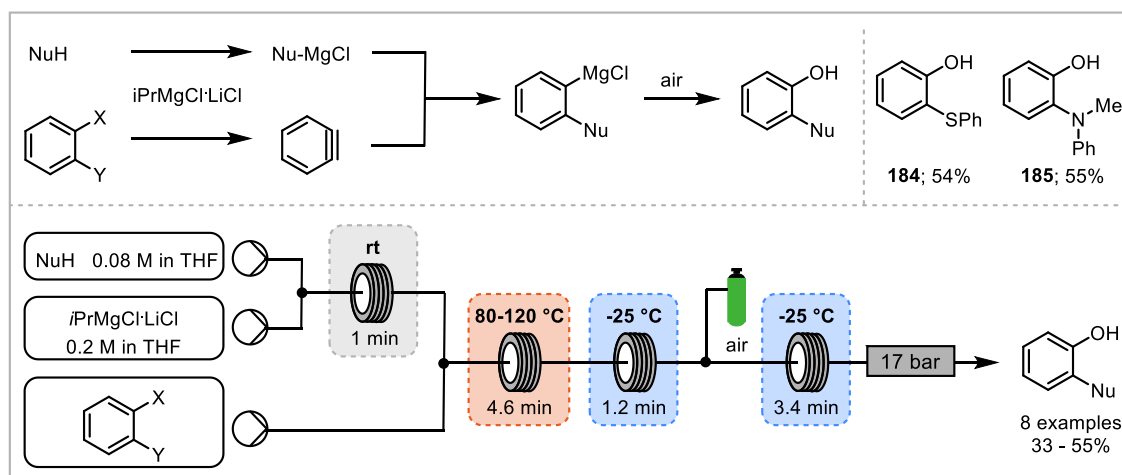
Scheme 4.7: On-line Reaction Monitoring of Benzyne Formation and Consumption Including Observed Products^[20]

The continuous formation of the Kobayashi precursor derivatives and nonaflyl alternatives has been investigated by Michel and Greaney in 2014 (Scheme 4.8). They were able to simplify the reaction procedure for this type of benzyne precursor (benzyne formation through C-Si bond cleavage) from a four step, two pot procedure to a single flow procedure. This was possible through the use of harsh reactions conditions such as the use of *n*-BuLi and improved reaction control to avoid side reactions. Also, they developed the nonaflyl substituted analogues to the Kobayashi type precursor as a more inexpensive and stable alternative. In this manner Michel and Greaney synthesised 12 different precursors and demonstrated their use in five different benzyne reactions ([4+2] cycloaddition, Pd catalysed triphenylene synthesis, σ bond insertion into an amide, benzyne Fischer indole reaction and σ bond insertion into a β -ketoester).^[21]



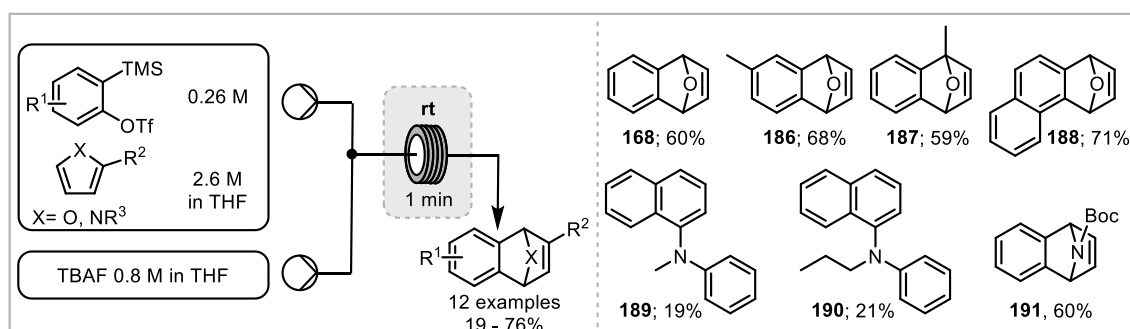
Scheme 4.8: Multistep Synthesis of Trimethylsilyl Phenyl Perfluorosulfonate Benzyne Precursors^[21]

Jamison and co-workers utilised the formation of benzyne for the synthesis of functionalised phenols (Scheme 4.9).^[22] Initially, the nucleophile was deprotonated with a Grignard reagent before merging with a stream of dihalidebenzene. At elevated temperatures magnesium halide exchange and elimination produced benzyne that was then intercepted by the deprotonated nucleophile and the magnesium halide to form a new Grignard reagent. The newly formed Grignard reagent then underwent aerobic oxidation under biphasic gas-liquid conditions to form the desired nucleophile-substituted phenol. The accurate control of temperatures and residence times to intercept intermediates and the use of biphasic conditions in the oxidation step increasing the mass transfer enabled this reaction to be performed in a three-step one-flow procedure.



Scheme 4.9: Synthesis of Functionalised Phenols by Oxidation of Grignard Reagents^[22]

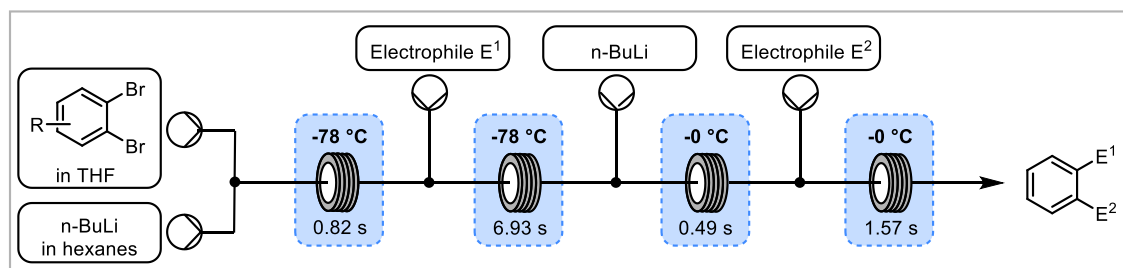
Later Khadra and Organ used three different Kobayashi type precursors for the Diels-Alder reaction with five-membered heterocycles under continuous flow conditions (Scheme 4.10).^[23] They used three differently substituted precursors ($R^1 = \text{H, Me, naphth}$) and tested up to five different furans and pyrroles for each of them. Interestingly, the reaction of *N*-alkyl pyrroles gave a different product than expected, a *N*-alkyl-*N*-phenylnaphthaleneamine (**189**, **190**). The benzyne and pyrrole first underwent the Diels-Alder reaction to give the expected dihydroepiminonaphthalene. This then further reacted with another equivalent of benzyne to ring open and give the observed product. This pathway was not observed with the Boc protected pyrrole where the reaction stopped at the Diels-Alder product (**191**).



Scheme 4.10: Kobayashi Type Precursors for the Diels-Alder Reaction of Heterocycles^[23]

Yoshida and co-workers developed a microreactor for the selective lithium-halogen exchange for a S_EAr with electrophiles under cryogenic conditions (Scheme 4.11).^[24] The main challenge was to avoid the formation of benzyne from the intermediate *o*-bromophenyllithium but instead to successfully intercept it with an electrophile. The authors accomplished that by working at low temperatures ($-78\text{ }^\circ\text{C}$) and short residence

times (0.8 s and 0.49 s) for the lithiation. They were able to develop a sequential reaction to exchange both bromides with electrophiles.



Scheme 4.11: Formation of *o*-Bromophenyllithium Without Benzyne Formation^[24]

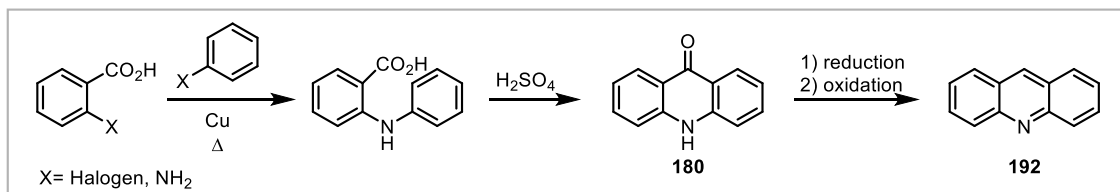
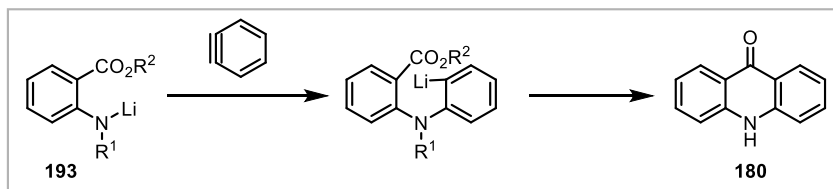
A similar approach has been applied to the multistep synthesis of phenylboronic acids via the *ortho* lithiation of a fluorobenzene by a collaboration of Cambridge Reactor Design, Dow Chemical Company and the laboratory of S.V. Ley in Cambridge.^[25] Important features are the use of a flow reactor platform that achieves cryogenic temperatures without the use of cryogenics (Polar Bear Plus) and the precise control of temperatures especially at points of mixing. The group has applied their synthesis to a scale up to make over 100 g of their target molecule.

1.5 Acridones

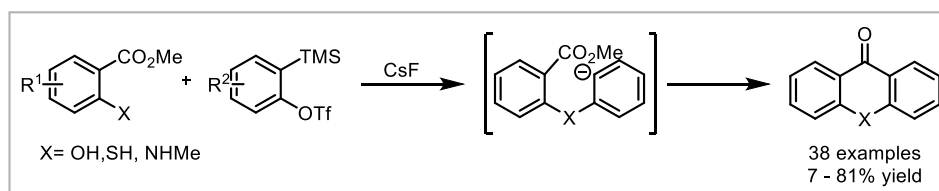
Acridones are of interest for the organic chemistry community as they are chemotherapeutic agents and show antimalarial activity.^[26]

Usual syntheses involve an Ullmann-Jourdan or Buchwald-Hartwig coupling and subsequent cyclisation under strongly acidic conditions (Scheme 4.12).^[3, 26a] Acridones (**180**) can be easily converted into acridines (**192**) via a reduction-oxidation sequence. Acridines are also chemotherapeutic agents but are also employed as organic photoredox catalysts.^[27]

The formation from benzyne has first been demonstrated by Watanabe in 1984 from lithiated methyl *N*-methylantranilate (**193**) (Scheme 4.13).^[28] Watanabe *et al.* produced benzyne from chlorobenzene and investigated different lithiating agents for the preparation of the the lithium anthranilate starting material. The use of lithium *N*-isopropylcyclohexylamine (LiICA) was found to be most effective and the authors demonstrated their method in the synthesis of four differently substituted acridones in 37-68% yield.

Scheme 4.12: Classical Synthesis of Acridones^[26a]Scheme 4.13: Acridone from Benzyne, Watanabe *et al.*^[28]

Larock and co-workers demonstrated the formation of acridones, xanthenes and thioxanthenes from the Kobayashi benzyne precursor (Scheme 4.14).^[29] The use of six different benzyne precursors and a range of anthranilates, salicylates and thiosalicylates gave them in total 38 different examples from poor to excellent yields. Importantly, the use of unsymmetrical benzyne precursors (such as 3-methyl) gave a mixture of regioisomers (1:1 ratio). Later, Larock and co-workers extended the scope of the reaction to the synthesis of acridines when reacting 2-aminoarylketones with benzyne.^[30]

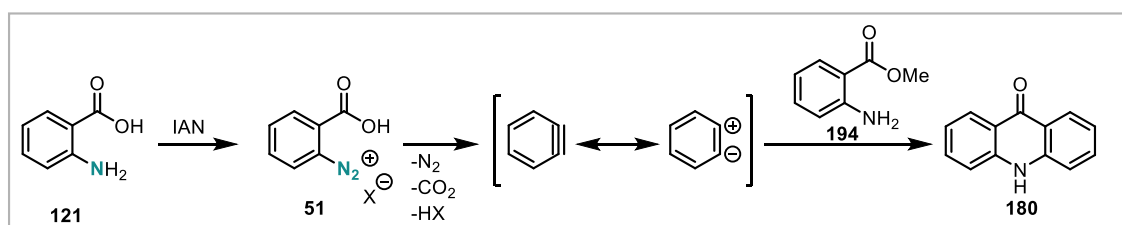
Scheme 4.14: Synthesis of Acridones, Xanthenes and Thioxanthenes^[29]

2 Results and Discussion

In this work, the *in situ* benzyne formation from anthranilic acid (**121**) and subsequent trapping in a nucleophilic addition is investigated under continuous flow conditions. After the nucleophilic attack the resulting phenyl anion is then quenched by an electrophile in a multicomponent reaction. That electrophile can be a proton in the simplest case, or by any other external nucleophile. However, this electrophile can also be part of the same molecule as the nucleophile, in which case an intramolecular cyclisation takes place. Few reactions using benzenediazonium-2-carboxylate (**51**) as a benzyne precursor are reported for an intramolecular multicomponent reaction.

The use of continuous flow methods allows the controlled and safe formation of the diazonium salt and its use without isolation in the next step. In addition, the precise temperature control in the second step allows the controlled release of benzyne.

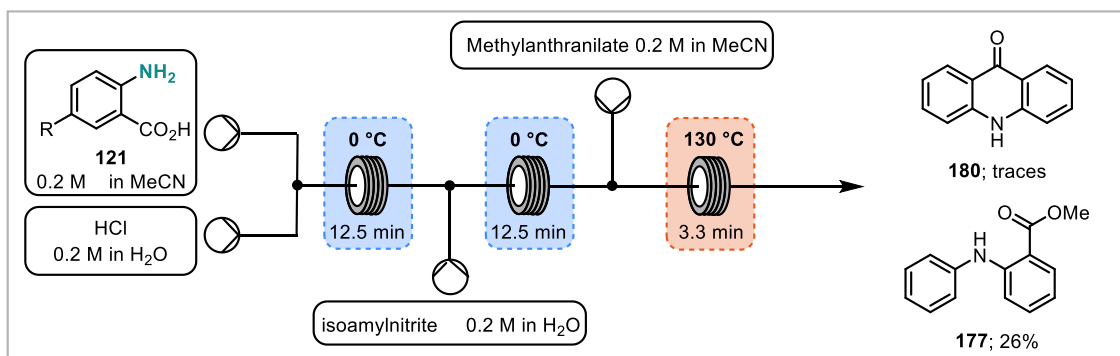
The reaction investigated in this work is the multistep formation of acridones (**180**) from benzyne. For this methyl anthranilate (**194**) functions as a nucleophile and electrophile as an example of an intramolecular multicomponent reaction (Scheme 4.15). Benzenediazonium-2-carboxylate (**51**) is formed from anthranilic acid (**121**) and isoamyl nitrite in the first step. Decomposition under elevated temperatures reveals the benzyne which can then react immediately with methyl anthranilate (**194**) in a second step. The amine group of methyl anthranilate attacks the benzyne nucleophilically and the benzyne can then ring close by attacking the ester moiety.



Scheme 4.15: Formation of Acridones from Benzyne

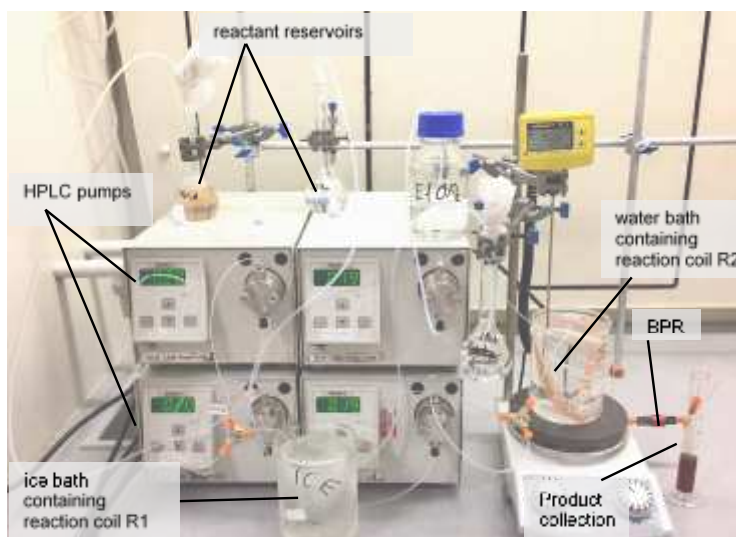
An initial reaction setup (Scheme 4.16) first merged an anthranilic acid (**121**) stream with an HCl stream, which passed through a small mixing coil. This stream then merged with an isoamyl nitrite stream to perform the diazotisation step in a cooled reaction coil. The diazonium salt solution then merged with a stream of methyl anthranilate (**194**) before entering a heated reaction coil. In that reaction coil the benzyne was unmasked and could react with the methyl anthranilate (**194**) already present in the reaction mixture to avoid side reactions. The formation of gas indicated the formation of benzyne to be

successful. After collection of the solution exiting the setup without further quenching the product was isolated by extraction and column chromatography.



Scheme 4.16: Initial Setup for the Formation of Acridones

The acyclic, *N*-arylated compound **177** resulting from the protonation instead of the envisioned ring closing was identified as a major product in the initial setup. The compound **177** has already been identified by Ley and co-workers as a side product in the reaction. The formation of the *N*-arylated compound **177** is probably due to the diazotisation being performed in acidic conditions and this excess of acid still being present during the reaction of benzyne with methyl anthranilate. Therefore, the diazotisation was performed under neutral conditions from then on. Further modifications of the initial setup included the incorporation of a BPR (Back Pressure Regulator, 250 psi, 17 bar) and a stream of EtOAc. The BPR avoided outgassing ensuring a homogenous reaction solution and an accurate residence time in the last reaction coil. The EtOAc was necessary to avoid precipitation of acridone product, which has a low solubility in the reaction solvent.



Picture 4.1: Reaction Setup

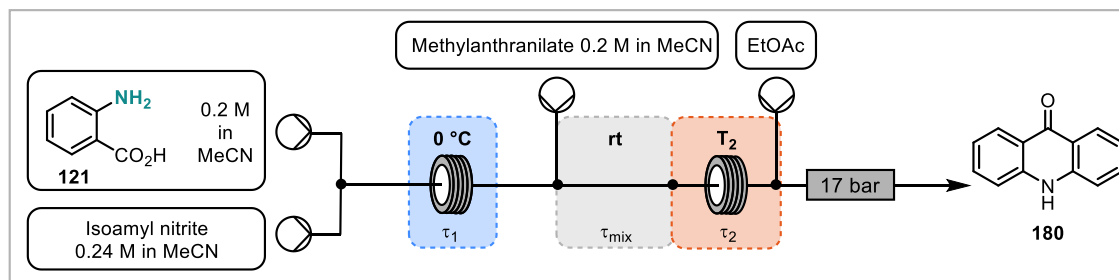
With a working setup in hand (Picture 4.1), an optimisation of reaction parameters including residence time for the diazotisation, temperature and residence time for the benzyne formation and trapping was performed (Table 4.1, entry 1-13). Quickly, a maximum of about 40% was observed for a wide range of reaction conditions. This could not be improved by stirring of the collection for a longer time and immediate quenching (entry 4 and 5).

As the reaction could potentially be limited by inefficient mixing of the diazonium salt and methylantranilate stream, which would lead to the formation of side products derived from benzyne reacting with itself, the mixing time was changed before the stream entered the elevated temperature zone. This was achieved by including different lengths of tubing before the elevated temperature reaction section (entry 14-16). However, no differences could be observed for the three lengths investigated.

The use of a BPR could potentially change the rate of benzyne being formed due to the formation of nitrogen and carbon dioxide as the side products. This includes both the gases forming bubbles and the gases dissolved in solution. The formation of gaseous products would be suppressed when the reaction solution is pressurised if the reaction was an equilibrium. In the case of the benzyne formation gas is released in form of bubbles that form slugs of gas. Control experiments without BPR are not possible without changing the residence time due to the gas release during the benzyne formation pushing out slugs of liquid. The amount of gas is dependent on the conversion of diazonium salt and therefore changes along the length of the reactor coil. Control experiments with similar residence times showed that the BPR did not affect the product yield significantly.

The equivalents of methylantranilate and isoamyl nitrite were increased and with 1.2 equiv of isoamyl nitrite an isolated yield of 51% was achieved (entry 19). The product was still formed when anthranilic acid was used instead of methylantranilate but as expected the yield decreased (36%, entry 20).

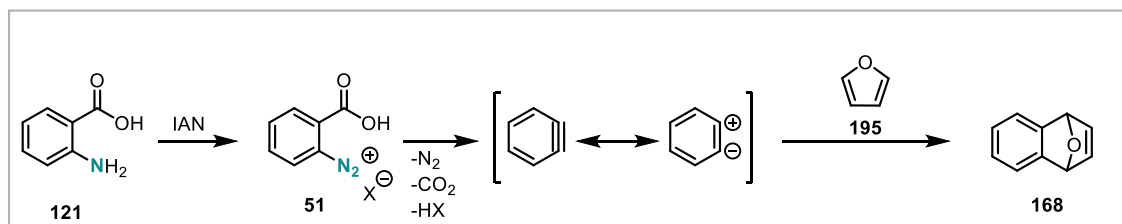
Table 4.1: Optimisation of the Formation of Acridones



entry	V ₁	T ₁ [min]	V ₂	T ₂ [min]	T [°C]	yield ^a %
1	2	5	1	1.67	90	29
2	7.5	18.75	1	1.67	90	27
3	5	12.5	1	1.67	90	32
4 ^b	5	12.5	2	3.33	90	36
5 ^c	5	12.5	2	3.33	90	43
6	5	12.5	2	3.33	90	41
7	7.5	18.75	2	3.33	90	43
8	5	12.5	3	5	90	37
9	5	12.5	4	6.67	90	41
10	5	12.5	5	8.33	90	40
11	5	12.5	3	5	70	34
12	7.5	18.75	3	5	90	37
13	5	12.5	2	3	110	39
14 ^d	5	12.5	2	3.33	90	39
15 ^e	5	12.5	2	3.33	90	41
16 ^f	5	12.5	2	3.33	90	37
17 ^{f,g}	5	12.5	2	3.33	90	46
18 ^{d,g}	5	12.5	2	3.33	90	31
19^{d,h}	5	12.5	2	3.33	90	51
20 ^{d,h,i}	5	12.5	2	3.33	90	36

a: isolated yields; b: collection stirred for another 30 min; c: collection into NaHCO₃ quench; d: mixing time before elevated temperature range 20 cm; e: mixing time before elevated temperature range 40 cm; f: mixing time before elevated temperature section 60 cm; g: 0.4 M methylantranilate; h: 0.24 M isoamyl nitrite; i: anthranilic acid instead of methylantranilate

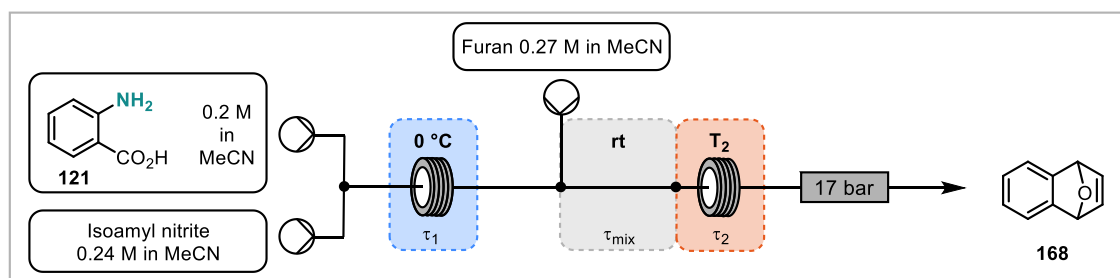
At this point it was decided to simplify the reaction system and instead investigate the Diels-Alder reaction with furan (**195**) as a model reaction for the formation of dihydroepoxynaphthalene (**168**) (Scheme 4.17). An extensive optimisation was performed using GC analysis for yield determination with mesitylene as internal standard. The yield plateaued just under 70% with a residence time of 7.5 min in the first coil and 3.3 min and 70 °C showing the best compromise of time and mild temperatures with 67% GC yield (Table 4.2, entry 8).



Scheme 4.17: Diels-Alder Reaction of Benzyne and Furan to Form Dihydroepoxynaphthalene

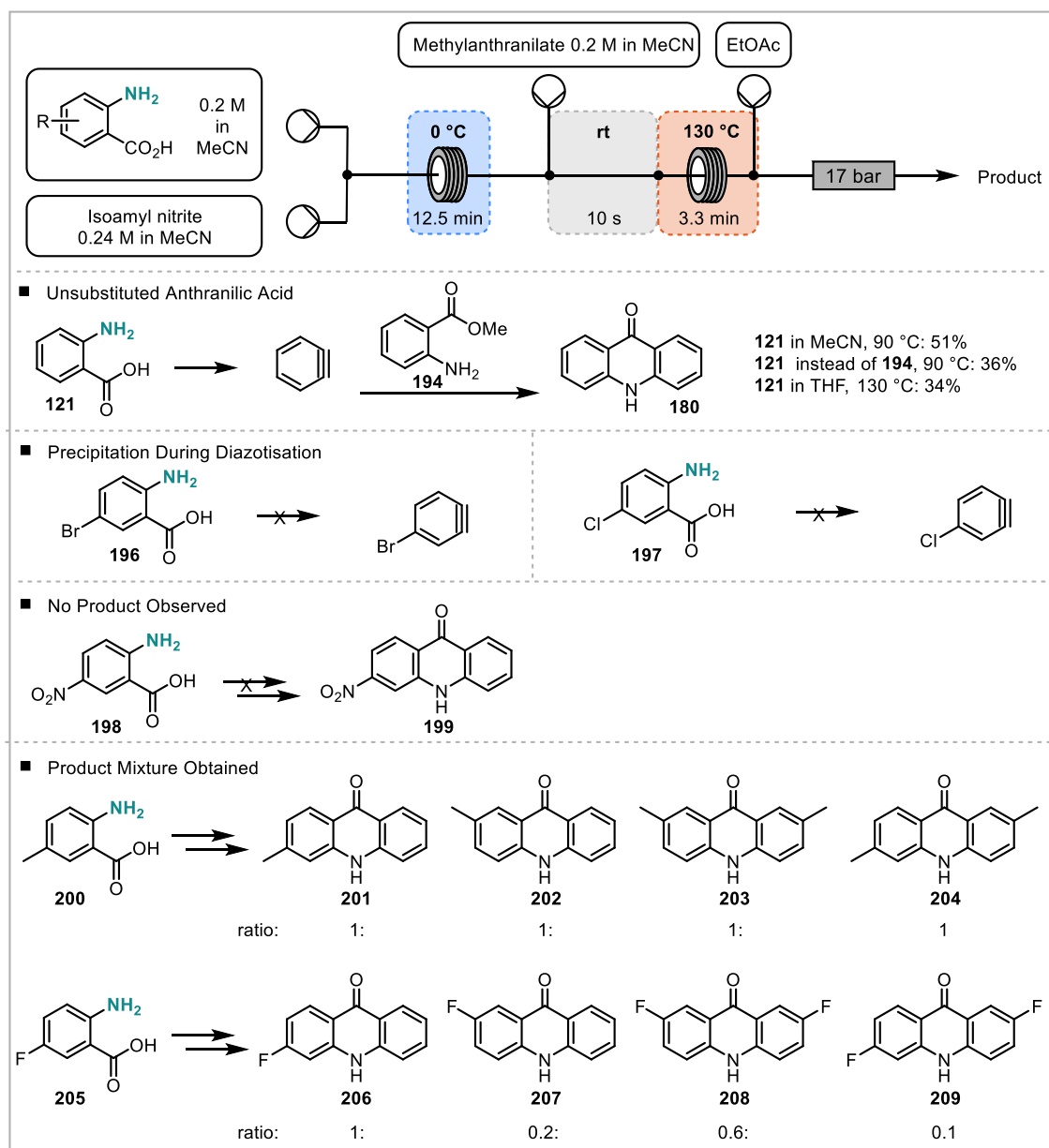
As substituted anthranilic acids are not well soluble in acetonitrile, different solvents were investigated. Benzyne reactions are often performed in benzene, dichloroethane or THF so that the solubility of 4-bromoanthranilic acid was tested. However, only THF could dissolve the substituted anthranilic acid. In addition acetone, diglyme and mixtures of acetonitrile and aqueous HCl were tested in the reaction as these are known to dissolve anthranilic acid and related products. Diglyme was not compatible with the GC method but product could be observed. Acetone and THF (entry 16 and 17) showed promising results but acetone was not further investigated due to its electrophilic nature and the increased possibility of side reactions.

When using THF as a solvent for the anthranilic acid stream (entry 17-22), decreased yields could be observed even if the reaction temperature was increased. A maximum yield could be observed when increasing the temperature to 130 °C (57%, entry 20). This second reaction condition screening proved, that the conditions established for the acridones were already optimised and no new set of parameters except for the solvents could be established. THF offers an alternative solvent system for the reaction of substituted anthranilic acids.

Table 4.2: Optimisation for the Diels-Alder Reaction of Benzynes and Furan to Form Dihydroepoxynaphthalene

entry	T ₁ min	T ₂ min	T ₂ °C	GC yield [%]
1	12.5	3.3	90	69
2 ^a	12.5	3.3	90	66
3 ^b	12.5	3.3	90	64
4	7.5	3.3	90	63
5	18.8	3.3	90	66
6	12.5	1.7	90	66
7	12.5	5	90	64
8	12.5	3.3	70	67
9	12.5	3.3	110	69
10	7.5	1.7	110	67
11	12.5	1.7	110	64
12	7.5	1.7	90	61
13	12.5	3.3	50	41
14	7.5	3.3	50	41
15	7.5	1.7	50	30
16 ^c	12.5	3.3	70	52
17 ^d	12.5	3.3	70	46
18 ^d	12.5	3.3	90	48
19 ^d	12.5	3.3	110	54
20 ^d	12.5	3.3	130	57
21 ^d	7.5	3.3	90	53
22 ^d	18.8	3.3	90	51

T_{mix} = 10 s; a: T_{mix} = 20 s; b: T_{mix} = 30 s; c: anthranilic acid in acetone; d: anthranilic acid in THF

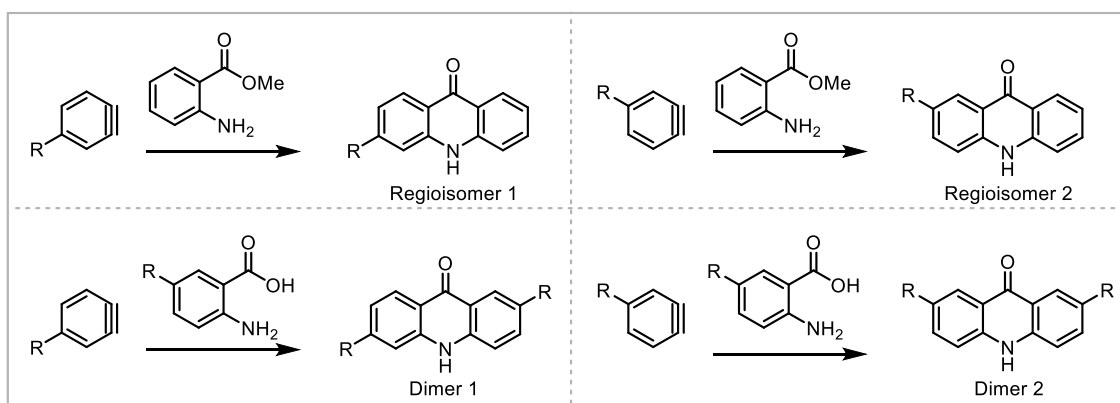


Scheme 4.18: Substrate Scope with Substituted Anthranilic Acids to Form Substituted Acridones

Having determined optimum conditions, a scope of acridones was performed (Scheme 4.18).

First, different substituted anthranilic acids were investigated for the formation of the acridone. The reactions with the bromo, chloro and nitro substituted anthranilic acids (**196**, **197**, **198**) were unsuccessful. The bromo and chloro substituted benzenediazonium-2-carboxylates precipitated in the first reaction coil and the reactions were aborted to avoid build-up of large quantities of potentially explosive diazonium salt precipitate. The reaction with the nitro substituted anthranilic acid **198** was performed smoothly, however no desired acridone product **199** could be observed.

Only the reaction of the methyl and fluoro substituted anthranilic (**200**, **205**) acids yielded a mixture of the desired products (**201 – 204** and **206 – 209**). The first two products **201/206** and **202/207** are regioisomers where the benzyne can react either way round to give the 3- or 2- substituted acridone (top row Scheme 4.19). The second two products **203/208** and **204/209** are derived from benzyne reacting with unreacted anthranilic acid starting material, giving a disubstituted acridone and its regioisomer (referred to as dimers, bottom row Scheme 4.18). The product mixtures were analysed by NMR (^1H , ^{13}C and ^{19}F for the fluorinated acridones). For both reactions, product mixtures with four nitrogen and four carbonyl environments could be identified and HRMS confirmed the existence of the expected products. For the methyl substituted product a ratio of approximately 1:1:1:1 (**201 – 204**) could be determined from the ^1H NMR, however no further assignment was possible. The combined yield was determined to be 33%. The ratio obtained is consistent with the ratio observed by Larock and co-workers when using methyl substituted benzyne for the preparation of acridones, xanthenes and thioxanthenes.^[29] The presence of both the mono- and dimethyl substituted acridones was confirmed by HRMS.



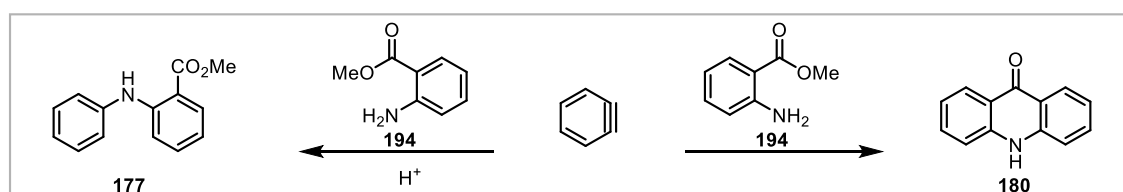
Scheme 4.19: Observed Products with Substituted Anthranilic Acids

For the reaction of the fluoro substituted anthranilic acid two of the four products could be partially separated. Examination of ^1H and ^{19}F revealed that these two products were a mixture of the 2-fluoro and the 2,7-difluoroacridone (**207** and **208**) which allowed the assignment of all products in the other fraction. The products were obtained in a total ratio of 1:0.2:0.6:0.1 (2-fluoro **207**, 3-fluoro **206**, 2,7-difluoro **208**, 3,7-difluoro **209**). Impurities with the same R_F prevented the calculation of an accurate yield. However, quantitative conversion of anthranilic acid to the four products is assumed as no evidence of unconverted anthranilic acid could be obtained and impurities are minor, according to

NMR. The presence of both the mono- and difluoro substituted acridones was confirmed by HRMS.

The regioselectivity for fluoro substituted benzyne reactions is mainly based on steric hindrance and inductive electronic effects. The regioselectivity is not based on resonance effects because of the reactive π bond being orthogonal to the aromatic system.^[2] The inductive electronic effect of fluorine favours one regioisomer through polarisation and stabilisation of the resulting carbanion whereas the methyl group shows only a weak electron donating capacity resulting in a nearly 1:1 ratio of the regioisomers. The fluorine group shows strong electron withdrawing capacity, resulting in the position *para* to fluorine preferably reacting with the nucleophile. Garg and co-workers investigated the regioselectivity on indolynes and showed that a distortion of the aromatic ring is the cause of this effect.^[31] Electron withdrawing substituents cause an unsymmetrical distortion and nucleophiles prefer the attack at the flatter, more positive end of the aromatic. Reports suggest that the inductively electron withdrawing capacity of a 3-methoxy group on benzyne only affords a single stereoisomer.^[29, 32]

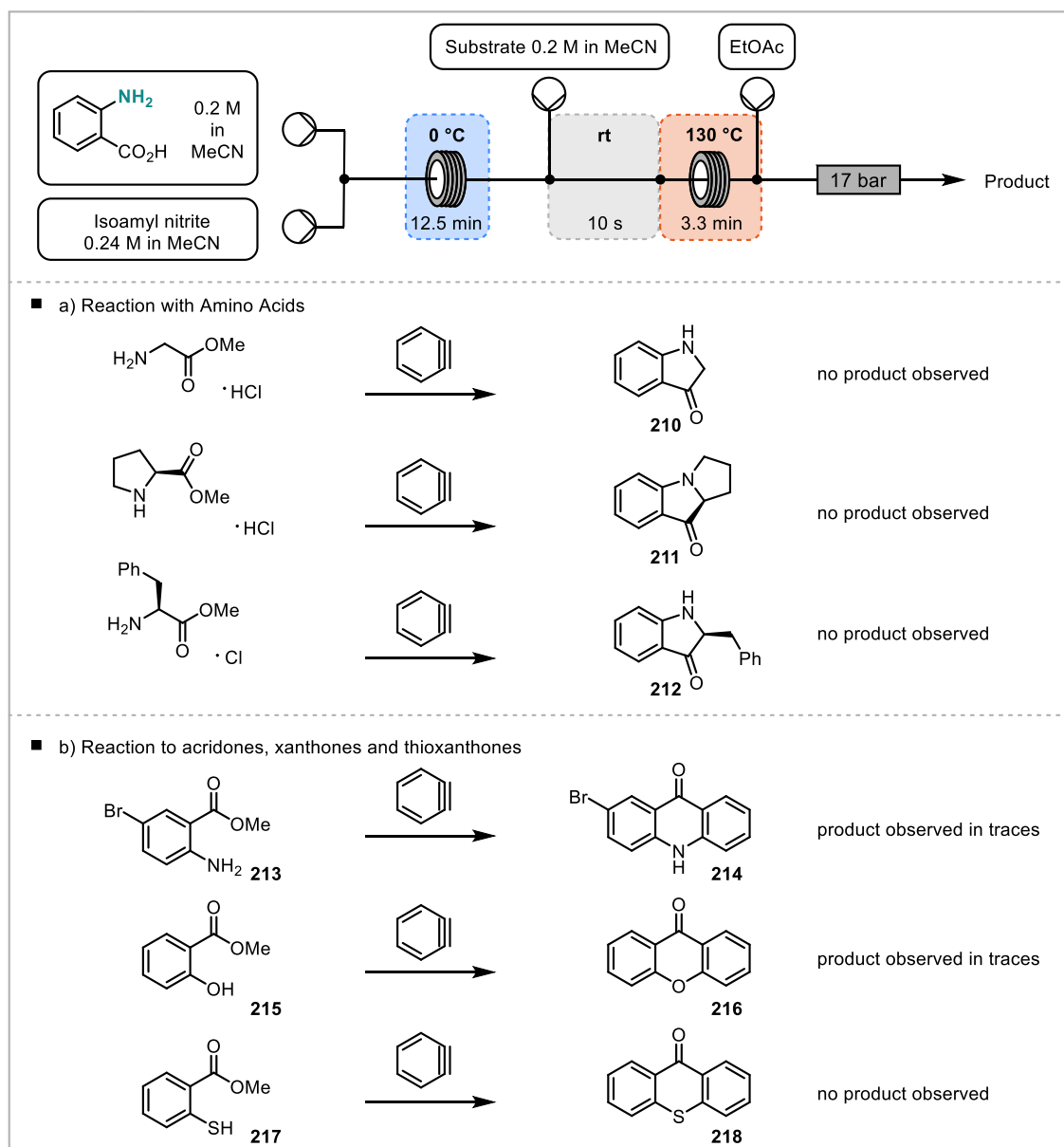
The uncyclised, *N*-arylated product **177** observed in initial studies was targeted by modifying the standard setup using a mixture of MeCN and aqueous HCl (3:1, 1 M HCl) for the anthranilic acid stream (Scheme 4.20). However, only cyclized product was observed. Compared to the initial results, the standard conditions vary also in the temperature and the concentration. Lowering the temperature, still no product **177** could be observed. This suggests, that the increased concentration in the standard reaction setup favours the formation of the acridone over the formation of the *N*-arylated product.



Scheme 4.20: Switch to Uncyclised, *N*-arylated Product **177 with Acid**

The reaction of benzyne with the methyl esters of three different amino acids (glycine, proline and phenylalanine) were investigated as substrates to form substituted indolinones **210** - **212** (Scheme 4.21, a). However, none of the reactions showed evidence of the desired product being formed by GCMS, NMR and TLC so that amino acid esters were not investigated further as substrates. Next, the reactions with a substituted methyl anthranilate (**213**), methyl salicylate (**215**) and methyl thiosalicylate (**217**) to form brominated acridone **214**, xanthone **216** and thioxanthone **218** were

performed (Scheme 4.21, b). GCMS showed traces of the brominated acridone **214** and the xanthone **216**, however the products could not be isolated. There was no evidence that the thioxanthone **218** was formed under the reaction conditions. Methyl salicylate **215** and thiosalicylate **217** were expected to be less suitable substrates due to the different strengths in nucleophilicity compared to methyl anthranilate **194**.



Scheme 4.21: Substrate Investigation with Amino Acids to Form Indolinones (a, left) and with Substituted Methyl Anthranilate, Methyl Salicylate and Methyl Thiosalicylate to Form a Substituted Acridone, Xanthone and Thioxanthone (b, right)

3 Conclusion and Outlook

The reaction of anthranilic acid to form benzyne and subsequent Diels-Alder reaction with furan and the reaction with methyl anthranilate to form acridones was investigated. A working continuous flow setup was developed and the reaction was optimised using this setup (51% acridone, 69% dihydroepoxynaphthalene). A few substrate variations were performed with mixed success. The reaction with substituted anthranilic acids demonstrated the limitation of solubility of starting materials and corresponding diazonium salts and highlighted the effects of benzyne substituents on the regioselectivity. The reactions with amino acids, substituted methyl anthranilates, methyl salicylate and methyl thiosalicylate did not yield the desired products.

In some reactions acridone **180** was observed as a byproduct. This byproduct resulted from undiazotised anthranilic acid reacting with benzyne proving that the diazotisation was not complete even under optimised conditions. This means that the residence time of the diazotisation needs to be adjusted to be longer for a complete reaction. *In situ* monitoring by IR or NMR might be useful tools to monitor the reaction and adjust parameters for complete conversion. The incomplete diazotisation will have been one of the reasons for relatively low yields.

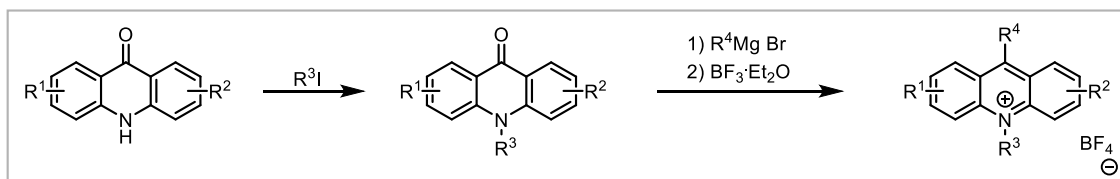
Another reason for the low yields could be the high reactivity of benzyne leading to undesired side reactions. For example, adducts of benzyne and isoamylalcohol and acetonitrile have been observed in GCMS. Unmasking benzyne under more controlled conditions could avoid these side reactions. This could include lower temperatures but longer reaction times in the second reaction coil to unmask benzyne more slowly but still give the reaction enough time to go to completion. Diluting the reactant stream might result in a lower amount of benzyne reacting with itself and thus increasing the chance to react with the desired product. Increasing the flow rates might lead to increased mixing and also benefit the reaction of benzyne with the desired substrate.

Future work on this project could include the further investigation of the synthesis of substituted acridones both *via* substituted anthranilic acids and substituted methyl anthranilates. For the anthranilic acids the substituents and their position can be carefully chosen to avoid regioisomers.

The change of solvent to acetone or diglyme could prevent precipitation of the diazonium salts. Other diazonium salt reactions are carried out in DMF, DMA or NMP which would present another alternative choice of solvent. However, especially in the case of acetone,

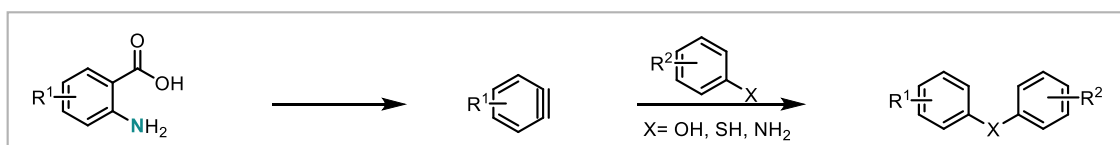
undesired products resulting from the solvent reacting with the reaction mixture have to be considered and avoided.

Acridones could be further derivatised to acridinium organic photoredox catalysts described by Nicewicz and co-workers (Scheme 4.22).^[33] The first step involves the arylation of the nitrogen, the followed by Grignard addition and aromatisation to the acridinium and counter ion exchange to afford the acridinium tetrafluoroborate.



Scheme 4.22: Further Derivatisation of Acridones to Acridinium Organic Photoredox Catalysts

The reaction of benzyne with nucleophiles in a more general term can be investigated (Scheme 4.23). This can offer a metal free alternative to traditional heteroatom-aryl coupling reactions such as Buchwald-Hartwig or Chan Lam couplings. The reaction with nucleophiles and benzyne from other precursors is known, however the reaction from benzenediazonium-2-carboxylate precursor has not been investigated in detail.^[2] A main side reaction can be the formation of a triazene (or other nucleophile analogues) that then decomposes in a radical pathway rather than giving the benzyne as discussed by Buxton *et al.* (Scheme 4.5).^[10] The addition of an acid might help the equilibrium of diazonium salt and triazene towards the diazonium salt and thereby towards the benzyne formation.



Scheme 4.23: Reaction of Benzyne with Other Nucleophiles

Different classes of nucleophiles can be investigated and are expected to require separate optimisation that differ from the acridone formation conditions (Scheme 4.23). The investigation of the reaction with different nucleophiles can be expanded by including amino acids and anthranilates as substrates to form *N*-arylated and ring closed products. The incorporation of amino acids might be an especially useful tool for the synthesis of indolinones bearing a stereocentre. The use of the amino acids directly, rather than their

methyl esters, is a possible alternative to the conditions applied in this work. The use of anthranilates could demonstrate how the same starting materials give two different products under different conditions applied (cyclic or acyclic).

4 References

- [1] a) H. Hart, in *Triple Bonded Functional Groups (1994)*, John Wiley & Sons, Ltd, **2004**, pp. 1017-1134; b) A. V. Dubrovskiy, N. A. Markina, R. C. Larock, *Org. Biomol. Chem.* **2013**, *11*, 191-218; c) P. M. Tadross, B. M. Stoltz, *Chem. Rev.* **2012**, *112*, 3550-3577; d) C. M. Gampe, E. M. Carreira, *Angew. Chem. Int. Ed.* **2012**, *51*, 3766-3778; e) A. Bhunia, S. R. Yetra, A. T. Biju, *Chem. Soc. Rev.* **2012**, *41*, 3140-3152; f) H. Pellissier, M. Santelli, *Tetrahedron* **2003**, *59*, 701-730.
- [2] H. Yoshida, in *Comprehensive Organic Synthesis II (Second Edition)*, Elsevier, Amsterdam, **2014**, pp. 517-579.
- [3] S. Kessar, in *Comprehensive Organic Synthesis (II), Volume 4: Additions to and Substitutions at C-C π -Bonds* (Ed.: I. Fleming), Pergamon, Oxford, **1991**, pp. 483-515.
- [4] H. Yoshio, S. Takaaki, K. Hiroshi, *Chem. Lett.* **1983**, *12*, 1211-1214.
- [5] a) S. Z. Tasker, P. J. Hergenrother, *Nature Chem.* **2017**, *9*, 504; b) S. P. Ross, T. R. Hoye, *Nature Chem.* **2017**, *9*, 523; c) V. D. Pogula, T. Wang, T. R. Hoye, *Org. Lett.* **2015**, *17*, 856-859; d) F. Xu, X. Xiao, T. R. Hoye, *J. Am. Chem. Soc.* **2017**, *139*, 8400-8403; e) T. R. Hoye, B. Baire, D. Niu, P. H. Willoughby, B. P. Woods, *Nature* **2012**, *490*, 208.
- [6] A. Hantzsch, W. B. Davidson, *Ber. Dtsch. Chem. Ges.* **1896**, *29*, 1522-1536.
- [7] M. Stiles, R. G. Miller, *J. Am. Chem. Soc.* **1960**, *82*, 3802-3802.
- [8] a) M. Stiles, R. G. Miller, U. Burckhardt, *J. Am. Chem. Soc.* **1963**, *85*, 1792-1797; b) L. Friedman, F. M. Logullo, *J. Am. Chem. Soc.* **1963**, *85*, 1549-1549; c) L. Friedman, F. M. Logullo, *J. Org. Chem.* **1969**, *34*, 3089-3092.
- [9] a) J. M. Sullivan, *Chemical & Engineering News Archive* **1971**, *49*, 5-7; b) T. F. Mich, E. J. Nienhouse, T. E. Farino, J. J. Tufariello, *J. Chem. Educ.* **1968**, *45*, 272; c) F. M. Logullo, A. H. Seitz, L. Friedman, *Org. Synth.* **1973**, 12-12.
- [10] P. Christopher Buxton, M. Fensome, H. Heaney, K. G. Mason, *Tetrahedron* **1995**, *51*, 2959-2968.
- [11] L. Castedo, C. González, E. Guitián, G. Nikonov, in *Encyclopedia of Reagents for Organic Synthesis*, John Wiley & Sons, Ltd, **2001**.
- [12] C. May, C. J. Moody, *J. Chem. Soc., Chem. Commun.* **1984**, 926-927.
- [13] S. S. Bhojgude, A. Bhunia, A. T. Biju, *Acc. Chem. Res.* **2016**, *49*, 1658-1670.
- [14] a) J. D. Roberts, H. E. Simmons, L. A. Carlsmith, C. W. Vaughan, *J. Am. Chem. Soc.* **1953**, *75*, 3290-3291; b) H. Heaney, *Chem. Rev.* **1962**, *62*, 81-97.

- [15] J. M. Medina, J. H. Ko, H. D. Maynard, N. K. Garg, *Macromolecules* **2017**, *50*, 580-586.
- [16] H. Seidl, R. Huisgen, R. Knorr, *Chem. Ber.* **1969**, *102*, 904-914.
- [17] J. H. Rigby, S. Laurent, *J. Org. Chem.* **1998**, *63*, 6742-6744.
- [18] D. K. Rayabarapu, K. K. Majumdar, T. Sambaiah, C.-H. Cheng, *J. Org. Chem.* **2001**, *66*, 3646-3649.
- [19] a) N. Atanes, L. Castedo, E. Guitian, C. Saa, J. M. Saa, R. Suau, *J. Org. Chem.* **1991**, *56*, 2984-2988; b) L. Castedo, E. Guitián, J. M. Saá, R. Suau, *Tetrahedron Lett.* **1982**, *23*, 457-458.
- [20] D. L. Browne, S. Wright, B. J. Deadman, S. Dunnage, I. R. Baxendale, R. M. Turner, S. V. Ley, *Rapid Commun. Mass Spectrom.* **2012**, *26*, 1999-2010.
- [21] B. Michel, M. F. Greaney, *Org. Lett.* **2014**, *16*, 2684-2687.
- [22] Z. He, T. F. Jamison, *Angew. Chem.* **2014**, *126*, 3421-3425.
- [23] A. Khadra, M. G. Organ, *J. Flow Chem.* **2016**, *6*, 293-296.
- [24] H. Usutani, Y. Tomida, A. Nagaki, H. Okamoto, T. Nokami, J.-i. Yoshida, *J. Am. Chem. Soc.* **2007**, *129*, 3046-3047.
- [25] a) J. A. Newby, D. W. Blaylock, P. M. Witt, J. C. Pastre, M. K. Zacharova, S. V. Ley, D. L. Browne, *Org. Process Res. Dev.* **2014**, *18*, 1211-1220; b) J. A. Newby, D. W. Blaylock, P. M. Witt, R. M. Turner, P. L. Heider, B. H. Harji, D. L. Browne, S. V. Ley, *Org. Process Res. Dev.* **2014**, *18*, 1221-1228.
- [26] a) P. Belmont, J. Bosson, T. Godet, M. Tiano, *Anti-Cancer Agents in Medicinal Chemistry- Anti-Cancer Agents* **2007**, *7*, 139-169; b) J. X. Kelly, M. J. Smilkstein, R. Brun, S. Wittlin, R. A. Cooper, K. D. Lane, A. Janowsky, R. A. Johnson, R. A. Dodean, R. Winter, *Nature* **2009**, *459*, 270; c) W. S. Alwan, A. A. Mahajan, R. A. Rane, A. A. Amritkar, S. S. Naphade, M. C. Yerigiri, R. Karpoornath, *Anti-Cancer Agents in Medicinal Chemistry- Anti-Cancer Agents* **2015**, *15*, 1012-1025.
- [27] a) J. A. Smith, R. M. West, M. Allen, *J. Fluoresc.* **2004**, *14*, 151-171; b) A. Joshi-Pangu, F. Lévesque, H. G. Roth, S. F. Oliver, L.-C. Campeau, D. Nicewicz, D. A. DiRocco, *J. Org. Chem.* **2016**, *81*, 7244-7249.
- [28] M. Watanabe, A. Kurosaki, S. Furukawa, *Chem. Pharm. Bull.* **1984**, *32*, 1264-1267.
- [29] J. Zhao, R. C. Larock, *J. Org. Chem.* **2007**, *72*, 583-588.
- [30] D. C. Rogness, R. C. Larock, *J. Org. Chem.* **2010**, *75*, 2289-2295.
- [31] a) P. H.-Y. Cheong, R. S. Paton, S. M. Bronner, G.-Y. J. Im, N. K. Garg, K. Houk, *J. Am. Chem. Soc.* **2010**, *132*, 1267-1269; b) G.-Y. J. Im, S. M. Bronner, A. E. Goetz, R. S. Paton, P. H.-Y. Cheong, K. Houk, N. K. Garg, *J. Am. Chem. Soc.* **2010**, *132*, 17933-17944.

- [32] a) Z. Liu, R. C. Larock, *Org. Lett.* **2004**, *6*, 99-102; b) H. Yoshida, S. Sugiura, A. Kunai, *Org. Lett.* **2002**, *4*, 2767-2769; c) Z. Liu, R. C. Larock, *Org. Lett.* **2003**, *5*, 4673-4675.
- [33] N. A. Romero, K. A. Margrey, N. E. Tay, D. A. Nicewicz, *Science* **2015**, *349*, 1326-1330.

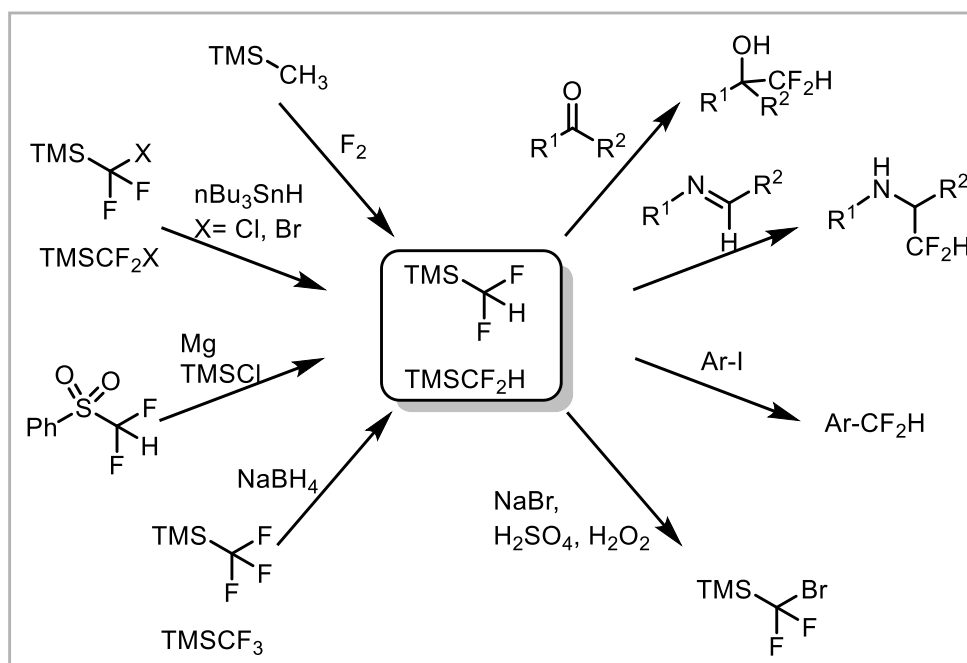
Chapter 5: Continuous Flow Reaction Monitoring for the Optimisation of Space-Time Yield of an Exothermic Reaction

Table of Contents

1	Introduction.....	128
2	Results and Discussion	133
2.1	Temperature Measurements.....	133
2.2	NMR Measurements.....	139
2.3	Hybrid Flow - Batch Large Scale Reaction.....	146
3	Conclusions and Outlook.....	151
4	References	152

1 Introduction

The synthesis of commodity chemicals is of great importance for the chemical industry. Especially the introduction of new commodity chemicals. This presents a challenge as viable routes for their large scale production have to be established. One such example of these chemicals is TMSCF_2H (difluoromethyl trimethyl silane). TMSCF_2H is a nucleophilic difluoromethylation agent, but due to its higher price and reduced reactivity, compared to the Ruppert Prakash reagent TMSCF_3 (trifluoromethyl trimethyl silane), applications are still few. However, in the last few years, the field is expanding.^[1] The nucleophilic difluoromethylation of carbonyls, imines, and iodides has been demonstrated since. TMSCF_2H is a precursor to TMSCF_2Br which can be converted into difluorinated acetonitrile and is used as a precursor for difluorocarbenes (Scheme 5.1). Recently, the Browne group has demonstrated use of TMSCF_2H in the formation of difluoromethyl thioethers.^[2]



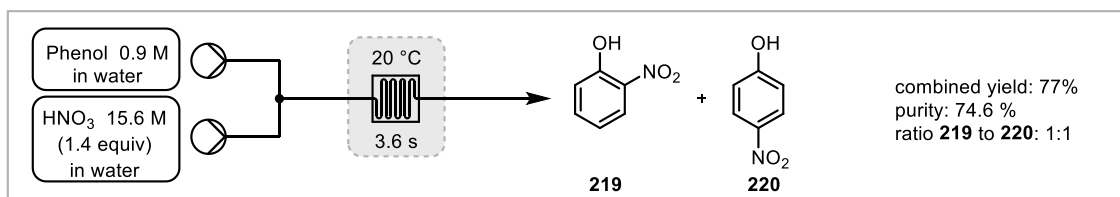
Scheme 5.1: TMSCF_2H Preparation and Its Synthetic Uses

TMSCF_2H can be prepared *via* the fluorination of tetramethylsilane with fluorine gas.^[3] However, safety concerns due to the use of fluorine gas and low selectivities make this approach unattractive. TMSCF_2H can also be prepared *via* the reductive monodehalogenation of TMSCF_2X ($\text{X} = \text{Cl, Br}$) or the reductive difluoromethylation of chlorosilanes from sulfides, sulfoxides or sulfones (Scheme 5.1).^[4] The reductive difluoromethylation of chlorosilanes is magnesium mediated and affords the disulfide as a byproduct. However, the most direct preparation is the method introduced by

Igoumnov and co-workers in 2011 where the Ruppert-Prakash reagent TMSCF_3 is reduced with sodium borohydride.^[5] Notably, this process is highly exothermic and is described by the authors as vigorous. Depending on the solvent, for example in DMF, even outbursts and small explosions of the reaction mixture are possible. The authors report the reaction in diglyme both for safety reasons but also due to the formation of fewer side products. The reaction is performed by suspending sodium borohydride in diglyme and adding the TMSCF_3 slowly to the ice cold solution. Even if this is done carefully, thermal runaways are still possible and scale up requires even longer addition times and lower temperatures. This has been verified within the Browne group. The reaction is completed by stirring the reaction mixture over night. A double distillation is then necessary to obtain the clean TMSCF_2H . The mechanism of this reaction is intriguing and potentially complex.

Safety issues due to large heat releases in chemical reactions often create challenges in the development of procedures, especially for large scale production.^[6] A qualitative way to describe whether a reactor is in a stable operation condition is the Semenov diagram. This diagram visually takes the heat transfer rate and heat production rate into account in order to identify a stable operation condition. The heat transfer rate has to be higher than the heat production rate for the operation conditions to be stable and avoid a thermal runaway. This means the heat has to be removed from the system faster than it is produced. This is explained in the Semenov diagram by the curve of the heat production rate having a lower value than the heat transfer rate. The necessary data thereby has to be acquired using calorimetric experiments.

Continuous flow methods can allow improved access to highly exothermic reactions as the surface area to volume ratio is high and heat can be dissipated effectively which means the heat transfer rate is hugely increased (see chapter 1.2.1 Introduction – Continuous Flow Processing – Heat Transfer).^[7] Generally, flow reactors with inner diameters smaller than 1 mm can cope with heat production rates 1000 fold higher than classical batch reactors which allows a broader scope of reaction types to be possible.^[8] The applicability to highly exothermic reactions has been investigated in the nitration of phenols where Ducry and Roberge measured exotherms using a calorimeter (Scheme 5.2). The exotherm control during nitration of phenols is of particular importance, as runaway reactions would lead to potential explosions. The authors first investigated the reaction exotherm using a calorimeter and DSC measurements before transferring the reaction into a glass microreactor. The authors could successfully control the exotherm and run the reaction under more concentrated conditions. This led to a more efficient process resulting in higher yields and selectivities during the reaction avoiding the usual polymeric side products, which characterise a poorly controlled reaction.



Scheme 5.2: Nitration of Phenols, Optimised Conditions

Since this report, other exothermic reactions, such as the use of organometallic reagents have been performed under continuous flow conditions to take advantage of the improved heat dissipation.^[9]

In this work, the use of a hybrid continuous flow – batch approach was envisaged to control the exotherm occurring during the reduction of TMSCF₃ with sodium borohydride at room temperature. This would avoid the use of low temperatures which are often costly to achieve. The continuous flow part of the reactor would allow the safe dissipation of the bulk of the exotherm during the early part of the reaction. The outlet of this would then drop into a heated batch vessel, where the reaction would be completed at elevated temperatures while the product was being removed by distillation. The flow part would therefore be key to control the exotherm safely and the batch part would decrease the reaction time significantly through the use of elevated temperatures for the slower part of the reaction. Key to realising this hybrid approach is the determination of a temperature profile of the reaction and then the decision of when to transfer the reaction from flow into batch (safety cut-off point, ScoP) (Figure 5.1). In the first scenario (ScoP 1), the safety cut-off point has been chosen at an early point during the reaction at a low conversion. The conversion of the reaction is proportional to the release of heat as the reaction slows down towards the end. Thus, the exotherm might not be fully dissipated at this early stage of the reaction. The early transfer into a batch vessel presents a potential risk of a runaway reaction. In the second scenario (ScoP 2), the safety cut-off point was chosen later in the reaction profile when the conversion only increases minimally over time. At this point, the bulk of the exotherm has been dissipated and the reaction progress is slow in the flow part of the reactor. This means, the reactor space is not used optimally, but the process is safe. In the third scenario (ScoP 3), an ideal balance between safety and reactor space is chosen. The bulk of the exotherm has been dissipated and the later, slower part of the reaction can be performed in a batch reactor.

The choice of where this safety cut-off point will be, is thereby highly dependent on individual operator targets and safety regulations within the institution where the reaction is performed.

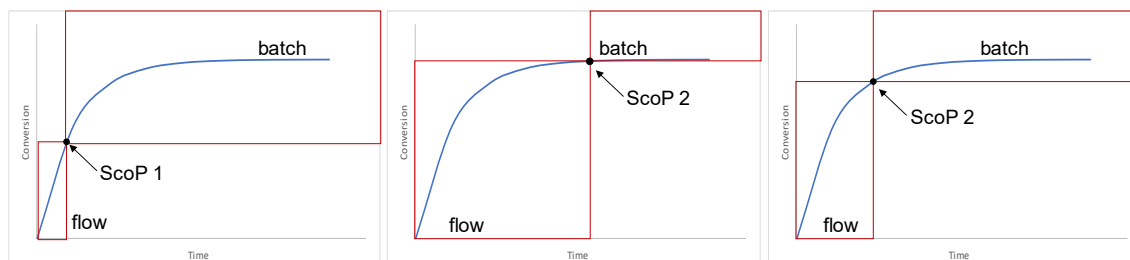


Figure 5.1: Identification of Safety Cut-Off Point (ScoP)

To link a temperature profile along the tubular reactor to a yield of the reaction, *in line* NMR monitoring was envisioned. Various *in line* and on-line measurements have been established for continuous flow processing such as UV/Vis, IR, MS, LC and NMR methods (see Chapter 1.2.6).^[10] NMR spectroscopy is most familiar to the day-to-day practise of an organic chemist, it provides quantitative information and offers the prospect of providing structural information. On-line monitoring using NMR has been widely established when coupled to a HPLC system.^[11] The introduction of benchtop spectrometers made the use of NMR methods for on-line or *in line* monitoring of reactions a widely available method.^[12] Fyfe and co-workers reported a flow NMR cell that could be used with a normal NMR machine in 1977 for the use of flow and stopped-flow reaction investigations.^[13] Later, Astra Zeneca (2010) and Bruker also developed flow NMR cells that could be used without the need of any modifications.^[14]

In this work, the Bruker InsightMR is used for the ¹⁹F NMR monitoring of the reduction of TMSCF₃ to TMSCF₂H. The flow cell, called InsightMR flow tube, consists of a normal NMR tube, a holder and tubing going into and out of the cell. The cell is inserted into a normal NMR machine instead of a normal NMR tube. This approach has the advantage of using high-field NMR spectrometers with high resolution and good sensitivity allowing the acquisition of spectra every few seconds leading to a good temporal resolution. Other methods to achieve high resolution have been developed but highly modified systems such as detector coils have to be used.^[11a, 15] The use of common NMR machines with the Bruker InsightMR allows the performance of multinuclear experiments such as those required in this work. The InsightMR tube is designed to accurately control the temperature by the incorporation of a recirculating chiller. Up to date, the InsightMR has only been used for the on-line monitoring of batch reactions.^[14]

The use of ^{19}F NMR for yield determination avoids the use of deuterated solvents or solvent suppression pulse sequences while acquiring high resolution spectra on crude reaction mixtures. To date, only one other report has used *in line* ^{19}F NMR for the monitoring of a continuous flow process.^[16] Rehm and co-workers developed a synthesis platform that included a NMRReady-60e benchtop NMR. They demonstrated its use in the investigation of a Krapcho decarboxylation, Ruppert Prakash perfluoroalkylation and the photochemical arylation of furan and used the benchtop NMR to monitor reaction progress.

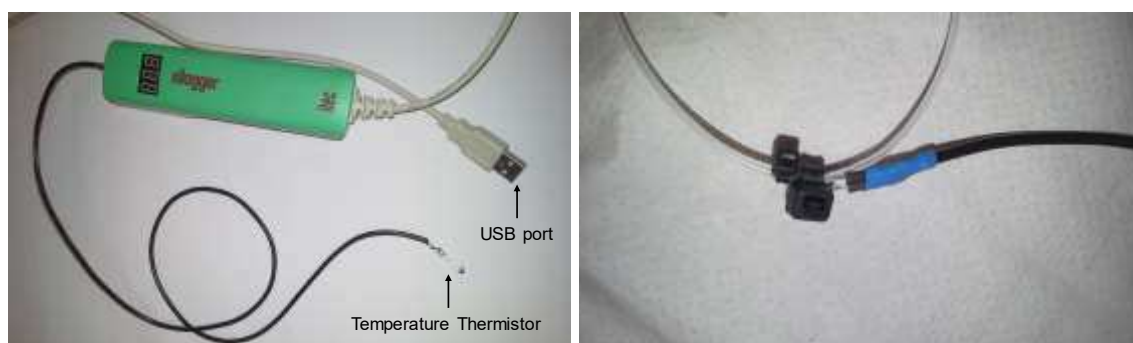
Flow NMR cells are usually limited by the maximum flow rate they can tolerate. The maximum flow rate tolerated by the Bruker InsightMR is 4 mL/min. This is due to the pressure resistance of the glass tube but also to ensure accurate measurements. At a higher flow rate, nuclei that are excited by the radiofrequency pulse have left the sample chamber before their FID can be recorded making the measurement inaccurate. The Bruker InsightMR has an internal volume of 1.5 mL, which has to be taken into account when waiting for steady state. The mixing properties within the glass tube are different than in the flow reactor and measurements should be taken long enough apart to have replaced all the internal volume.^[14c]

2 Results and Discussion

2.1 Temperature Measurements

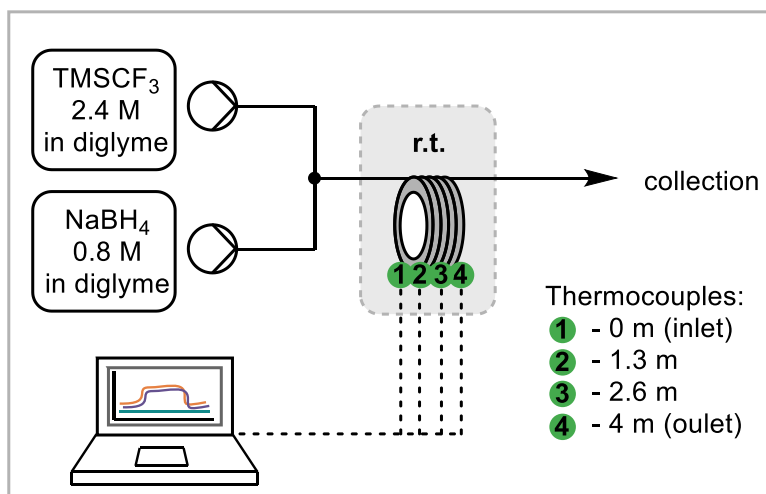
The sodium borohydride reduction of TMSCF_3 to TMSCF_2H was transferred into flow by making one solution of sodium borohydride in diglyme and one solution of TMSCF_3 in diglyme. These solutions were to be mixed in a T-piece and then enter the reaction coil (0.8 mm ID, 1.2 mm OD, PFA, 2 mL, 4 m). The maximum concentration of sodium borohydride in diglyme (0.8 M) was chosen. To have the same molar ratio of sodium borohydride and TMSCF_3 as in batch (1:3), the concentration of TMSCF_3 in diglyme was set to 2.4 M.

The temperature profile of the sodium borohydride reduction of TMSCF_3 to TMSCF_2H was investigated first. To quantify the temperature profile, commercially available thermocouples (xlogger, Itec) were used which were connected to a computer via USB.^[17] The data was then recorded and processed in an Excel spreadsheet using the xlogger plug-in software. These thermocouples were connected to the outside of the flow tubing (Picture 5.1). Four thermocouples were connected along the tubing (T1: inlet, 1 cm; T2: 1/3 of the length, 1.3 m; T3: 2/3 of the length, 2.6 m; T4: outlet, 4 m).

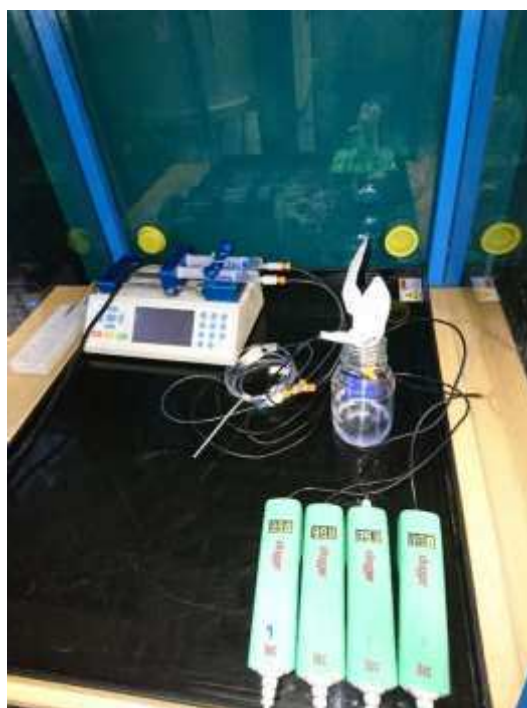


Picture 5.1: xlogger Thermocouples with Temperature Thermistor Attached to Flow Tubing

Initial experiments showed that temperature changes, depending on the flow rate, could be detected outside of the tubing. Offline NMR measurements showed that TMSCF_3 was converted into TMSCF_2H . However, the reaction proved to not be completed and TMSCF_3 was still present. These experiments also showed that the system was very sensitive towards draughts and temperature changes in the environment. The areas around the sensors were therefore insulated with a small amount of cotton wool and the experiments were performed in a thermostatically controlled room (18 °C) without the use of extraction fans. Using this modified setup, the temperature changes along the tubing for different flow rates were measured (Scheme 5.3 and Picture 5.2).



Scheme 5.3: Modified Flow Setup for Temperature Measurements



Picture 5.2: Picture of Flow Setup for Temperature Measurements

The temperature was recorded upon starting the pumps. Reaching steady state (here in terms of constant temperature) took 6-8 residence times, which is due to the need of the temperature equilibrating outside the tubing. A typical measurement is shown in Figure 5.2 and Figure 5.3 (3 mL/min, 0.7 min residence time). The raw data (Figure 5.2) was calibrated for all sensors to start at room temperature (Figure 5.3). The time until the first response of the sensors is dependent on their position along the tubing as the reaction mixture takes different times to pass the sensor.

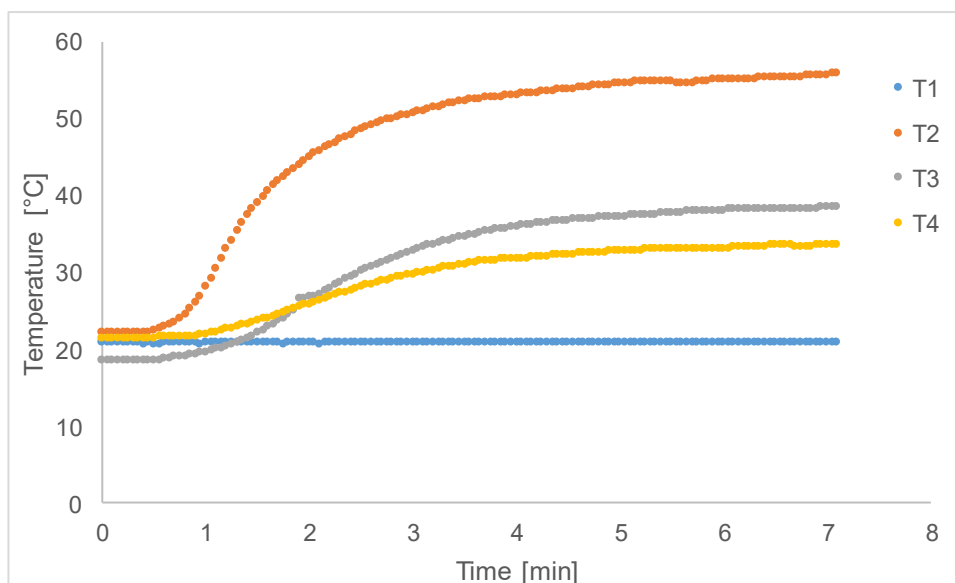


Figure 5.2: Crude Temperature Measurement for One Flow Rate (3 mL/min, 0.7 min Residence Time)

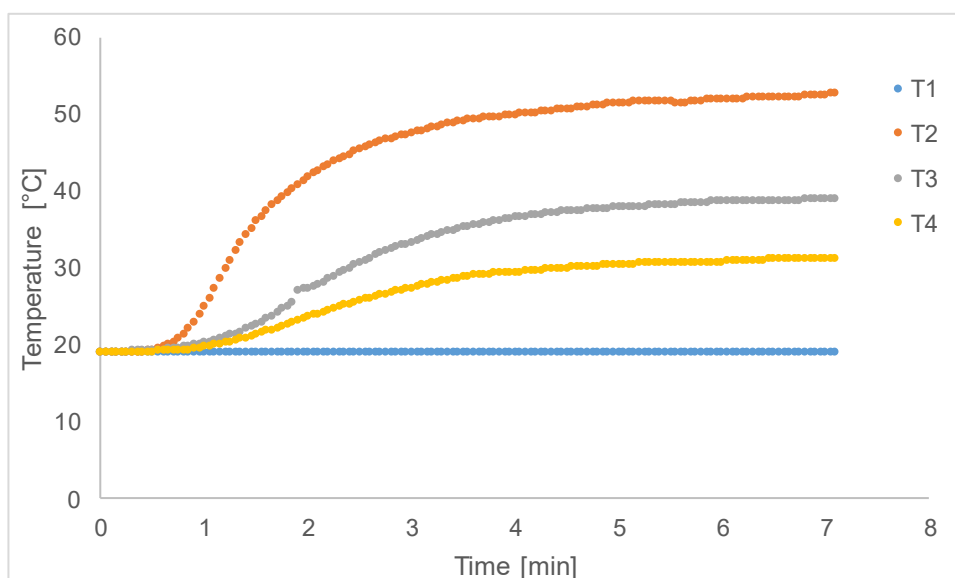


Figure 5.3: Calibrated Temperature Measurement for One Flow Rate (0.3 mL/min, 0.7 min Residence Time)

The temperature along the tubing was measured for 5 different flow rates (0.5 - 4 mL/min) (Table 5.1). The use of a finite number of thermocouples leads to the fact, that the exact position of the maximum cannot not be determined and will always be in between two thermocouples. In this work four thermocouples were used and the approximate position of the exotherm was estimated. At all flow rates tested, the temperature went through a maximum and decreased over the length of the tubing with the exact value of the temperature depending on the flow rate (Figure 5.4).

At slow flow rates (0.5 mL/min and 1 mL/min), the exotherm is negligible and the temperature hardly increases. For the other three flow rates tested (2 mL/min, 3 mL/min and 4 mL/min), the maximum temperature measured was at the second point along the tubing (T2, 1.3 m) with the highest temperature observed for the highest flow rate (58 °C at 4 mL/min). For all flow rates, the temperature then decreases further along the tubing which means the maximum of the exotherm has been successfully dissipated. Notably, the temperature at the inlet stays at room temperature independent of the flow rate which indicates that the reaction has not yet started to produce heat. This is due to incomplete mixing in the beginning of the reaction coil. The temperature difference along the tubing is larger at higher flow rates and the maximum exotherm is always near the second point along the tubing (T2) as it gives the highest reading for each flow rate.

Notably, the tubing for the slow flow rates always felt cold to the touch, indicating that no temperature increase was missed by the exact placement of the thermocouples.

Table 5.1: Temperature Measurement Results

entry	flowrate [mL/min]	residence time [min]	T1 [°C]	T2 [°C]	T3 [°C]	T4 [°C]
1	4	0.5	20	58	46	39
2	3	0.7	20	55	41	33
3	2	1	20	45	33	29
4	1	2	19	25	25	22
5	0.5	4	21	21	21	20

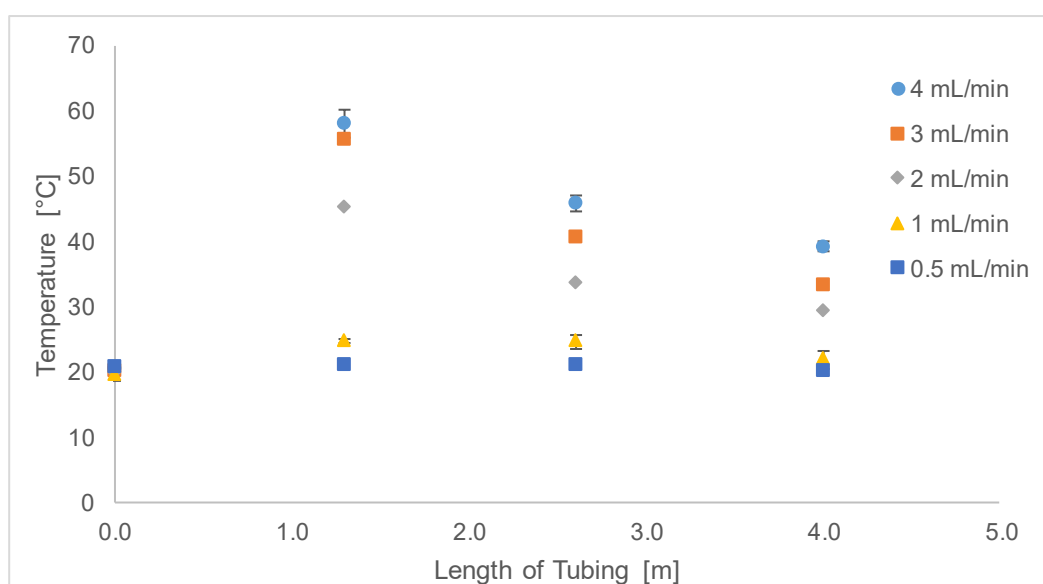


Figure 5.4: Temperature Profile Along the Length of the Tubing

Measurements for two flow rates (4 mL/min and 1 mL/min) were repeated two more times to assess errors. The errors in the mean were a maximum of 2 °C. Notably, the outside temperatures are reported rather than internal temperatures.

The temperature measured is the result of the heat transfer rate (cooling in the reactor) and the heat production rate (exotherm) which both have to be taken into account when explaining the observations.

The maximum of the heat production rate, or the maximum of the exotherm, corresponds to the maximum rate of reaction. The maximum rate of reaction should always be at the same time during the reaction progress if other factors such as mixing and temperatures are constant. This should result in a shift of the maximum exotherm along the tubing; for low flow rates it should be at the beginning of the reactor, for fast flow rates it should move towards the end.

The heat transfer rate is highly dependent on the surface area. For a fast flow rate, one aliquot of the flow reaction mixture is, in the same amount of time, in contact with a larger surface area compared to an aliquot during slow flow rate. This results in a higher heat transfer rate and a more efficient heat dissipation for faster flow rates.

The combination of the effects of heat production and heat transfer rate should result in a temperature profile with an early, high temperature maximum for slow flow rates and a later, lower maximum for faster flow rates. The opposite is observed. To justify the observed results against the hypothesized results, other factors such as mixing must be taken into account.

In the setup applied, the maximum exotherms occur at approximately the same point along the tubing, as far as can be determined using this method, independent of the flow rate. This indicates that the reaction rate changes with the flow rate. At faster flow rates the mixing of the reactants is more efficient due to the transition from a laminar to a turbulent flow regime. This can result in a reaction rate enhancement. This would lead to the heat production maximum of fast flow rates occurring earlier than expected as the reaction rate is increased. This becomes apparent when the temperature is shown vs the residence time (Figure 5.5).

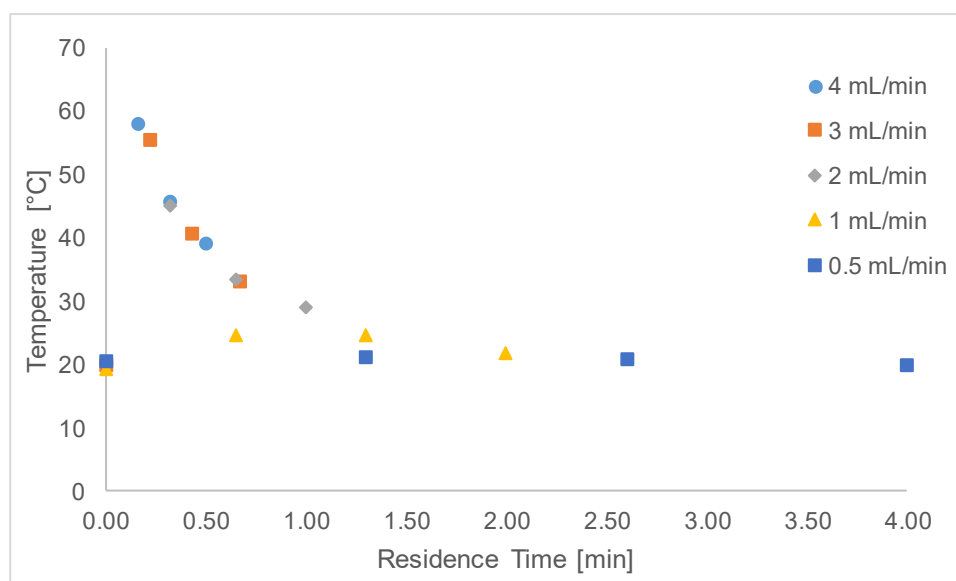


Figure 5.5: Temperature Profile for Different Residence Times

The maximum temperatures for low flow rates (0.5 mL/min and 1 mL/min) are lower than the temperatures for the other flow rates at the same point in time. This means that the heat production rate is higher for the fast flow rates due to an increased reaction rate.

Due to a higher reaction rate, the maximum heat production rate occurs earlier along the tubing. At the point of the maximum temperature, the reaction mixture has passed through a shorter length of tubing compared to the reaction without a reaction rate enhancement. This decreases the experienced surface area and therefore the heat transfer rate and results in an increase in the measured temperature. As the maximum exotherm for a slow and a fast flow rate occur approximately at the same point along the tubing, the surface area experienced by the reaction mixtures are very similar. Therefore, the surface area is not the main difference on the heat transfer rate but instead it is the time the reaction mixture has to dissipate the heat. For a slow flow rate reaction, the exotherm can be dissipated during a longer time resulting in a lower temperature.

In addition, the temperature increase of the reaction mixture could increase the reaction rate further in accordance to Arrhenius' law. This means that, reactions performed at faster flow rates (higher temperatures observed) would require less time than a reaction performed at a slower flow rate (lower temperatures observed).

Mixing effects and heat transfer in microreactors have been discussed in the literature (see Chapter 1.2.1 and 1.2.2). However the combination of those, in this case the increased heat production rate due to increased mixing, has not been discussed.

The temperature measurements showed, that the maximum of the exotherm is dissipated at all flow rates tested which was the main objective of the temperature measurements.

In addition, these measurements showed that the flow rate has a detrimental effect on the temperature profile. The change in flow rate likely resulted in a change of flow regime from laminar to turbulent which increased the mixing of the reactants. This resulted in an increased reaction rate for fast flow rate and changed the temperature significantly. The reaction rates were even further increased due to the reaction being performed at temperatures above room temperature.

However, no quantitative conclusion about the reaction yield could be made other than that it is not finished at the outlet. Therefore, *in line* ^{19}F NMR measurements, through the use of the Bruker InsightMR flow tube, were incorporated.

2.2 NMR Measurements

The InsightMR flow tube is joined to a connector box through a jacketed tubing (Figure 5.6). The connector box attaches the jacket to a recirculating chiller for temperature control and the tubing inside to an inlet and an outlet. The flow cell (Picture 5.3) consists of a holder and a spinner like adapter to which the glass tube is attached. The inlet tubing (0.5 mm ID, 0.8 mm OD, PTFE) inside the jacket leads from the connector box to the flow cell, through the spinner into the bottom of the glass tube. The outlet tubing leads from the top of the glass tube through the spinner back to the connector box.

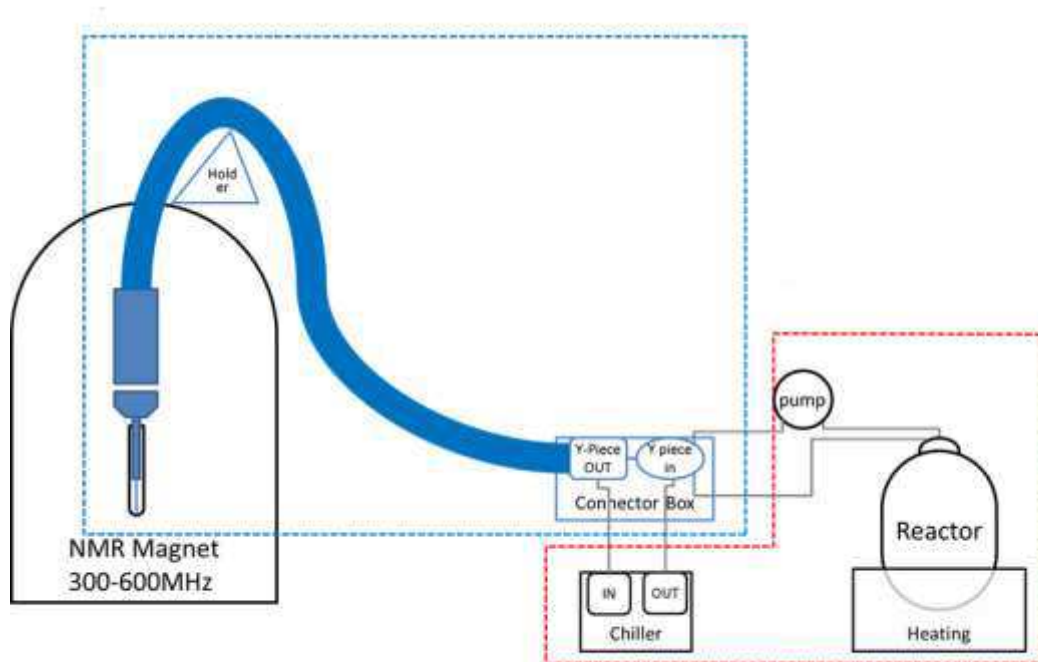


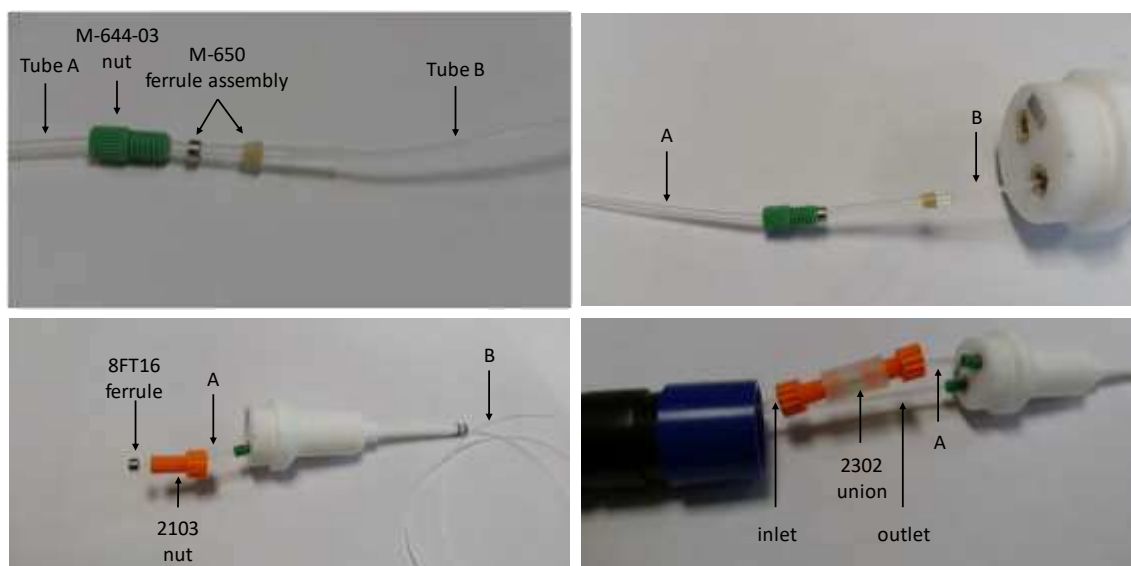
Figure 5.6: InsightMR Setup^[18]



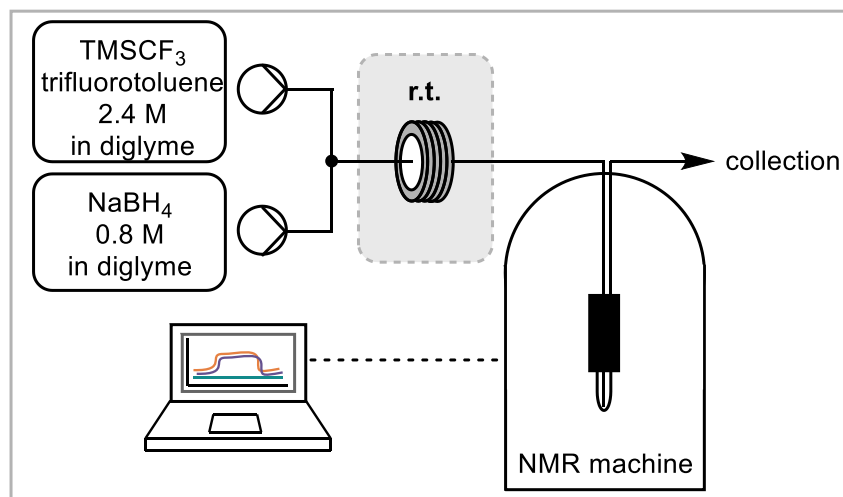
Picture 5.3: InsightMR Flow Tube

To compare the *in situ* NMR measurements to the temperature measurements (standard PFA 0.8 mm ID and 1.2 mm OD tubing), it was necessary to modify the InsightMR setup in terms of tubing diameter and material. The assembly, including part numbers from the IDEX catalogue, is described in Picture 5.4. A short piece of the smaller diameter tubing (tube B) was needed to go through the spinner of the flow cell into the bottom of the glass tube. This was sleeved by the standard tubing (tube A) and fixed to the spinner through the tightening of the nut (green) and ferrule assembly. The other end of tube A was connected to the standard nut (orange) and ferrule to connect to the reactor coil (2 mL, 4 m) through a union. The outlet (standard tubing) was connected to the spinner through

a nut (green) and ferrule assembly. Both the outlet and the inlet were fed through the holder.



Picture 5.4: Modifications to the InsightMR Flow Tube



Scheme 5.4: Flow Setup for the NMR Measurements¹

¹ The NMR measurements were performed together with Joseph L. Howard.



Picture 5.5: Picture of the Working System¹

The inlet of the reactor coil was attached to a T-piece that was connected to two pumps and the reactant solutions. The flow NMR cell was then inserted into the NMR machine (Scheme 5.4 and Picture 5.5). In this work, a dual syringe pump was used because the pump stops in the case of a pressure build up. This avoids potential spillage in the NMR machine in the event of a burst tube due to an increased pressure. The addition of trifluorotoluene as a ^{19}F NMR standard to the TMSCF_3 solution enabled the quantification of both the starting material and the product. The use of a 500 MHz machine (Bruker AscendTM500) could obtain quantitative data in a single scan so that spectra could be measured up to every 7 seconds.

The modified setup was then employed to measure yields at different flow rates and residence times acquiring ^{19}F NMR spectra using the Bruker InsightMR software. The system was flushed with a solution of trifluorotoluene (1.6 M) in diglyme. After stopping the pumps, the spectrometer was set to optimise the shim settings on the ^1H spectrum of the solution using solvent peaks and then tune back to ^{19}F . Following this, the reaction

measurements were started by pumping a solution of TMSCF_3 (2.4 M) and trifluorotoluene (1.6 M) in diglyme and a solution of sodium borohydride (0.8 M in diglyme) through the setup according to Scheme 5.4 using a dual syringe pump. At each flow rate, the system was stabilised for three residence times and then integrals of TMSCF_2H were measured in comparison to the trifluorotoluene standard for one residence time. Thereby each spectrum was acquired using only one scan and the frequency of spectra acquisition was adjusted depending on the flow rate. For fast flow rates the frequency was high (highest frequency possible approximately every 7 s) and for slower flow rates the frequency was lower (e.g. 0.66 mL/min flow rate, 30 min residence time, 2 min frequency of spectra acquired). Typical ^{19}F NMRs spectra during one experiment are shown in Figure 5.7 where the spectra are overlaid.

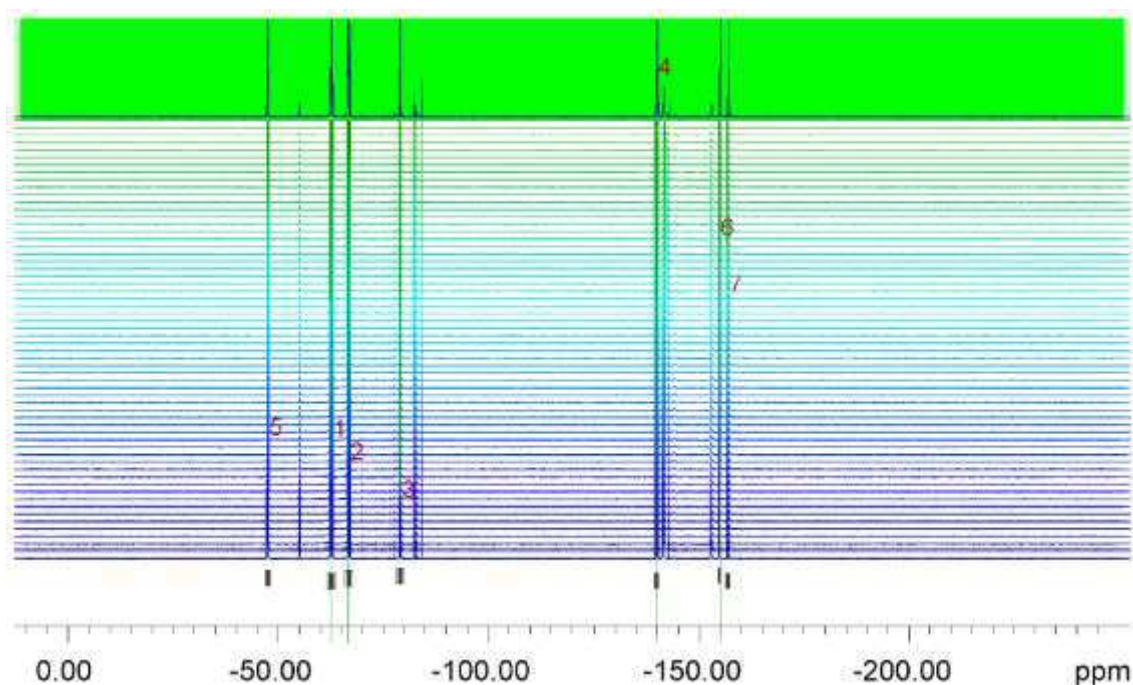


Figure 5.7: ^{19}F NMR During One Measurement

The acquired spectra were integrated using the InsightMR software, the data exported into Excel and converted into a graph illustrating the integration over time (Figure 5.8, example for 0.67 mL/min flow rate, 3 min residence time). In the example shown in figure 5.8, the tubing was filled with reactants before the pumps and measurement were started. The main integrals from top to bottom are: trifluorotoluene (-63.7 ppm, blue), TMSCF_3 (-67.9 ppm, orange), TMSCF_2H (-141.3 ppm, grey). The bottom three integrals are suspected $\text{NaBF}_x\text{H}_{4-x}$ species (-165.3 ppm, green), CF_3H (-80.5 ppm, yellow), which can be formed in a reaction of TMSCF_3 and water, and TMSF (-158.2 ppm, dark blue). After one residence time the content of the tube is replaced with a new stream of

reactants, which explains the sudden change in integration at about 3 min residence time. After that, the integral of trifluorotoluene stays constant whereas the integrals of TMSCF_3 and TMSCF_2H reach a plateau and are stable after about three residence times (9 min). The prolonged time to reach steady state can be explained by the additional 1.5 mL internal volume of the flow NMR cell.

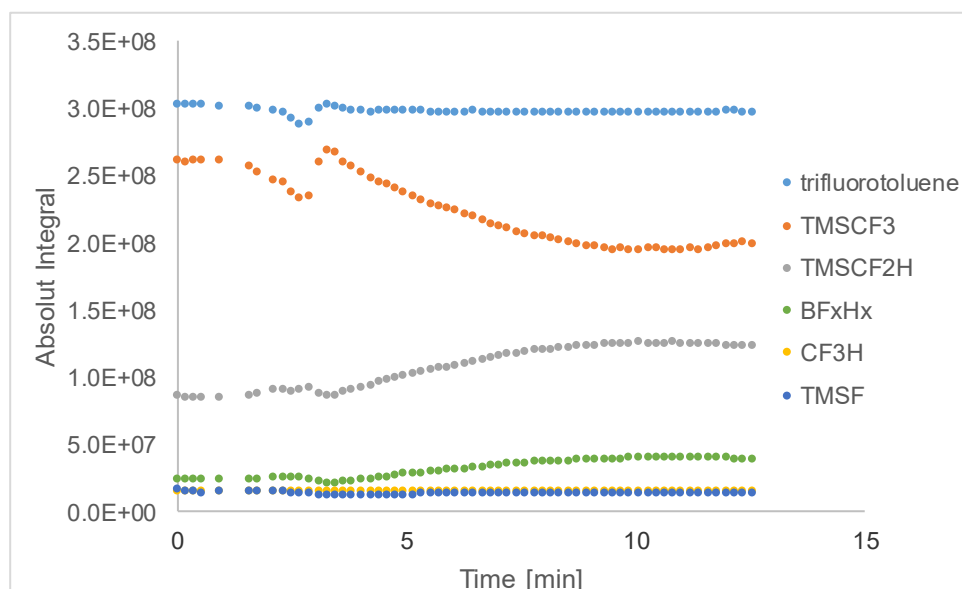


Figure 5.8: Integration over Time, Example for 0.67 mL/min Flow Rate, 3 min Residence Time

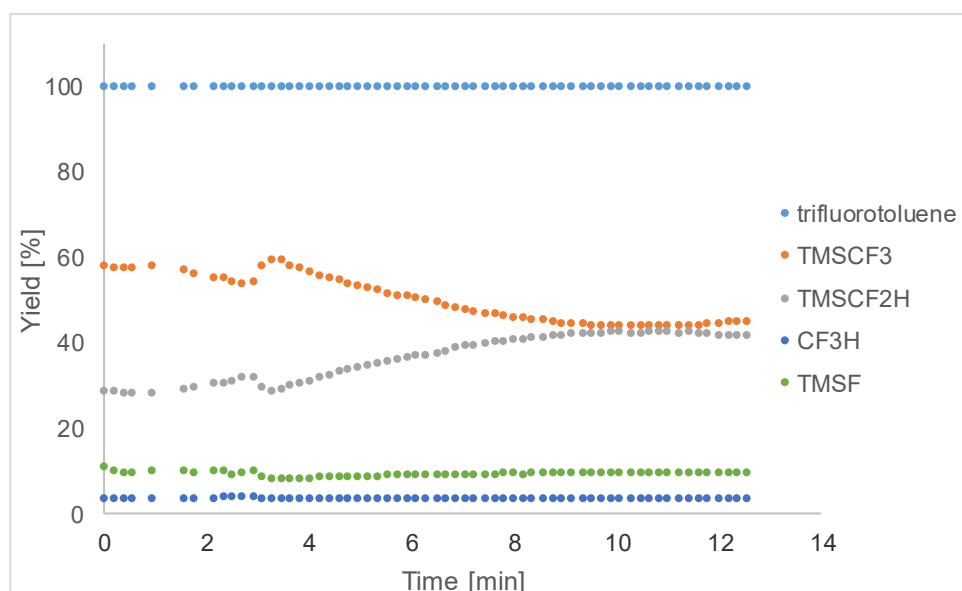


Figure 5.9: Yields over Time, Example for 0.67 mL/min Flow Rate, 3 min Residence Time

The yields (Y) were calculated from the integral of the trifluorotoluene standard and the integral of the compound (Figure 5.9) after stabilisation (after 3 residence times),

averaged and the standard error in the mean calculated, which proved to be a maximum of 0.3% for all measurements.

$$Y = \frac{I_{TMSCF_2H}}{I_{trifluorotoluene}} \cdot 100\%$$

Applying this method for all measurements gave the TMSCF₂H yield for different residence times resulting from the change in flow rates (Table 5.2, Figure 5.10). At the shortest residence time measured (30 s, 4 mL/min) the yield is comparably low at 27%. The yield increases with longer residence times (slower flow rates) and plateaus after about 10 min residence time (flow rate 0.2 mL/min) at approximately 50%. Notably, the reaction continued in the collection flask as intended.

Table 5.2: Results *in line* NMR measurements

entry	flow rate [mL/min]	residence time [min]	yield [%]	error [%]
1	0.066	30	52	0.3
2	0.1	20	53	0.3
3	0.2	10	50	0.1
4	0.4	5	46	0.1
5	0.50	4	45	0.1
6	0.67	3	42	0.1
7	1	2	36	0.1
8	2	1	30	0.2
9	4	0.5	27	0.2

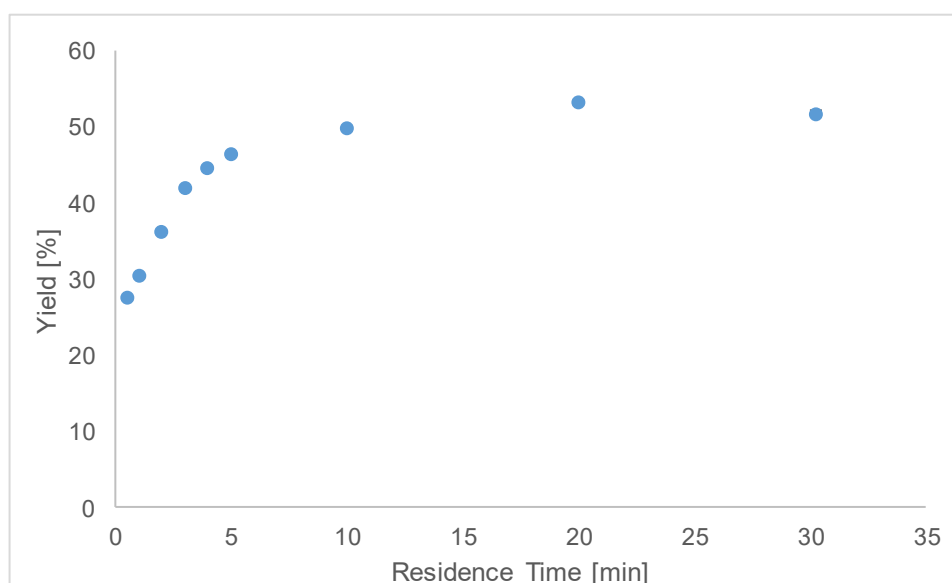


Figure 5.10: Yields for Different Residence Times Resulting from the Change of Flow Rates

2.3 Hybrid Flow - Batch Large Scale Reaction

With the information about the performance of the reaction in hand in terms of temperature and yield, the setup was to be used to its full advantage and scale the reaction up (50 g of TMSCF_3 starting material) in a hybrid reaction. This hybrid setup was to first quench the exotherm in flow, then continue the reaction in a hot batch vessel and also include distillation of the product. The appropriate flow rate had to be found that would be most productive but still safe.

Space time yields (STY) and productivities (P) for the flow part of the reaction were calculated for the different flow rates tested assuming a 60 min operation time at steady state. The STY was calculated from the mass of TMSCF_2H ($m_{\text{TMSCF}_2\text{H}}$, calculated from the flow rate, time, molecular mass, maximum concentration possible and yield), the volume processed in 60 min (V , calculated from the flow rate) and the time (t). Importantly, only the reaction mixture volume that has been processed was considered and not the volume of the setup and pumps. The maximum possible concentration of TMSCF_2H (c_{max}) is thereby the concentration achieved if all TMSCF_3 had been converted into TMSCF_2H , which is the same as the initial concentration of TMSCF_3 in the reactor (1.2 M).

$$STY = \frac{m_{\text{TMSCF}_2\text{H}}}{V \cdot t} = \frac{\dot{V} \cdot t \cdot M_{\text{TMSCF}_2\text{H}} \cdot c_{\text{max}} \cdot Y}{\dot{V} \cdot t \cdot t}$$

$m_{\text{TMSCF}_2\text{H}}$: Mass of TMSCF_2H

V : Volume

t : time (60 min)

\dot{V} : flow rate

$M_{\text{TMSCF}_2\text{H}}$: Molecular mass of TMSCF_2H

c_{max} : Maximum possible concentration of TMSCF_2H (1.2 M)

Y : Yield

For the example of 4 mL/min (27%) the STY is calculated according to the following equations:

$$STY = \frac{\dot{V} \cdot t \cdot M_{\text{TMSCF}_2\text{H}} \cdot c_{\text{max}} \cdot Y}{\dot{V} \cdot t \cdot t} = \frac{4 \frac{\text{mL}}{\text{min}} \cdot 60 \text{ min} \cdot 124.2 \frac{\text{g}}{\text{mol}} \cdot 1.2 \frac{\text{mol}}{\text{L}} \cdot 27\%}{4 \frac{\text{mL}}{\text{min}} \cdot 60 \text{ min} \cdot 60 \text{ min}}$$

$$= \frac{124.2 \cdot 1.2 \cdot 27 \text{ kg}}{10^5 \text{ hL}} = 0.040 \frac{\text{kg}}{\text{hL}}$$

The productivity (P) is the mass that can be produced per hour.

$$P = \frac{m_{TMSCF_2H}}{t} = \frac{\dot{V} \cdot t \cdot M_{TMSCF_2H} \cdot c_{max} \cdot Y}{t}$$

For the example of 4 mL/min (27%) P is calculated:

$$STY = \frac{\dot{V} \cdot t \cdot M_{TMSCF_2H} \cdot c_{max} \cdot Y}{t} = \frac{4 \frac{\text{mL}}{\text{min}} \cdot 60 \text{ min} \cdot 124.2 \frac{\text{g}}{\text{mol}} \cdot 1.2 \frac{\text{mol}}{\text{L}} \cdot 27\%}{60 \text{ min}}$$

$$= 4 \cdot 60 \cdot 124.2 \cdot 1.2 \cdot 27 \cdot 10^{-5} \frac{\text{g}}{\text{h}} = 9.7 \frac{\text{g}}{\text{h}}$$

Table 5.3: STY and P for the Flow Reaction

flow rate [mL/min]	residence time [min]	yield [%]	T _{max} [°C]	STY [kg/(L·h)]	P [g/h]
4	0.5	27	58	0.040	9.7
2	1	37	55	0.055	6.6
1	2	42	25	0.063	3.8
0.5	4	52	21	0.078	2.3

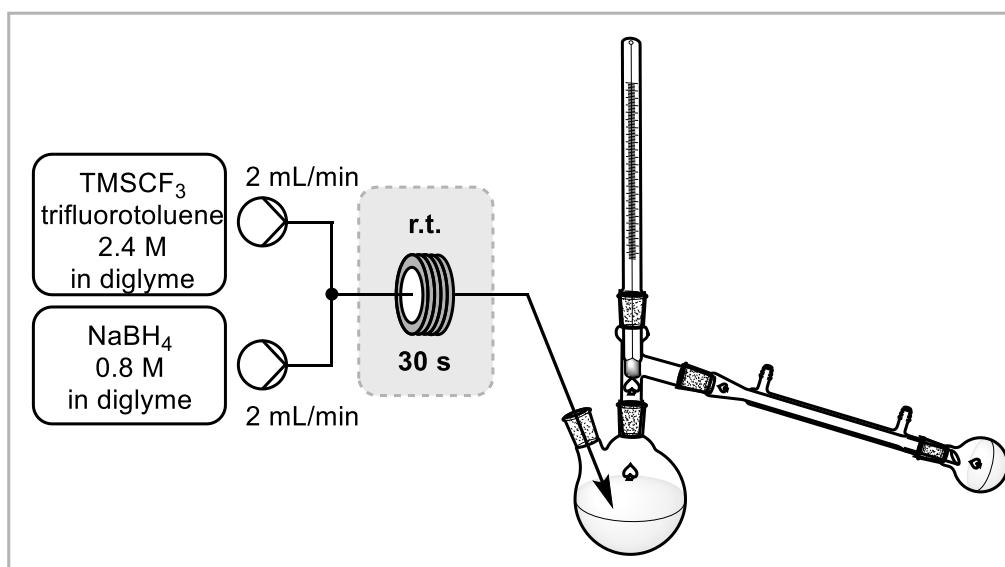
The STY decreases with the increase in flow rate from 0.078 kgL⁻¹h⁻¹ (0.5 mL/min) to 0.040 kgL⁻¹h⁻¹ (4 mL/min), mainly due to the differences in yields (Table 5.3). The productivity however, increases with the increase in flow rate from 2.3 g/h (0.5 mL/min) to 9.7 g/h (4 mL/min) which is due to the increased throughput at faster flowrates. In the telescoped setup the reaction is supposed to go to completion in the batch reaction vessel so that the increased productivity is more important for the scale up which would make the fastest flow rate most attractive.

As the maximum of the exotherm is quenched at all flow rates, even the fastest flow rate was deemed as safe even though the reaction mixture was still warm upon exiting the reactor.

For the telescoped reaction, the flow output is collected in a distillation flask to link the flow part of the reaction and use the collection vessel directly for distillation (Scheme 5.5, Picture 5.6).

Initially, the reaction outlet was fed into the flask stirred at 50 °C and the distillation immediately started after collection by increasing the temperature to 170 °C. Notably, the reaction performed smoothly in the collection vessel at 50 °C, without any obvious signs of an uncontrolled exotherm. However, upon immediate distillation, a mixture of TMSCF_2H and starting material TMSCF_3 was obtained. That meant, that the reaction was not completely finished in the collection flask when the distillation was started. As the boiling point of TMSCF_3 (54 °C) is lower than the boiling point of TMSCF_2H (65 °C) it was observed in the product mixture after distillation. The procedure was therefore modified by stirring the reaction solution for another 30 min in the collection flask before starting the distillation.

50 g of starting material were processed in a total of 105 min. Subsequent distillation gave the prepurified product with traces of solvent. A second distillation gave the TMSCF_2H product (25 g, 56%).



Scheme 5.5: Scheme of Telescoped Reaction Process²

² The experiment of the telescoped reaction process was performed by Joseph L. Howard.

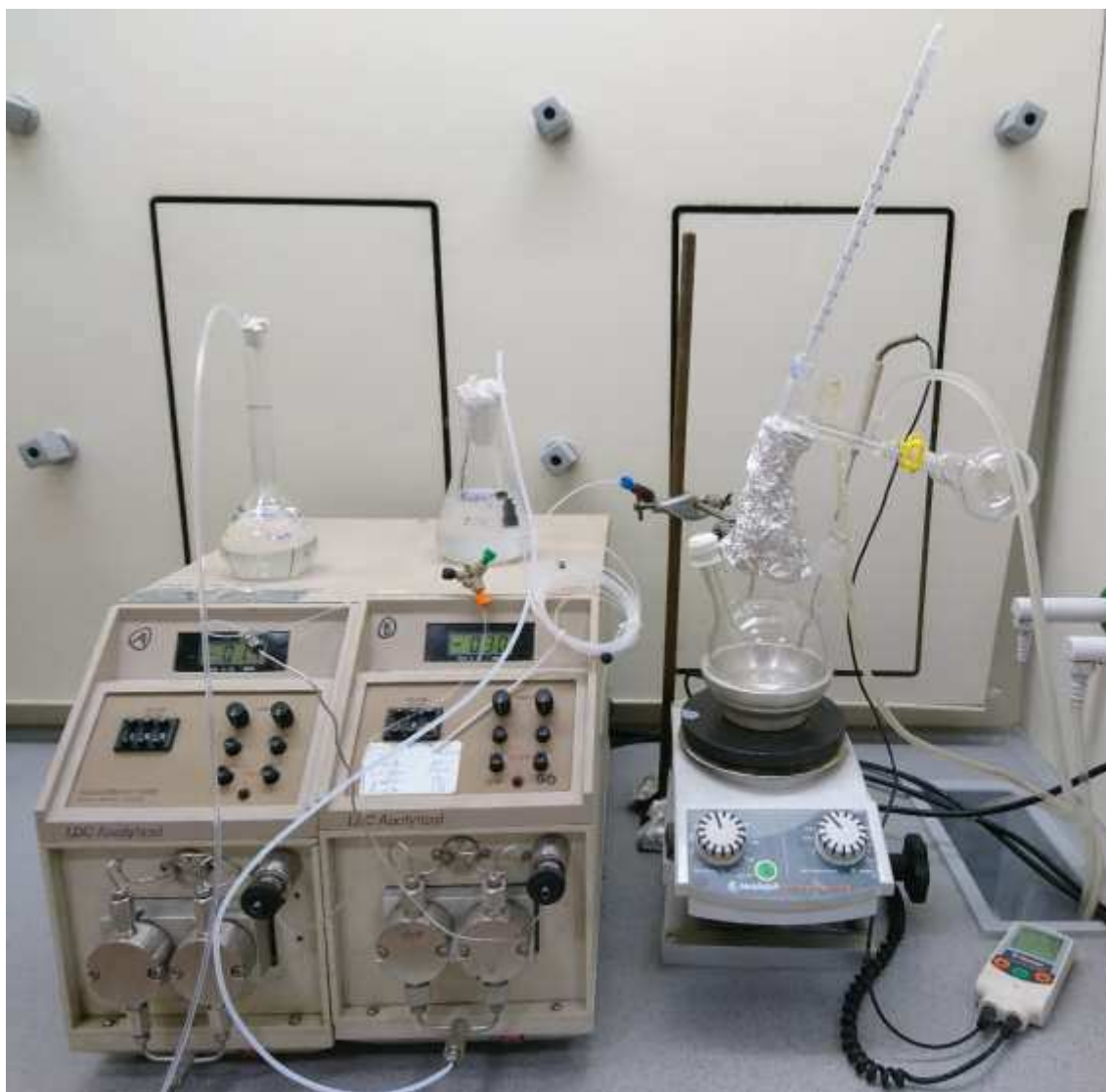


Figure 5.6: Picture of Telescoped Reaction Process²

The STY and P for the telescoped process was calculated taking the processed volume (300 mL), the yield (56%, 25 g) and the time (105 min) into account before starting the distillation.

$$STY = \frac{m_{TMSCF_2H}}{V \cdot t} = \frac{25 \text{ g}}{300 \text{ mL} \cdot 105 \text{ min}} = 0.048 \frac{\text{kg}}{\text{hL}}$$

$$P = \frac{m_{TMSCF_2H}}{t} = \frac{25 \text{ g}}{105 \text{ min}} = 14.3 \frac{\text{g}}{\text{h}}$$

These results permitted the comparison of the STY of the hybrid process to the batch process. Goossen and co-workers processed 20 g of $TMSCF_3$ to yield 12 g $TMSCF_2H$

(71% yield) in 12 h using approximately 62 mL reaction volume in batch giving a STY of $0.016 \text{ kgL}^{-1}\text{h}^{-1}$ and a P of $1 \text{ g/h}^{[10]}$

This described process does not only allow the control of the exotherm enabling the scale up of the reaction, but also has a three fold space time yield and a 14 fold productivity compared to the batch process. It therefore offers the opportunity for the preparation of useful commodity chemicals such as TMSCF_2H .

3 Conclusions and Outlook

A telescoped hybrid flow-batch-distillation process for the monitoring and control of an exothermic reaction, the reduction of TMSCF_3 , has been established. The exotherm was monitored via commercially available thermocouples and the yield determined by *in line* NMR measurements. This enabled the identification of a safe reaction regime and allowed scale up of the process in a telescoped semi-continuous approach including distillation. 50 g of starting material were processed in 105 min total reaction time and a yield of 25 g (56%) of clean material after distillation was achieved. Compared to the batch process a three fold STY and a 14 fold productivity was achieved.

The mixing effect on the temperature could be further investigated. This could include yield measurements at different lengths of tubing and to compare yields for different residence times without the need to change the flow rate ensuring the same mixing conditions. In addition, the use of mixers could be explored.

In general, kinetic or computational studies could determine the mechanism and could quantify the energy release during the exothermic step. These studies could also identify the rate determining step. This information could then help to understand why the reaction first produces a large exotherm but then takes relatively long to go to completion (over night at room temperature). Preliminary efforts on this show the reaction to be highly complex.

4 References

- [1] a) D. Chen, C. Ni, Y. Zhao, X. Cai, X. Li, P. Xiao, J. Hu, *Angew. Chem. Int. Ed.* **2016**, *55*, 12632-12636; b) J. Hu, C. Ni, in *Encyclopedia of Reagents for Organic Synthesis*, John Wiley & Sons, Ltd, **2001**; c) Y. Zhao, W. Huang, J. Zheng, J. Hu, *Org. Lett.* **2011**, *13*, 5342-5345; d) A. A. Tyutyunov, V. E. Boyko, S. M. Igoumnov, *Fluorine notes* **2011**, *1*, 78; e) P. S. Fier, J. F. Hartwig, *J. Am. Chem. Soc.* **2012**, *134*, 5524-5527; f) X.-L. Jiang, Z.-H. Chen, X.-H. Xu, F.-L. Qing, *Organic Chemistry Frontiers* **2014**, *1*, 774-776; g) Y. Gu, X. Leng, Q. Shen, *Nat. Commun.* **2014**, *5*; h) C. Matheis, K. Jouvin, L. J. Goossen, *Org. Lett.* **2014**, *16*, 5984-5987; i) G.-F. Du, Y. Wang, C.-Z. Gu, B. Dai, L. He, *RSC Advances* **2015**, *5*, 35421-35424; j) D. Zhu, Y. Gu, L. Lu, Q. Shen, *J. Am. Chem. Soc.* **2015**, *137*, 10547-10553; k) S.-Q. Zhu, X.-H. Xu, F.-L. Qing, *Organic Chemistry Frontiers* **2015**, *2*, 1022-1025; l) J.-B. Han, H.-L. Qin, S.-H. Ye, L. Zhu, C.-P. Zhang, *J. Org. Chem.* **2016**, *81*, 2506-2512; m) K. Jouvin, C. Matheis, L. J. Goossen, *Chemistry–A European Journal* **2015**, *21*, 14324-14327; n) J. Wu, Y. Gu, X. Leng, Q. Shen, *Angew. Chem. Int. Ed.* **2015**, *54*, 7648-7652; o) B. Bayarmagnai, C. Matheis, K. Jouvin, L. J. Goossen, *Angew. Chem. Int. Ed.* **2015**, *54*, 5753-5756; p) E. Obijalska, G. Utecht, M. K. Kowalski, G. Mlostoń, M. Rachwalski, *Tetrahedron Lett.* **2015**, *56*, 4701-4703; q) O. M. Michurin, D. S. Radchenko, I. V. Komarov, *Tetrahedron* **2016**, *72*, 1351-1356; r) M. Nagase, Y. Kuninobu, M. Kanai, *J. Am. Chem. Soc.* **2016**, *138*, 6103-6106; s) J. Hartwig, P. Fier, **2016**; t) M. D. Kosobokov, A. D. Dilman, V. V. Levin, M. I. Struchkova, *J. Org. Chem.* **2012**, *77*, 5850-5855; u) G. K. S. Prakash, S. K. Ganesh, J.-P. Jones, A. Kulkarni, K. Masood, J. K. Swabeck, G. A. Olah, *Angew. Chem. Int. Ed.* **2012**, *51*, 12090-12094; v) Q. Glenadel, E. Ismalaj, T. Billard, *J. Org. Chem.* **2016**, *81*, 8268-8275; w) L. Wang, J. Wei, R. Wu, G. Cheng, X. Li, J. Hu, Y. Hu, R. Sheng, *Organic Chemistry Frontiers* **2017**, *4*, 214-223; x) J. Xu, S. Zhang, S. Wu, S. Bi, X. Li, Y. Lu, L. Wang, *Tetrahedron* **2017**, *73*, 494-499; y) J. R. Bour, S. K. Kariofillis, M. S. Sanford, *Organometallics* **2017**, *36*, 1220-1223; z) C. Lu, Y. Gu, J. Wu, Y. Gu, Q. Shen, *Chem. Sci.* **2017**, *8*, 4848-4852; aa) C. D. Sessler, M. Rahm, S. Becker, J. M. Goldberg, F. Wang, S. J. Lippard, *J. Am. Chem. Soc.* **2017**, *139*, 9325-9332; ab) E. Pietrasiak, A. Togni, *Organometallics* **2017**, *36*, 3750-3757; ac) S.-Q. Zhu, X.-H. Xu, F.-L. Qing, *Chem. Commun.* **2017**, *53*, 11484-11487.
- [2] J. L. Howard, C. Schotten, S. T. Alston, D. L. Browne, *Chem. Commun.* **2016**, *52*, 8448-8451.
- [3] E. K. S. Liu, R. J. Lagow, *J. Organomet. Chem.* **1978**, *145*, 167-182.

- [4] a) V. Broicher, D. Geffken, *J. Organomet. Chem.* **1990**, *381*, 315-320; b) G. K. S. Prakash, J. Hu, G. A. Olah, *J. Org. Chem.* **2003**, *68*, 4457-4463.
- [5] a) A. Tyutyunov, V. Boyko, S. Igoumnov, *Fluorine notes* **2011**, *1*, 74; b) I. Ruppert, K. Schlich, W. Volbach, *Tetrahedron Lett.* **1984**, *25*, 2195-2198.
- [6] N. Kockmann, P. Thenee, C. Fleischer-Trebes, G. Laudadio, T. Noel, *React. Chem. Eng.* **2017**, *2*, 258-280.
- [7] M. Movsisyan, E. I. P. Delbeke, J. K. E. T. Berton, C. Battilocchio, S. V. Ley, C. V. Stevens, *Chem. Soc. Rev.* **2016**, *45*, 4892-4928.
- [8] M. Gödde, C. Liebner, H. Hieronymus, *Chem. Ing. Tech.* **2009**, *81*, 73-78.
- [9] a) R. J. Bogaert-Alvarez, P. Demena, G. Kodersha, R. E. Polomski, N. Soundararajan, S. S. Wang, *Org. Process Res. Dev.* **2001**, *5*, 636-645; b) D. Webb, T. F. Jamison, *Org. Lett.* **2011**, *14*, 568-571; c) M. Baumann, I. R. Baxendale, L. J. Martin, S. V. Ley, *Tetrahedron* **2009**, *65*, 6611-6625; d) A. A. Kulkarni, *Beilstein J. Org. Chem.* **2014**, *10*, 405-424.
- [10] D. C. Fabry, E. Sugiono, M. Rueping, *React. Chem. Eng.* **2016**, *1*, 129-133.
- [11] a) K. Albert, E. Bayer, *TrAC Trends in Analytical Chemistry* **1988**, *7*, 288-293; b) K. Albert, *On-line LC-NMR and related techniques*, John Wiley & Sons, **2003**.
- [12] a) M. Maiwald, H. H. Fischer, Y.-K. Kim, H. Hasse, *Anal. Bioanal. Chem.* **2003**, *375*, 1111-1115; b) S. S. Zalesskiy, E. Danieli, B. Blümich, V. P. Ananikov, *Chem. Rev.* **2014**, *114*, 5641-5694; c) V. Sans, L. Porwol, V. Dragone, L. Cronin, *Chem. Sci.* **2015**, *6*, 1258-1264; d) N. Zientek, K. Meyer, S. Kern, M. Maiwald, *Chem. Ing. Tech.* **2016**, *88*, 698-709; e) M. V. Gomez, A. de la Hoz, *Beilstein J. Org. Chem.* **2017**, *13*, 285; f) M. Goldbach, E. Danieli, J. Perlo, B. Kaptein, V. M. Litvinov, B. Blümich, F. Casanova, A. L. L. Duchateau, *Tetrahedron Lett.* **2016**, *57*, 122-125; g) M. A. Vargas, M. Cudaj, K. Hailu, K. Sachsenheimer, G. Guthausen, *Macromolecules* **2010**, *43*, 5561-5568; h) M. Maiwald, H. H. Fischer, Y.-K. Kim, K. Albert, H. Hasse, *J. Magn. Reson.* **2004**, *166*, 135-146; i) V. Röntzsch, M. Wilhelm, G. Guthausen, *Magn. Reson. Chem.* **2016**, *54*, 494-501; j) M. A. Bernstein, M. Štefinović, C. J. Sleight, *Magn. Reson. Chem.* **2007**, *45*, 564-571; k) A. Nordon, C. A. McGill, D. Littlejohn, *Analyst* **2001**, *126*, 260-272; l) M. V. Silva Elipe, R. R. Milburn, *Magn. Reson. Chem.* **2016**, *54*, 437-443; m) B. Picard, B. Gouilleux, T. Lebleu, J. Maddaluno, I. Chataigner, M. Penhoat, F.-X. Felpin, P. Giraudeau, J. Legros, *Angew. Chem. Int. Ed.* **2017**, *56*, 7568-7572; n) D. A. Foley, C. W. Doecke, J. Y. Buser, J. M. Merritt, L. Murphy, M. Kissane, S. G. Collins, A. R. Maguire, A. Kaerner, *J. Org. Chem.* **2011**, *76*, 9630-9640; o) B. Ahmed-Omer, E. Sliwinski, J. P. Cerroti, S. V. Ley, *Org. Process Res. Dev.* **2016**, *20*, 1603-1614.

- [13] C. A. Fyfe, M. Cocivera, S. W. H. Damji, *Acc. Chem. Res.* **1978**, *11*, 277-282.
- [14] a) M. Khajeh, M. A. Bernstein, G. A. Morris, *Magn. Reson. Chem.* **2010**, *48*, 516-522; b) D. A. Foley, E. Bez, A. Codina, K. L. Colson, M. Fey, R. Krull, D. Piroli, M. T. Zell, B. L. Marquez, *Anal. Chem.* **2014**, *86*, 12008-12013; c) A. M. R. Hall, J. C. Chouler, A. Codina, P. T. Gierth, J. P. Lowe, U. Hintermair, *Catal. Sci. Tech.* **2016**, *6*, 8406-8417; d) D. A. Foley, A. L. Dunn, M. T. Zell, *Magn. Reson. Chem.* **2016**, *54*, 451-456; e) D. A. Foley, J. Wang, B. Maranzano, M. T. Zell, B. L. Marquez, Y. Xiang, G. L. Reid, *Anal. Chem.* **2013**, *85*, 8928-8932; f) A. M. R. Hall, R. Broomfield-Tagg, M. Camilleri, D. R. Carbery, A. Codina, D. T. E. Whittaker, S. Coombes, J. P. Lowe, U. Hintermair, *Chem. Commun.* **2018**, *54*, 30-33.
- [15] a) J. Y. Buser, A. D. McFarland, *Chem. Commun.* **2014**, *50*, 4234-4237; b) J. Bart, A. J. Kolkman, A. J. Oosthoek-de Vries, K. Koch, P. J. Nieuwland, H. Janssen, J. van Bentum, K. A. M. Ampt, F. P. J. T. Rutjes, S. S. Wijmenga, H. Gardeniers, A. P. M. Kentgens, *J. Am. Chem. Soc.* **2009**, *131*, 5014-5015; c) G. Finch, A. Yilmaz, M. Utz, *J. Magn. Reson.* **2016**, *262*, 73-80.
- [16] T. H. Rehm, C. Hofmann, D. Reinhard, H.-J. Kost, P. Lob, M. Besold, K. Welzel, J. Barten, A. Didenko, D. V. Sevenard, B. Lix, A. R. Hillson, S. D. Riegel, *React. Chem. Eng.* **2017**, *2*, 315-323.
- [17] <http://www.xllogger.com/html/sensors.html>, accessed 20.02.2018.
- [18] A. Codina, Bruker Benelux Workshop, **2016**.

Chapter 6: Experimental

1	Table of Contents	
1	General Methods	157
2	Chapter 2 - Triazenes	159
2.1	Batch Procedure.....	159
2.2	General Method for the Preparation of Triazenes 26 - 41 in Flow	161
2.3	General Method for the Preparation of Triazenes 41 - 50 in Flow	176
2.4	General Procedure for the Preparation of Diazonium Salts 51 - 58	184
2.5	DSC Spectra	187
2.5.1	Triazenes.....	187
2.5.2	Diazonium Salts.....	194
3	Chapter 3 - Indoles	198
3.1	Method for the Optimisation of the Multistep Indole Synthesis	198
3.1.1	Optimisation of the Microwave Step.....	198
3.1.2	Investigating the hydrazide formation by ¹⁹ F NMR	199
3.1.3	Optimisation of the Telescoped Process.....	201
3.2	General Method for the Synthesis of Indoles 85 and 92 - 104 : Aniline Screen 202	
3.2.1	Anthranilic Acid Product.....	209
3.3	General Method for the Synthesis of Indoles 85 and 105 - 113 : Ketone Screen 210	
3.4	Sumatriptan Synthesis.....	216
3.5	General Method for the Synthesis of Indoles 129 and 136 - 144 : Zolmitriptan Plus Analogues	217
3.6	General Method for the Preparation of Pyrazoles	224
4	Chapter 4 - Benzyne	228
4.1	Initial Setup.....	228
4.2	Optimisation	228

4.2.1	Optimisation Acridone.....	228
4.2.2	Optimisation Dihydroepoxynaphtalene 168	230
4.3	Substrate Investigation	232
4.3.1	Substituted Anthranilic Acids.....	233
4.4	Switch to Uncyclised Product 177 with Acid.....	235
4.5	Product Characterisation	236
5	Chapter 5 – Exotherm Monitoring	239
5.1	General Methods	239
5.2	Batch Reaction	239
5.3	Temperature Measurements.....	240
5.4	Flow NMR Modifications	242
5.5	Flow NMR Measurements	243
5.6	Telescoped Large Scale Reaction	246
6	References	247

1 General Methods

All reagents and solvents were commercially available and were used without further purification unless stated otherwise. Petroleum ether refers to the 40-60 °C fraction.

For the measurement of ^1H , ^{13}C and ^{19}F NMR spectra a Bruker Fourier³⁰⁰ (300 MHz), 400 UltraShieldTM (400 MHz) or AscendTM500 (500 MHz) were used. The obtained chemical shifts δ are reported in ppm and are referenced to the residual solvent signal or to the standard trifluorotoluene (-63.72 ppm) in ^{19}F NMR. Spin-spin coupling constants J are given in Hz and refer to apparent multiplicities rather than true coupling constants. Data is reported as: chemical shift, multiplicity and integration. Carbon shifts are reported to the nearest 0.5 ppm and the number of signals rounded to the same value is indicated in brackets. Carbons in an identical environment giving one signal are not indicated further.

The flow setup consisted of PFA tubing of an 0.8 mm internal diameter (ID) and 1.2 mm outer diameter (OD) and the necessary number of pumps. The residence coils were made from the tubing by taking the appropriate length for the desired volume.

Gas chromatography analysis was carried out using Bruker Scion 456 gas chromatograph. An Agilent 19091J-413HP-5 column (30.0 m \times 320 μm \times 0.25 μm nominal) was employed for all the separations using the following conditions: initial column temperature, 40 °C, initial hold time 2 min; 4 °C/min gradient to 100 °C, hold time, 5 min; 15 °C/min gradient to final temperature 300 °C, final hold time 5 min; injection temperature 250 °C; injection volume 1 μL ; detection temperature 300 °C; split mode. The effluent was combusted in an H_2 /air flame and detected using FID (flame ionization detector). The GC yield of products was determined by using the internal standard method. The response factor (RF) of analytes was determined by analysing known quantities of internal standard (trifluorotoluene) against known quantities of substrate and product.

GCMS was performed on a Shimadzu GCMS-QP2010 SE. An Agilent 19091J-413HP-5 column (30.0 m \times 320 μm \times 0.25 μm nominal) was employed for all the separations using the following conditions: initial column temperature, 40 °C, initial hold time 2 min; 15 °C/min gradient to final temperature 300 °C, final hold time 5 min; injection temperature 250 °C; injection volume 1 μL ; detection temperature 300 °C; split mode. The effluent detected using the mass spectrometer.

LCMS was performed on a Bruker Amazon SL mass spectrometer operating in positive electrospray mode that was coupled to a Thermo Ultimate HPLC with a C_{18} column that was held at 40 °C during measurements. The mobile phase consisted of a mixture of

water (with 0.1% formic acid) and acetonitrile (12 min at 98%, 2 min at 2%, 2 min at 98%).

Column chromatography was performed using 60 Å (40-64 micron) silica and solvent mixtures of petroleum ether and ethyl acetate unless stated otherwise.

DSC measurements were performed using a TA instruments Q100. The samples were heated to 200 °C at a 20 °Cmin⁻¹ gradient. Some samples were heated to 300 °C to show starting transitions.

High resolution mass spectra (HRMS) were obtained on a Waters MALDI-TOF mx at Cardiff University or on a Thermo Scientific LTQ Orbitrap XL by the EPSRC UK National Mass Spectrometry Facility at Swansea University.

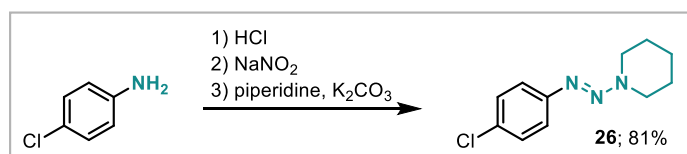
IR spectra were obtained from a Shimadzu IR-Affinity-1S FTIR and melting points from a Gallenkamp apparatus and are reported uncorrected.

References to spectroscopic data are given for known compounds.

2 Chapter 2 - Triazines

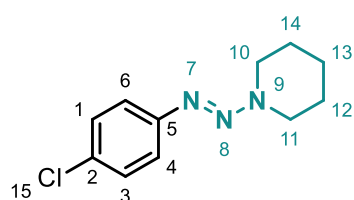
2.1 Batch Procedure

1-((4-chlorophenyl)diazenyl)piperidine (**1**)^[1]



Scheme 6.1: Batch Procedure for the Preparation of Compound 26

Following the procedure from Huang and co-workers^[1], *p*-chloroaniline (0.128 g, 1 mmol) was dissolved in a mixture of water and MeCN (H₂O: MeCN 1:2, 0.5 mL: 1 mL). After cooling to 0 °C, conc. HCl was added slowly (0.33 mL, 4 mmol, 4 equiv). The solution was further cooled down to -5 °C and NaNO₂ (0.140 g, 1.5 mmol, 1.5 equiv) in water (1.5 mL) was added slowly. The solution was stirred for 30 min at -5 to 0 °C. Then it was added to a solution of piperidine (0.346 g, 2.5 mmol, 2.5 equiv) and K₂CO₃ (0.719 g, 5.2 mmol, 5.2 equiv) in water and MeCN ((H₂O: MeCN 1:2, 2 mL: 4 mL). The solution was vigorously stirred for 1 h at room temperature. The product was extracted with EtOAc (3 x 10 mL). The combined organic layers were washed with brine, dried over MgSO₄, filtered and the solvent removed under reduced pressure. The crude product was taken up in DCM and filtered through a plug of silica. Removal of the solvent yielded the product **26** as a pale yellow solid in 81% yield (0.181 g, 0.81 mmol).



¹H NMR (400 MHz, CDCl₃, rt) δ 7.38 – 7.34 (m, 2H, ArH), 7.31 – 7.25 (m, 2H, ArH), 3.83 – 3.71 (m, 4H, CH₂^{10,11}), 1.77 – 1.63 (m, 6H, CH₂^{12,13,14}) ppm.

¹³C NMR (101 MHz, CDCl₃, -30 °C) δ 149.0 (ArC⁵), 130.5 (ArC²), 129.0 (ArCH), 121.5 (ArCH), 53.0 (CH₂), 43.5 (CH₂), 26.0 (CH₂), 24.0 (CH₂) ppm.

¹³C NMR (101 MHz, CDCl₃, rt) δ 149.5 (ArC⁵), 131.0 (ArC²), 129.0 (ArCH), 122.0 (ArCH), 25.5 (CH₂), 24.5 (CH₂) ppm.

¹³C NMR (101 MHz, CDCl₃, 50 °C) δ 150.0 (ArC⁵), 131.0 (ArC²), 129.0 (ArCH), 122.0 (ArCH), 48.5 (CH₂), 25.5 (CH₂), 24.5 (CH₂) ppm.

mp (DCM): 53 - 54 °C.

IR: 2936, 2853, 1329, 831, 521 cm⁻¹.

HRMS (EI+): [C₁₁H₁₄N₃Cl] Calcd. 223.0876, Found 223.0883.

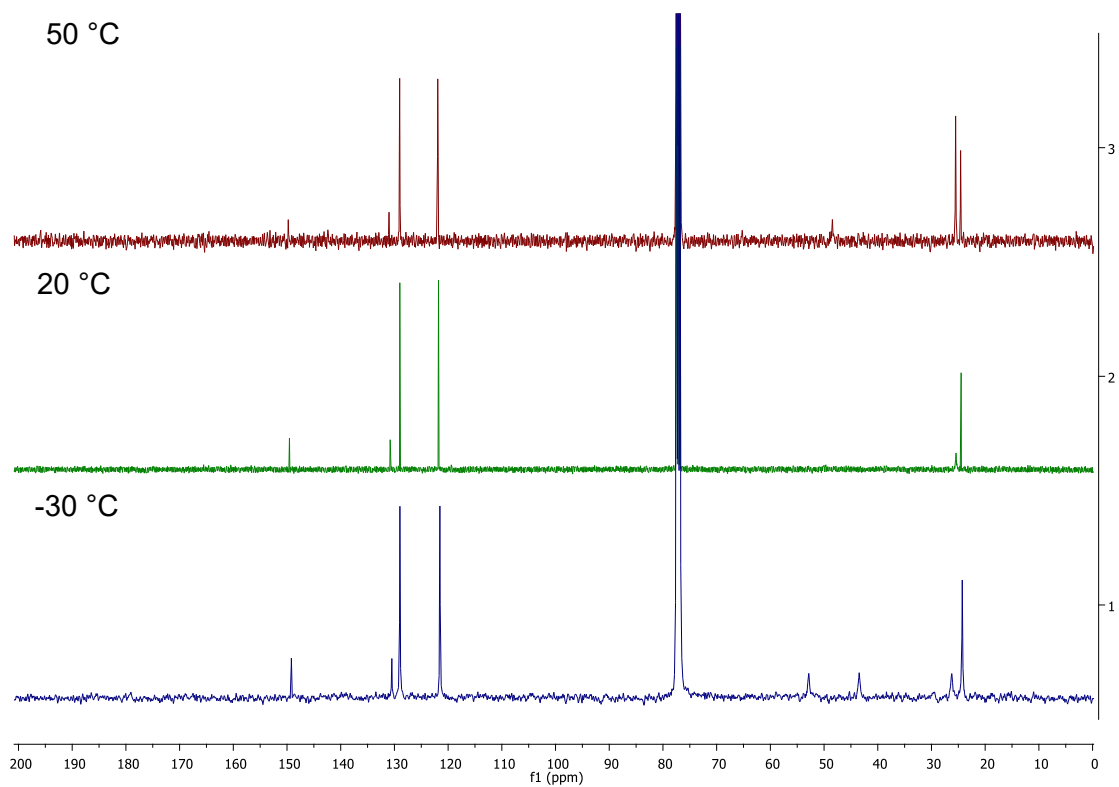


Figure 6.1: VT ^{13}C NMR for Compound 26

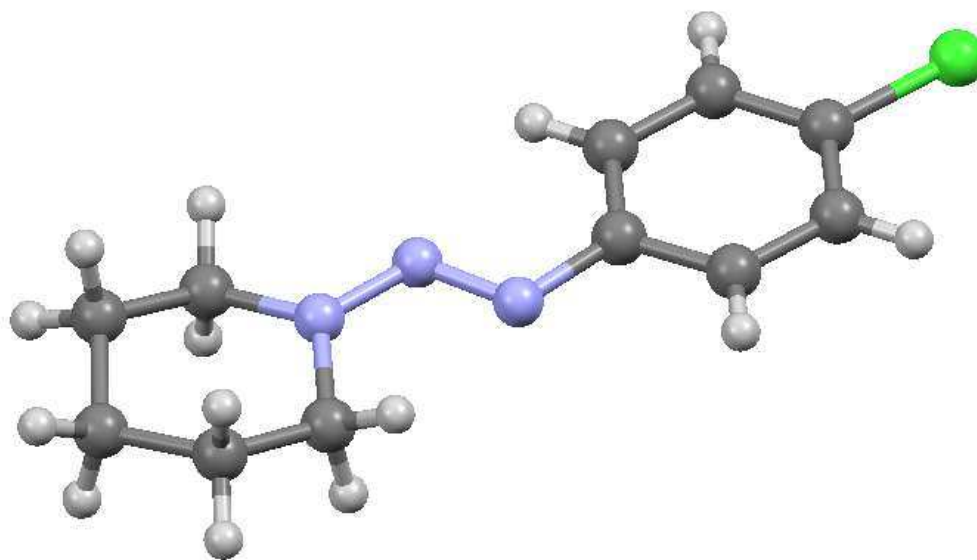
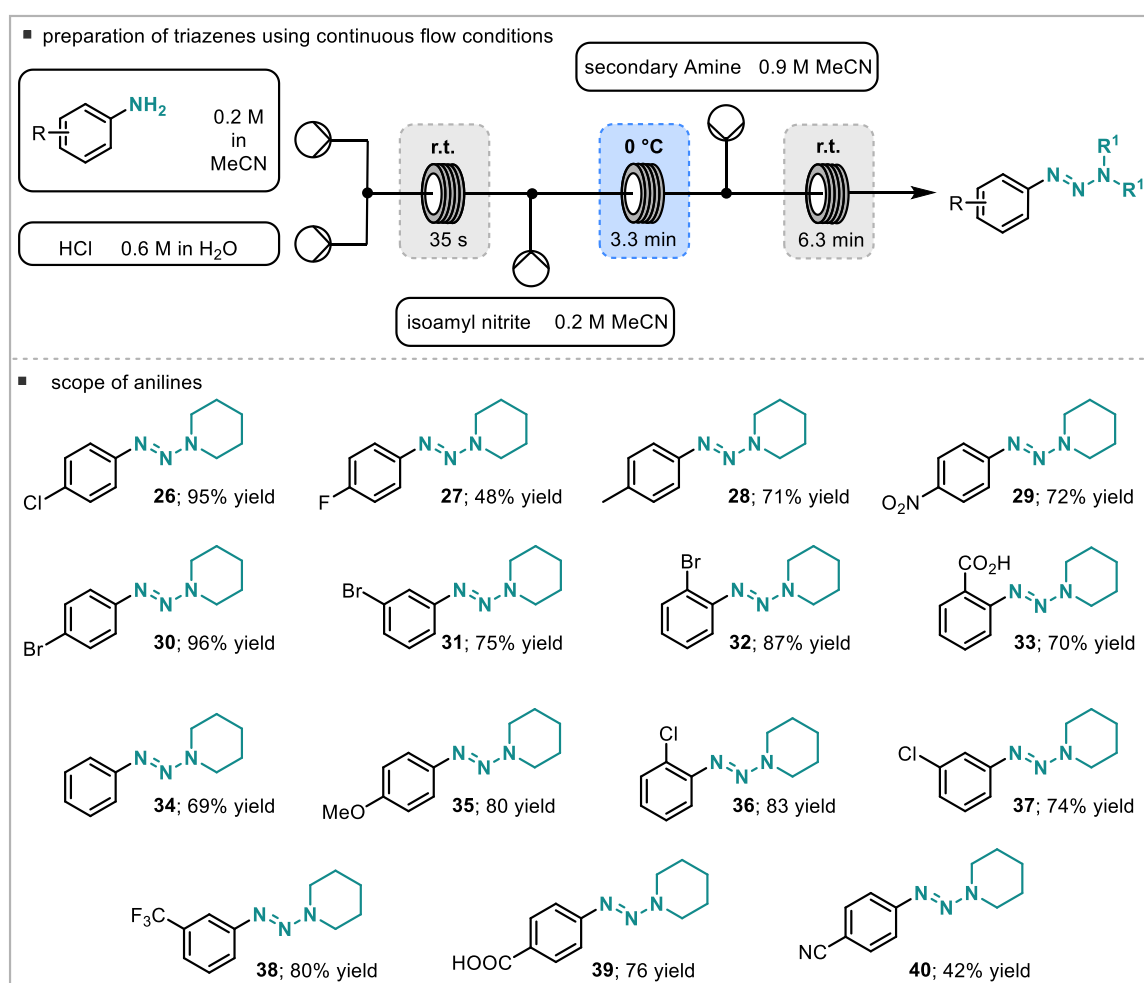


Figure 6.2: Crystal Structure of Compound 26

2.2 General Method for the Preparation of Triazenes **26** - **41** in Flow

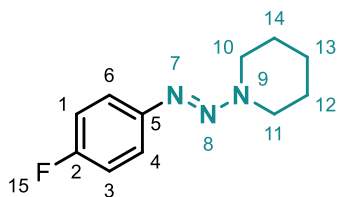
Solutions of the aniline (0.2 M in acetonitrile), HCl (0.6 M in water), isoamyl nitrite (0.2 M in acetonitrile) and piperidine (0.9 M in acetonitrile) were prepared. These were then pumped through the flow system (see Scheme 6.2) at a flow rate of 0.2 mL min⁻¹. After 20 min steady state was reached and an aliquot of 20 mL (1 mmol, 25 min) was collected. The reaction solution was neutralized with aqueous NaHCO₃, extracted with EtOAc (3 x 20 mL), washed with brine and dried over MgSO₄. After removing the solvent under reduced pressure, the crude product was further purified by column chromatography (0 to 10% EtOAc in petroleum ether).



Scheme 6.2: Preparation of Triazenes Using Continuous Flow Conditions: Aniline Scope

1-((4-chlorophenyl)diazenyl)piperidine (**26**)^[1]

Following the general procedure, the title compound **26** was obtained from 4-chloroaniline as a pale yellow solid in 95% yield (0.213 g). See characterisation data in 2.1)

1-((4-fluorophenyl)diazenyl)piperidine (27)^[2]

Following the general procedure, the title compound **27** was obtained from 4-fluoroaniline as a yellow oil in 62% yield (0.129 g).

¹H NMR (400 MHz, CDCl₃) δ 7.43 – 7.35 (m, 2H, ArH), 7.05 – 6.97 (m, 2H, ArH), 3.80 – 3.71 (m, 4H, CH₂^{10,11}), 1.77 – 1.62 (m, 6H, CH₂^{12,13,14}) ppm.

¹⁹F NMR (376 MHz, CDCl₃) δ -117.99 ppm.

¹³C NMR (101 MHz, CDCl₃, -30 °C) δ 161.0 (d, *J* = 243.4 Hz, ArC²), 147.0 (d, *J* = 2.8 Hz, ArC⁵), 121.5 (d, *J* = 8.1 Hz, ArCH^{4,6}), 115.5 (d, *J* = 22.3 Hz, ArCH^{1,3}), 52.5 (CH₂), 43.5 (CH₂), 26.0 (CH₂), 24.5 (CH₂), 24.5 (CH₂) ppm.

¹³C NMR (101 MHz, CDCl₃, rt) δ 161.0 (d, *J* = 243.7 Hz, ArC²), 147.5 (d, *J* = 2.8 Hz, ArC⁵), 122.0 (d, *J* = 8.1 Hz, ArCH^{4,6}), 116.0 (d, *J* = 22.4 Hz, ArCH^{1,3}), 25.5 (CH₂), 24.5 (CH₂) ppm.

¹³C NMR (101 MHz, CDCl₃, 50 °C) δ 161.5 (d, *J* = 243.9 Hz, ArC²), 147.5 (d, *J* = 2.9 Hz, ArC⁵), 122.0 (d, *J* = 8.1 Hz, ArCH^{4,6}), 115.5 (d, *J* = 22.5 Hz, ArCH^{1,3}), 48.5 (CH₂), 25.5 (CH₂), 24.5 (CH₂) ppm.

IR: 2938, 2857, 1595, 1497, 1437, 1221, 1177, 1101, 1088, 835, 821 cm⁻¹.

HRMS (EI⁺): [C₁₁H₁₄N₃F]⁺ Calcd. 207.1172, Found 207.1170.

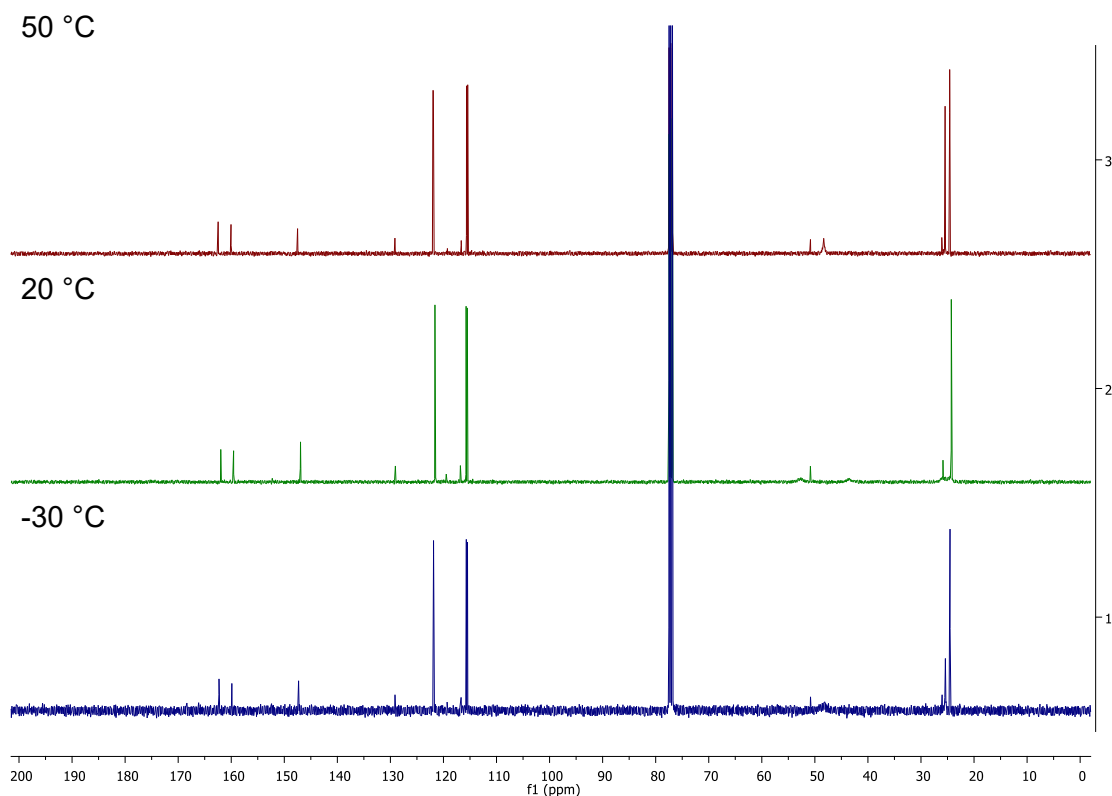
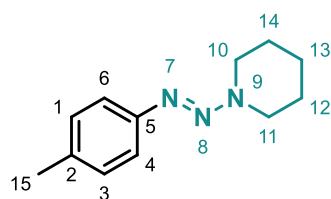


Figure 6.3: VT ¹³C NMR for Compound 27

1-((4-methylphenyl)diazenyl)piperidine (28)^[1]

Following the general procedure, the title compound **28** was obtained from toluidine as an orange oil in 87% yield (0.176 g).

¹H NMR (400 MHz, CDCl₃, rt) δ 7.37 – 7.31 (m, 2H, ArH), 7.14 (d, *J* = 8.1 Hz, 2H, ArH), 3.86 – 3.67 (m, 4H, CH₂^{10,11}), 2.34 (s, 3H, CH₃¹⁵), 1.87 – 1.62 (m, *J* = 7.8 Hz, 6H, CH₂^{12,13,14}) ppm.

¹³C NMR (101 MHz, CDCl₃, -30 °C) δ 148.5 (ArC), 135.5 (ArC), 129.5 (ArCH), 120.0 (ArCH), 24.5 (CH₃), 21.5 (CH₂) ppm.

¹³C NMR (101 MHz, CDCl₃, rt) δ 148.5 (ArC), 135.5 (ArC), 129.5 (ArCH), 120.5 (ArCH), 48.5 (CH₂), 25.5 (CH₂), 24.5 (CH₃), 21.0 (CH₂) ppm.

¹³C NMR (101 MHz, CDCl₃, 50 °C) δ 149.0 (ArC), 135.5 (ArC), 129.5 (ArCH), 120.5 (ArCH), 48.5 (CH₂), 25.5 (CH₂), 24.5 (CH₃), 21.0 (CH₂) ppm.

mp (DCM): 36 - 38 °C.

IR : 2949, 2938, 2928, 2853, 2361, 1435, 1350, 1180, 1099, 824, 521 cm⁻¹.

HRMS (EI+): [C₁₂H₁₇N₃] Calcd. 203.1422, Found 203.1423.

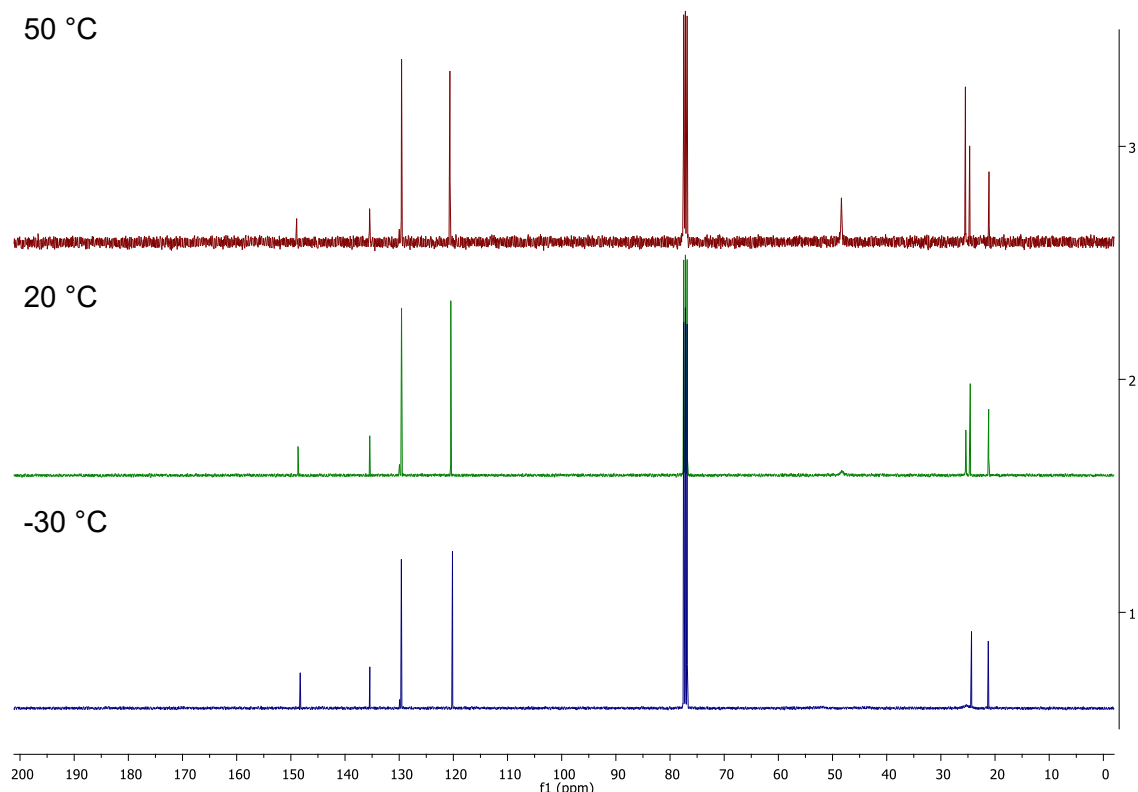
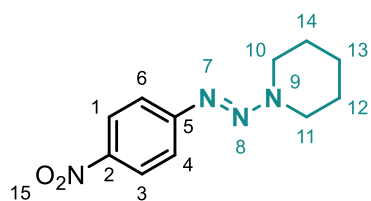


Figure 6.4: VT ¹³C NMR for Compound **28**

1-((4-nitrophenyl)diazenyl)piperidine (29)^[1]

Following the general procedure, the title compound **29** was obtained from 4-nitroaniline as an orange solid in 72% yield (0.168 g).

¹H NMR (400 MHz, CDCl₃, rt) δ 8.25 – 8.08 (m, 2H, ArH), 7.57 – 7.42 (m, 2H, ArH), 4.01 – 3.72 (s, 4H, CH₂^{10,11}), 1.90 – 1.57 (s, 6H, CH₂^{12,13,14}) ppm.

¹³C NMR (101 MHz, CDCl₃, -30 °C) δ 156.0 (ArC), 144.0 (ArC), 125.0 (ArCH), 120.5 (ArCH), 53.5 (CH₂), 43.5 (CH₂), 26.5 (CH₂), 24.5 (CH₂), 24.0 (CH₂) ppm.

¹³C NMR (101 MHz, CDCl₃, rt) δ 156.0 (ArC), 145.0 (ArC), 125.0 (ArCH), 120.5 (ArCH), 24.5 (CH₂) ppm.

¹³C NMR (101 MHz, CDCl₃, 50 °C) δ 156.0 (ArC), 125.0 (ArCH), 121.0 (ArCH), 24.5 (CH₂) ppm.

mp (DCM): 96 - 98 °C.

IR: 2945, 2855, 2361, 1506, 1285, 1098, 851, 694 cm⁻¹.

HRMS (FTMS+ p NSI): [C₁₁H₁₄N₄O₂] Calcd. 234.1117, Found 234.1118.

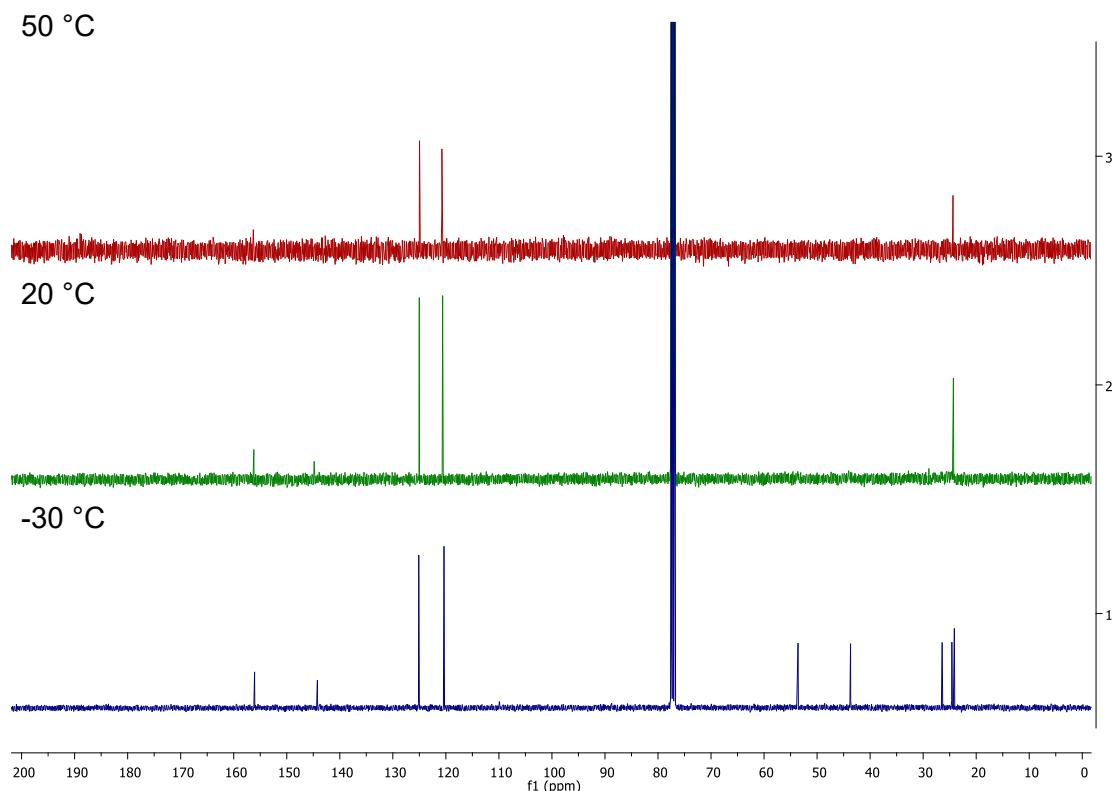
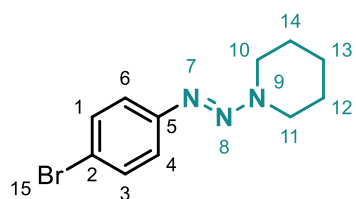


Figure 6.5: VT ¹³C NMR for Compound 29

1-((4-bromophenyl)diazenyl)piperidine (30)^[3]

Following the general procedure, the title compound **30** was obtained from 4-bromoaniline as a pale orange solid in 96% yield (0.257 g).

¹H NMR (400 MHz, CDCl₃, rt) δ 7.46 – 7.39 (m, 2H, ArH), 7.34 – 7.27 (m, 2H, ArH), 3.85 – 3.69 (m, 4H, CH₂^{10,11}), 1.78 – 1.63 (m, 6H, CH₂^{12,13,14}) ppm.

¹³C NMR (101 MHz, CDCl₃, -30 °C) δ 149.5 (ArC), 132.0 (ArCH), 122.0 (ArCH), 118.5 (ArC), 53.0 (CH₂), 43.5 (CH₂), 26.0 (CH₂), 24.5 (CH₂) ppm.

¹³C NMR (101 MHz, CDCl₃, rt) δ 150.0 (ArC), 132.0 (ArCH), 122.0 (ArCH), 118.5 (ArC), 25.5 (CH₂), 24.5 (CH₂) ppm.

¹³C NMR (101 MHz, CDCl₃, 50 °C) δ 150.0 (ArC), 132.0 (ArCH), 122.5 (ArCH), 119.0 (ArC), 25.5 (CH₂), 24.5 (CH₂) ppm.

mp (DCM): 58 - 60 °C.

IR: 2934, 2851, 2361, 1427, 1109, 1186, 827, 704, 629, 517 cm⁻¹.

HRMS (FTMS+ p NSI): [C₁₁H₁₄N₃Br] Calcd. 267.0371, Found 267.0372

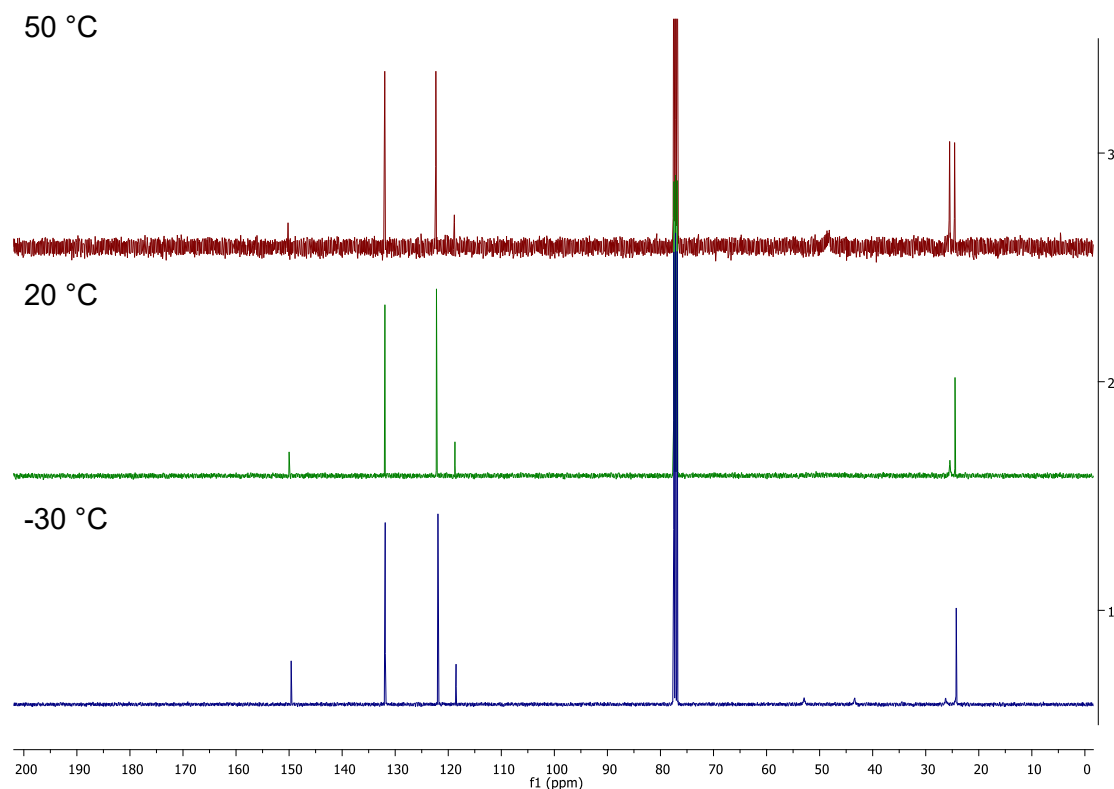
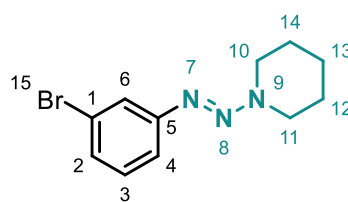


Figure 6.6: VT ¹³C NMR for Compound **30**

1-((3-bromophenyl)diazenyl)piperidine (31)^[1]

Following the general procedure, the title compound **31** was obtained from 3-bromoaniline as a pale orange oil in 75% yield (0.201 g).

¹H NMR (400 MHz, CDCl₃, rt) δ 7.61 (t, J = 1.9 Hz, 1H, ArH), 7.36 – 7.31 (m, 1H, ArH), 7.28 – 7.23 (m, 1H, ArH), 7.19 (t, J = 7.9 Hz, 1H), 3.84 – 3.72 (m, 4H, CH₂^{11,10}), 1.79 – 1.62 (m, 6H, CH₂^{12,13,14}) ppm.

¹³C NMR (101 MHz, CDCl₃, -30 °C) δ 152.0 (ArC), 130.5 (ArCH), 128.0 (ArCH), 123.0 (ArC), 122.5 (ArCH), 120.0 (ArCH), 53.0 (CH₂), 43.5 (CH₂), 26.5 (CH₂), 24.5 (CH₂), 24.0 (CH₂) ppm.

¹³C NMR (101 MHz, CDCl₃, rt) δ 152.5 (ArC), 130.0 (ArCH), 128.0 (ArCH), 123.0 (2 ArC), 120.0 (ArCH), 25.5 (CH₂), 24.5 (CH₂) ppm.

¹³C NMR (101 MHz, CDCl₃, 50 °C) δ 152.5 (ArC), 130.0 (ArCH), 128.0 (ArCH), 123.0 (2 ArC), 120.0 (ArCH), 48.5 (CH₂), 25.5 (CH₂), 24.5 (CH₂) ppm.

IR: 2938, 2855, 1584, 1564, 1433, 1404, 1352, 1180, 1103, 775, 683 cm⁻¹.

HRMS (EI⁺): [C₁₁H₁₄N₃Br]⁺ Calcd 267.0371, Found 267.0372.

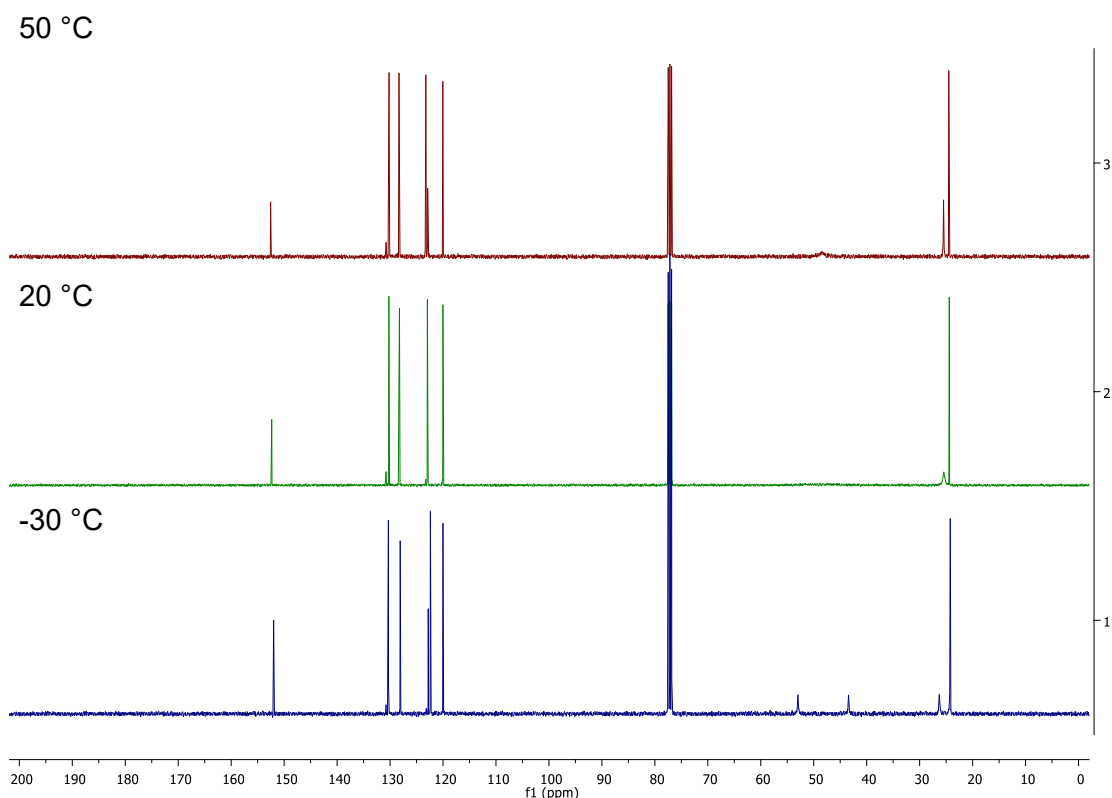
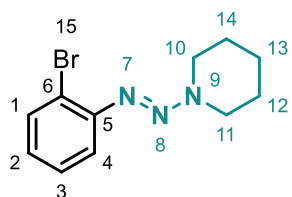


Figure 6.7: VT ¹³C NMR for Compound 31

1-((2-bromophenyl)diazenyl)piperidine (32)^[1]

Following the general procedure, the title compound **32** was obtained from 2-bromoaniline as a pale orange oil in 87% yield (0.233 g).

¹H NMR (400 MHz, CDCl₃, rt) δ 7.85 (d, *J* = 7.9 Hz, 1H, ArH), 7.38 (d, *J* = 8.0 Hz, 1H, ArH), 7.28 (t, *J* = 7.6 Hz, 1H, ArH), 6.93 – 6.81 (m, 1H, ArH), 4.24 – 3.51 (m, 4H, CH₂^{10,11}), 1.85-1.65 (m, 6H, CH₂^{12,13,14}) ppm.

¹³C NMR (101 MHz, CDCl₃, -30 °C) δ 149.5 (ArC), 139.0 (ArCH), 129.0 (ArCH), 127.0 (ArCH), 117.5 (ArCH), 97.0 (ArC), 53.0 (CH₂), 44.0 (CH₂), 26.5 (CH₂), 24.5 (CH₂), 24.0 (CH₂) ppm.

¹³C NMR (101 MHz, CDCl₃, rt) δ 150.0 (ArC), 139.0 (ArCH), 129.0 (ArCH), 127.0 (ArCH), 117.5 (ArCH), 97.0 (ArC), 24.5 (CH₂) ppm.

¹³C NMR (101 MHz, CDCl₃, 50 °C) δ 148.5 (ArC), 133.0 (ArCH), 128.0 (ArCH), 126.5 (ArCH), 120.0 (ArCH), 119.0 (ArC), 25.5 (CH₂), 24.5 (CH₂) ppm.

IR: 2938, 2853, 2361, 1464, 1418, 1107, 1028, 853, 756 cm⁻¹.

HRMS (FTMS+ p NSI): [C₁₁H₁₄N₃Br] Calcd. 267.0371, Found 267.0374.

50 °C

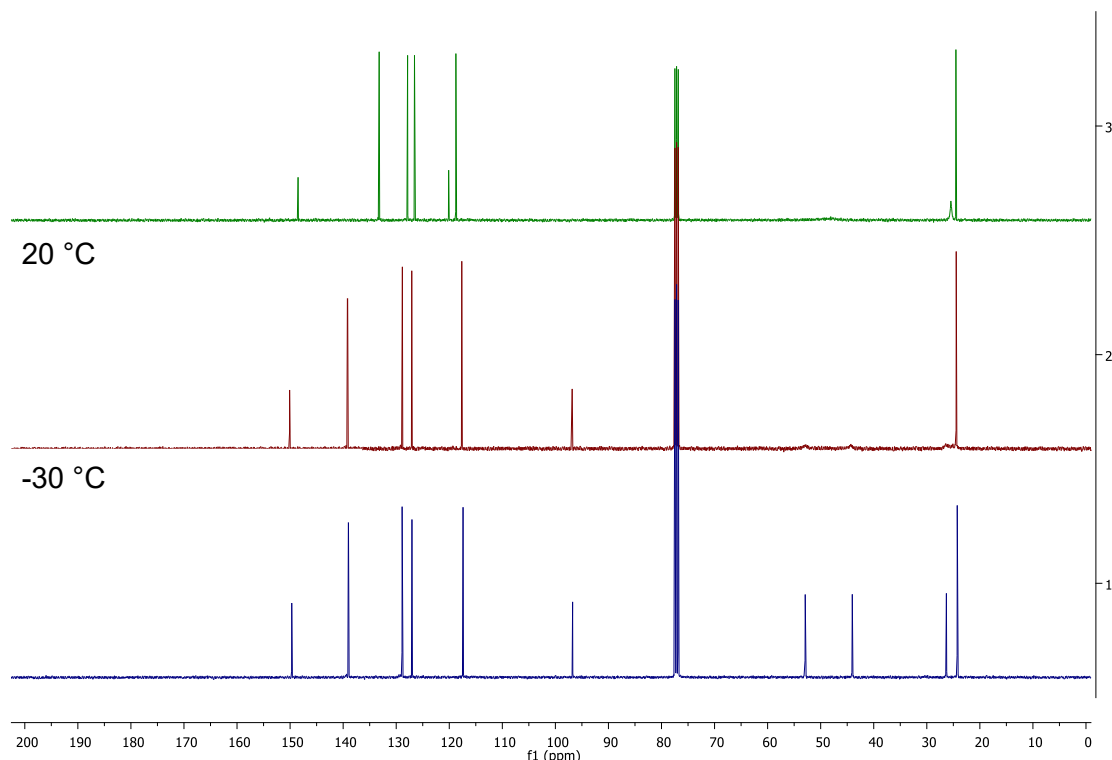
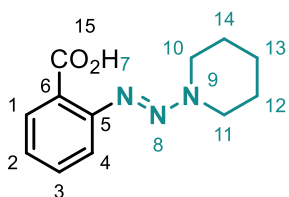


Figure 6.8: VT ¹³C NMR for Compound 32

2-(piperidin-1-yl diazenyl)benzoic acid (33)

Following the general procedure, the title compound **33** was obtained from anthranillic acid as a pale yellow solid in 70% yield (0.235 g).

^1H NMR (400 MHz, CDCl_3 , rt) δ 14.04 (s, 1H, COOH), 8.29 – 8.22 (m, 1H, ArH), 7.73 – 7.67 (m, 1H, ArH), 7.55 – 7.45 (m, 1H, ArH), 7.32 – 7.23 (m, 1H, ArH), 4.03 – 3.75 (m, 4H, $\text{CH}_2^{10,11}$), 1.95 – 1.70 (m, 6H, $\text{CH}_2^{12,13,14}$) ppm.

^{13}C NMR (101 MHz, CDCl_3 , $-30\text{ }^\circ\text{C}$) δ 168.0 (COOH), 148.5 (ArC), 134.0 (ArC), 132.0 (ArC), 126.0 (ArC), 121.0 (ArC), 115.5 (ArC), 54.0 (CH_2), 45.0 (CH_2), 26.0 (CH_2), 24.0 (CH_2), 23.5 (CH_2) ppm.

^{13}C NMR (101 MHz, CDCl_3 , rt) δ 167.5 (COOH), 148.5 (ArC), 133.5 (ArCH), 132.5 (ArCH), 126.0 (ArCH), 122.0 (ArC), 116.0 (ArCH), 54.0 (CH_2), 45.0 (CH_2), 26.0 (CH_2), 24.0 (CH_2), 23.5 (CH_2) ppm.

^{13}C NMR (101 MHz, CDCl_3 , $50\text{ }^\circ\text{C}$) δ 167.5 (COOH), 149.0 (ArC), 133.5 (ArCH), 132.5 (ArCH), 126.5 (ArC)H, 122.5 (ArC), 116.0 (ArCH), 25.0 (CH_2), 23.5 (CH_2) ppm.

mp (acetone): 88 - 90 $^\circ\text{C}$.

IR: 2945, 1703, 1704, 1593, 1410, 1109, 766, 692, 608 cm^{-1} .

HRMS (EI $^+$): [$\text{C}_{12}\text{H}_{15}\text{O}_2\text{N}_3$] Calcd. 233.1164, Found 233.1162.

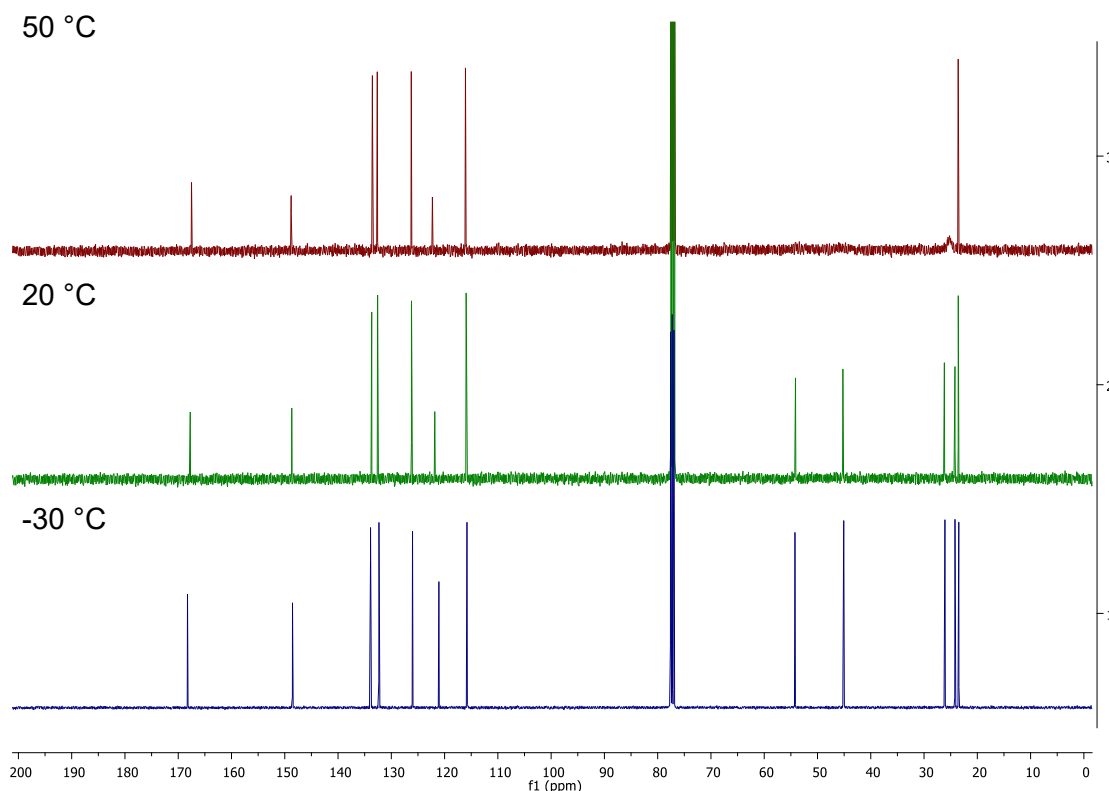
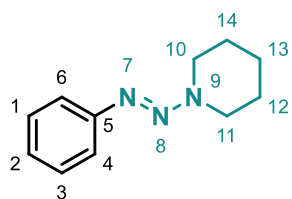


Figure 6.9: VT ^{13}C NMR for Compound **33**

1-(phenyldiazenyl)piperidine (34)^[1]

Following the general procedure, the title compound **34** was obtained from aniline as an orange oil in 69% yield (0.130 g).

¹H NMR (400 MHz, CDCl₃, rt) δ 7.46 – 7.40 (m, 2H, ArH), 7.37 – 7.30 (m, 2H, ArH), 7.19 – 7.12 (m, *J* = 7.3 Hz, 1H, ArH²), 3.84 – 3.71 (m, 4H, CH₂^{10,11}), 1.77 – 1.64 (m, 6H, CH₂^{12,13,14}) ppm.

¹³C NMR (101 MHz, CDCl₃, -30 °C) δ 150.5 (ArC), 129.0 (ArCH), 125.5 (ArC), 120.5 (ArCH), 52.5 (CH₂), 43.5 (CH₂), 26.0 (CH₂), 24.5 (CH₂), 24.0 (CH₂) ppm.

¹³C NMR (101 MHz, CDCl₃, rt) δ 151.0 (ArC), 129.0 (ArCH), 126.0 (ArC), 120.5 (ArCH), 25.5 (CH₂), 24.5 (CH₂) ppm.

¹³C NMR (101 MHz, CDCl₃, 50 °C) δ 151.0 (ArC), 129.0 (ArCH), 126.0 (ArC), 121.0 (ArCH), 48.5 (CH₂), 25.5 (CH₂), 24.5 (CH₂) ppm.

IR: 2940, 2922, 2855, 1591, 1580, 1483, 1408, 1186, 764, 694 cm⁻¹.

HRMS (EI⁺): [C₁₁H₁₅N₃] Calcd. 189.1266, Found 189.1263.

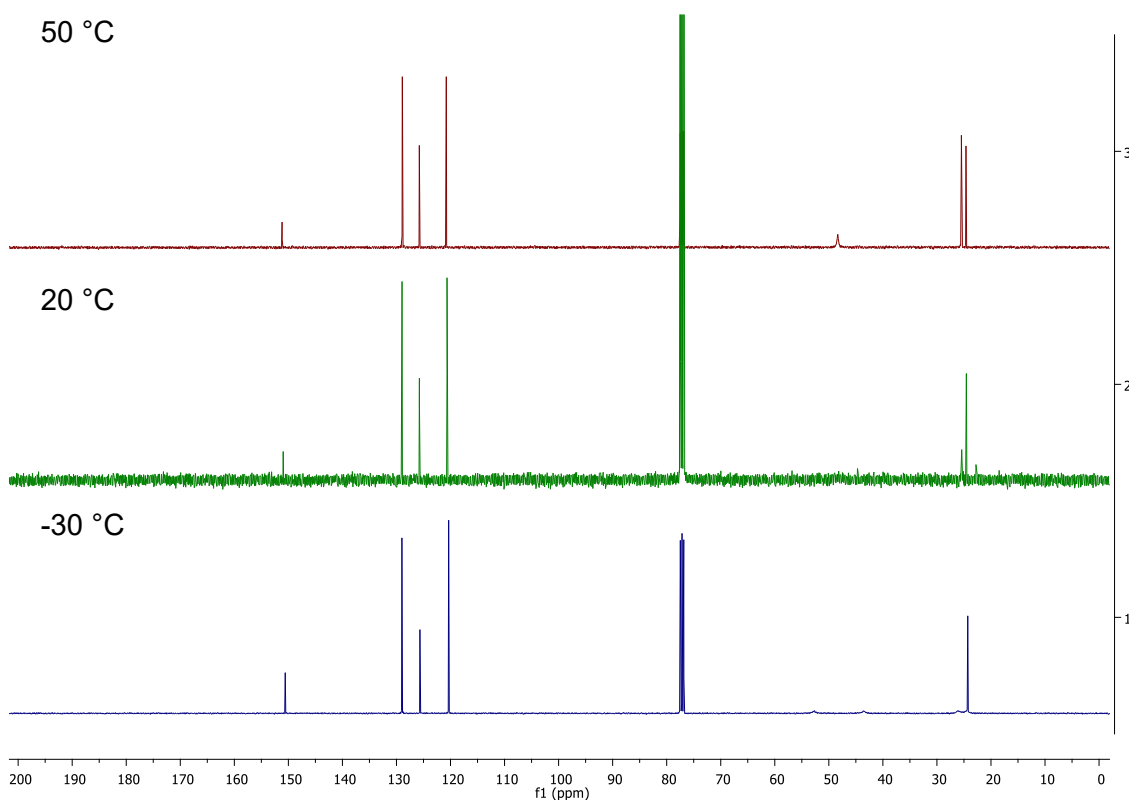
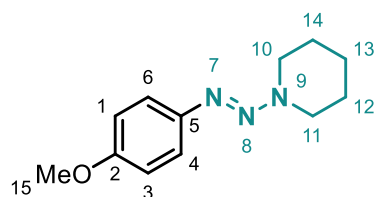


Figure 6.10: VT ¹³C NMR for Compound **34**

1-((4-methoxyphenyl)diazenyl)piperidine (35)

Following the general procedure, the title compound **35** was obtained from *p*-anisidine as an orange oil in 80% yield (0.176 g).

$^1\text{H NMR}$ (400 MHz, CDCl_3 , rt) δ 7.44 – 7.37 (m, 2H, ArH), 6.92 – 6.85 (m, 2H, ArH), 3.81 (s, 3H, CH_3^{15}), 3.77 – 3.68 (m, 4H, $\text{CH}_2^{10,11}$), 1.87 – 1.52 (m, 6H, $\text{CH}_2^{12,13,14}$) ppm.

$^{13}\text{C NMR}$ (101 MHz, CDCl_3 , $-30\text{ }^\circ\text{C}$) δ 157.5 (ArC), 144.5 (ArC), 121.5 (ArCH), 114.0 (ArCH), 55.5 (CH_3^{15}), 25.0 (CH_2), 24.5 (CH_2) ppm.

$^{13}\text{C NMR}$ (101 MHz, CDCl_3) δ 158.0 (ArC), 145.0 (ArCH), 121.5 (ArCH), 114.0 (ArC), 55.5 (CH_3^{15}), 48.5 (CH_2), 25.5 (CH_2), 24.5 (CH_2) ppm.

$^{13}\text{C NMR}$ (101 MHz, CDCl_3) δ 158.0 (ArC), 145.0 (ArCH), 121.5 (ArCH), 114.0 (ArC), 55.5 (CH_3^{15}), 48.5 (CH_2), 25.5 (CH_2), 24.5 (CH_2) ppm.

IR: 2936, 2833, 2359, 1506, 1456, 1246, 1101, 835 cm^{-1} .

HRMS (FTMS+ *p* NSI): $[\text{C}_{12}\text{H}_{18}\text{ON}_3]$ Calcd. 220.1444, Found 220.1444.

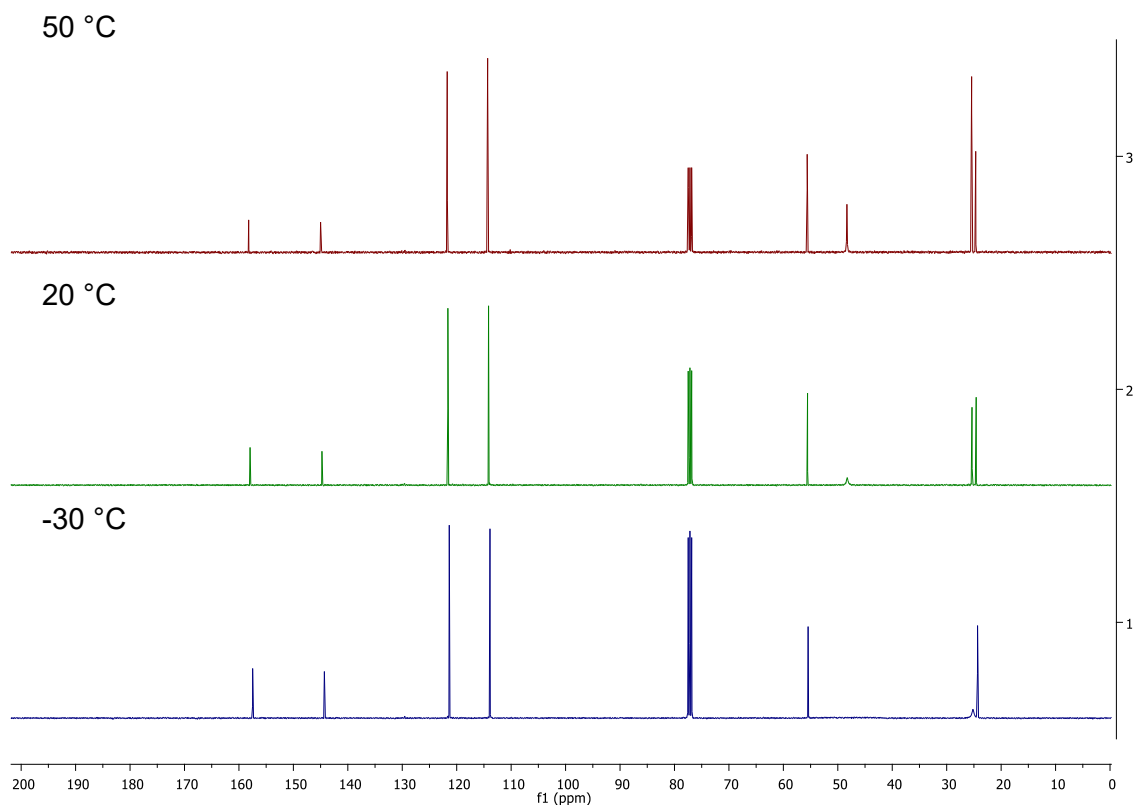
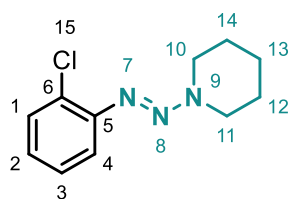


Figure 6.11: VT $^{13}\text{C NMR}$ for Compound 35

1-((2-chlorophenyl)diazenyl)piperidine (36)

Following the general procedure, the title compound **36** was obtained from *o*-chloroaniline as an orange oil in 83% yield (0.185 g).

^1H NMR (400 MHz, CDCl_3 , rt) δ 7.44 (dd, $J = 8.1, 1.6$ Hz, 1H, ArH), 7.38 (dd, $J = 8.0, 1.4$ Hz, 1H, ArH), 7.23 – 7.17 (m, 1H, ArH), 7.09 – 7.03 (m, 1H, ArH), 3.93 – 3.74 (m, 4H, $\text{CH}_2^{10,11}$), 1.81 – 1.64 (m, 6H, $\text{CH}_2^{12,13,14}$) ppm.

^{13}C NMR (101 MHz, CDCl_3 , -30 °C) δ 147.0 (ArC), 130.0 (ArCH), 129.0 (ArC), 127.5 (ArCH), 126.0 (ArHC), 118.5 (ArCH), 53.0 (CH_2), 43.5 (CH_2), 26.5 (CH_2), 24.0 (CH_2) ppm.

^{13}C NMR (101 MHz, CDCl_3 , rt) δ 147.5 (ArC), 130.0 (ArCH), 129.5 (ArC), 127.0 (ArCH), 126.0 (ArCH), 118.5 (ArCH), 24.5 (CH_2) ppm.

^{13}C NMR (101 MHz, CDCl_3 , 50 °C) δ 147.5 (ArC), 130.0 (ArCH), 129.5 (ArC), 127.0 (ArCH), 126.0 (ArCH), 119.0 (ArCH), 25.5 (CH_2), 24.5 (CH_2) ppm.

IR: 2945, 2855, 1468, 1402, 1184, 760, 698, 556 cm^{-1} .

HRMS (FTMS+ p NSI): $[\text{C}_{11}\text{H}_{14}\text{N}_3\text{Cl}]$ Calcd. 224.0949, Found 224.0950.

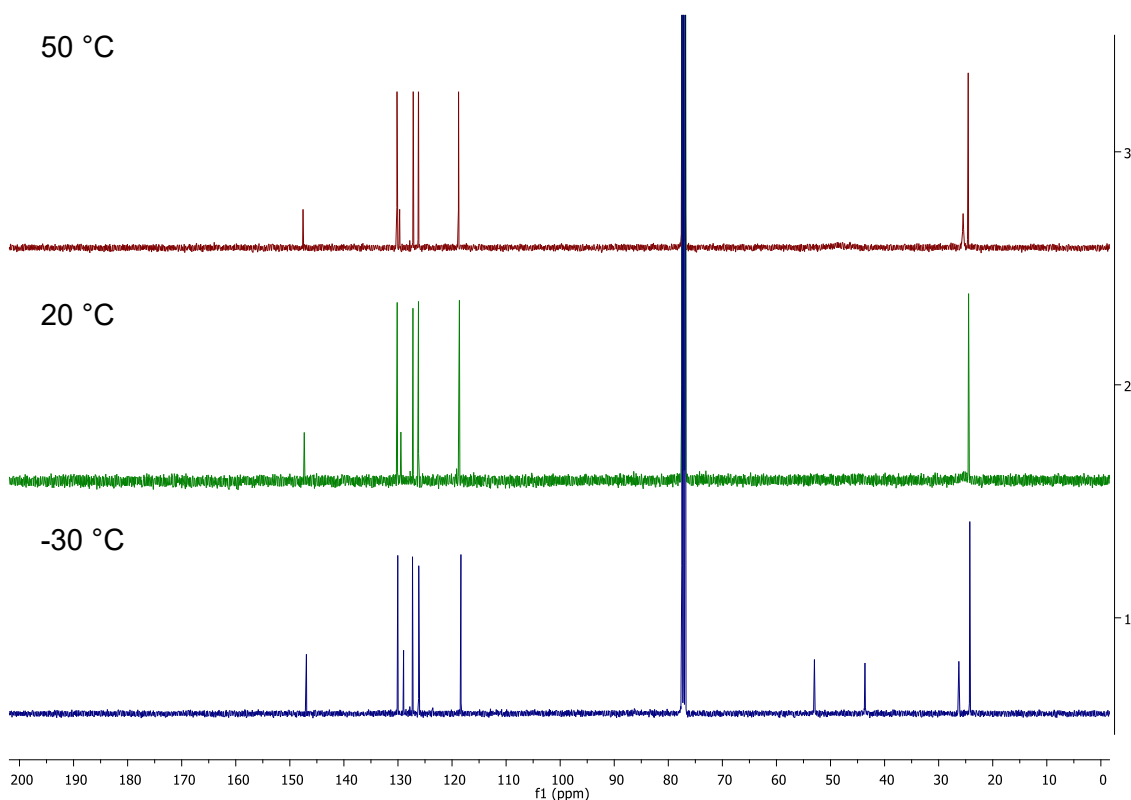
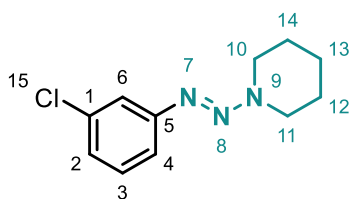


Figure 6.12: VT ^{13}C NMR for Compound 36

1-((3-chlorophenyl)diazenyl)piperidine (37)

Following the general procedure, the title compound **37** was obtained from *m*-chloroaniline as a red oil in 74% yield (0.165 g).

^1H NMR (400 MHz, CDCl_3 , rt) δ 7.44 (t, $J = 1.9$ Hz, 1H, ArH), 7.31 – 7.27 (m, 1H, ArH), 7.24 (t, $J = 7.8$ Hz, 1H, ArH), 7.12 – 7.08 (m, 1H, ArH), 3.86 – 3.74 (m, 4H, $\text{CH}_2^{10,11}$), 1.77 – 1.65 (m, 6H, $\text{CH}_2^{12,13,14}$) ppm.

^{13}C NMR (101 MHz, CDCl_3 , -30 °C) δ 152.0 (ArC), 134.5 (ArC), 130.0 (ArCH), 125.0 (ArCH), 119.5 (2 ArCH), 53.0 (CH_2), 43.5 (CH_2), 26.5 (CH_2), 24.0 (CH_2) ppm.

^{13}C NMR (101 MHz, CDCl_3 , rt) δ 152.5 (ArC), 134.5 (ArC), 130.0 (ArCH), 125.5 (ArCH), 120.0 (ArCH), 119.5 (ArCH), 24.5 (CH_2) ppm.

^{13}C NMR (101 MHz, CDCl_3 , 50 °C) δ 152.5 (ArC), 135.0 (ArC), 130.0 (ArCH), 125.5 (ArCH), 120.5 (ArCH), 119.5 (ArCH), 48.5 (CH_2), 25.5 (CH_2), 24.5 (CH_2) ppm.

IR: 2938, 2855, 2361, 1418, 1362, 1107, 997, 854, 781, 687 cm^{-1} .

HRMS (FTMS+ p NSI): $[\text{C}_{11}\text{H}_{15}\text{N}_3\text{Cl}]$ Calcd. 224.0949, Found 224.0950.

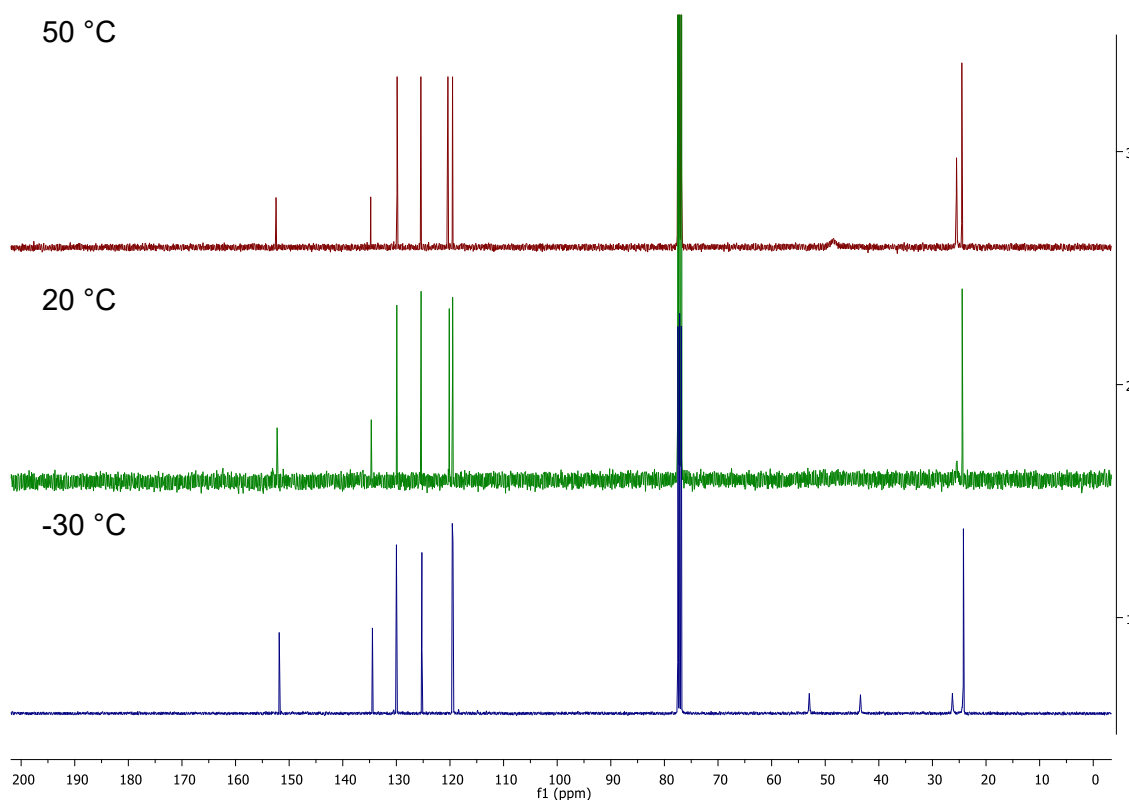
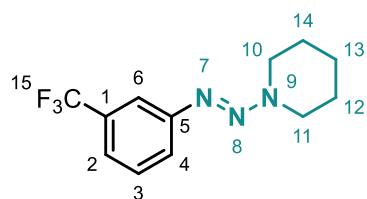


Figure 6.13: VT ^{13}C NMR for Compound 37

1-((3-(trifluoromethyl)phenyl)diazenyl)piperidine (38)

Following the general procedure, the title compound **38** was obtained from *m*-trifluoromethylaniline as a red oil in 80% yield (0.206 g).

^1H NMR (400 MHz, CDCl_3 , rt) δ 7.69 (s, 1H), 7.59 (d, $J = 7.8$ Hz, 1H), 7.45 – 7.35 (m, 2H), 3.89 – 3.75 (m, $J = 5.5$ Hz, 4H), 1.79 – 1.66 (m, 6H) ppm.

^{13}C NMR (101 MHz, CDCl_3 , -30 °C) δ 152.0 (ArC), 134.5 (ArC), 130.0 (ArCH), 125.5 (ArCH), 119.5 (2 ArCH), 53.0 (CH_2), 43.5 (CH_2), 26.5 (CH_2), 24.0 (CH_2) ppm.

^{13}C NMR (101 MHz, CDCl_3 , rt) δ 151.5 (ArC), 131.5 (q, $J = 32.1$ Hz, ArC¹), 129.5 (ArCH), 124.5 (q, $J = 272.3$ Hz, CF_3^{15}), 124.0 (ArC), 122.0 (q, $J = 3.8$ Hz, ArCH), 117.5 (q, $J = 3.8$ Hz, ArCH), 25.5 (CH_2), 24.5 (CH_2) ppm.

^{13}C NMR (101 MHz, CDCl_3 , 50 °C) δ 151.5 (ArC), 129.5 (ArCH), 124.0 (ArCH), 122.0 (ArC), 117.5 (ArC), 25.5 (CH_2), 24.5 (CH_2) ppm.

IR: 2941, 2859, 2359, 1558, 1541, 1508, 1456, 1331, 1128, 1065, 899, 799 cm^{-1} .

HRMS (FTMS+ p NSI): $[\text{C}_{12}\text{H}_{14}\text{N}_3\text{F}_3]$ Calcd. 257.1140, Found 257.1140.

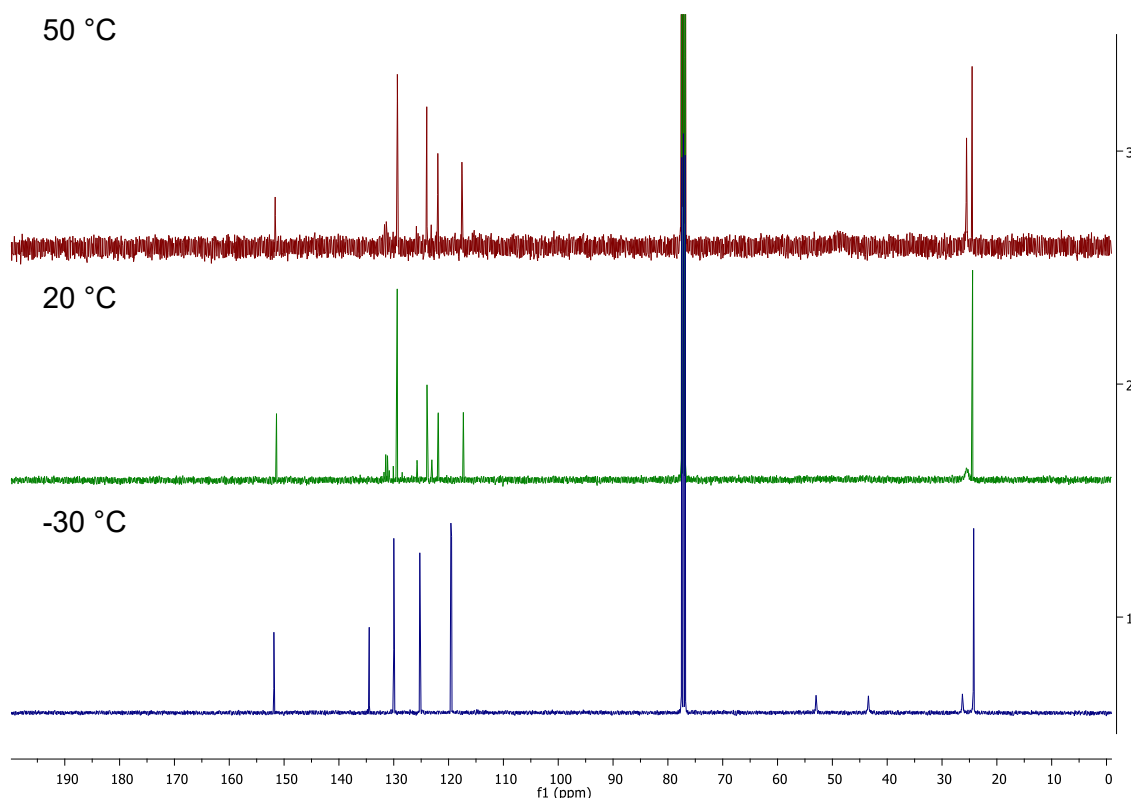
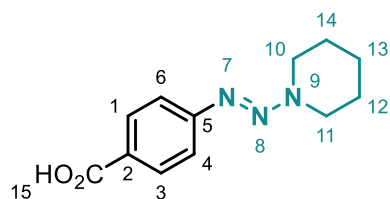


Figure 6.14: VT ^{13}C NMR for Compound **38**

4-(piperidin-1-yl diazenyl)benzoic acid (39)

Following the general procedure, the title compound **39** was obtained from 4-aminobenzoic acid as an off-white solid in 76% yield (0.178 g).

$^1\text{H NMR}$ (400 MHz, CDCl_3 , rt) δ 8.11 – 8.04 (m, 2H, ArH), 7.53 – 7.45 (m, 2H, ArH), 3.95 – 3.76 (m, 4H, $\text{CH}_2^{10,11}$), 1.83 – 1.64 (m, 6H, $\text{CH}_2^{12,13,14}$) ppm.

$^{13}\text{C NMR}$ (101 MHz, CDCl_3 , $-30\text{ }^\circ\text{C}$) δ 173.0 (COOH), 155.0 (ArC), 131.5 (ArCH), 125.5 (ArC), 120.0 (ArCH), 53.5 (CH_2), 43.5 (CH_2), 26.5 (CH_2), 24.5 (CH_2), 24.0 (CH_2) ppm.

$^{13}\text{C NMR}$ (101 MHz, CDCl_3 , rt) δ 172.5 (COOH), 155.5 (ArC), 131.5 (ArCH), 126.0 (ArC), 120.5 (ArCH), 30.0 (CH_2), 25.5 (CH_2), 24.5 (CH_2) ppm.

$^{13}\text{C NMR}$ (101 MHz, CDCl_3 , $50\text{ }^\circ\text{C}$) δ 172.0 (COOH), 155.5 (ArC), 131.5 (ArCH), 126.0 (ArC), 120.5 (ArCH), 30.0 (CH_2), 25.5 (CH_2), 24.5 (CH_2) ppm.

mp (DCM): 152 - 154 $^\circ\text{C}$.

IR: 2943, 2851, 2531, 1668, 1599, 1423, 1402, 1281, 1099, 856, 515 cm^{-1} .

HRMS (EI $^+$): $[\text{C}_{12}\text{H}_{15}\text{N}_3\text{O}_2]^+$ Calcd. 233.1164, Found 233.1157.

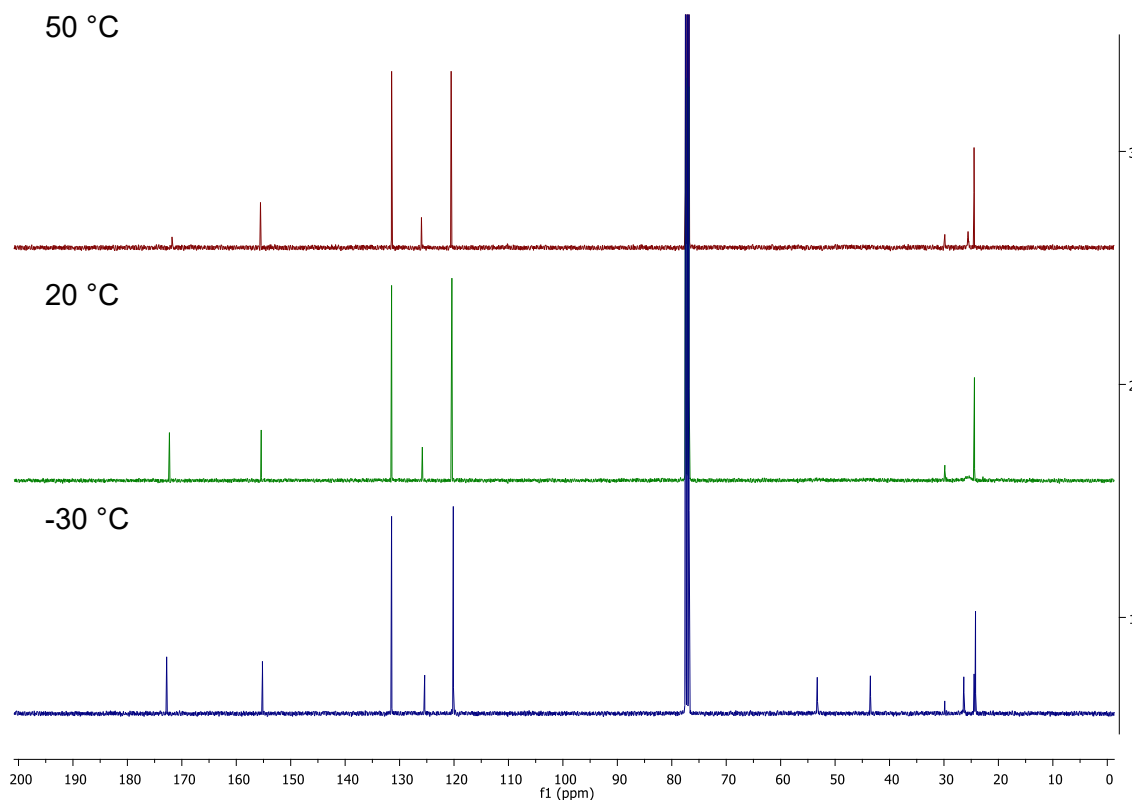
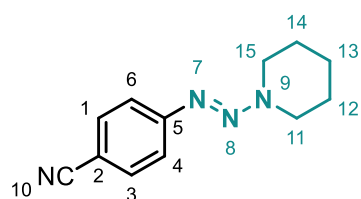


Figure 6.15: VT $^{13}\text{C NMR}$ for Compound 39

4-(piperidin-1-ylidiazenyl)benzonitrile (40)

Following the general procedure, the title compound **40** was obtained from 4-aminobenzonitrile as an orange solid in 83% yield (0.178 g).

^1H NMR (400 MHz, CDCl_3 , rt) δ 7.63 – 7.56 (m, 2H, ArH), 7.50 – 7.44 (m, 2H, ArH), 3.97 – 3.73 (m, 4H, $\text{CH}_2^{11,15}$), 1.82 – 1.60 (m, 6H, $\text{CH}_2^{12,13,14}$) ppm.

^{13}C NMR (101 MHz, CDCl_3 , $-30\text{ }^\circ\text{C}$) δ 154.0 (ArC), 133.0 (ArCH), 120.5 (ArCH), 120.0 (CN), 107.5 (ArC), 53.5 (CH_2), 43.5 (CH_2), 26.5 (CH_2), 24.5 (CH_2), 24.0 (CH_2) ppm.

^{13}C NMR (101 MHz, CDCl_3 , rt) δ 154.5 (ArC), 133.0 (ArCH), 121.0 (ArCH), 120.0 (CN), 108.0 (ArC), 24.5 (CH_2) ppm.

^{13}C NMR (101 MHz, CDCl_3 , $50\text{ }^\circ\text{C}$) δ 154.5 (ArC), 133.0 (ArCH), 121.0 (ArCH), 119.5 (CN), 108.0 (ArC), 25.5 (CH_2), 24.5 (CH_2) ppm.

mp (DCM): 74 - 76 $^\circ\text{C}$.

IR: 2918, 2359, 1668, 1597, 1386, 1280, 939, 856, 698 cm^{-1} .

HRMS (FTMS+ p NSI): $[\text{C}_{12}\text{H}_{14}\text{N}_4]$ Calcd. 215.1297, Found 215.1307.

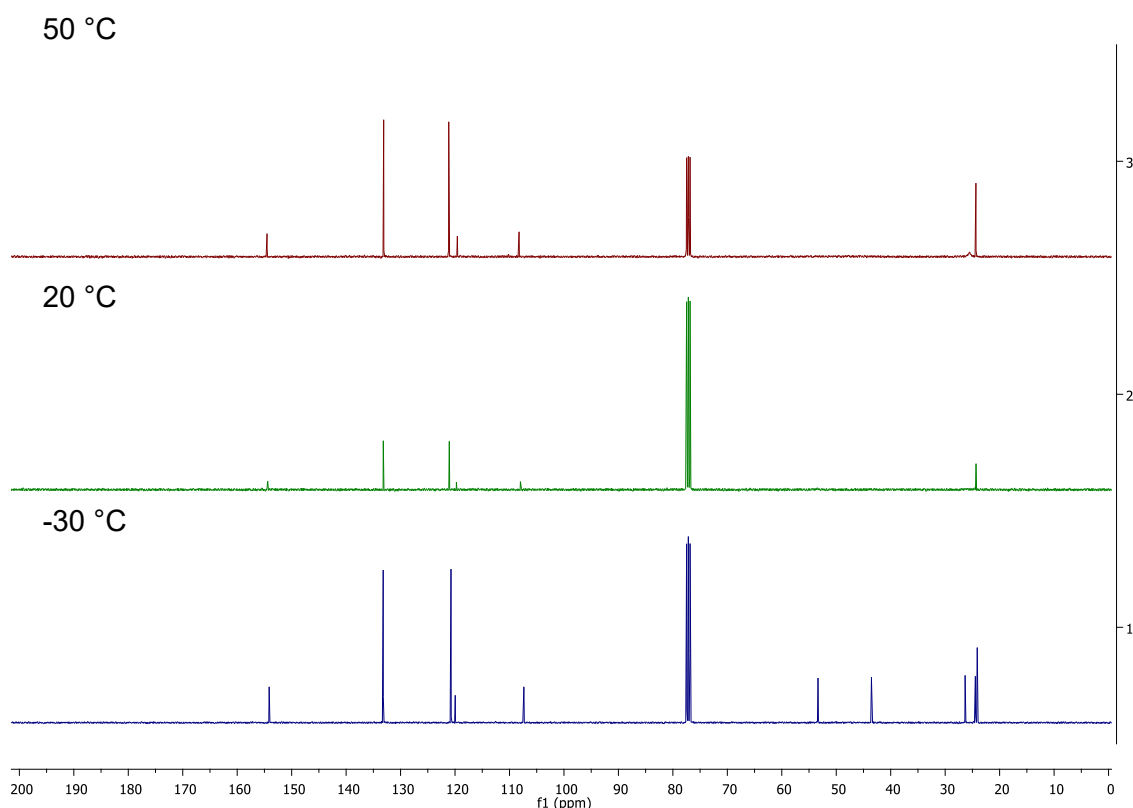
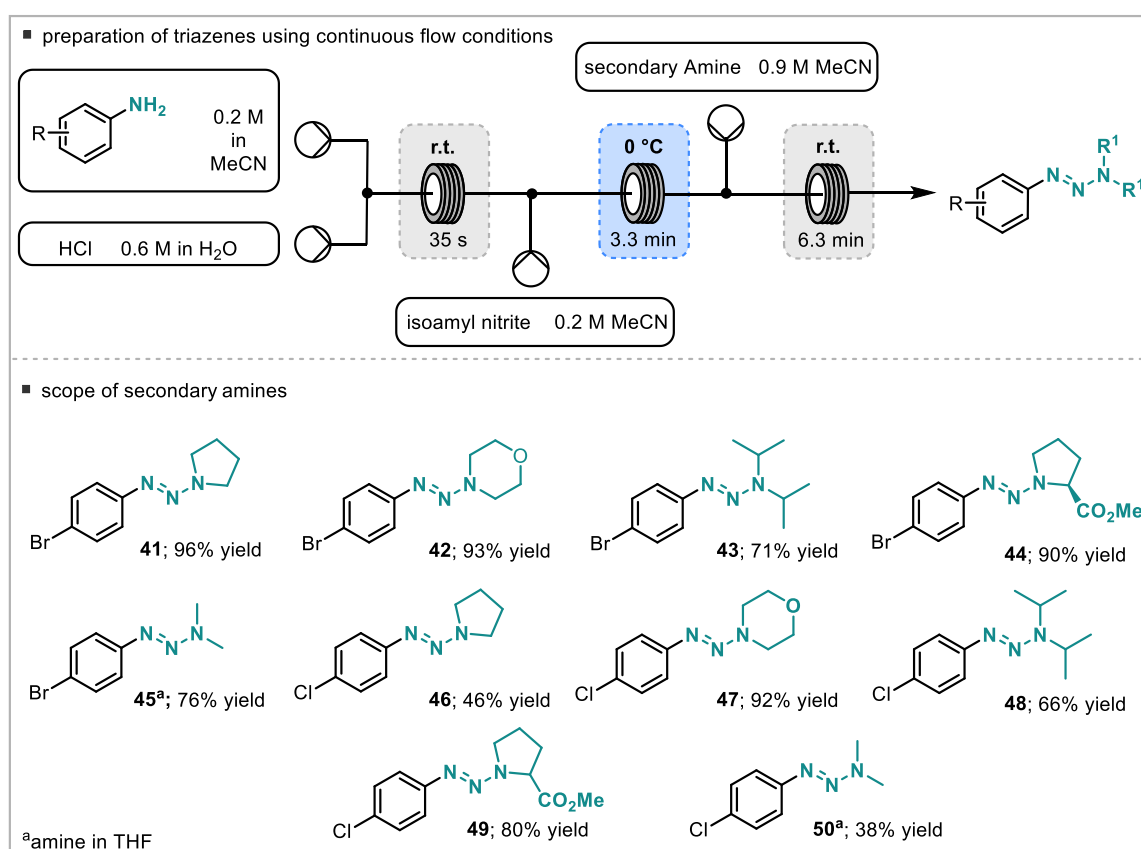


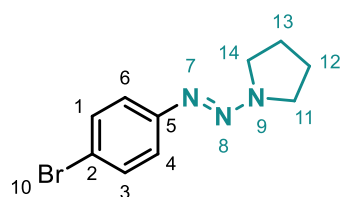
Figure 6.16: VT ^{13}C NMR for Compound **40**

2.3 General Method for the Preparation of Triazenes **41** - **50** in Flow

Solutions of *p*-chloroaniline or *p*-bromoaniline (0.2 M in acetonitrile), HCl (0.6 M in water), isoamylnitrite (0.2 M in acetonitrile) and the secondary amine (0.9 M in acetonitrile) were prepared. These were then pumped through the flow system (see Scheme 6.3) at a flow rate of 0.2 mL min⁻¹. After 20 min steady state was reached and an aliquot of 20 mL (1 mmol, 25 min) was collected. The reaction solution was neutralized with aqueous NaHCO₃, extracted with EtOAc (3 x 20 mL), washed with brine and dried over MgSO₄. After removing the solvent under reduced pressure, the crude product was further purified by column chromatography (0 to 10% EtOAc in petroleum ether).



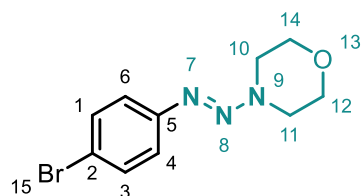
Scheme 6.3: Preparation of Triazenes Using Continuous Flow Conditions: Amine Scope

1-((4-bromophenyl)diazenyl)pyrrolidine (41)^[4]

Following the general procedure, the title compound **41** was obtained from pyrrolidine as a pale yellow solid in 96% yield (0.244 g).

¹H NMR (400 MHz, CDCl₃, rt) δ 7.44 – 7.39 (m, 2H, ArH), 7.31 – 7.26 (m, 2H, ArH), 4.08 – 3.37 (m, 4H, CH₂^{11,14}), 2.14 – 1.88 (m, 4H, CH₂^{12,13}) ppm.

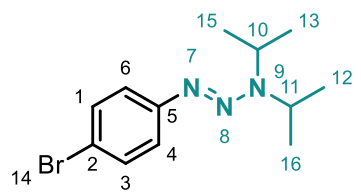
¹³C NMR (126 MHz, CDCl₃, rt) δ 150.5 (ArC), 132.0 (ArCH), 122.0 (ArCH), 118.0 (ArC), 51.0 (CH₂), 46.5 (CH₂), 24.0 (CH₂) ppm.

4-((4-bromophenyl)diazenyl)morpholine (42)^[5]

Following the general procedure, the title compound **42** was obtained from morpholine as pale yellow solid in 93% yield (0.250 g).

¹H NMR (400 MHz, CDCl₃, rt) δ 7.52 – 7.42 (m, 2H, ArH), 7.37 – 7.28 (m, 2H, ArH), 3.89 – 3.82 (m, 4H, CH₂), 3.82 – 3.75 (m, 4H, CH₂) ppm.

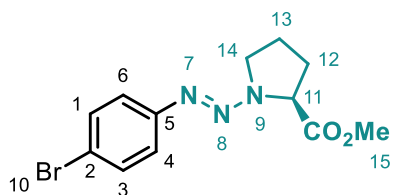
¹³C NMR (101 MHz, CDCl₃, rt) δ 149.0 (ArC), 132.0 (ArCH), 122.5 (ArCH), 120.0 (ArC), 66.5 (CH₂) ppm.

1-(4-bromophenyl)-3,3-diisopropyltriaz-1-ene (43)^[6]

Following the general procedure, the title compound **43** was obtained from diisopropylamine as an orange oil in 71% yield (0.201 g).

¹H NMR (400 MHz, CDCl₃, rt) δ 7.44 – 7.38 (m, 2H, ArH), 7.31 – 7.26 (m, 2H, ArH), 5.63 – 5.06 (m, 1H, CH), 4.27 – 3.72 (m, 1H, CH), 1.51 – 1.00 (m, 12H, CH₃^{12,13,15,16}) ppm.

¹³C NMR (126 MHz, CDCl₃, rt) δ 151.0 (ArC), 132.0 (ArCH), 122.0 (ArCH), 117.5 (ArC), 49.0 (CH), 46.0 (CH), 24.0 (CH₃), 19.5 (CH₃) ppm.

methyl(4-bromophenyl)diazenyl)-L-prolinate (44)

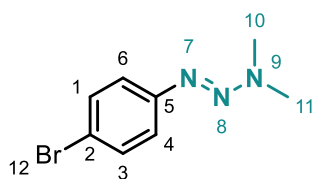
Following the general procedure, the title compound **44** was obtained from L-proline methyl ester as pale yellow oil in 90% yield (0.280 g).

^1H NMR (500 MHz, CDCl_3 , rt) δ 7.45 – 7.39 (m, 2H, ArH), 7.31 – 7.25 (m, 2H, ArH), 4.86 – 4.49 (m, 1H, CH^{11}), 4.22 – 3.55 (m, 2H, CH_2^{14}), 3.75 (s, 3H, CH_3^{15}), 2.41 – 2.28 (m, 1H, CH_2), 2.23 – 2.10 (m, 2H, CH_2), 2.10 – 1.97 (m, 1H, CH_2) ppm.

^{13}C NMR (126 MHz, CDCl_3 , rt) δ 172.5 (COOH), 140.5 (COOH), 131.5 (2 ArCH), 122.5 (ArCH), 119.0 (ArC), 63.5 (CH_2), 59.5 (CH_2), 52.5 (OCH₃), 51.0 (CH_2), 47.0 (CH_2), 29.0 (CH_2), 23.0 (CH_2) ppm.

IR: 2951, 2876, 1740, 1479, 1427, 1392, 1323, 1148, 1067, 827 cm^{-1} .

HRMS (EI⁺): [$\text{C}_{12}\text{H}_{15}\text{N}_3\text{O}_2\text{Br}$]⁺ Calcd. 312.0348, Found 312.0351.

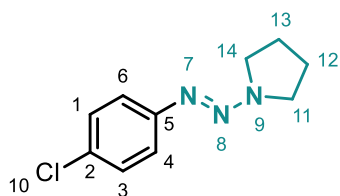
1-(4-bromophenyl)-3,3-dimethyltriaz-1-ene (45)^[7]

Following the general procedure, solutions of the 4-bromoaniline (0.2 M in acetonitrile), HCl (0.6 M in water), isoamyl nitrite (0.2 M in acetonitrile) and a dimethylamine (0.9 M in THF) were prepared. The title compound **45** was

obtained from dimethylamine as a red oil in 76% yield (0.173 g).

^1H NMR (400 MHz, CDCl_3 , rt) δ 7.46 – 7.40 (m, 2H, ArH), 7.33 – 7.27 (m, 2H, ArH), 3.71 – 3.00 (m, 6H, CH_3) ppm.

^{13}C NMR (126 MHz, CDCl_3 , rt) δ 150.0 (ArCH), 132.0 (ArC), 122.0 (ArC), 118.50 (ArCH) ppm.

1-((4-chlorophenyl)diazenyl)pyrrolidine (46)

Following the general procedure, the title compound **46** was obtained from pyrrolidine as a pale yellow solid in 46% yield (0.096 g).

^1H NMR (400 MHz, CDCl_3 , rt) δ 7.35 – 7.29 (m, 2H, ArH), 7.25 (d, $J = 7.5$ Hz, 2H, ArH), 4.05 – 3.50 (m, 4H, $\text{CH}_2^{11,14}$), 2.08 – 1.93 (m, 4H, $\text{CH}_2^{12,13}$) ppm.

^{13}C NMR (101 MHz, CDCl_3 , -30 °C) δ 150.0 (ArC), 130.0 (ArC), 129.0 (ArCH), 121.5 (ArCH), 51.5 (CH_2), 46.5 (CH_2), 24.0 (CH_2), 23.5 (CH_2) ppm.

^{13}C NMR (101 MHz, CDCl_3 , rt) δ 150.0 (ArC), 130.5 (ArC), 129.0 (ArCH), 122.0 (ArCH), 24.0 (CH_2) ppm.

^{13}C NMR (101 MHz, CDCl_3 , 50 °C) δ 150.0 (ArC), 130.5 (ArC), 129.0 (ArCH), 121.5 (ArCH), 24.0 (CH_2) ppm.

mp (DCM): 48 - 50 °C.

IR: 3952, 2963, 2837, 2785, 2172, 1659, 1639, 1248, 1090, 1040, 883 cm^{-1} .

HRMS(FTMS+ p NSI): $[\text{C}_{10}\text{H}_{13}\text{N}_3\text{Cl}]$ Calcd. 210.0798, Found 210.0797.

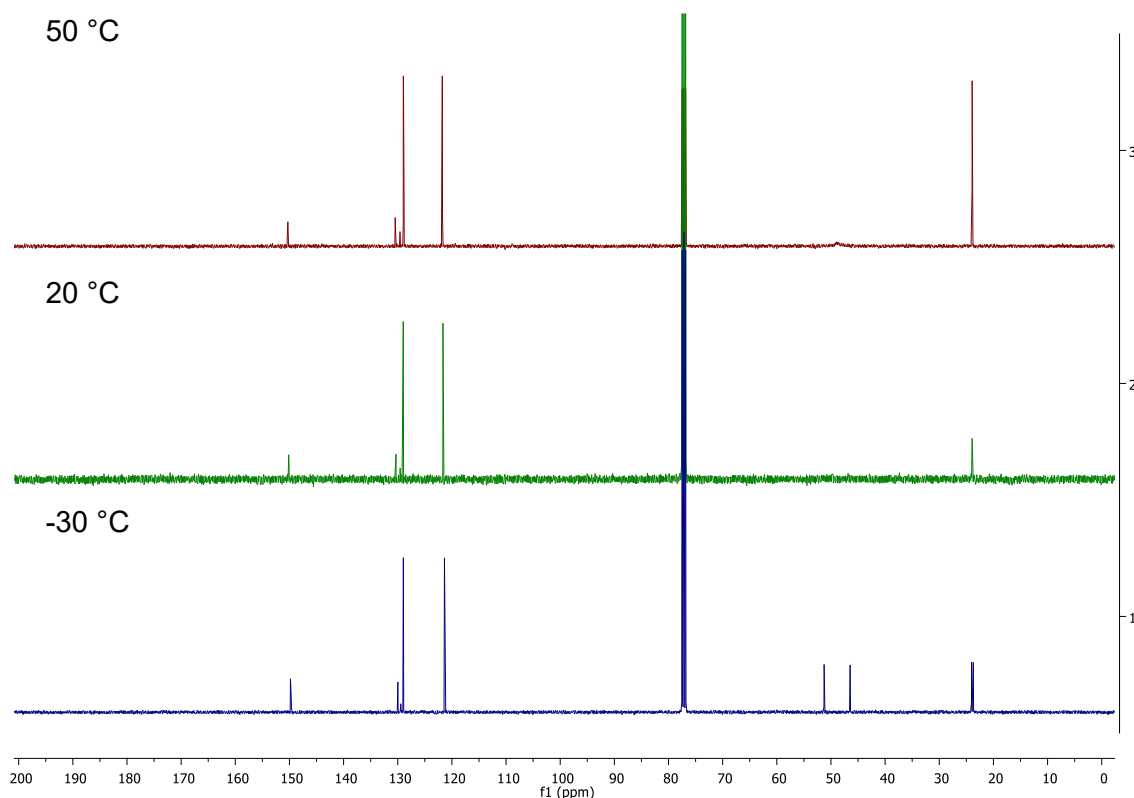
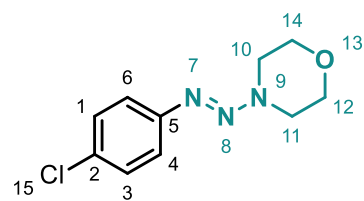


Figure 6.17: VT ^{13}C NMR for Compound 46

4-((4-chlorophenyl)diazenyl)morpholine (47)



Following the general procedure, the title compound **47** was obtained from morpholine as an orange solid in 92% yield (0.208 g).

^1H NMR (400 MHz, CDCl_3 , rt) δ 7.39 (d, $J = 8.7$ Hz, 2H, ArH), 7.31 (d, $J = 8.7$ Hz, 2H, ArH), 3.88 – 3.82 (m, 4H, CH_2), 3.82 – 3.76 (m, 4H, CH_2) ppm.

^{13}C NMR (101 MHz, CDCl_3 , -30 °C) δ 148.5 (ArC), 131.5 (ArC), 129.0 (ArCH), 122.0 (ArCH), 66.5 (CH_2), 51.5 (CH_2), 44.0 (CH_2) ppm.

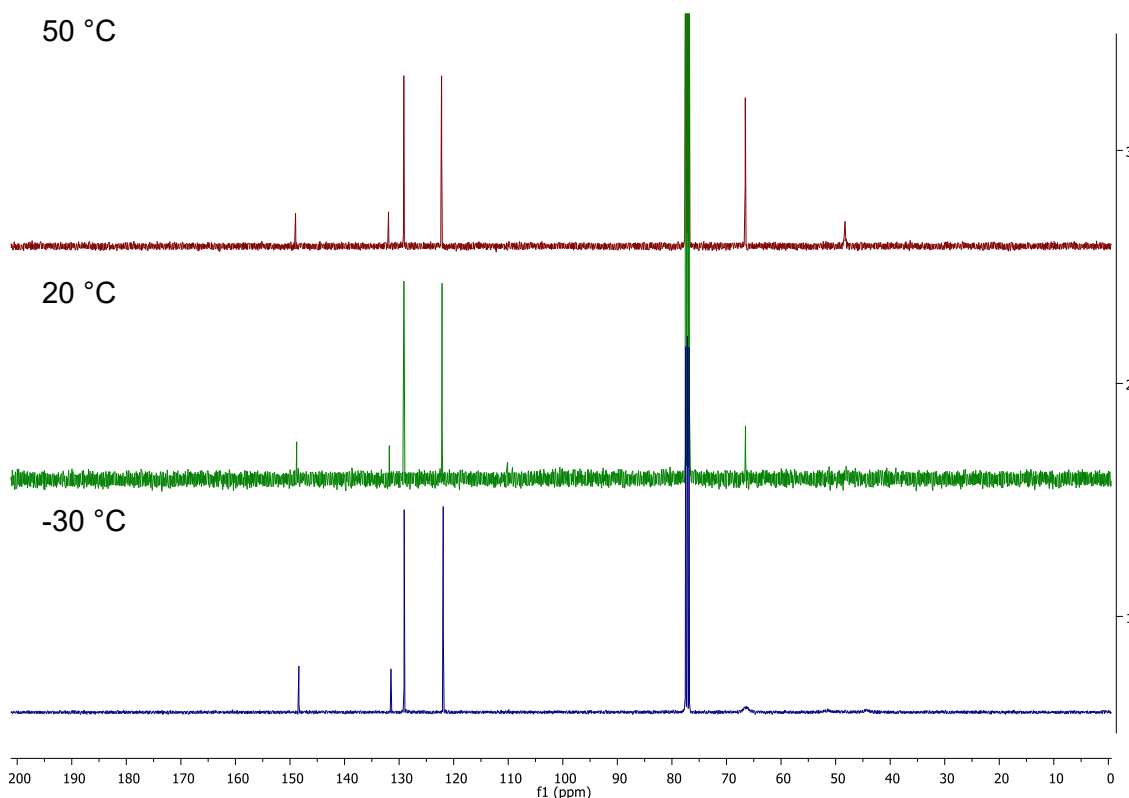
^{13}C NMR (101 MHz, CDCl_3 , rt) δ 149.0 (ArC), 132.0 (ArC), 129.0 (ArCH), 122.0 (ArCH), 66.5 (CH_2) ppm.

^{13}C NMR (101 MHz, CDCl_3 , 50 °C) δ 149.0 (ArC), 132.0 (ArC), 129.0 (ArCH), 122.0 (ArCH), 66.5 (CH_2), 48.0 (CH_2) ppm.

mp (DCM): 40 - 42 °C.

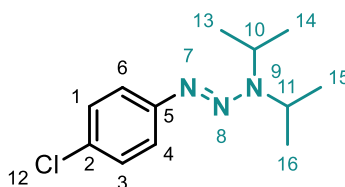
IR: 2858, 1437, 1400, 1342, 1153, 1099, 1004, 937, 626, 549 cm^{-1} .

HRMS (EI^+): [$\text{C}_{10}\text{H}_{12}\text{ClN}_3\text{O}$] Calcd. 225.0669, Found 225.0677.



6.18: VT ^{13}C NMR for Compound 47

1-(4-chlorophenyl)-3,3-diisopropyltriaz-1-ene (48)



Following the general procedure, the title compound **48** was obtained from diisopropylamine as an orange oil in 66% yield (0.157 g).

^1H NMR (400 MHz, CDCl_3 , rt) δ 7.34 (d, $J = 8.7$ Hz, 2H, ArH), 7.27 (d, $J = 8.7$ Hz, 2H, ArH), 4.49 – 4.88 (m, 1H, CH), 4.21 – 3.69 (m, 1H, CH), 1.49 – 1.08 (m, 12H, CH_3) ppm.

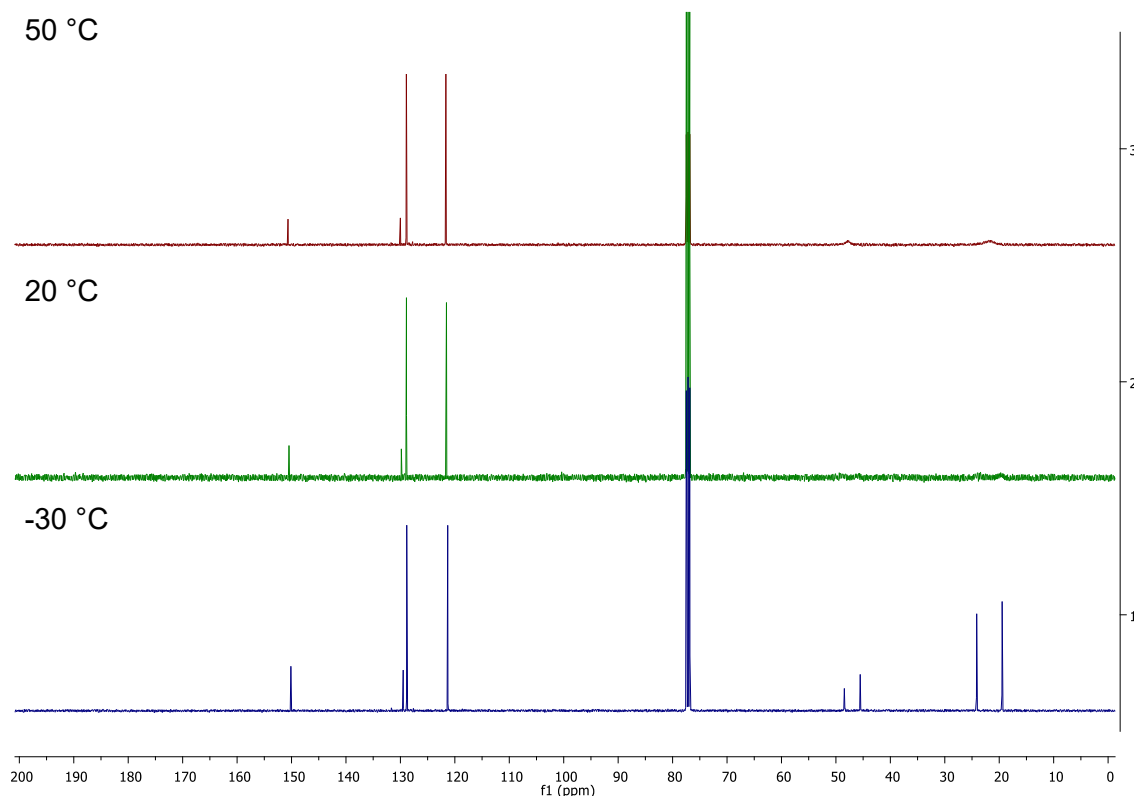
^{13}C NMR (101 MHz, CDCl_3 , -30 °C) δ 150.0 (ArC), 129.5 (ArC), 129.0 (ArC), 121.5 (ArC), 48.5 (CH), 46.5 (CH), 24.0 (CH_3), 19.5 (CH_3) ppm.

^{13}C NMR (101 MHz, CDCl_3 , rt) δ 150.5 (ArC), 130.0 (ArC), 129.0 (ArCH), 121.5 (ArCH) ppm.

^{13}C NMR (101 MHz, CDCl_3 , 50 °C) δ 155.5 (ArC), 130.0 (ArC), 129.0 (ArCH), 121.5 (ArCH), 48.0 (CH), 21.5 (CH_2) ppm.

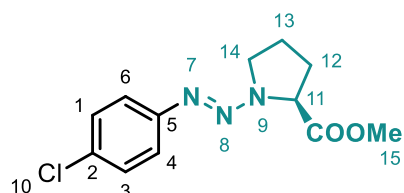
IR: 2972, 1481, 1296, 1159, 1087, 831, 536, 486 cm^{-1} .

HRMS: $[\text{C}_{12}\text{H}_{19}\text{N}_3\text{Cl}]$ Calcd. 240.1267, Found 240.1268.



6.19: VT ^{13}C NMR for Compound 48

methyl-((4-chlorophenyl)diazenyl)-L-prolinate (**49**)



Following the general procedure, the title compound **49** was obtained from L-proline methyl ester hydrochloride as an orange oil in 80% yield (0.215 g).

^1H NMR (400 MHz, CDCl_3 , rt) δ 7.38 – 7.32 (m, 2H, ArH), 7.30 – 7.25 (m, 2H, ArH), 4.87 – 4.47 (m, 1H, CH^{10}), 4.24 – 3.48 (m, 2H, CH_2^{14}), 3.75 (s, 3H, CH_3^{15}), 2.43 – 2.27 (m, 1H, CH_2), 2.28 – 1.95 (m, 3H, CH_{2z}) ppm.

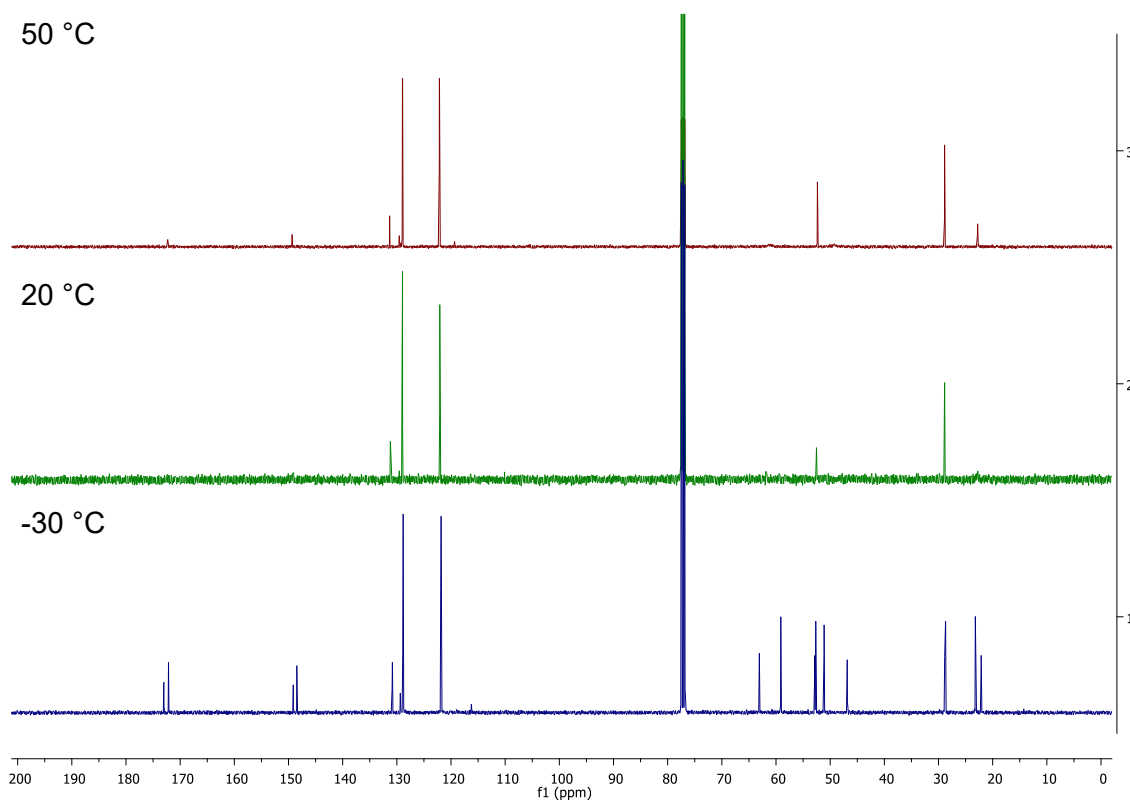
^{13}C NMR (101 MHz, CDCl_3 , -30 °C) δ 173.0 (COOH), 172.0 (COOH), 149.0 (ArC), 148.5 (ArC), 131.0 (2 ArC), 129.0 (2 ArC), 122.0 (2 ArC), 63.0 (CH), 59.0 (CH), 53.0 (CH), 52.5 (CH), 51.0 (CH), 47.0 (CH), 29.0 (CH), 28.5 (CH), 23.0 (CH), 22.0 (CH) ppm.

^{13}C NMR (101 MHz, CDCl_3 , rt) δ 131.0 (ArC), 129.0 (ArC), 122.0 (ArC), 52.5 (CH), 29.0 (CH) ppm.

^{13}C NMR (101 MHz, CDCl_3 , 50 °C) δ 171.5 (COOH), 148.5 (ArC), 130.5 (ArC), 128.0 (ArC), 121.0 (ArC), 51.5 (CH), 28.0 (CH), 22.0 (CH) ppm.

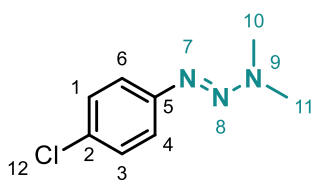
IR: 2951, 1740, 1429, 1325, 1200, 1088, 831, 521 cm^{-1} .

HRMS (EI⁺): [$\text{C}_{12}\text{H}_{15}\text{N}_3\text{O}_2\text{Cl}$] Calcd. 268.0853, Found 268.0849.



6.20: VT ^{13}C NMR for Compound 49

1-(4-chlorophenyl)-3,3-dimethyltriaz-1-ene (50)



The general procedure was slightly modified for the preparation of title compound **50**. The dimethylamine solution was prepared in THF and the general procedure followed for all other steps to yield the product as a pale orange solid in

38% yield (0.097 g).

^1H NMR (400 MHz, CDCl_3 , rt) δ 7.36 (d, J = 8.6 Hz, 2H, ArH), 7.28 (d, J = 8.7 Hz, 2H, ArH), 3.34 (bs, 6H) ppm.

^{13}C NMR (101 MHz, CDCl_3 , -30 °C) δ 149.5 (ArC), 130.0 (ArC), 129.0 (ArCH), 121.5 (ArCH), 43.5 (CH_2), 36.0 (CH_2) ppm.

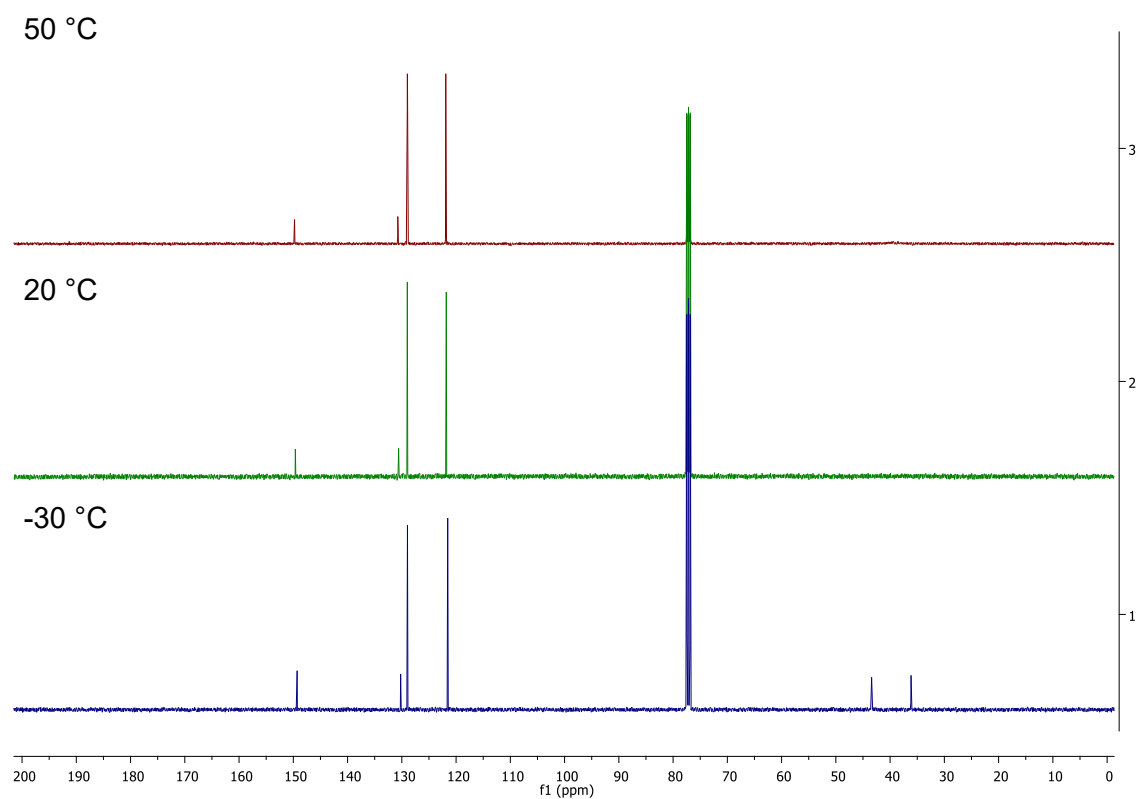
^{13}C NMR (101 MHz, CDCl_3 , rt) δ 149.5 (ArC), 130.5 (ArC), 129.0 (ArCH), 122.0 (ArCH) ppm.

^{13}C NMR (101 MHz, CDCl_3 , 50 °C) δ 150.0 (ArC), 130.5 (ArC), 129.0 (ArCH), 122.0 (ArCH) ppm.

mp (DCM) 47 - 49 °C.

IR: 2924, 2905, 1441, 1381, 1333, 1314, 1080, 833, 816, 515 cm^{-1} .

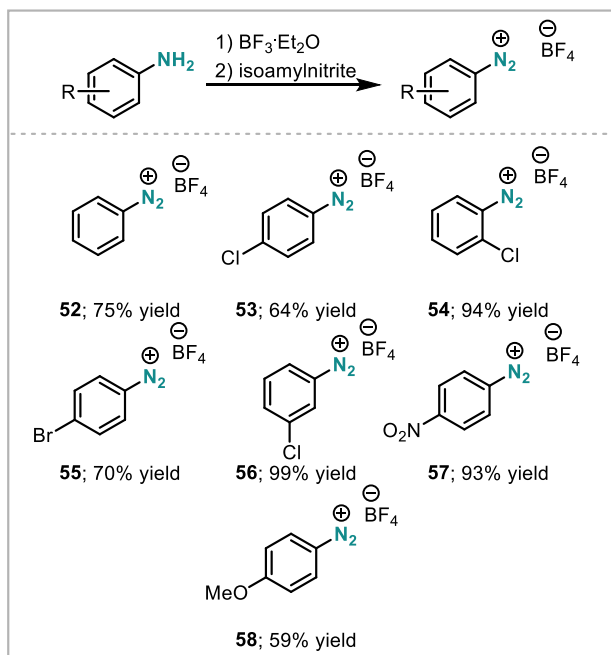
HRMS (FTMS+ p NSI): $[\text{C}_8\text{H}_{11}\text{N}_3\text{Cl}]$ Calcd. 184.0636, Found 184.0635.



6.21: VT ^{13}C NMR for Compound 50

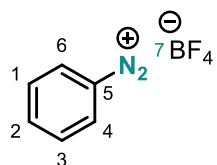
2.4 General Procedure for the Preparation of Diazonium Salts **51 - 58**

The aniline (5.0 mmol) was dissolved in MeCN (10 mL). After cooling with ice-water $\text{BF}_3 \cdot \text{Et}_2\text{O}$ (0.95 mL, 7.5 mmol, 1.5 equiv) was added. Isoamylnitrite (0.709 g, 6.0 mmol, 1.2 equiv) in MeCN (5 mL) was then added slowly at 0 °C and the reaction mixture stirred for 30 min. After precipitation with Et_2O (30 mL) the product was suction filtered, washed with Et_2O and air dried to yield the corresponding diazonium salt (Scheme 3).



Scheme 6.4: Preparation of Diazonium Salts

benzenediazonium tetrafluoroborate (**52**)^[8]



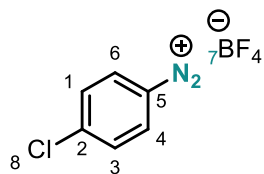
Following the general procedure, the title compound **52** was obtained from aniline as an off-white solid in 75% yield (0.351 g).

$^1\text{H NMR}$ (400 MHz, DMSO) δ 8.73 – 8.59 (m, 2H, ArH), 8.26 (t, J = 7.7 Hz, 1H, ArH²), 7.98 (t, J = 8.2 Hz, 2H, ArH^{1,4}) ppm.

$^{13}\text{C NMR}$ (101 MHz, DMSO) δ 141.5 (ArC), 133.0 (ArC), 131.5 (ArC) ppm.

IR: 3107, 2295, 1570, 1462, 1312, 1020, 754, 665 cm^{-1} .

HRMS (EI⁺): $[\text{C}_6\text{H}_5\text{N}_2]$ Calcd. 105.0453, Found 105.0452.

4-chlorobenzenediazonium tetrafluoroborate (53)^[8]

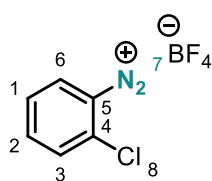
Following the general procedure, the title compound **53** was obtained from aniline as a colourless solid in 63% yield (0.712 g).

¹H NMR (400 MHz, DMSO) δ 8.71 – 8.65 (m, 2H, ArH), 8.14 – 8.08 (m, 2H, ArH) ppm.

¹³C NMR (101 MHz, DMSO) δ 146.5 (ArC), 134.5 (ArC), 131.5 (ArC), 115.0 (ArC) ppm.

IR: 3107, 2295, 1570, 1462, 1312, 1020, 754, 665 cm⁻¹.

HRMS (EI+): [C₆H₄N₂Cl]⁺ Calcd. 139.0063, Found 139.0059.

2-chlorobenzenediazonium tetrafluoroborate (54)^[9]

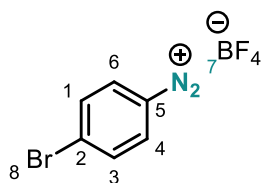
Following the general procedure, the title compound **54** was obtained from aniline as a colourless solid in 94% yield (1.063 g).

¹H NMR (400 MHz, DMSO) δ 8.85 (dd, *J* = 8.3, 1.5 Hz, 1H, ArH), 8.32 – 8.24 (m, 1H, ArH), 8.20 (dd, *J* = 8.3, 1.1 Hz, 1H, ArH), 7.99 – 7.91 (m, 1H, ArH) ppm.

¹³C NMR (101 MHz, DMSO) δ 142.5 (ArC), 135.5 (ArC), 134.5 (ArC), 132.5 (ArC), 130.0 (ArC), 116.5 (ArC) ppm.

IR: 3100, 2361, 2291, 1566, 1474, 1464, 1034, 773, 677 cm⁻¹.

HRMS (EI+): [C₆H₄N₂Cl]⁺ Calcd. 139.0063, Found 139.0057.

4-bromobenzenediazonium tetrafluoroborate (55)^[8]

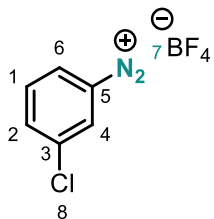
Following the general procedure, the title compound **55** was obtained from aniline as a colourless solid in 70% yield (0.949 g).

¹H NMR (400 MHz, DMSO) δ 8.62 – 8.52 (m, 1H, ArH), 8.29 – 8.21 (m, 1H, ArH) ppm.

¹³C NMR (101 MHz, DMSO) δ 136.5 (ArC), 134.5 (ArC), 134.0 (ArC), 115.0 (ArC) ppm.

IR: 3105, 2290, 1555, 1022, 1011, 829, 521 cm⁻¹.

HRMS (ES+): [C₆H₄N₂Br]⁺ Calcd. 182.9558, Found 182.9555.

3-chlorobenzenediazonium tetrafluoroborate (56)^[9]

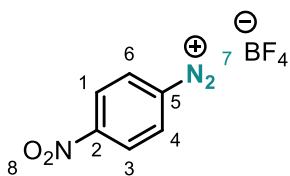
Following the general procedure, the title compound **56** was obtained from aniline as a slightly pink solid in 99% yield (1.118 g).

¹H NMR (400 MHz, DMSO) δ 8.86 (t, J = 2.0 Hz, 1H, ArH), 8.69 – 8.63 (m, 1H, ArH), 8.40 – 8.34 (m, 1H, ArH), 8.01 (t, J = 8.3 Hz, 1H, ArH) ppm.

¹³C NMR (101 MHz, DMSO) δ 141.0 (ArC), 134.5 (ArC), 133.0 (ArC), 131.5 (ArC), 131.5 (ArC), 118.0 (ArC) ppm.

IR: 3103, 2359, 2305, 1558, 1466, 1020, 885, 793, 652, 519 cm⁻¹.

HRMS (EI⁺): [C₆H₄N₂Cl]⁺ Calcd. 139.0058, Found 139.0054.

4-nitrobenzenediazonium tetrafluoroborate (57)^[8]

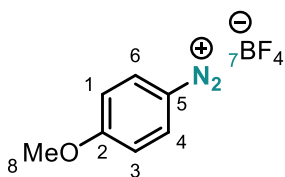
Following the general procedure, the title compound **57** was obtained from aniline as a grey solid in 93% yield (1.102 g).

¹H NMR (400 MHz, DMSO) δ 8.97 – 8.89 (m, 2H, ArH), 8.77 – 8.67 (m, 2H, ArH) ppm.

¹³C NMR (101 MHz, DMSO) δ 153.5 (ArC), 134.5 (ArC), 126.0 (ArC), 122.0 (ArC) ppm.

IR: 3119, 2359, 2307, 1539, 1336, 1317, 1030, 866, 743, 662, 525 cm⁻¹.

HRMS (EI⁺): [C₆H₄N₃O₂]⁺ Calcd. 150.0304, Found 150.0302.

4-methoxybenzenediazonium tetrafluoroborate (58)^[8]

Following the general procedure, the title compound **58** was obtained from aniline as a brown solid in 59% yield (0.659 g).

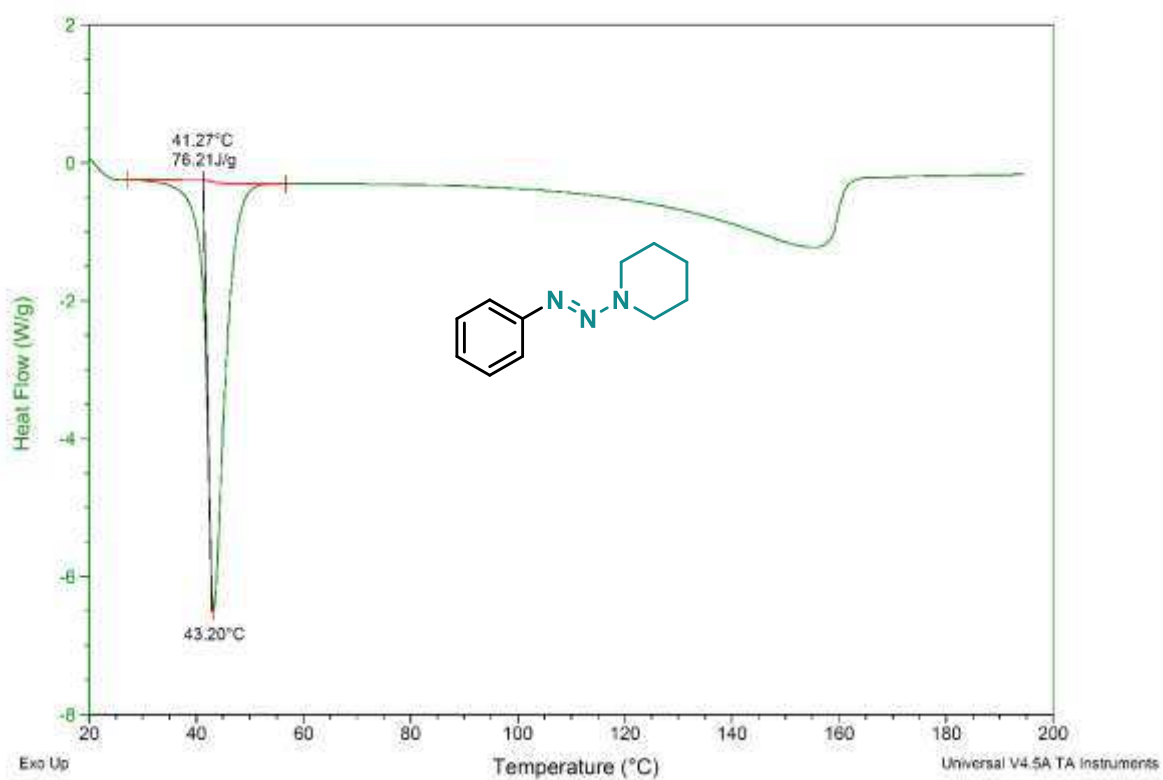
¹H NMR (400 MHz, DMSO) δ 8.64 – 8.56 (m, 2H, ArH), 7.52 – 7.44 (m, 2H, ArH), 4.04 (s, 3H, OCH₃) ppm.

¹³C NMR (101 MHz, DMSO) δ 169.0 (ArC), 136.0 (ArC), 117.5 (ArC), 103.5 (ArC), 57.5 (OCH₃) ppm.

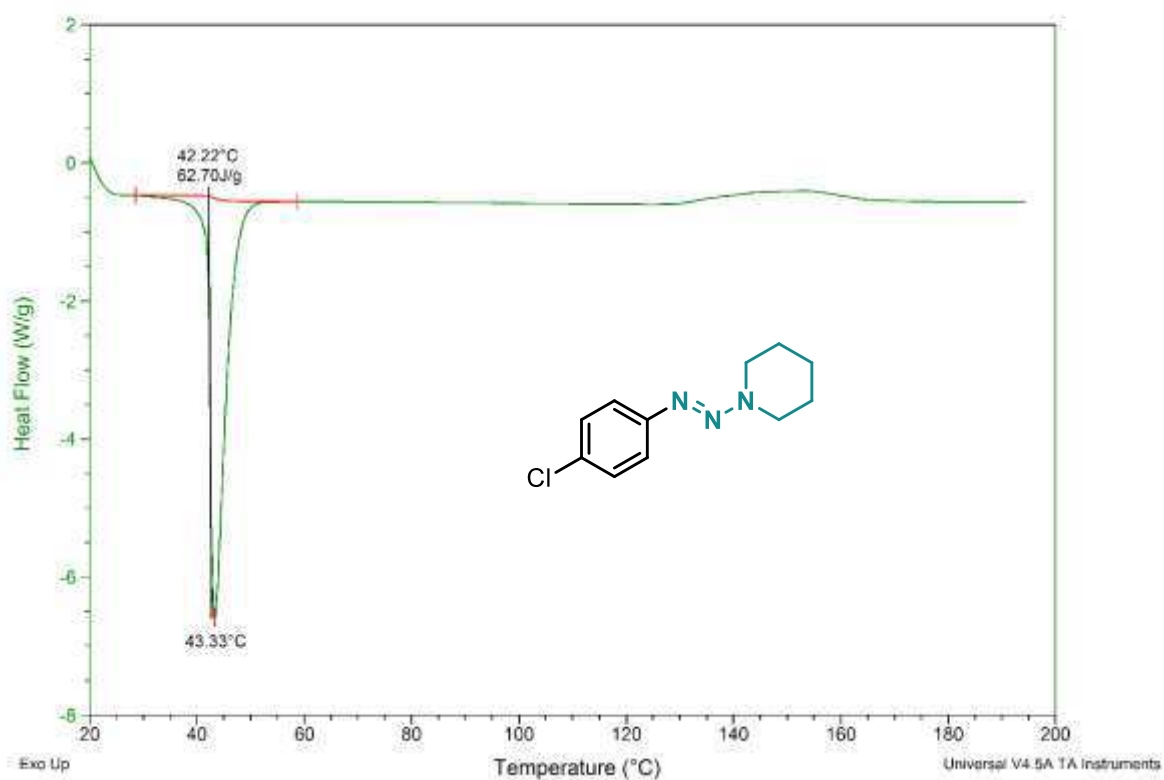
IR: 3121, 2251, 1582, 1568, 1493, 1441, 1344 ; 1287, 1030, 997, 841, 685 cm⁻¹.

HRMS (EI⁺): [C₇H₇O₁N₂]⁺ calc. 135.0553, found 135.0549.

DSC

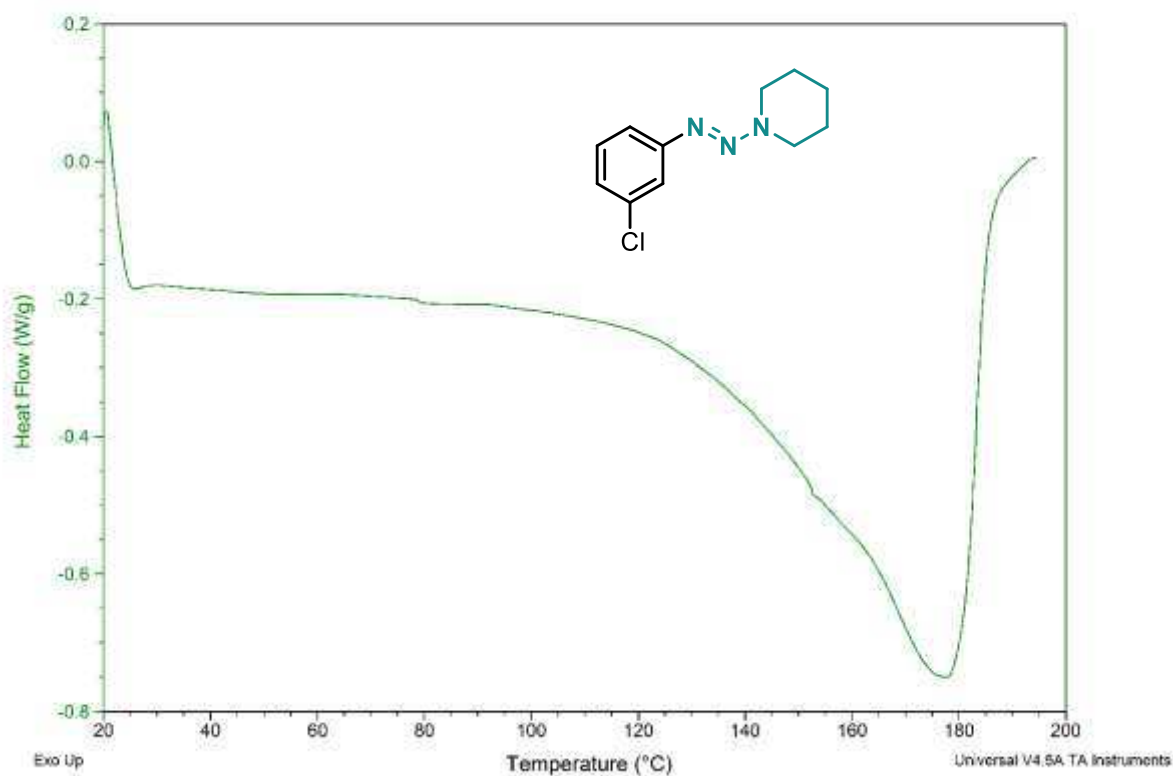


DSC

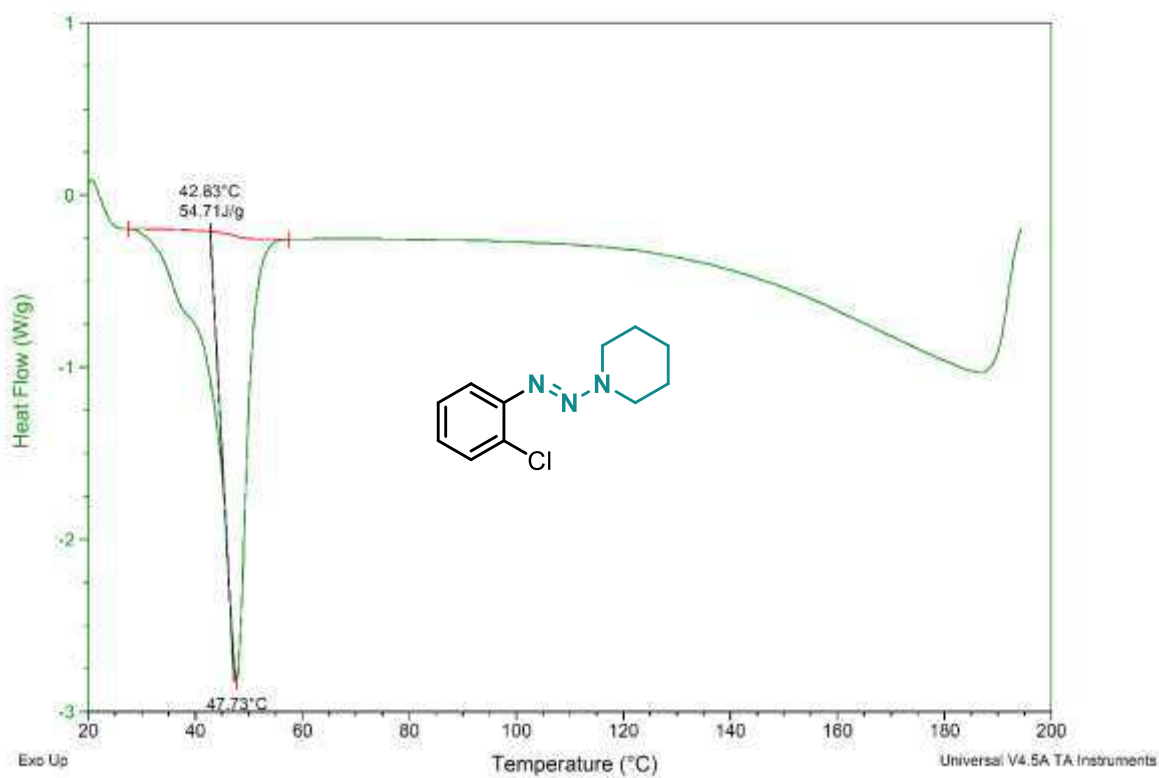


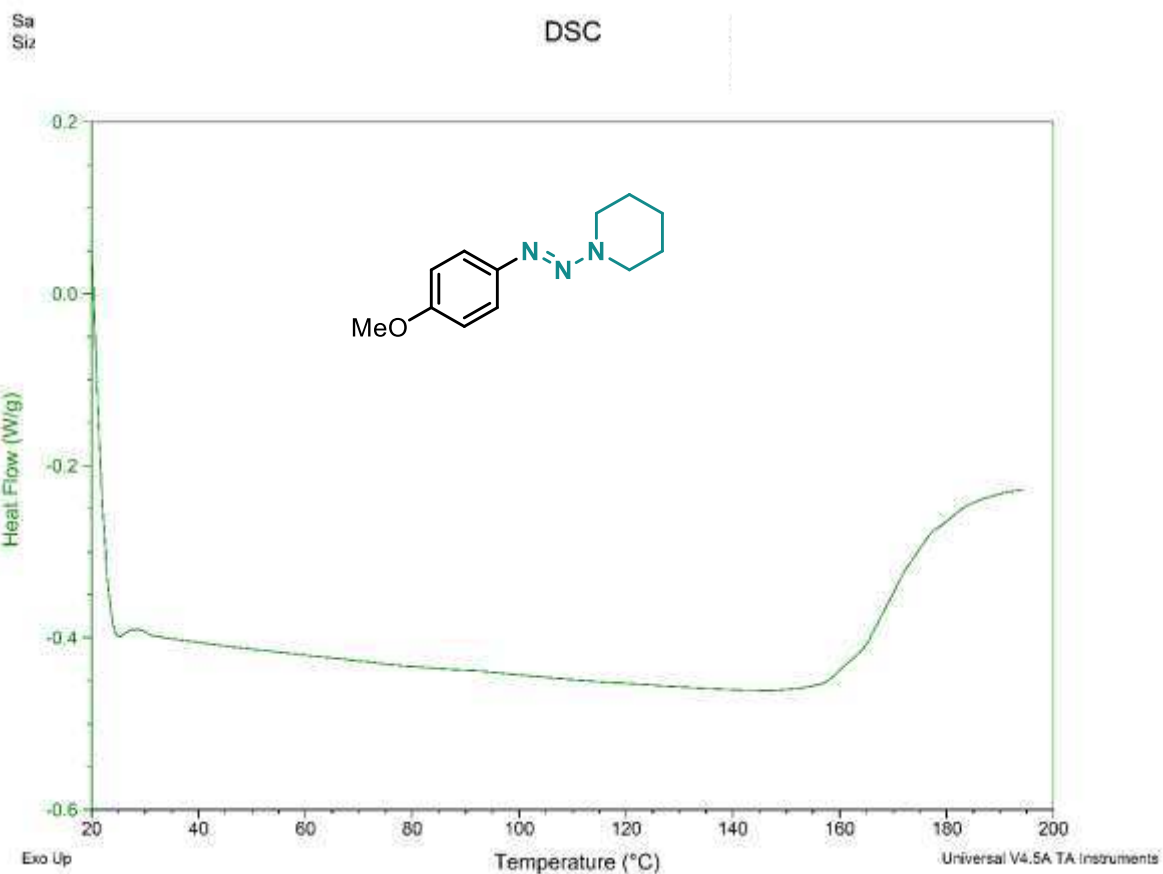
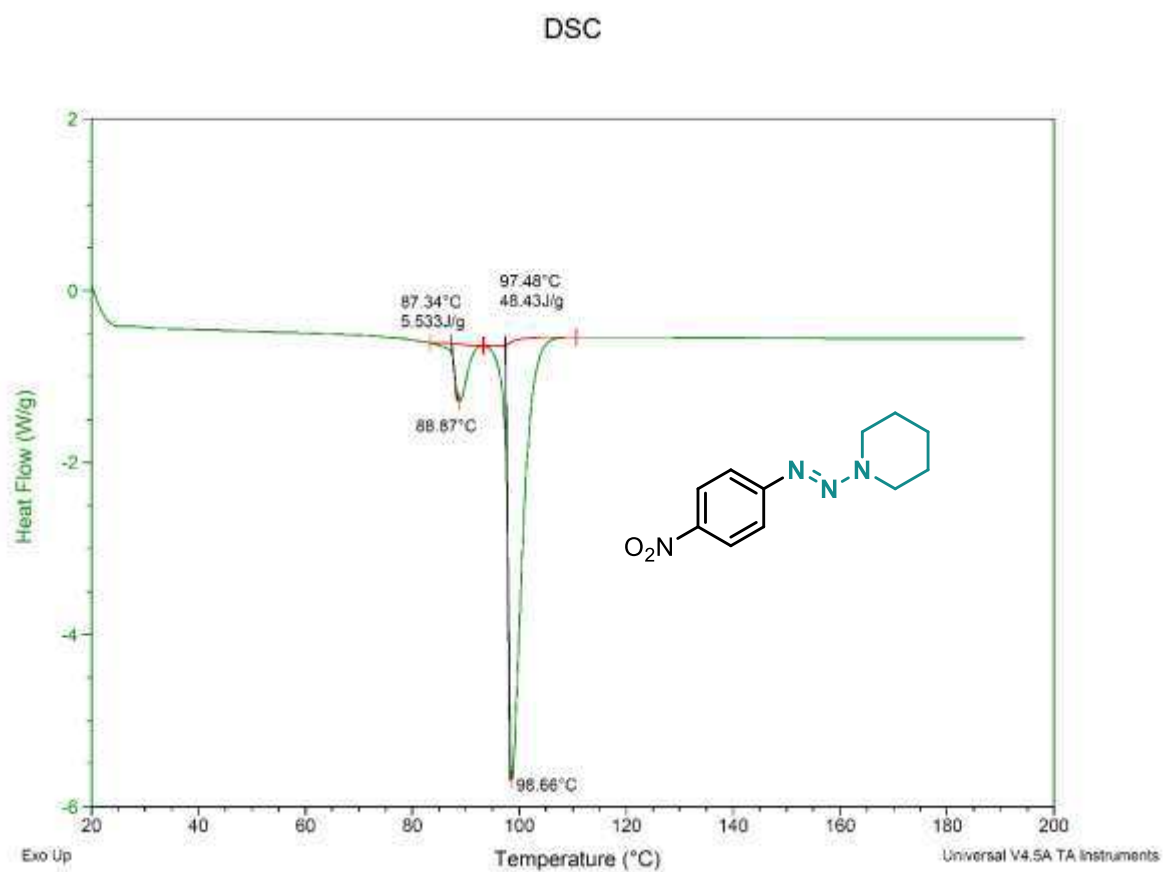
DSC

101

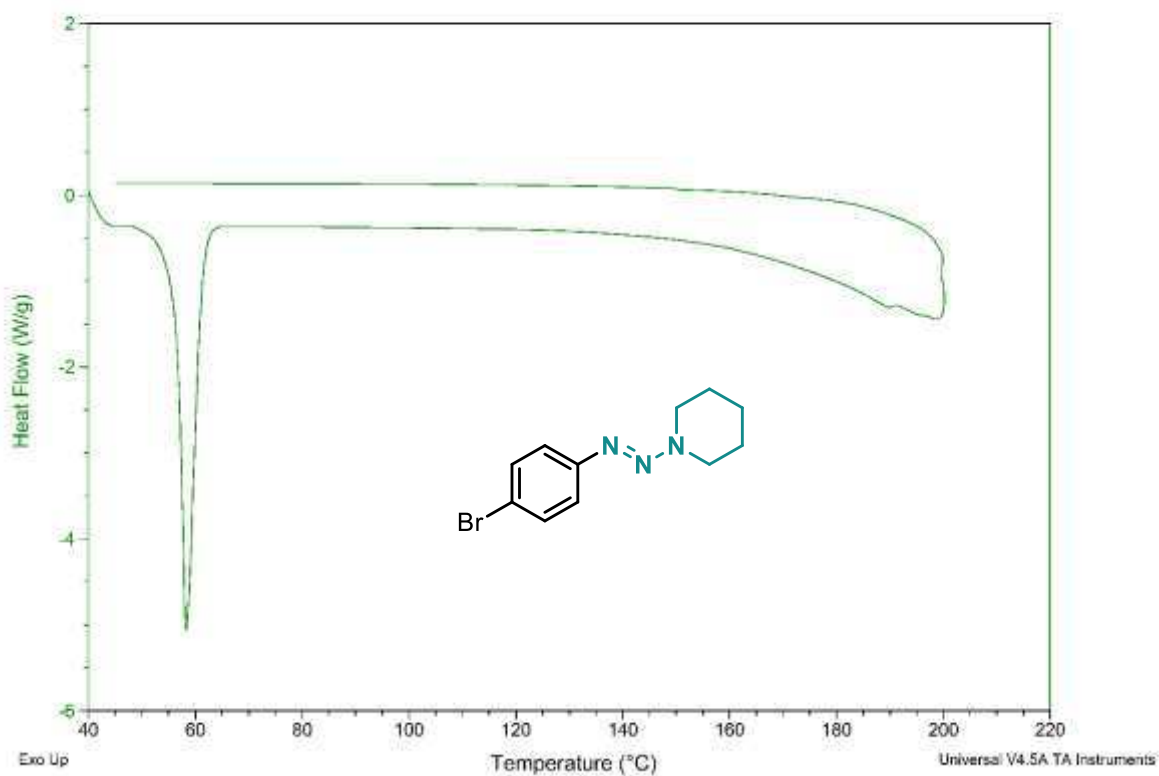


DSC

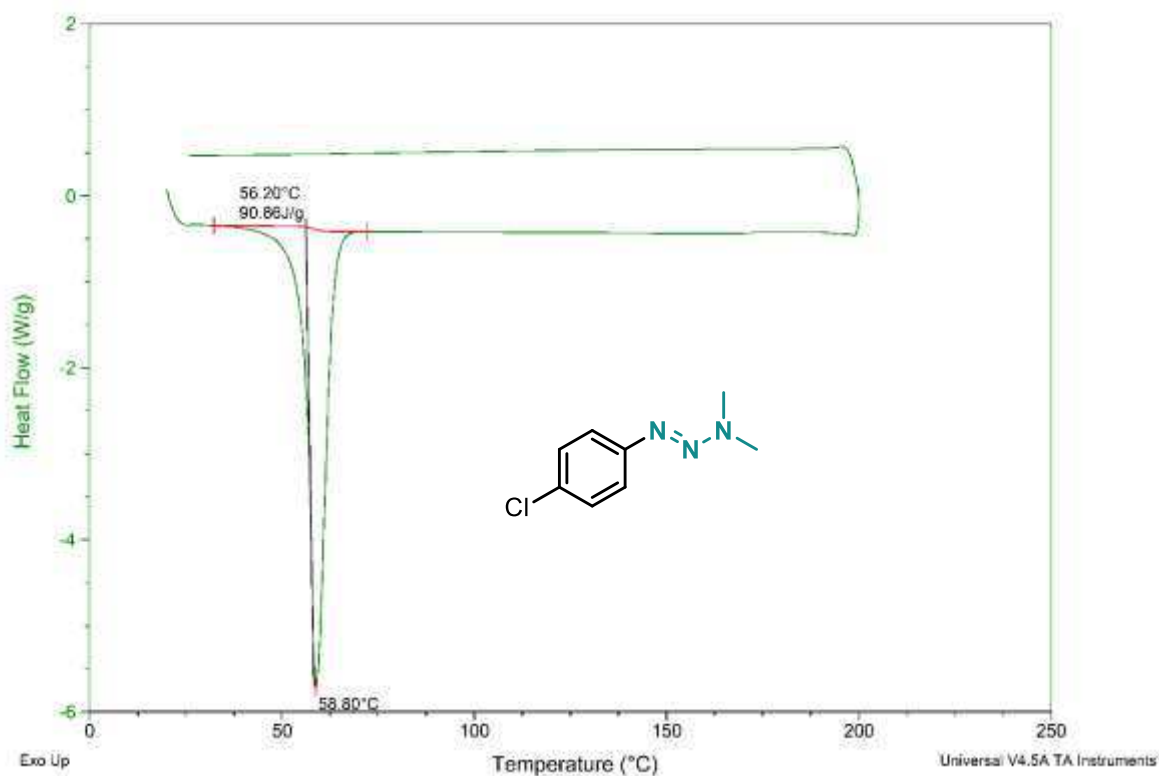




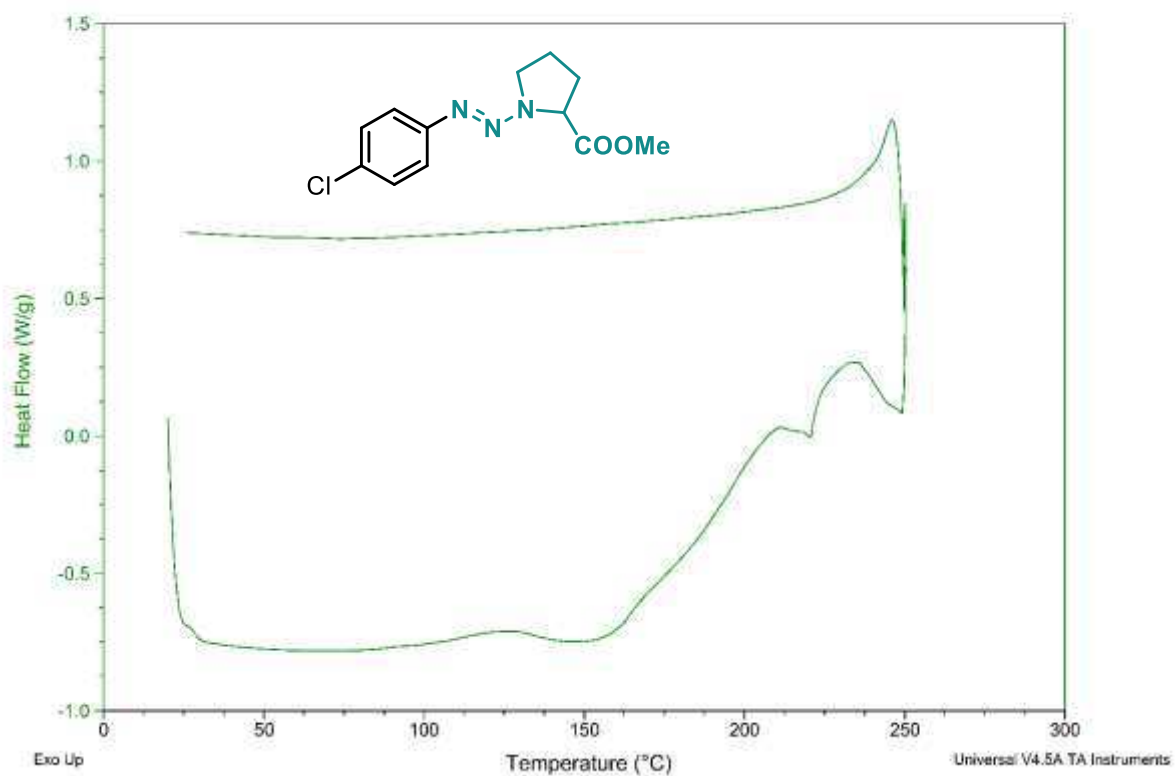
DSC



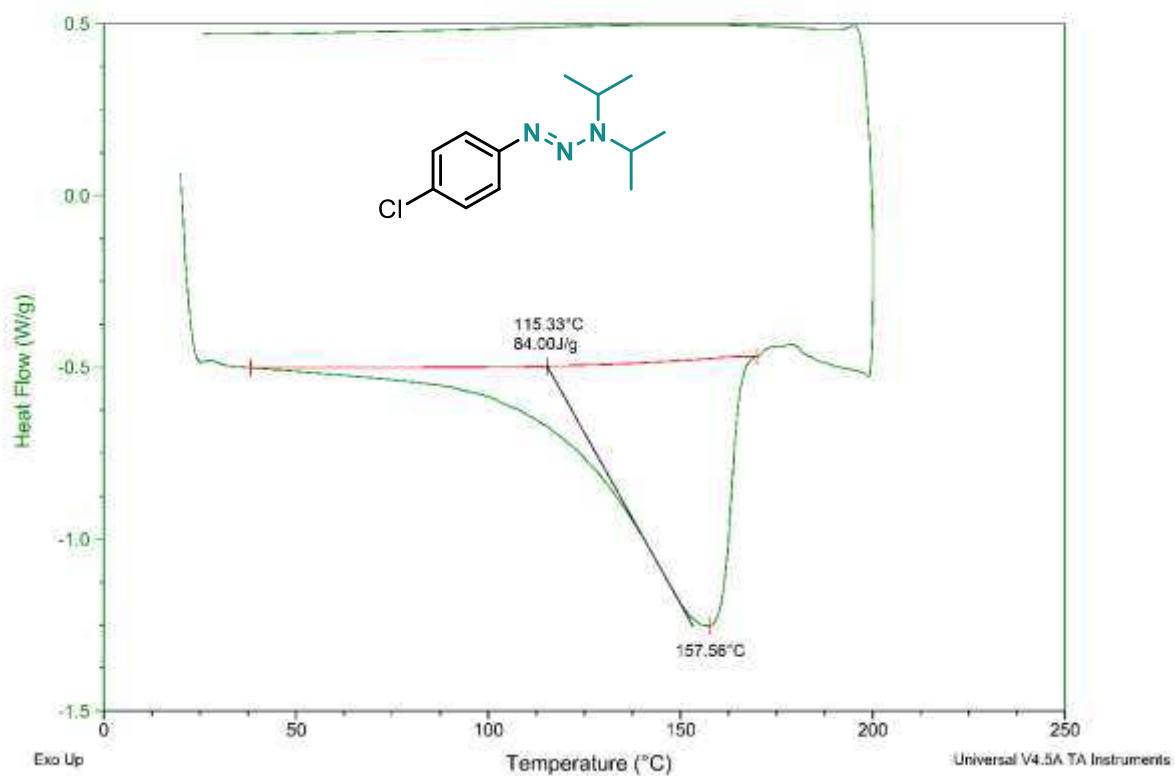
DSC

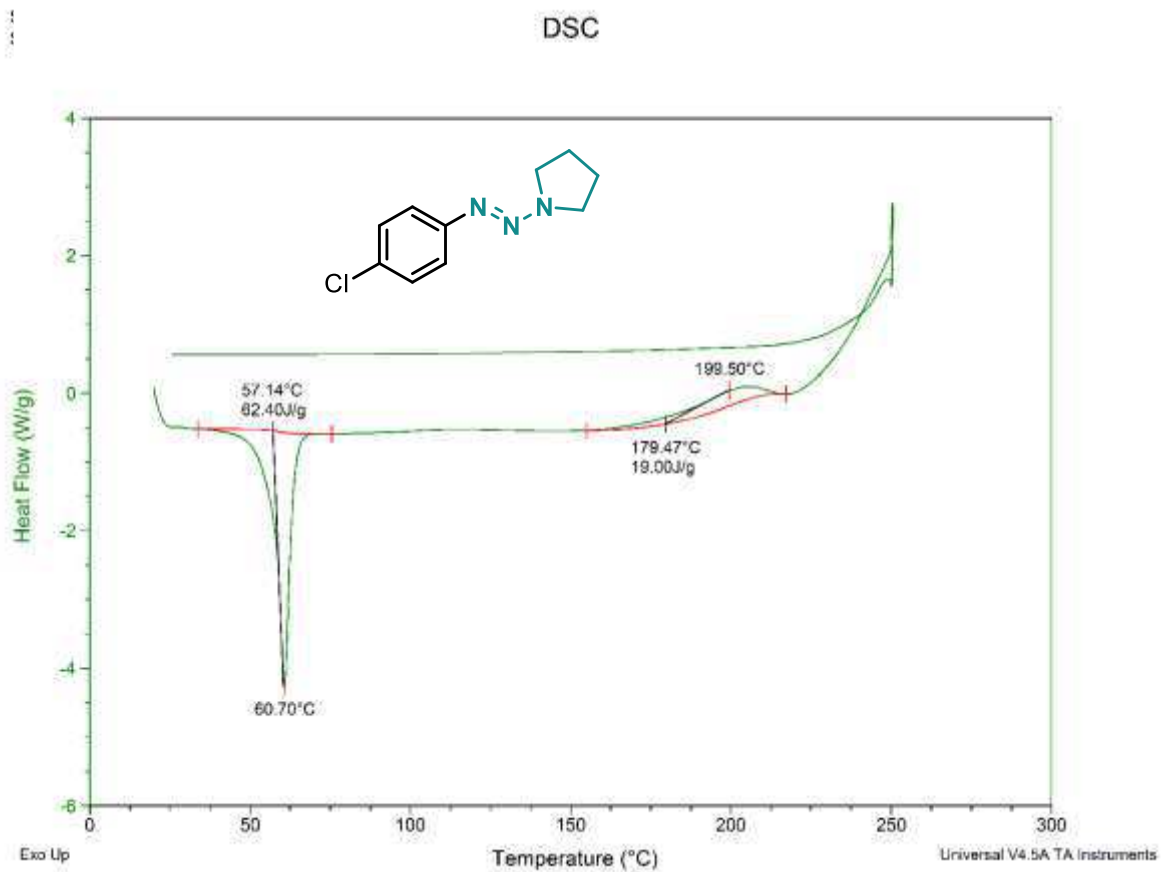
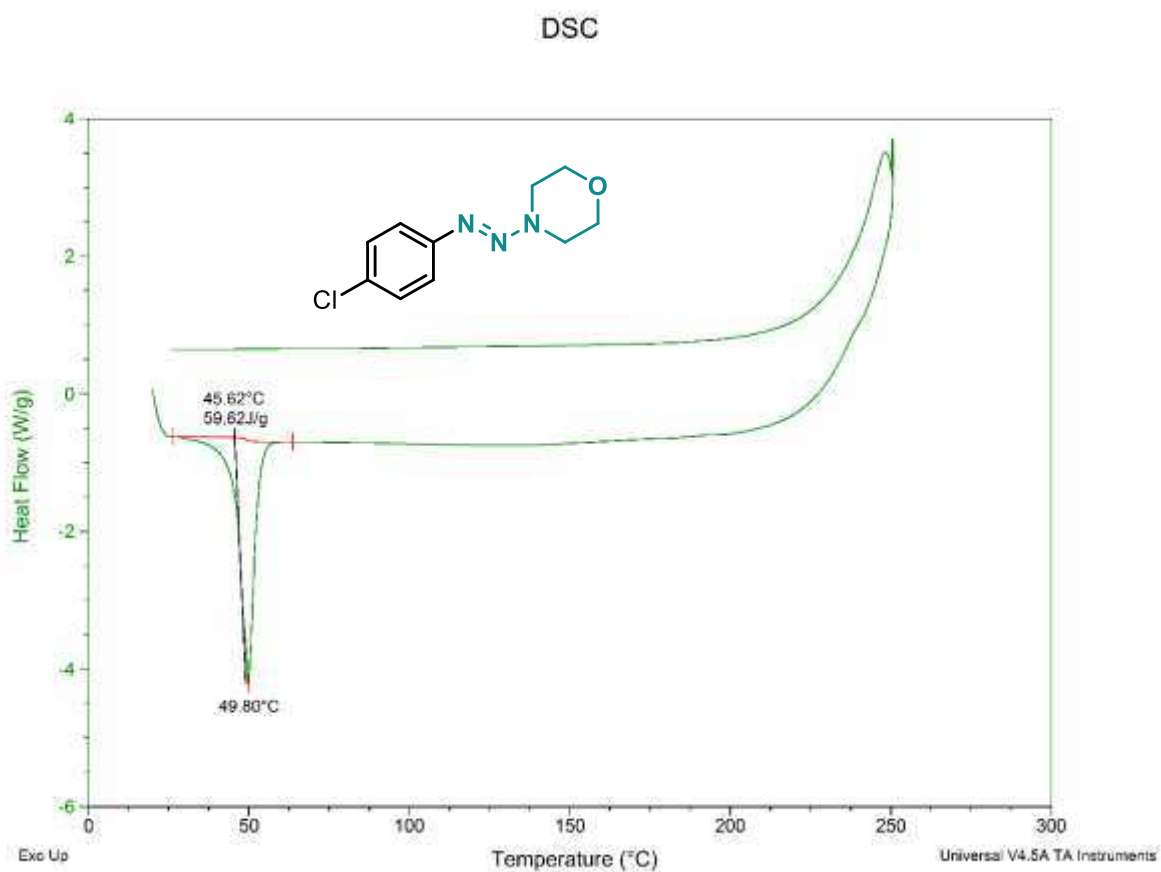


DSC



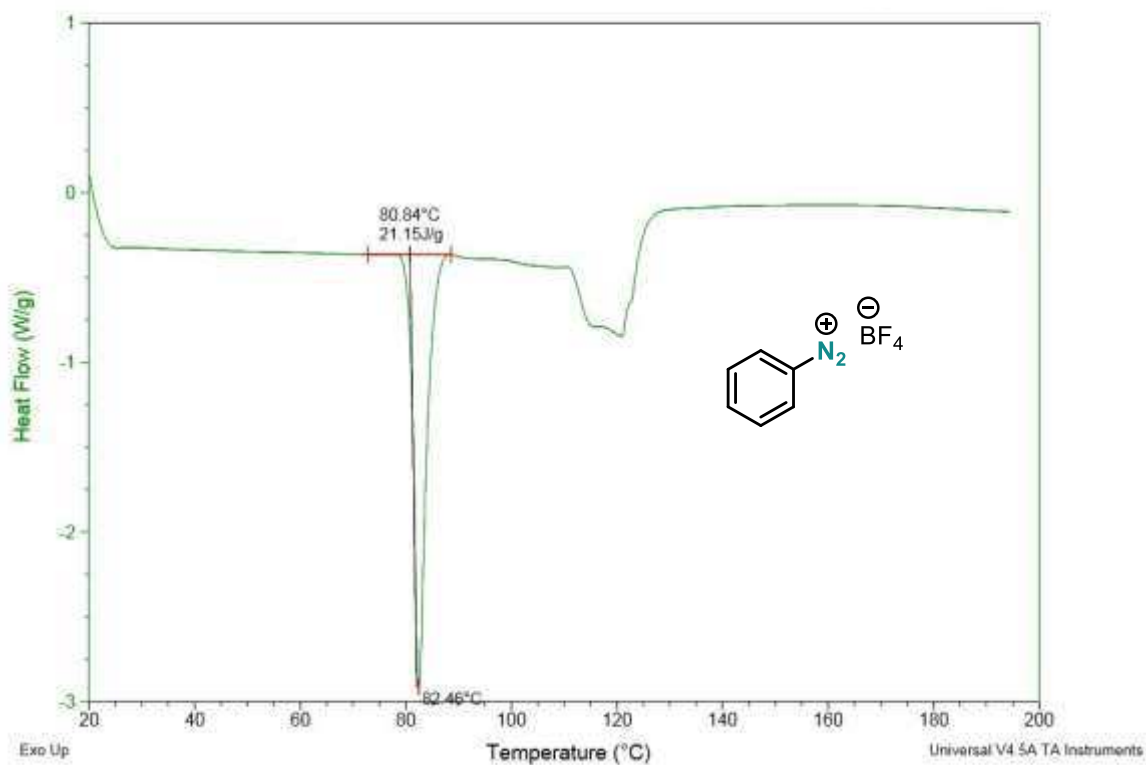
DSC



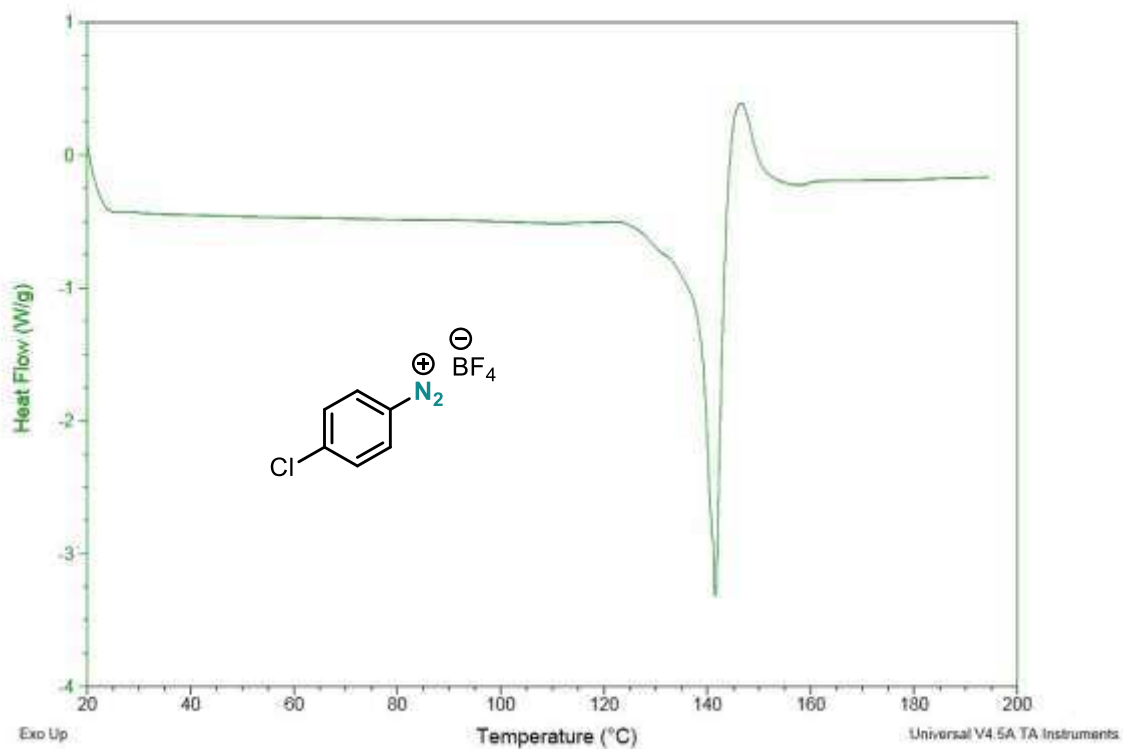


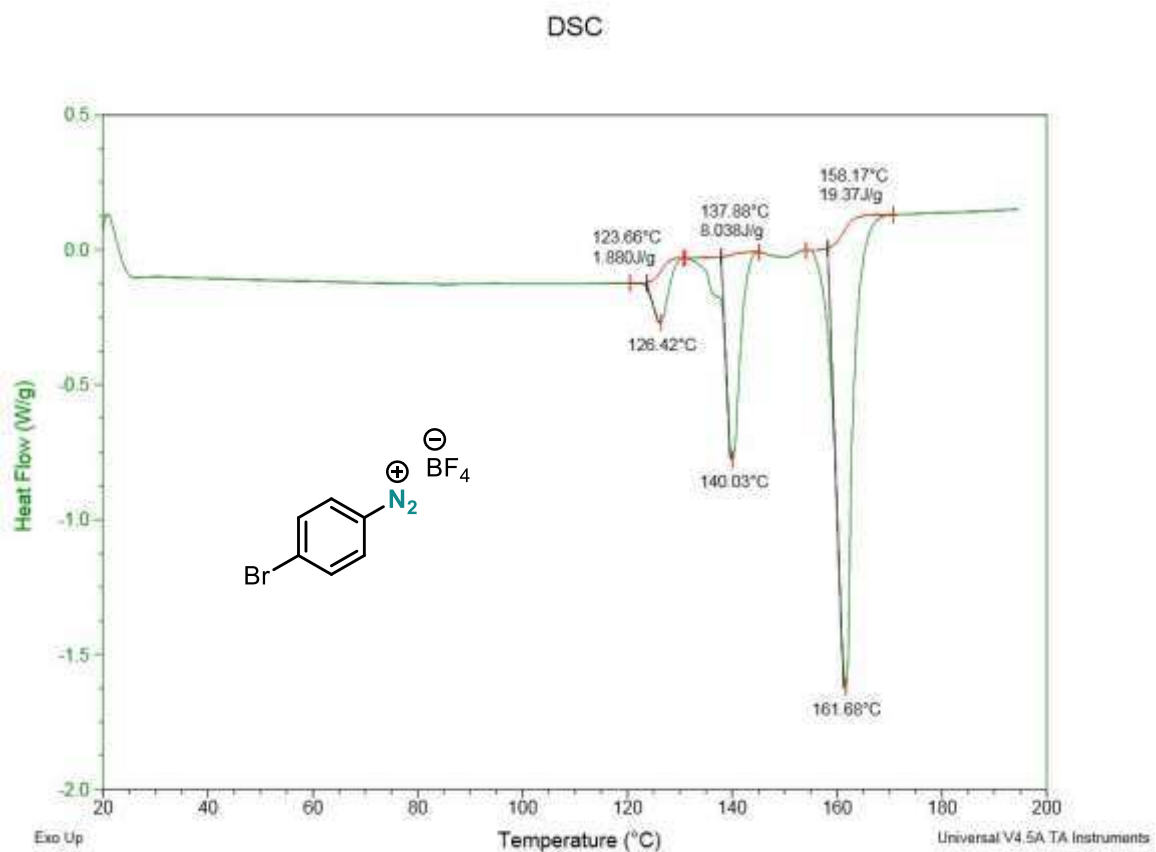
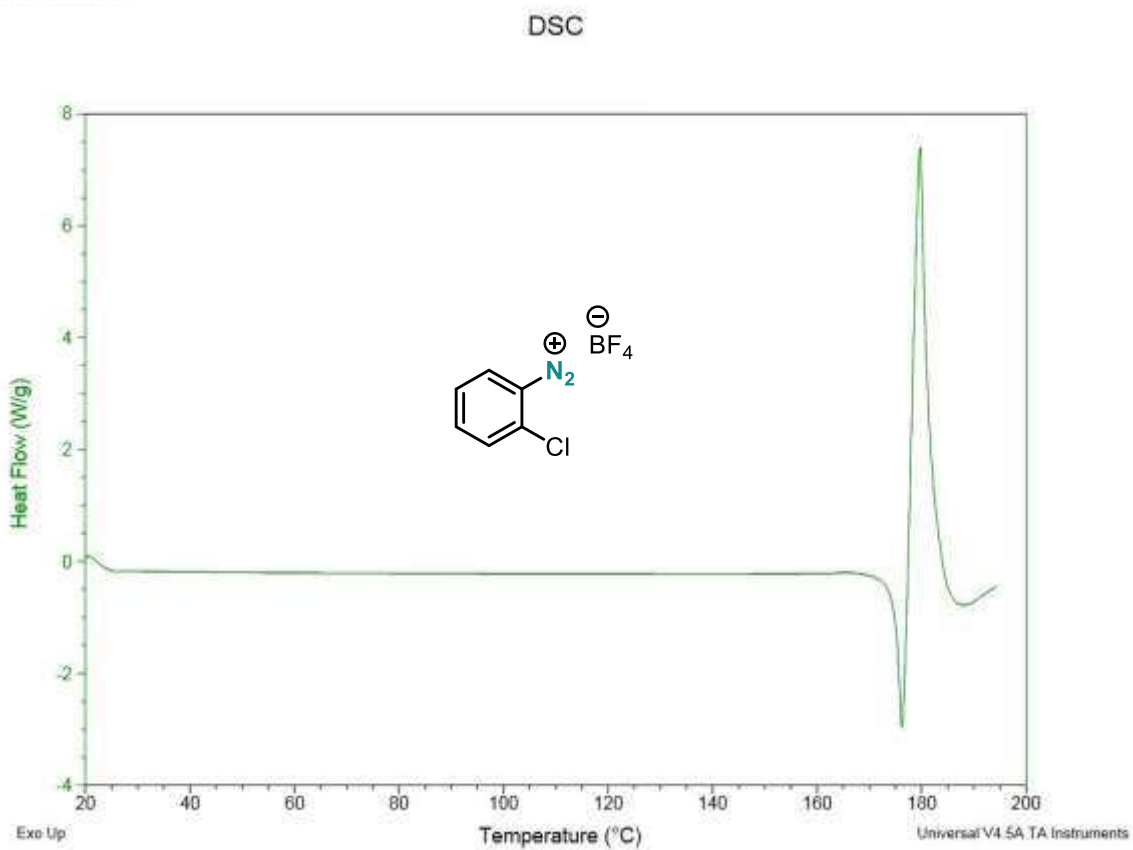
2.5.2 Diazonium Salts

DSC

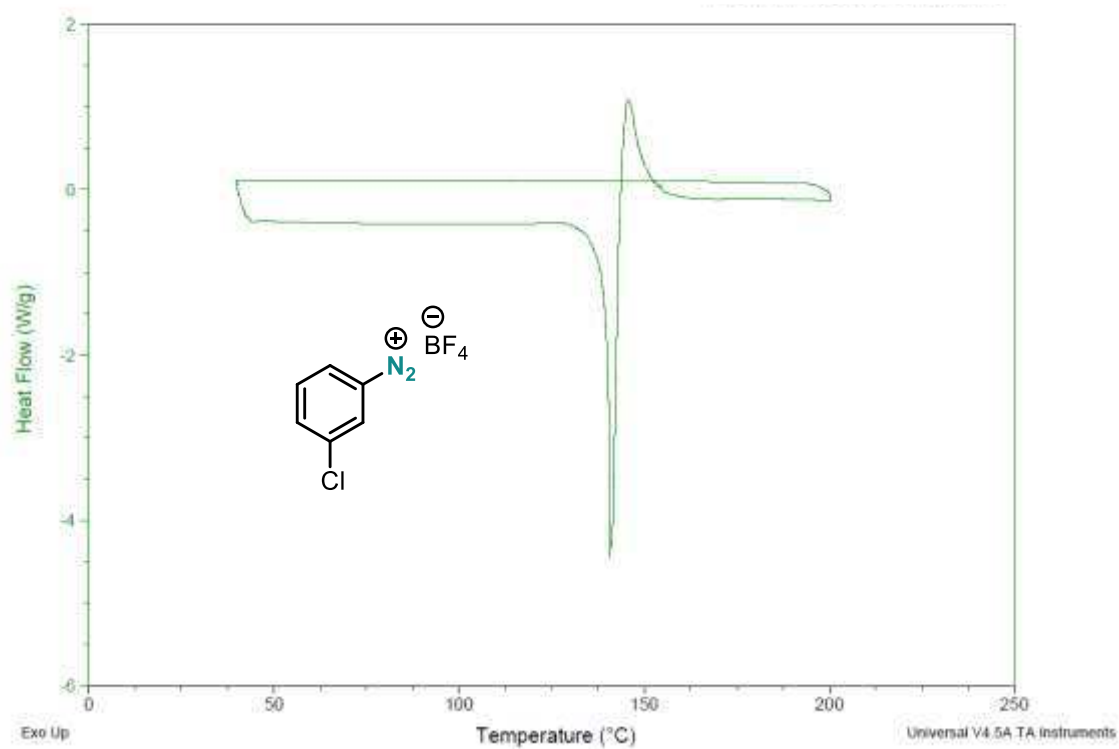


DSC

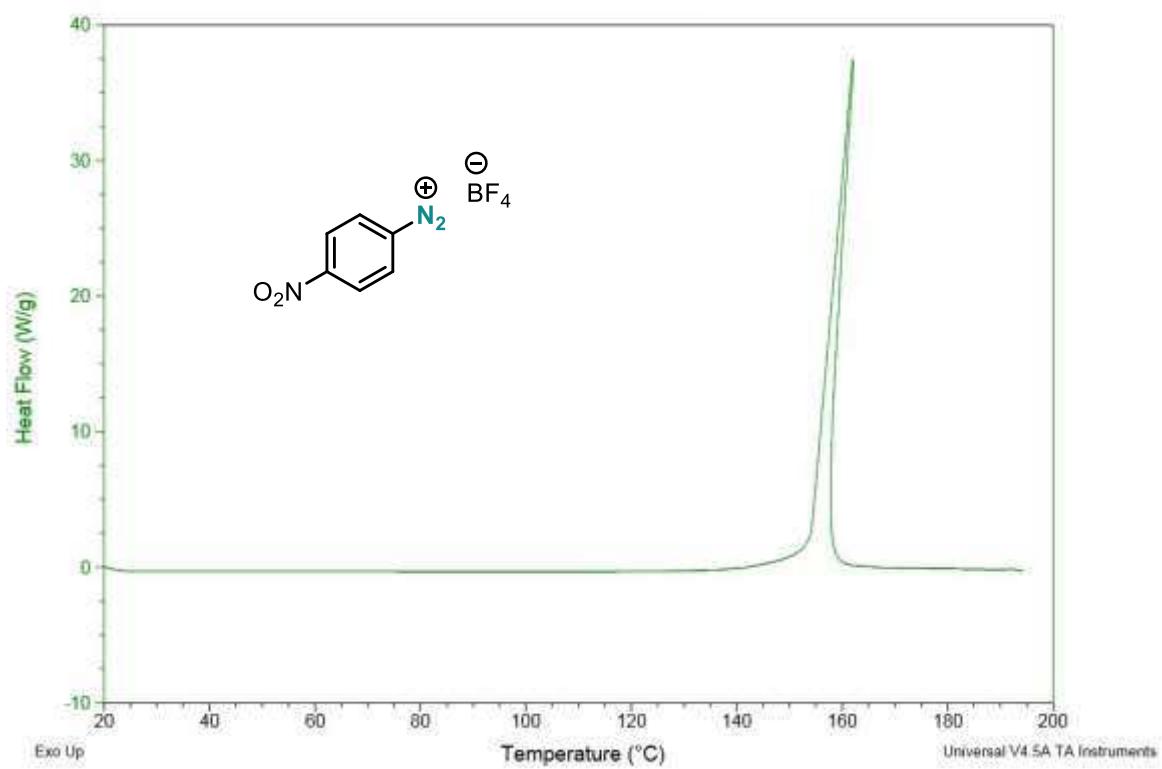


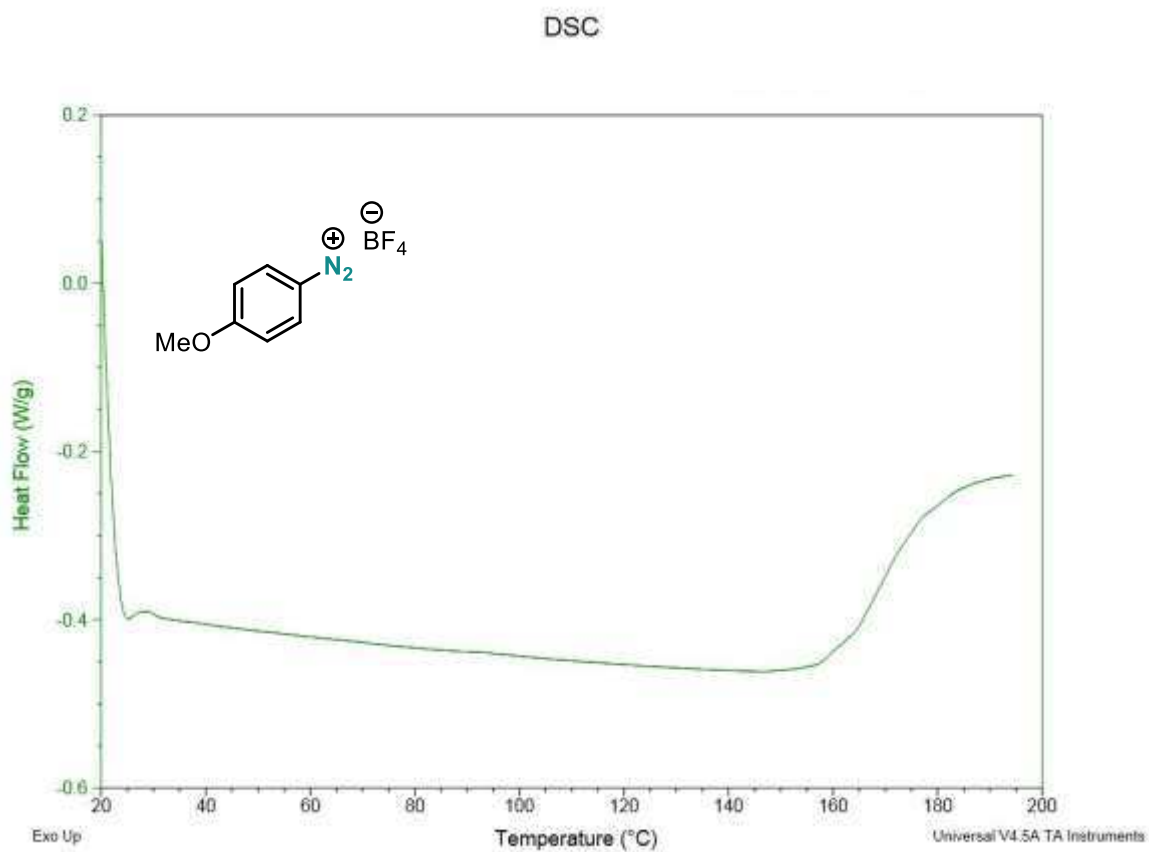


DSC



DSC





3 Chapter 3 - Indoles

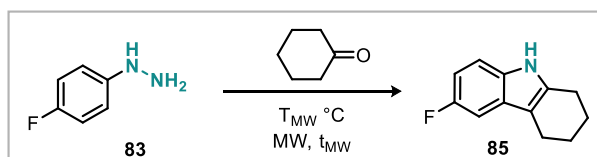
3.1 Method for the Optimisation of the Multistep Indole Synthesis

3.1.1 Optimisation of the Microwave Step

To a solution of *p*-fluorophenylhydrazine hydrochloride (0.163 g, 1 mmol) in acetonitrile (10 mL) and aqueous HCl (0.2 M, 5 mL) in a 35 mL microwave vial neat cyclohexanone was added (0.098 g, 1 mmol, 1 equiv). The reaction mixture was heated in the microwave for 10 min at 120 °C. After cooling to room temperature, the product conversion was determined via ¹⁹F NMR from the crude reaction mixture (98%). The NMR solution was then combined with the rest of the reaction mixture. This was then diluted with 10 mL H₂O and the product extracted with DCM (3 x 20 mL). The combined organic layers were washed with brine (20 mL), dried over MgSO₄ and the solvent was removed under reduced pressure to give the product **85** in 97% isolated yield (0.184 g, 0.97 mmol).

To a solution of *p*-fluoroaniline (0.111 g, 1 mmol) in acetonitrile (5 mL) in a 35 mL microwave vial a solution of HCl (0.2 M in water, 5 mL, 1 mmol, 1 equiv) was added. After cooling to 0 °C, isoamyl nitrite (0.117 g, 1 mmol, 1 equiv) in acetonitrile (5 mL) was added slowly. The ice bath was removed and a solution of ascorbic acid (0.176 g, 1 mmol, 1 equiv) in water (5 mL) was added. The reaction mixture was left to stir for 30 min before neat cyclohexanone was added (0.098 g, 1 mmol, 1 equiv). The reaction mixture was heated in the microwave for the appropriate time and temperature. After cooling to room temperature, the product conversion was determined via ¹⁹F NMR from the crude reaction mixture.

Table 6.1: Optimisation of Microwave Parameters (Step 2)



entry	hydrazine source	T_{MW} [°C]	t_{MW} [min]	^{19}F yield [%]
1	commercial	120	10	98 (97)
2	<i>in situ</i> prepared	120	10	15
3	<i>in situ</i> prepared	140	10	30
4	<i>in situ</i> prepared	160	10	52 (47)
5	<i>in situ</i> prepared	180	10	46
6	<i>in situ</i> prepared	160	30	48
7 ^a	<i>in situ</i> prepared	160	10	67
8^{a,b}	in situ prepared	160	10	73

isolated yields in parenthesis; batch hydrazine formation: 1 mmol *p*-fluoroaniline, 1 mmol HCl, 1 mmol isoamyl nitrite, 1 mmol Vit C; ^a 5 mmol of HCl; ^b 1.2 mmol isoamyl nitrite

3.1.2 Investigating the hydrazide formation by ^{19}F NMR

p-Fluoroaniline (0.111 g, 1 mmol) was dissolved in MeCN (5 mL) in a 50 mL RBF equipped with a stirrer bar and trifluorotoluene (41 μL , 0.33 mmol, 0.33 equiv) added as the internal standard. To that reaction solution aqueous HCl (5 mL, 1 M, 5 mmol, 5 equiv) was added and a ^{19}F NMR taken. After recombining the solutions and cooling in ice-water isoamyl nitrite (0.117 g, 1 mmol, 1 equiv) in MeCN (5 mL) was added and another ^{19}F NMR was taken. After recombining, ascorbic acid (0.176 g, 1 mmol, 1 equiv) in water (5 mL) was added at room temperature and the reaction monitored over time via ^{19}F NMR.

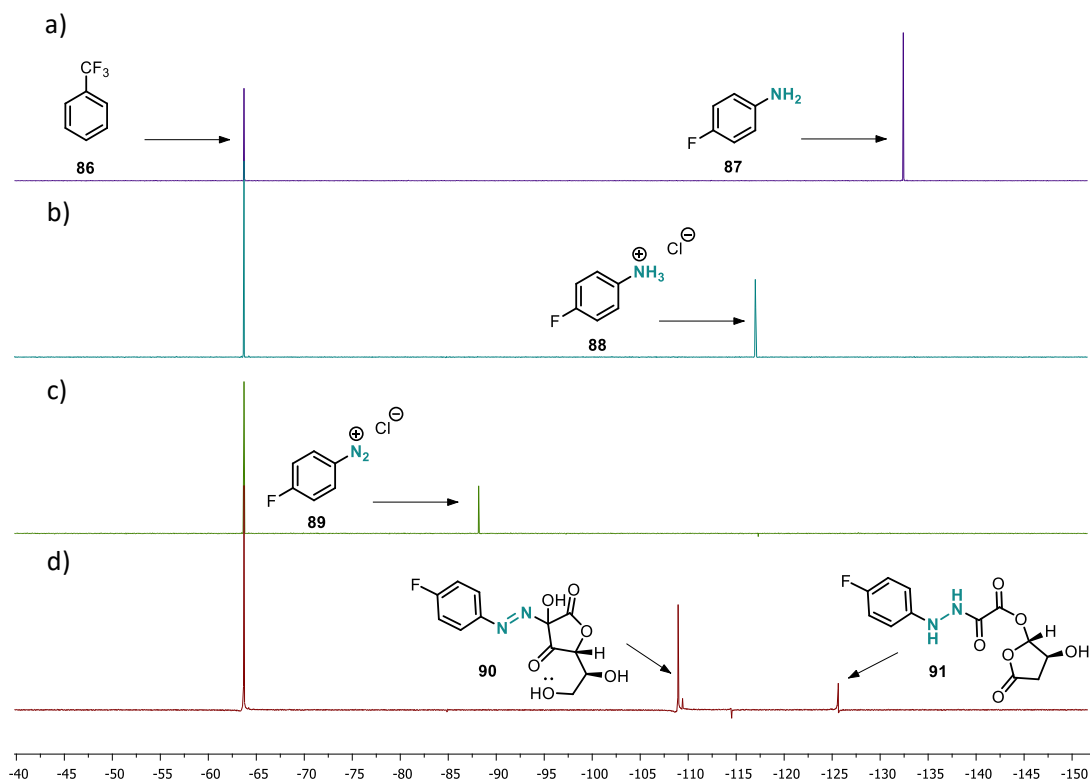


Figure 6.22: ^{19}F NMR Monitoring of the Reaction with Internal Standard; a) *p*-fluoroaniline (87) in MeCN; b) after addition of HCl; c) after addition of isoamyl nitrite, diazonium salt (88); d) after addition of ascorbic acid, two new peaks observed

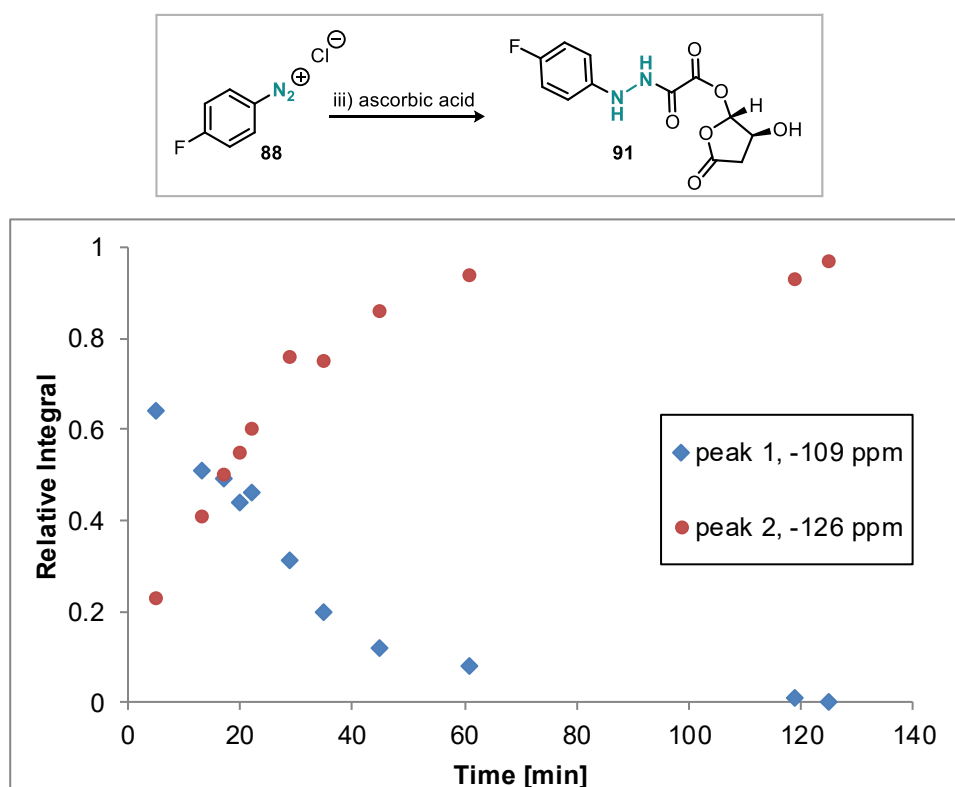
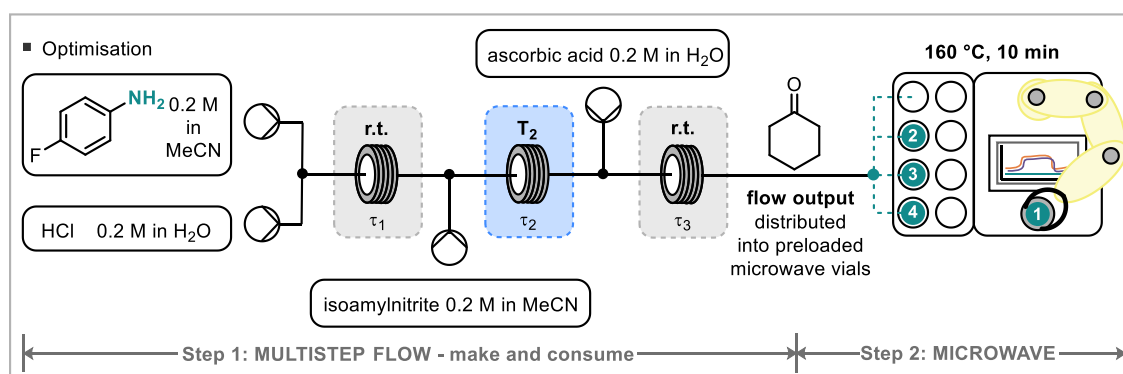


Figure 6.23: ^{19}F NMR Monitoring of the Reaction over Time after Addition of Ascorbic Acid

3.1.3 Optimisation of the Telescoped Process

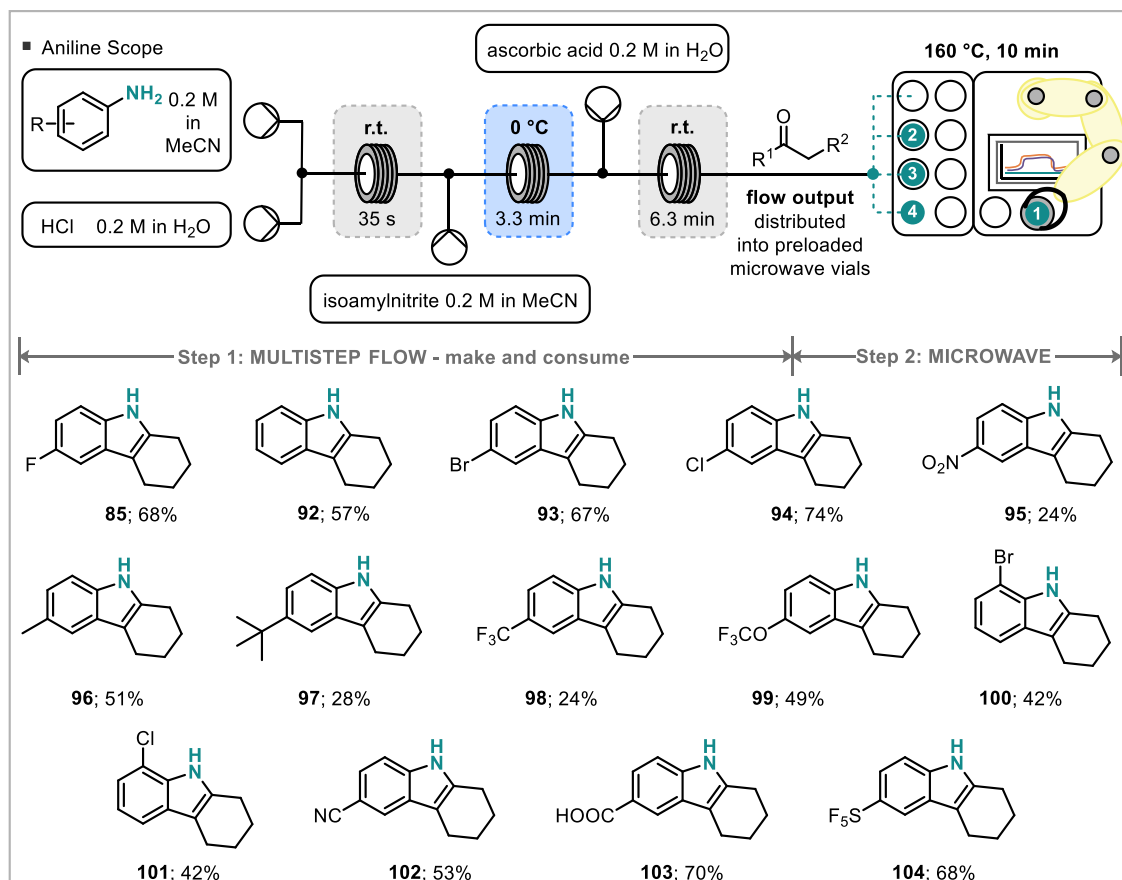
Solutions of *p*-fluoroaniline (0.2 M in acetonitrile), HCl (in water), isoamylnitrite (in acetonitrile) and ascorbic acid (in water) were prepared. These were then pumped through the flow system (see Scheme 1) at a flow rate of 0.2 mL min⁻¹. After waiting for steady state for 20 min, fractions of 20 mL (1 mmol, 25 min) were collected. The neat cyclohexanone (0.098 g, 1 mmol) was added into a 35 mL microwave vial equipped with a stirrer bar and the reaction solution was added. The reaction mixture was heated in the microwave for the 10 min at 160 °C. After cooling to room temperature trifluorotoluene (0.041 mL, 0.33 mmol) was added and yield determined by ¹⁹F NMR.

Table 6.2: Optimisation of the Telescoped Process



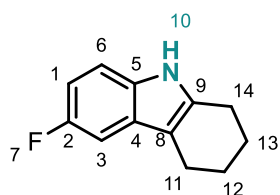
entry	c (HCl) [mol/L]	c (isoamylnitrite) [mol/L]	c (Vit C) [mol/L]	T ₂ [°C]	T ₁ [min]	T ₂ [min]	T ₃ [min]	¹⁹ F yield [%]
1	0.2	0.24	0.2	0	0.6	3.3	3.3	41
2	1	0.2	0.2	0	0.6	3.3	3.3	72
3	1	0.24	0.24	0	0.6	3.3	3.3	62
4	1	0.24	0.2	rt	0.6	3.3	3.3	53
5	1	0.24	0.2	0	5	3.3	3.3	60
6	1	0.24	0.2	0	0.6	1.7	3.3	64
7	1	0.24	0.2	0	0.6	8.3	3.3	65
8	1	0.24	0.2	0	0.6	3.3	2.5	64
9	1	0.24	0.2	0	0.6	3.3	12.5	64
10	1	0.24	0.2	0	0.6	3.3	3.3	74 (68)

3.2 General Method for the Synthesis of Indoles **85** and **92** - **104**: Aniline Screen



Scheme 6.5: Aniline Substrate Scope

Solutions of the aniline (2 mmol, 10 mL of 0.2 M solution in acetonitrile), HCl (10 mL of 1 M aqueous solution), isoamyl nitrite (0.281 g, 2.4 mmol, 10 mL of 0.24 M solution in acetonitrile) and ascorbic acid (0.352 g, 2 mmol, 10 mL of 0.2 M aqueous solution) were prepared. These were then pumped through the flow system (see Scheme 6.5) at a flow rate of 0.2 mL min^{-1} . After waiting for steady state for 20 min, fractions of 20 mL (1 mmol, 25 min) were collected. The neat cyclohexanone (0.098 g, 1 mmol) was added into a 35 mL microwave vial equipped with a stirrer bar and the reaction solution added. The reaction mixture was heated in the microwave (160 °C, 10 min). After cooling to room temperature, the reaction mixture was diluted with 10 mL water and extracted with DCM (3 x 20 mL). The combined organic layers were washed with brine (20 mL), dried over MgSO_4 , filtered and the solvent was removed under reduced pressure. The crude product was then further purified via column chromatography (EtOAc in petroleum ether, 0 to 5%).

6-Fluoro-2,3,4,9-tetrahydro-1H-carbazole (85)^[10]

Following the general procedure, **85** was synthesized from *p*-fluoroaniline (2 mmol, 0.222 g) and obtained as a yellow solid (68%, 0.128 g, 0.68 mmol).

¹H NMR (400 MHz, CDCl₃) δ 7.66 (bs, 1H, NH¹⁰), 7.17 (dd, *J*=8.6, 4.3 Hz, 1H, ArH), 7.10 (d, *J*=9.6 Hz, 1H, ArH), 6.84 (t, *J*=9.0 Hz, 1H, ArH), 2.74 - 2.69 (m, 4H, CH₂^{11,14}), 1.96–1.79 (m, 4H, CH₂^{12,13}) ppm.

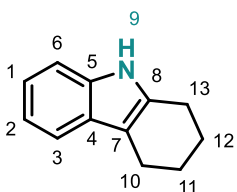
¹³C NMR (101 MHz, CDCl₃) δ 158.0 (d, *J*=233.5 Hz, ArC²), 136.5 (ArC), 132.0 (ArC), 128.0 (d, *J*=9.6 Hz, ArC⁴), 111.0 (d, *J*=9.7 Hz, ArCH⁶), 110.5 (d, *J*=4.4 Hz, ArC⁸), 109.0 (d, *J*=26.1 Hz, ArCH³), 103.0 (d, *J*=23.2 Hz, ArCH¹), 23.5 (3xCH₂), 21.0 (CH₂) ppm.

¹⁹F NMR (376 MHz, CDCl₃) δ -125.43 ppm.

mp (DCM): 96 - 98 °C.

IR: 3404, 2931, 2850, 1615, 1581, 1479, 1444, 1319, 1251, 1230, 1180, 1128, 1107, 1062, 920, 854, 792, 704, 601, 472 cm⁻¹.

HRMS (AP⁺): [C₁₂H₁₂FN]⁺ Calcd. 189.0954; Found 189.0953.

2,3,4,9-Tetrahydro-1H-carbazole (92)^[10]

Following the general procedure, **92** was synthesized from aniline (2 mmol, 0.186 g) and obtained as a yellow solid (57%, 0.097 g, 0.57 mmol).

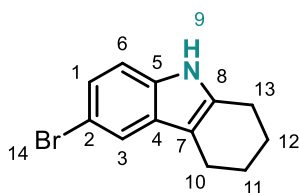
¹H NMR (400 MHz, CDCl₃) δ 7.63 (bs, 1H, NH⁹), 7.48 (d, *J* = 7.4 Hz, 1H, ArH³), 7.28 (d, *J*=7.9 Hz, 1H, ArH⁶), 7.16 - 7.06 (m, 2H, ArH), 2.73 - 2.96 (m, 4H, CH₂^{10,13}), 1.99 - 1.83 (m, 4H, CH₂^{11,12}) ppm.

¹³C NMR (101 MHz, CDCl₃) δ 136.0 (ArC), 134.5 (ArC), 128.0 (ArC), 121.0 (ArCH), 119.5 (ArCH), 118.0 (ArCH), 110.5 (ArCH), 110.0 (ArC), 23.5 (3xCH₂), 21.0 (CH₂) ppm.

mp: 106 - 108 °C.

IR: 3394, 3016, 2926, 2846, 1591, 1613, 1467, 1438, 1363, 1325, 1303, 1234, 1143, 1108, 918, 8134, 636, 596, 578, 542, 478, 426 cm⁻¹.

HRMS (EI⁺): [C₁₂H₁₃N]⁺ Calcd. 170.0970; Found 170.0974.

6-Bromo-2,3,4,9-tetrahydro-1H-carbazole (93)^[11]

Following the general procedure, **93** was synthesized from *p*-bromoaniline (2 mmol, 0.344 g) and obtained as a yellow solid (64%, 0.159 g, 0.64 mmol).

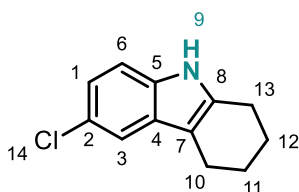
¹H NMR (400 MHz, CDCl₃) δ 7.69 (bs, 1H, NH⁹), 7.57 (s, 1H, ArH³), 7.18 (d, *J* = 8.5 Hz, 1H, ArH), 7.13 (d, *J* = 8.5 Hz, 1H, ArH), 2.73-2.64 (m, 4H, CH₂^{10,13}), 1.97 - 1.79 (m, 4H, CH₂^{11,12}) ppm.

¹³C NMR (101 MHz, CDCl₃) δ 136.5 (ArC), 134.5 (ArC), 130.0 (ArC), 123.5 (ArCH), 120.5 (ArCH), 112.5 (ArC), 112.0 (ArCH), 110.0 (ArC), 23.5 (2xCH₂), 23.0 (CH₂), 21.0 (CH₂) ppm.

mp (DCM): 146 - 147 °C.

IR: 3402, 2937, 2846, 1737, 1433, 1309, 1232, 1045, 975, 862, 796, 743, 640, 584, 478 cm⁻¹.

HRMS (AP⁺): [C₁₂H₁₂BrN]⁺ Calcd. 250.0231; Found 250.0242.

6-Chloro-2,3,4,9-tetrahydro-1H-carbazole (94)^[12]

Following the general procedure, **94** was synthesized from *p*-chloroaniline (2 mmol, 0.254 g) and obtained as a yellow solid (74%, 0.131 g, 0.74 mmol).

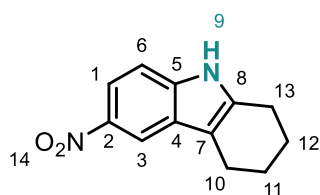
¹H NMR (400 MHz, CDCl₃) δ 7.66 (bs, 1H, NH⁹), 7.42 (s, 1H, ArH³), 7.16 (d, *J* = 8.5 Hz, 1H, ArH), 7.06 (d, *J* = 8.5 Hz, 1H, ArH), 2.73 - 2.65 (m, 4H, CH₂^{10,13}), 1.96 - 1.82 (m, 4H, CH₂^{11,12}) ppm.

¹³C NMR (101 MHz, CDCl₃) δ 136.0 (ArC), 134.0 (ArC), 129.0 (ArC), 125.0 (ArC), 121.0 (ArCH), 117.5 (ArCH), 111.0 (ArCH), 110.0 (ArC), 23.5 (2xCH₂), 23.0 (CH₂), 21.0 (CH₂) ppm.

mp (DCM): 140 - 141 °C.

IR: 3400, 2937, 2846, 1737, 1577, 1467, 1435, 1354, 1311, 1230, 1055, 972, 900, 862, 798, 655, 640, 590, 476 cm⁻¹.

HRMS (AP⁺): [C₁₂H₁₂ClN]⁺ Calcd. 206.0737; Found 206.0745.

6-Nitro-2,3,4,9-tetrahydro-1H-carbazole (95)^[10]

Following the general procedure, **95** was synthesized from *p*-nitroaniline (2 mmol, 0.276 g) and obtained as a yellow solid (24%, 0.052 g, 0.24 mmol).

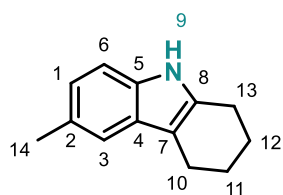
¹H NMR (400 MHz, CDCl₃) δ 8.42 (s, 1H, NH⁹), 8.15 - 7.92 (m, 2H, ArH), 7.31 - 7.22 (m, 1H, ArH), 2.86 - 2.64 (m, 4H, CH₂^{10,13}), 2.04 - 1.82 (m, 4H, CH₂^{11,12}) ppm.

¹³C NMR (126 MHz, CDCl₃) δ 141.5 (ArC), 139.0 (ArC), 137.5 (ArC), 127.5 (ArC), 117.0 (ArCH), 115.0 (ArCH), 113.0 (ArC), 110.0 (ArCH), 23.5 (CH₂), 23.0 (2xCH₂), 21.0 (CH₂) ppm.

mp (DCM): 156 - 158 °C.

IR: 3331, 2924, 2817, 1625, 1579, 1506, 1473, 1438, 1396, 1357, 1307, 1205, 1149, 1078, 881, 823, 651, 599 cm⁻¹.

HRMS (EI⁺): [C₁₂H₁₂N₂O₂]⁺ Calcd. 216.0899; Found 216.0899.

6-Methyl-2,3,4,9-tetrahydro-1H-carbazole (96)^[10]

Following the general procedure, **96** was synthesized from *p*-toluidine (2 mmol, 0.214 g) and obtained as a yellow solid (51%, 0.087 g, 0.51 mmol).

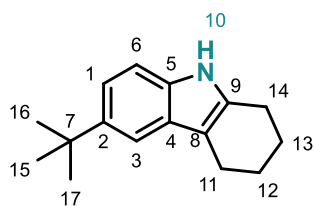
¹H NMR (400 MHz, CDCl₃) δ 7.45 (bs, 1H, NH⁹), 7.16 (s, 1H, ArH³), 7.06 (d, *J*=8.2 Hz, 1H, ArH), 6.85 (d, *J*=8.0 Hz, 1H, ArH), 2.66 - 2.55 (m, 4H, CH₂^{10,13}), 2.36 (s, 3H, CH₃¹⁴), 1.88 - 1.73 (m, 4H, CH₂^{11,12}) ppm.

¹³C NMR (101 MHz, CDCl₃) δ 134.5 (ArC), 134.0 (ArC), 128.5 (ArC), 128.0 (ArC), 122.5 (ArCH), 117.5 (ArCH), 110.0 (ArCH + ArC), 23.5 (3xCH₂), 22.0 (CH₃), 21.0 (CH₂) ppm.

mp (DCM): 132 - 133 °C.

IR: 3390, 2927, 2846, 1589, 1436, 1313, 797, 594, 4673 cm⁻¹.

HRMS (AP⁺): [C₁₃H₁₄N]⁺ Calcd. 184.1121; Found: 184.1120.

6-(Tert-butyl)-2,3,4,9-tetrahydro-1H-carbazole (97)^[13]

Following the general procedure, **97** was synthesized from *p*-tertbutylaniline (2 mmol, 0.298 g) and obtained as a yellow solid (28%, 0.064 g, 0.28 mmol).

¹H NMR (400 MHz, CDCl₃) δ 7.58 (bs, 1H, NH¹⁰), 7.44 (s, 1H, ArH³), 7.23 - 7.16 (m, 2H, ArH^{1,6}), 2.71 (t, *J*=5.3 Hz, 4H, CH₂^{11,14}), 1.94 - 1.83 (m, 4H, CH₂^{12,13}), 1.38 (s, 9H, CH₃^{15,16,17}) ppm.

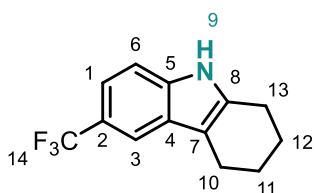
^{13}C NMR (101 MHz, CDCl_3) δ 142.5 (ArC), 134.5 (ArC), 134.0 (ArC), 128.0 (ArC), 119.5 (ArCH), 114.0 (ArCH), 110.5 (ArC), 110.0 (ArCH), 35.0 (CH_2), 32.0 (CH_2), 23.5 ($3\times\text{CH}_3$), 21.5 (CH_2) ppm.

mp (DCM): 114 - 115 °C.

IR: 3390, 2929, 2852, 1475, 1361, 1313, 1236, 869, 804, 624, 482, 449 cm^{-1} .

HRMS (EI⁺): [$\text{C}_{16}\text{H}_{21}\text{N}$]⁺ Calcd. 227.1674; Found 227.1672.

6-(Trifluoromethyl)-2,3,4,9-tetrahydro-1H-carbazole (98)



Following the general procedure, **98** was synthesized from *p*-(trifluoromethyl)aniline (2 mmol, 0.322 g) and obtained as a yellow solid (24%, 0.057 g, 0.24 mmol).

^1H NMR (500 MHz, CDCl_3) δ 7.89 (s, 1H, NH^9), 7.54 (s, 1H, ArCH^3), 7.51 (d, $J = 8.3$ Hz, 1H, ArCH), 7.31 (d, $J = 8.2$ Hz, 1H, ArCH), 2.77 (t, $J = 5.9$ Hz, 2H, CH_2), 2.72 (t, $J = 5.8$ Hz, 2H, CH_2), 1.99 – 1.82 (m, 4H, $\text{CH}_2^{11,12}$) ppm.

^{13}C NMR (126 MHz, CDCl_3) δ 137.5 (ArC), 134.5 (ArC), 130.5 (ArC), 125.5 (q, $J = 271.3$ Hz, CF_3^{14}), 123.0 (q, $J = 31.6$ Hz, ArC^2), 118.0 (ArCH), 116.0 (q, $J = 3.6$ Hz, ArCH), 111.0 (ArC), 108.0 (q, $J = 4.3$ Hz, ArCH), 23.5 ($2\times\text{CH}_2$), 23.0 (CH_2), 21.0 (CH_2) ppm.

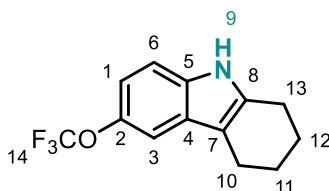
^{19}F -NMR (471 MHz, CDCl_3) δ -60.09 ppm.

mp (DCM): 120 - 121 °C.

IR: 3460, 3408, 2931, 2854, 1583, 1478, 1427, 1323, 1267, 1147, 1098, 1051, 908, 873, 813, 711, 813, 711, 640, 463 cm^{-1} .

HRMS (EI⁺): [$\text{C}_{13}\text{H}_{12}\text{F}_3\text{N}$]⁺ Calcd. 239.0922; Found 239.0924.

6-(Trifluoromethoxy)-2,3,4,9-tetrahydro-1H-carbazole (99)^[13]



Following the general procedure, **99** was synthesized from *p*-(trifluoromethoxy)aniline (2 mmol, 0.354 g) and obtained as a yellow solid (49%, 0.126 g, 0.49 mmol).

^1H NMR (400 MHz, CDCl_3) δ 7.76 (s, 1H, NH^9), 7.30 (s, 1H, ArCH^3), 7.22 (d, $J = 8.7$ Hz, 1H, ArCH), 6.98 (d, $J = 8.7$ Hz, 1H, ArCH), 2.73 (t, $J = 5.4$ Hz, 2H, CH_2), 2.68 (t, $J = 5.4$ Hz, 2H, CH_2), 1.97 – 1.82 (m, 4H, $\text{CH}_2^{11,12}$) ppm.

^{13}C NMR (126 MHz, CDCl_3) δ 143.0 (ArC), 136.5 (ArC), 134.0 (ArC), 128.0 (ArC), 121.0 (q, $J = 254.5$ Hz, OCF_3^{14}), 115.0 (ArCH), 111.0 (ArCH + ArC), 110.5 (ArCH), 23.5 (2x CH_2), 23.0 (CH_2), 21.0 (CH_2) ppm.

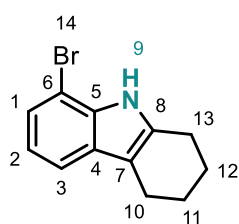
^{19}F NMR (376 MHz CDCl_3) δ -58.05 ppm.

mp (DCM): 58 - 60 °C.

IR: 3404, 2958, 2846, 1583, 1479, 1449, 1211, 1151, 869, 798, 688, 599, 482 cm^{-1} .

HRMS (EI $^+$): $[\text{C}_{13}\text{H}_{12}\text{F}_3\text{NO}]^+$ Calcd. 255.0871; Found 255.0868.

8-Bromo-2,3,4,9-tetrahydro-1H-carbazole (100)



Following to the general procedure, **100** was synthesized from *o*-bromoaniline (2 mmol, 0.344 g) and obtained as a yellow solid (42%, 0.106 g, 0.42 mmol).

^1H NMR (400 MHz, CDCl_3) δ 7.87 (s, 1H, NH^9), 7.39 (d, $J = 7.8$ Hz, 1H, ArH), 7.25 (d, $J = 7.1$ Hz, 1H, ArH), 6.95 (t, $J = 7.7$ Hz, 1H, ArH), 2.77 (t, $J = 5.9$ Hz, 2H, CH_2), 2.69 (t, $J = 5.7$ Hz, 2H, CH_2), 2.03 – 1.79 (m, 4H, $\text{CH}_2^{11,12}$) ppm.

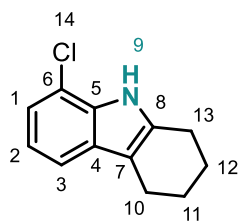
^{13}C NMR (101 MHz, CDCl_3) δ 135.0 (ArC), 134.5 (ArC), 129.0 (ArC), 123.5 (ArCH), 120.5 (ArCH), 117.0 (ArCH), 111.5 (ArC), 104.0 (ArC), 23.5 (2x CH_2), 23.0 (CH_2), 21.0 (CH_2) ppm.

mp (DCM): 56 - 57 °C.

IR: 3392, 2933, 2850, 1583, 1548, 1485, 1460, 1438, 1413, 1359, 1312, 1301, 1278, 1205, 1186, 1149, 1124, 954, 896, 769, 732, 640, 572, 426 cm^{-1} .

HRMS (EI $^+$): $[\text{C}_{12}\text{H}_{12}\text{BrN}]^+$ Calcd. 250.0231; Found 250.0242.

8-Chloro-2,3,4,9-tetrahydro-1H-carbazole (101)^[14]



Following the general procedure, **101** was synthesized from *o*-chloroaniline (2 mmol, 0.254 g) and obtained as a yellow solid (42%, 0.086 g, 0.42 mmol).

^1H NMR (400 MHz, CDCl_3) δ 7.91 (bs, 1H, NH^9), 7.35 (d, $J = 7.7$ Hz, 1H, ArH), 7.10 (d, $J = 7.6$ Hz, 1H, ArH), 7.00 (t, $J = 7.8$ Hz, 1H, ArH^2), 2.77 (t, $J = 5.5$ Hz, 2H, CH_2), 2.70 (t, $J = 5.5$ Hz, 2H, CH_2), 1.97–1.82 (m, 4H, CH_2) ppm.

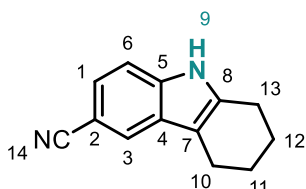
^{13}C NMR (126 MHz, CDCl_3) δ 135.0 (ArC), 133.0 (ArC), 129.5 (ArC), 120.5 (ArCH), 120.0 (ArCH), 116.5 (ArCH), 116.0 (ArC), 111.5 (ArC), 23.5 (CH_2), 23.0 (2x CH_2), 21.0 (CH_2) ppm.

mp (DCM): 57 - 58 °C.

IR: 3394, 2916, 2845, 1891, 1815, 1615, 1585, 1564, 1489, 1457, 1419, 1361, 1325, 1301, 1209, 1123, 1014, 908, 753, 726, 574, 462 cm⁻¹.

HRMS (EI⁺): [C₁₂H₁₂CIN]⁺ Calcd. 205.0658; Found: 205.0672.

2,3,4,9-tetrahydro-1H-carbazole-6-carbonitrile (**102**)^[13]



Following the general procedure, **102** was synthesized from *p*-aminobenzonitrile (2 mmol, 0.236 g) and obtained as an orange solid (53%, 0.104 g, 0.53 mmol).

¹H NMR (400 MHz, DMSO) δ 11.29 (s, 1H, NH⁹), 7.84 (s, 1H, ArH²), 7.39 (d, *J* = 8.3 Hz, 1H, ArH), 7.33 (dd, *J* = 8.4, 1.3 Hz, 1H, ArH), 2.72 (t, *J* = 5.7 Hz, 2H, CH₂), 2.63 (t, *J* = 5.7 Hz, 2H, CH₂), 1.90 - 1.71 (m, 4H, CH₂) ppm.

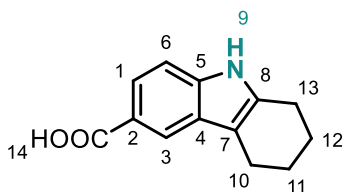
¹³C NMR (101 MHz, DMSO) δ 137.5 (ArC, CN), 127.0 (ArC), 123.0 (ArC), 122.5 (ArC), 121.0 (ArC), 111.5 (ArC), 109.5 (ArC), 100.0 (ArC), 22.5 (3xCH₂), 20.5 (CH₂) ppm.

mp (DCM): 106-108 °C.

IR: 3312, 2922, 2849, 2216, 1622, 1476, 1317, 1179, 799, 621 cm⁻¹.

HRMS (FTMS+ *p* NSI): [C₁₃H₁₃N₂]⁺ Calcd. 197.1073; Found 197.1071.

2,3,4,9-tetrahydro-1H-carbazole-6-carboxylic acid (**103**)



Following the general procedure, **103** was synthesized from *p*-aminobenzoic acid (2 mmol, 0.274 g) and obtained as an orange solid (70%, 0.150 g, 0.70 mmol).

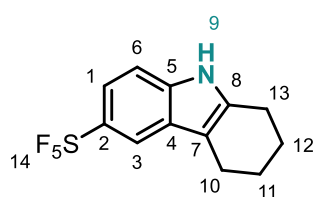
¹H NMR (400 MHz, DMSO) δ 12.31 (s, 1H, OH¹⁴), 11.02 (s, 1H, NH⁹), 8.01 (s, 1H, ArH³), 7.63 (dd, *J* = 8.5, 1.6 Hz, 1H, ArH), 7.28 (d, *J* = 8.5 Hz, 1H, ArH), 2.70 (t, *J* = 5.4 Hz, 2H, CH₂), 2.65 (t, *J* = 5.4 Hz, 2H, CH₂), 1.95 - 1.69 (m, 4H, CH₂) ppm.

¹³C NMR (101 MHz, DMSO) δ 168.5 (CO), 138.0 (ArC), 136.0 (ArC), 127.0 (ArC), 121.5 (ArC), 120.5 (ArC), 119.5 (ArC), 110.0 (ArC), 109.5 (ArC), 23.0 (CH₂), 22.5 (CH₂), 20.5 (CH₂) ppm.

mp (DCM): degradation >150 °C.

IR: 3397, 2941, 2905, 2849, 1668, 1614, 1245, 772, 494 cm⁻¹.

HRMS (FTMS+ *p* NSI): [C₁₃H₁₄O₂N₁]⁺ Calcd. 216.1019; Found 216.1020.

6-(pentafluorothio)-2,3,4,9-tetrahydro-1H-carbazole (104)

Following the general procedure, **104** was synthesized from *p*-pentafluorothioaniline (2 mmol, 0.281 g) and obtained as a light brown solid (68%, 0.181 g, 0.68 mmol).

$^1\text{H NMR}$ (500 MHz, CDCl_3) δ 7.90 (s, 1H, NH^9), 7.87 (d, $J = 2.1$ Hz, 1H, ArH^3), 7.50 (dd, $J = 8.9, 2.2$ Hz, 1H, ArH^1), 7.25 (d, $J = 9.9$ Hz, 1H, ArH^6), 2.78 – 2.65 (m, 4H, $\text{CH}_2^{10,13}$), 1.98 – 1.82 (m, 4H, $\text{CH}_2^{11,12}$) ppm.

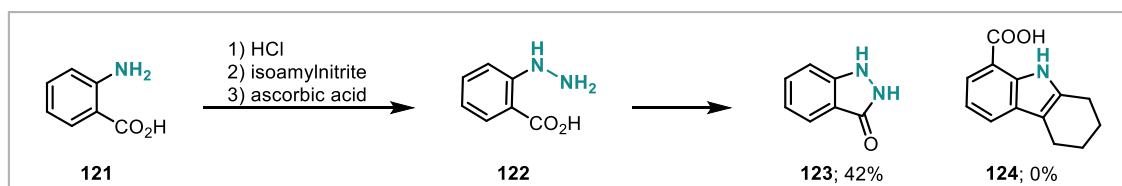
$^{13}\text{C NMR}$ (126 MHz, CDCl_3) δ 146.5 (ArC), 137.0 (ArC), 136.0 (ArC), 127.0 (ArC), 119.0 – 118.5 (m, ArC), 116.5 – 116.0 (m, ArC), 112.0 (ArC), 109.5 (ArC), 23.5 (CH_2), 23.0 ($2\times\text{CH}_2$), 21.0 (CH_2) ppm.

$^{19}\text{F NMR}$ (471 MHz, CDCl_3) δ 91.85 – 83.51 (m, 1F), 65.95 (d, $J = 150.0$ Hz, 4F) ppm.

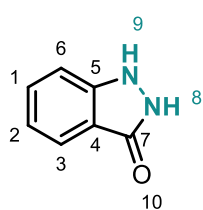
mp (DCM): 66–68 °C.

IR: 3482, 2922, 2855, 1474, 1323, 791, 613, 556 cm^{-1} .

HRMS (ASAP+): $[\text{C}_{12}\text{H}_{13}\text{F}_5\text{NS}]^+$ Calcd. 298.0689; Found 298.0683.

3.2.1 Anthranilic Acid Product**1,2-dihydro-3H-indazol-3-one (123)**

Solutions of anthranilic acid (0.274 g, 2 mmol, 10 mL of 0.2 M solution in acetonitrile), HCl (10 mL of 1 M aqueous solution), isoamyl nitrite (0.281 g, 2.4 mmol, 10 mL of 0.24 M solution in acetonitrile) and ascorbic acid (0.352 g, 2 mmol, 10 mL of 0.2 M aqueous solution) were prepared. These were then pumped through the flow system (see Scheme 6.4) at a flow rate of 0.2 mL min^{-1} . After waiting for steady state for 20 min, a fraction of 20 mL (1 mmol, 25 min) was collected. The neat cyclohexanone (0.098 g, 1 mmol) was added into a 35 mL microwave vial equipped with a stirrer bar and the reaction solution added. The reaction mixture was heated in the microwave (160 °C, 10 min). After cooling to room temperature, the reaction mixture was diluted with 10 mL water and extracted with DCM (3 x 20 mL). The combined organic layers were washed with brine (20 mL), dried over MgSO_4 , filtered and the solvent was removed under reduced pressure. The crude product was then further purified via column chromatography (EtOAc in petroleum ether, 0 to 5%) to yield the product **123** in 42% yield (0.056 g, 0.42 mmol) as an off white solid.



^1H NMR (400 MHz, DMSO) δ 11.33 (s, 1H, NH⁸), 10.58 (s, 1H, NH⁹), 7.61 (d, J = 8.1 Hz, 1H, ArH), 7.36 – 7.21 (m, 2H, ArH), 7.02 – 6.91 (m, 1H, ArH) ppm.

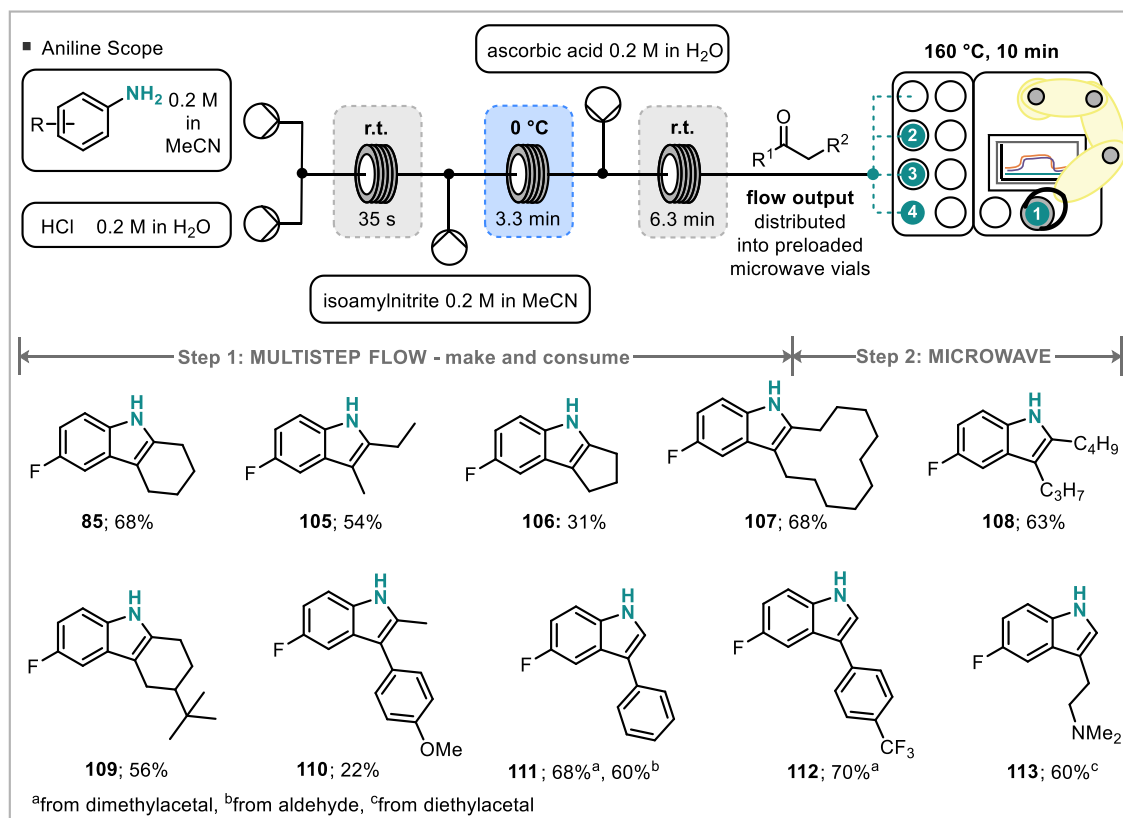
^{13}C NMR (126 MHz, DMSO) δ 156.0 (CO⁷), 142.5 (ArC), 127.0 (ArC), 120.0 (ArCH), 118.5 (ArCH), 112.5 (ArC), 110.0 (ArCH) ppm.

mp (DCM): degradation >190 °C.

IR: 3055, 2922, 2853, 1618, 1585, 1458, 1327, 1090, 897, 733, 670, 505 cm^{-1} .

HRMS (MAT 95 ^+Cl (NH₃)): [C₇H₇ON₂]⁺ Calcd. 135.0553; Found 135.0554.

3.3 General Method for the Synthesis of Indoles **85** and **105** - **113**: Ketone Screen

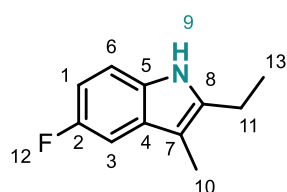


Scheme 6.6: Ketone Substrate Scope

Solutions of *p*-fluoroaniline (0.2 M in acetonitrile), HCl (1 M in water), isoamyl nitrite (0.24 M in acetonitrile) and ascorbic acid (0.2 M in water) were prepared. These were then pumped through the flow system (see Scheme 6.6) at a flow rate of 0.2 mL min⁻¹. After waiting for steady state for 20 min, fractions of 20 mL (1 mmol, 25 min) were collected. The neat ketone (1 mmol) was added into a 35 mL microwave vial equipped

with a stirrer bar and the reaction solution added. The reaction mixture was heated in the microwave (160 °C, 10 min). After cooling to room temperature trifluorotoluene (0.041 mL, 0.33 mmol) was added and yield determined by ^{19}F NMR. After recombining the NMR sample with the bulk solution, it was diluted with 10 mL water and extracted with DCM (3 x 20 mL). The combined organic layers were washed with brine (20 mL), dried over MgSO_4 , filtered and the solvent was removed under reduced pressure. The crude product was then further purified via column chromatography (EtOAc in petroleum ether, 0 to 5%).

3-Ethyl-5-fluoro-2-methyl-1H-indole (113)



Following the general procedure, **113** was synthesized from 3-pentanone (1 mmol, 0.086 g) and obtained as a yellow solid (54%, 0.096 g, 0.54 mmol).

^1H NMR (400 MHz, CDCl_3) δ 7.71 (s, 1H, NH^9), 7.19 - 7.14 (m, 1H, ArH), 7.11 (d, $J = 9.7$ Hz, 1H, ArH), 6.84 (t, $J = 9.1$ Hz, 1H, ArH), 2.75 (q, $J = 7.6$ Hz, 2H, CH_2^{11}), 2.19 (s, 3H, CH_3^{10}), 1.28 (t, $J = 7.6$ Hz, 3H, CH_3^{13}) ppm.

^{13}C NMR (126 MHz, CDCl_3) δ 158.0 (d, $J = 233.4$ Hz, ArC^2), 138.5 (ArC), 131.5 (ArC), 130.0 (d, $J = 9.6$ Hz, ArC), 110.5 (d, $J = 9.7$ Hz, ArC), 109.0 (d, $J = 26.2$ Hz, ArC^3), 106.71 (d, $J = 4.5$ Hz, ArC^7), 103.23 (d, $J = 23.2$ Hz, ArC^1), 19.5 (CH_3^{10}), 14.0 (CH_2^{11}), 8.5 (CH_3^{13}) ppm.

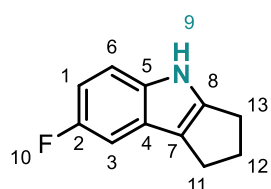
^{19}F NMR (376 MHz, CDCl_3) δ -125.49 ppm.

mp (DCM): 58 - 59 °C.

IR: 3392, 2976, 2863, 1842, 1624, 1581, 1483, 1446, 1325, 1288, 1180, 1055, 941, 848, 803, 607, 493 cm^{-1} .

HRMS (EI $^+$): $[\text{C}_{11}\text{H}_{12}\text{FN}_2]^+$ Calcd. 177.0954; Found 177.0954.

7-fluoro-1,2,3,4-tetrahydrocyclopenta[b]indole (114)



Following the general procedure, **114** was synthesized from cyclopentanone (1 mmol, 0.084 g) and obtained as a yellow solid (31%, 0.054 g, 0.31 mmol).

^1H NMR (400 MHz, CDCl_3) δ 7.82 (s, 1H, NH^9), 7.26 - 7.17 (m, 1H, ArH), 7.09 - 7.06 (m, 1H, ArH), 6.85 - 6.80 (m, 1H, ArH), 2.86 (t, $J = 7.1$ Hz, 2H, CH_2), 2.80 (t, $J = 6.9$ Hz, 2H, CH_2), 2.60 - 2.48 (m, 2H, CH_2^{12}) ppm.

^{13}C NMR (101 MHz, CDCl_3) δ 158.0 (d, $J = 233.5$ Hz, ArC^2), 146.0 (ArC), 137.5 (ArC), 125.0 (d, $J = 10.0$ Hz, ArC^4), 120.0 (d, $J = 4.3$ Hz, ArC^7), 111.5 (d, $J = 9.9$ Hz, ArCH^6),

108.5 (d, $J = 26.1$ Hz, ArCH), 104.0 (d, $J = 23.5$ Hz, ArCH), 28.5 (CH₂), 26.0 (CH₂), 24.5 (CH₂¹²) ppm.

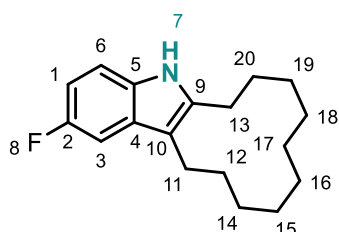
¹⁹F NMR (376 MHz, CDCl₃) δ -125.19 ppm.

mp (DCM): 80 - 83 °C.

IR: 3410, 2918, 2854, 1662, 1622, 1577, 1473, 1446, 1300, 1074, 850, 801, 599, 478, 413 cm⁻¹.

HRMS (EI⁺): [C₁₁H₁₀FN]⁺ Calcd. 175.0797; Found 175.0799.

2-fluoro-6,7,8,9,10,11,12,13,14,15-decahydro-5H-cyclododeca[b]indole (115)



Following the general procedure, **115** was obtained from cyclododecanone (1 mmol, 0.182 g). The product was

isolated as a pale yellow solid (68%, 0.129 g, 0.68 mmol).

¹H NMR (500 MHz, CDCl₃) δ 8.97 (bs, 1H, NH⁷), 7.40 - 7.27 (m, 2H, ArH), 7.09 (m, 1H, ArH), 3.17 - 2.75 (m, 4H, CH₂),

1.91 - 1.68 (m, 4H, CH₂), 1.68 - 1.02 (m, 12H, CH₂) ppm.

¹³C NMR (126 MHz, CDCl₃) δ 158.0 (d, $J = 236.7$ Hz, ArC²), 133.0 (d, $J = 33.4$ Hz, ArCH), 129.0 (d, $J = 9.3$ Hz, ArCH), 123.5 (d, $J = 5.7$ Hz (ArC¹⁰), 115.5 (d, $J = 27.0$ Hz, ArCH), 113.0 (d, $J = 9.4$ Hz, ArC), 106.0 (ArC), 105.5 (ArC), 41.0 (CH₂), 28.0 (CH₂), 26.5 (CH₂), 26.0 (CH₂), 24.5 (CH₂), 24.0 (CH₂), 23.0 (CH₂), 22.5 (CH₂), 22.0 (CH₂) ppm.

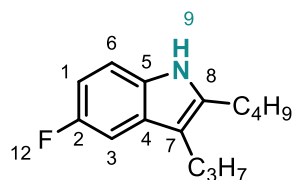
¹⁹F NMR (471 MHz, CDCl₃) δ -123.21 ppm.

mp (hexane): 190 - 192 °C.

IR: 3322, 2920, 2359, 1625, 1520, 1508, 1458, 1425, 1265, 1229, 1172, 1092, 1080, 1018, 810, 758, 667, 590, 486, 419 cm⁻¹.

HRMS (ES⁺): [C₁₈H₂₅FN]⁺ Calcd. 274.1971, Found 274.1981.

2-butyl-5-fluoro-3-propyl-1H-indole (116)



Following the general procedure, compound **116** was obtained from 5-nonanone (1 mmol, 0.142 g) as an orange oil (63%, 0.147 g, 0.63 mmol).

¹H NMR (400 MHz, CDCl₃) δ 7.69 (s, 1H, NH⁹), 7.19 - 7.11 (m, 2H, ArH), 6.83 (td, $J = 9.2, 2.5$ Hz, 1H, ArH), 2.75 - 2.68 (m, 2H, CH₂), 2.66 - 2.58 (m, 2H, CH₂), 1.69 - 1.56 (m, 4H, CH₂), 1.46 - 1.32 (m, 2H, CH₂), 0.96 (t, $J = 7.3$ Hz, 3H, CH₃), 0.95 (t, $J = 7.3$ Hz, 3H, CH₃) ppm.

¹³C NMR (101 MHz, CDCl₃) δ 158.0 (d, $J = 233.2$ Hz, ArC²), 137.5 (ArC), 132.0 (ArC), 129.5 (d, $J = 9.4$ Hz, ArCH⁶), 112.5 (d, $J = 4.5$ Hz, ArC⁷), 110.5 (d, $J = 9.7$ Hz, ArC⁴),

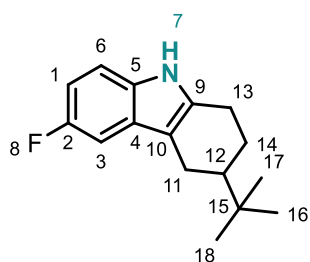
109.0 (d, $J = 26.1$ Hz, ArCH), 103.5 (d, $J = 23.2$ Hz, ArCH), 32.0 (CH₂), 26.5 (CH₂), 26.0 (CH₂), 24.0 (CH₂), 22.5 (CH₂), 14.5 (CH₃), 14.0 (CH₃) ppm.

¹⁹F NMR (376 MHz, CDCl₃) δ -125.63 ppm.

IR: 3420, 2957, 2930, 2359, 2342, 1608, 1508, 1483, 1456, 1364, 1287, 1236, 1175, 1074, 968, 847, 822, 793, 606, 419 cm⁻¹.

HRMS (FTMS+ p NSI): [C₁₅H₂₀FN]⁺ Calcd. 234.1653, Found 234.1654.

3-(tert-butyl)-6-fluoro-2,3,4,9-tetrahydro-1H-carbazole (117)



Following the general procedure, **117** was obtained from 4-tertbutylcyclohexanone (1 mmol, 0.154 g). The product was isolated as a colourless solid (56%, 0.137 g, 0.56 mmol).

¹H NMR (500 MHz, CDCl₃) δ 9.03 (bs, 1H, NH⁹), 7.37 (dd, $J = 8.3, 4.4$ Hz, 1H, ArH), 7.12 (dd, $J = 7.2, 1.9$ Hz, 1H, ArH), 7.07 - 6.95 (m, 1H, ArH), 2.82 - 2.71 (m, 2H, CH₂), 2.53 (d, $J = 14.5$

Hz, 1H, CH₂), 2.25 - 2.18 (m, 1H, CH), 1.88 (t, $J = 12.6$ Hz, 1H, CH₂), 1.24 (qd, $J = 12.6, 5.6$ Hz, 1H, CH¹²), 1.12 (t, $J = 13.7$ Hz, 1H), 0.89 (s, 9H) ppm.

¹³C NMR (126 MHz, CDCl₃) δ 185.0 (d, $J = 3.6$ Hz, ArC), 161.5 (d, $J = 245.7$ Hz, ArC²), 150.0 (d, $J = 2.1$ Hz, ArC), 139.5 (d, $J = 8.2$ Hz, ArC), 121.0 (d, $J = 8.6$ Hz, ArCH), 116.0 (d, $J = 23.5$ Hz, ArCH), 110.5 (d, $J = 24.8$ Hz, ArCH), 92.5 (ArC), 42.0 (CH), 37.0 (CH), 32.0 (CH₂), 29.5 (2xCH₂), 27.5 (CH₃) ppm.

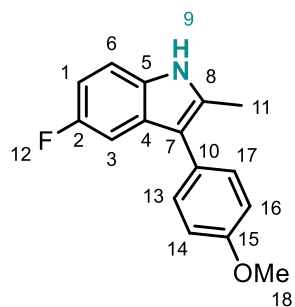
¹⁹F NMR (471 MHz, CDCl₃) δ -116.56 ppm.

mp (hexane): 125 - 126 °C.

IR: 2961, 2359, 1607, 1459, 1172, 1094, 870, 825, 799, 592, 538, 418 cm⁻¹.

HRMS (EI⁺): [C₁₆H₂₁FN]⁺ Calcd. 246.1658; Found 246.1647.

5-fluoro-3-(4-methoxyphenyl)-2-methyl-1H-indole (118)



Following the general procedure, compound **118** was obtained from 4-methoxyphenyl acetone (1 mmol, 0.164 g) to yield a yellow solid (22%, 0.056 g, 0.22 mmol).

¹H NMR (400 MHz, CDCl₃) δ 7.92 (s, 1H, NH⁹), 7.43 - 7.35 (m, 2H, ArH), 7.29 - 7.18 (m, 2H, ArH), 7.05 - 6.98 (m, 2H, ArH), 6.89 (td, $J = 9.0, 2.5$ Hz, 1H, ArH), 3.87 (s, 3H, OCH₃¹⁸), 2.48 (s, 3H, CH₃¹¹) ppm.

¹³C NMR (126 MHz, CDCl₃) δ 158.5 (d, $J = 233.9$ Hz, ArC²), 158.0 (ArC), 133.0 (ArC), 131.5 (ArC), 130.5 (ArCH), 128.5 (d, $J = 9.6$ Hz, ArC), 127.5 (ArC), 114.5 (d, $J = 4.4$ Hz,

ArC⁷), 114.0 (ArCH), 111.0 (d, $J = 9.7$ Hz, ArCH), 110.0 (d, $J = 26.2$ Hz, ArCH), 104.0 (d, $J = 24.0$ Hz, ArCH), 55.5 (OCH₃¹⁸), 12.5 (CH₃¹¹) ppm.

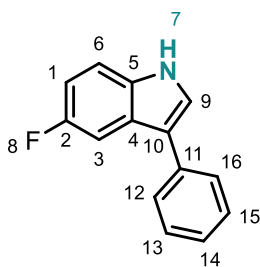
¹⁹F NMR (376 MHz, CDCl₃) δ -124.67 ppm.

mp (DCM): 120 - 124 °C

IR: 3347, 3001, 2963, 2920, 1510, 1487, 1452, 1236, 795, 615, 577 cm⁻¹.

HRMS (ES⁺): [C₁₆H₁₅FNO]⁺ Calcd. 256.1138, Found 256.1138.

5-fluoro-3-phenyl-1H-indole (119)^[15]



Following the general procedure, compound **119** was obtained as a brown solid from phenyl acetaldehyde (1 mmol, 0.120 g) and the corresponding acetal 2,2-dimethoxyethylbenzene (1 mmol, 0.166 g) in 60% (0.127 g, 0.60 mmol) and 68% (0.143 g, 0.68 mmol) respectively.

¹H NMR (500 MHz, CDCl₃) δ 8.23 (bs, 1H, NH⁹), 7.68 - 7.56 (m, 3H, ArH), 7.47 - 7.41 (m, 3H, ArH), 7.37 - 7.28 (m, 2H, ArH), 7.02 (m, 1H, ArH) ppm.

¹³C NMR (126 MHz, CDCl₃) δ 158.5 (d, $J = 234.9$ Hz, ArC²), 135.0 (Ar), 133.5 (Ar), 129.0 (ArCH), 127.5 (ArCH), 126.5 (ArCH), 126.5 (d, $J = 9.9$ Hz, ArCH), 123.5 (ArC), 118.5 (d, $J = 4.7$ Hz, ArC), 112.0 (d, $J = 9.7$ Hz, ArC), 111.0 (d, $J = 26.4$ Hz, ArCH), 105.0 (d, $J = 24.2$ Hz, ArCH) ppm.

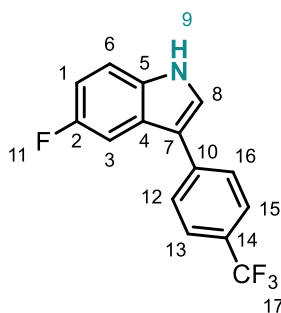
¹⁹F NMR (471 MHz, CDCl₃) δ -123.91 ppm.

mp (DCM): 94 - 95 °C.

IR: 3454, 3132, 2359, 1599, 1578, 1539, 1458, 1323, 1172, 1161, 1119, 920, 799, 758, 691, 691, 681, 592, 529, 486, 424 cm⁻¹.

HRMS (ASAP⁺): [C₁₄H₁₀FN]⁺ Calcd. 212.0876, Found 212.0881.

5-fluoro-3-(4-(trifluoromethyl)phenyl)-1H-indole (120)



Following the general procedure, compound **120** was obtained from 4-trifluoromethylphenyl acetaldehyde dimethyl acetal (1 mmol, 0.234 g) to yield yellow solid (70%, 0.196 g, 0.70 mmol).

¹H NMR (400 MHz, CDCl₃) δ 8.36 (s, 1H, NH⁹), 7.71 (q, $J = 8.5$ Hz, 4H, ArH), 7.56 (dd, $J = 9.8, 2.5$ Hz, 1H, ArH), 7.48 (d, $J = 2.7$ Hz, 1H, ArH), 7.38 (dd, $J = 8.9, 4.4$ Hz, 1H, ArH), 7.04 (td, $J = 8.9, 2.4$ Hz, 1H, ArH) ppm.

^{13}C NMR (126 MHz, CDCl_3) δ 158.5 (d, $J = 235.5$ Hz, ArC^2), 139.0 (ArC), 133.0 (ArC), 128.0 (q, $J = 32.5$ Hz ($\text{ArC}^{13,15}$), 127.0 (ArC), 126.0 (q, $J = 3.8$ Hz, ArC^{10}), 126.0 (d, $J = 9.8$ Hz, ArC^6), 124.53 (q, $J = 271.7$ Hz, CF_3^{17}), 124.5 (ArC), 117.5 (d, $J = 4.7$ Hz, ArC^7), 112.5 (d, $J = 9.7$ Hz, ArC^4), 111.5 (d, $J = 26.4$ Hz, ArC), 105.0 (d, $J = 24.3$ Hz, ArCH) ppm.

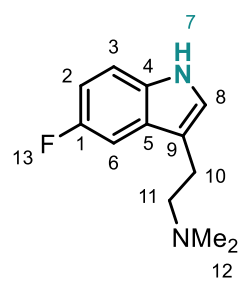
^{19}F NMR (376 MHz, CDCl_3) δ -62.28 (s, 3H), -123.02 (s, 1H) ppm.

mp (DCM): 55 - 58 °C.

IR: 3455, 2928, 2855, 1612, 1479, 1323, 1103, 924, 845, 800, 594 cm^{-1} .

HRMS (FTMS+ p APCI corona): $[\text{C}_{15}\text{H}_9\text{F}_4\text{N}]^+$ Calcd. 279.0666, Found 279.0665.

2-(5-fluoro-1H-indol-3-yl)-*N,N*-dimethylethan-1-amine (121)



Following the general procedure, compound **121** was obtained from 4-(dimethylamino)butyraldehyde diethylacetal (1 mmol, 0.189 g) and purified via column chromatography (0 to 10% Et_3N in EtOAc) to yield an orange solid (60%, 0.124 g, 0.70 mmol).

^1H NMR (500 MHz, CDCl_3) δ 8.30 (s, 1H, NH^9), 7.32 – 7.23 (m, 2H, ArH), 7.08 (s, 1H, ArH), 6.95 (t, $J = 9.0$ Hz, 1H, ArH), 2.97 – 2.89

(m, 2H, CH_2), 2.69 – 2.61 (m, 2H, CH_2), 2.38 (s, 6H, CH_3^{12}) ppm.

^{13}C NMR (126 MHz, CDCl_3) δ 157.5 (d, $J = 234.1$ Hz, ArC^1), 133.0 (ArCH), 128.0 (d, $J = 9.6$ Hz, ArCH), 123.5 (ArCH), 114.5 (d, $J = 4.7$ Hz, ArC^9), 112.0 (d, $J = 9.7$ Hz, ArC), 110.5 (d, $J = 26.4$ Hz, ArCH), 104.0 (d, $J = 23.2$ Hz, ArC), 60.0 (CH_2), 45.5 (CH_2), 24.0 (CH_3) ppm.

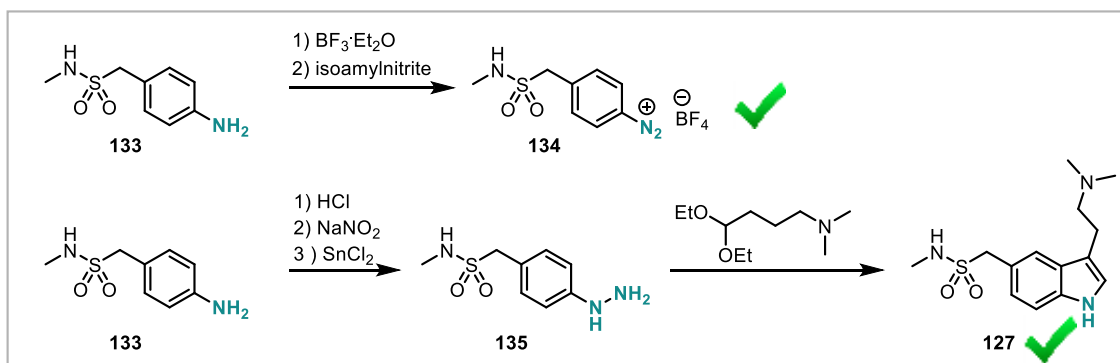
^{19}F NMR (471 MHz, CDCl_3) δ -125.06 (d, $J = 3.7$ Hz) ppm.

mp (DCM): 62 - 64 °C.

IR: 3136, 3049, 2947, 2859, 2822, 2770, 1582, 1464, 1445, 1155, 1032, 937, 843, 795, 713, 615, 422 cm^{-1} .

HRMS (FTMS + p NSI): $[\text{C}_{12}\text{H}_{16}\text{FN}_2]^+$ Calcd. 207.1292, Found 207.1292.

3.4 Sumatriptan Synthesis



Scheme 6.7: Sumatriptan Synthesis

4-((N-methylsulfonyl)methyl)benzenediazonium tetrafluoroborate 134

4-amino-*N*-methyl- α -toluene sulphonamide (1 g, 5 mmol) was dissolved in MeCN (15 mL) and the solution cooled to 0 °C. After the addition of boron trifluoride diethyl etherate (1.064 g, 7.5 mmol, 1.5 equiv), isoamyl nitrite (0.702 g, 6 mmol, 1.2 equiv) in MeCN (5 mL) was added slowly. The solution was stirred for another 30 min and turned bright orange. The product was precipitated with diethyl ether (50 mL), filtered and washed with ice cold diethyl ether. Further recrystallisations did not succeed in obtaining a satisfactory clean product by NMR. IR confirmed the diazonium salt N-N triple bond to be present.

1-(4-hydrazineylphenyl)-*N*-methylmethanesulfonamide 135^[16]

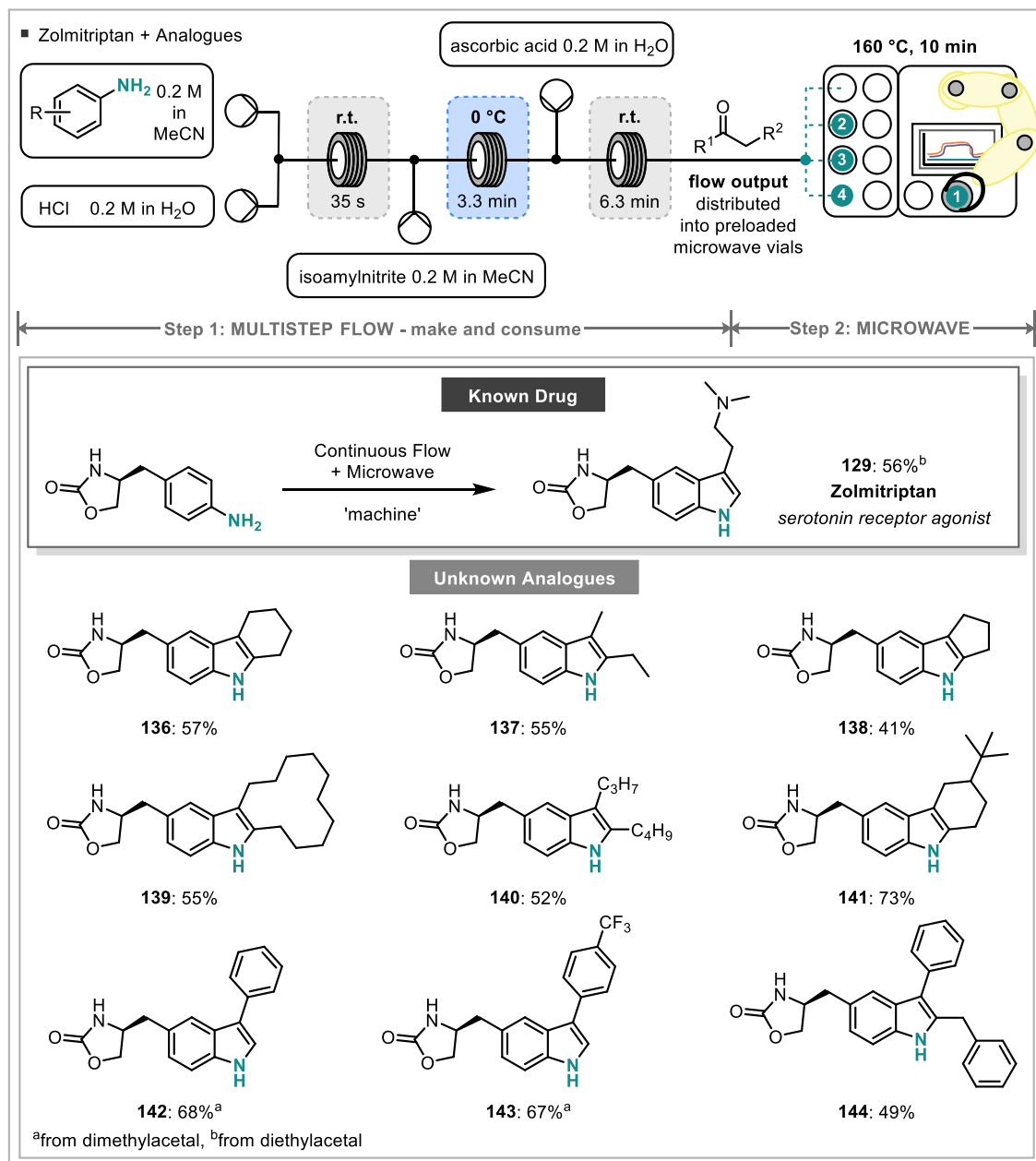
4-amino-*N*-methyl- α -toluene sulphonamide (0.50 g, 2.5 mmol) was dissolved in aqueous HCl (10 mL, 6 M) and the solution cooled to 0 °C. Sodium nitrite (0.181 g, 2.62 mmol, 1.05 equiv) in water (3 mL) was added dropwise. The solution was then stirred at 0 °C for 2.5 h. To the reaction mixture SnCl₂ (1.325 g, 6.99 mmol, 2.8 equiv) in aqueous HCl (15 mL, 6 M) was added and the reaction mixture stirred overnight. The pH was adjusted to 12 using aqueous NaOH (17 mL, 10 M) and the product extracted with EtOAc (3 x 50 mL). The combined organic layers were washed with brine, dried over MgSO₄, filtered and the solvent was removed under reduced pressure.

1-(3-(2-(dimethylamino)ethyl)-1H-indol-5-yl)-*N*-methylmethanesulfonamide 127(Sumatriptan)

The crude hydrazine **135** was transferred into a microwave vial and HCl (10 mL, 0.5 M), MeCN (10 mL) and 4-aminobutylaldehyde diethylacetal (0.189 g, 1 mmol) were added. The microwave vial was sealed and the mixture heated at 160 °C for 10 min. The mixture

was analysed using GCMS and showed the presence of the desired product. However, the product could not be isolated.

3.5 General Method for the Synthesis of Indoles **129** and **136** - **144**: Zolmitriptan Plus Analogues

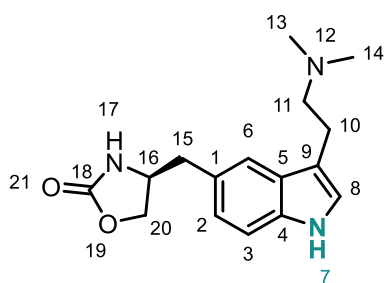


Scheme 6.8: Zolmitriptan Plus Analogues

Solutions of (S)-4-(4-aminobenzyl)-2-oxazolidinone (0.2 M in acetonitrile), HCl (1 M in water), isoamyl nitrite (0.24 M in acetonitrile) and ascorbic acid (0.2 M in water) were prepared. These were then pumped through the flow system (see Scheme 6.8) at a flow

rate of 0.2 mL min⁻¹. After waiting for steady state for 20 min, fractions of 20 mL (1 mmol, 25 min) were collected. The neat ketone (1 mmol) was added into a 35 mL microwave vial equipped with a stirrer bar and the reaction solution added. The reaction mixture was heated in the microwave (160 °C, 10 min). After cooling to room temperature, the reaction mixture was neutralised with 20 mL aqueous NaHCO₃ and extracted with EtOAc (3 x 20 mL). The combined organic layers were washed with brine (20 mL), dried over MgSO₄, filtered and the solvent was removed under reduced pressure. The crude product was then further purified via column chromatography (EtOAc in petroleum ether, 20 to 50%) unless otherwise stated

(S)-4-((3-(2-(dimethylamino)ethyl)-1H-indol-5-yl)methyl)oxazolidin-2-one, Zolmitriptan (129)^[17]



Following the general procedure, compound **129** was obtained from 4-aminobutyraldehyde diethylacetal (1 mmol, 0.189 g) and purified via column chromatography (10% Et₃N in EtOH) to yield a slightly brown solid (56%, 0.162 g, 0.56 mmol).

¹H NMR (500 MHz, DMSO) δ 10.71 (s, 1H, NH⁷), 7.77 (s, 1H, NH¹⁷), 7.35 (s, 1H, ArH⁸), 7.25 (d, *J* = 8.2 Hz, 1H, ArH³), 7.11 (d, *J* = 1.5 Hz, 1H, ArH⁶), 6.92 (d, *J* = 8.2 Hz, 1H, ArH²), 4.22 (t, *J* = 7.4 Hz, 1H, CH¹⁶), 4.10 – 3.94 (m, 2H, CH₂²⁰), 2.95 – 2.72 (m, 4H, CH₂), 2.55 – 2.46 (m, 2H, CH₂), 2.22 (s, 6H, CH₃^{13,14}) ppm.

¹H NMR (500 MHz, CDCl₃) δ 8.41 (s, 1H, NH⁷), 7.39 (s, 1H, ArH⁸), 7.28 (d, *J* = 8.2 Hz, 1H, ArH³), 7.02 (s, 1H, ArH⁶), 6.95 (d, *J* = 8.2 Hz, 1H, ArH²), 5.57 (s, 1H, NH¹⁷), 4.44 (t, *J* = 8.3 Hz, 1H, CH¹⁶), 4.24 – 4.03 (m, 2H, CH₂²⁰), 3.01 – 2.86 (m, 4H, CH₂), 2.71 – 2.57 (m, 2H, CH₂), 2.36 (s, 6H, CH₃^{13,14}) ppm.

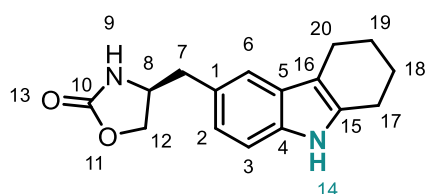
¹³C NMR (126 MHz, DMSO) δ 158.5 (CO¹⁸), 135.0 (ArC), 127.5 (ArC), 126.0 (ArC), 122.5 (2ArC), 119.0 (ArC), 112.5 (ArC), 111.0 (ArC), 68.0 (CH₂²⁰), 60.0 (CH₂¹¹), 53.0 (CH¹⁶), 45.0 (CH₃^{13,14}), 40.5 (CH₂¹⁵), 23.0 (CH₂¹⁰) ppm.

¹³C NMR (126 MHz, CDCl₃) δ 159.5 (CO¹⁸), 135.5 (ArC), 128.0 (ArC), 126.5 (ArC), 123.0 (ArC), 122.5 (ArC), 119.0 (ArC), 114.0 (ArC), 112.0 (ArC), 67.0 (CH₂²⁰), 60.0 (CH₂¹¹), 54.5 (CH¹⁶), 45.5 (CH₃^{13,14}), 42.0 (CH₂¹⁵), 23.5 (CH₂¹⁰) ppm.

mp (DCM): 40 - 45 °C.

IR: 3395, 3285, 2922, 2857, 2824, 2778, 2361, 1732, 1404, 1234, 1022, 727, 637 cm⁻¹.

HRMS (EI⁺): [C₁₆H₂₁ N₃O₂]⁺ Calcd. 287.1634, Found 287.1632.

(S)-4-((2,3,4,9-tetrahydro-1H-carbazol-6-yl)methyl)oxazolidin-2-one (136)

Following the general procedure, compound **136** was obtained from cyclohexanone (1 mmol, 0.098 g) to yield an off-white solid (57%, 0.155 g, 0.57 mmol).

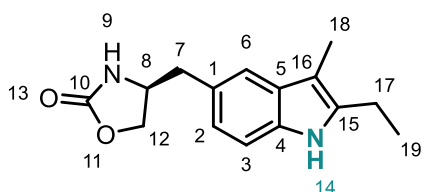
$^1\text{H NMR}$ (500 MHz, CDCl_3) δ 7.78 (s, 1H, NH^{14}), 7.24 (t, $J = 9.2$ Hz, 2H, ArH), 6.89 (dd, $J = 8.1, 1.6$ Hz, 1H, ArH^2), 5.14 (s, 1H, NH^9), 4.46 (t, $J = 8.4$ Hz, 1H, CH^8), 4.19 (dd, $J = 8.6, 5.6$ Hz, 1H, CH_2^{12}), 4.13 – 4.04 (m, 1H, CH_2^{12}), 3.02 – 2.84 (m, 2H, CH_2^7), 2.71 (dt, $J = 11.4, 5.5$ Hz, 4H, $\text{CH}_2^{17,20}$), 1.99 – 1.79 (m, 4H, $\text{CH}_2^{18,19}$) ppm.

$^{13}\text{C NMR}$ (126 MHz, CDCl_3) δ 159.5 (CO^{13}), 135.5 (ArC), 135.0 (ArC), 128.5 (ArC), 126.5 (ArC), 122.0 (ArC), 118.0 (ArC), 111.0 (ArC), 110.0 (ArC), 70.0 (CH_2^{12}), 54.5 (CH^8), 42.0 (CH_2^7), 23.5 (3CH_2), 21.0 (CH_2) ppm.

mp (DCM): 184 - 188 °C.

IR: 3391, 2918, 1753, 1719, 1477, 1396, 1244, 1018, 941, 480 cm^{-1} .

HRMS (FTMS + p NSI): $[\text{C}_{16}\text{H}_{19}\text{O}_2\text{N}_2]^+$ Calcd. 271.1441, Found 271.1444.

(S)-4-((2-ethyl-3-methyl-1H-indol-5-yl)methyl)oxazolidin-2-one (137)

Following the general procedure, compound **139** was obtained from 3-pentanone (1 mmol, 0.086 g) to yield a white solid (55%, 0.141 g, 0.55 mmol).

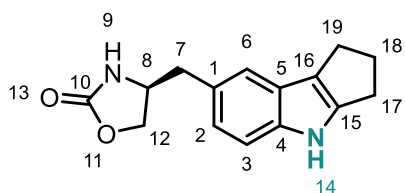
$^1\text{H NMR}$ (500 MHz, CDCl_3) δ 7.77 (s, 1H, NH^{14}), 7.27 – 7.25 (m, 1H, ArH^6), 7.23 (d, $J = 8.2$ Hz, 1H, ArH^3), 6.90 (dd, $J = 8.2, 1.7$ Hz, 1H, ArH^2), 4.95 (s, 1H, NH^9), 4.48 (t, $J = 8.3$ Hz, 1H, CH^8), 4.23 – 4.18 (m, 1H, CH_2^{12}), 4.14 – 4.06 (m, 1H, CH_2^{12}), 3.05 – 2.87 (m, 2H, CH_2^7), 2.76 (q, $J = 7.6$ Hz, 2H, CH_2^{17}), 2.22 (s, 3H, CH_2^{18}), 1.28 (t, $J = 7.6$ Hz, 3H, CH_3^{19}) ppm.

$^{13}\text{C NMR}$ (126 MHz, CDCl_3) δ 159.0 (CO^{10}), 137.5 (ArC), 134.5 (ArC), 130.0 (ArC), 126.5 (ArC), 122.0 (ArC), 118.5 (ArC), 111.0 (ArC), 106.0 (ArC), 70.0 (CH_2^{12}), 54.5 (CH^8), 42.0 (CH_2^7), 19.5 (CH_2^{17}), 14.0 (CH_3^{18}), 8.5 (CH_3^{19}) ppm.

mp (DCM): 60 - 64 °C

IR: 3387, 3267, 2970, 2914, 2363, 1732, 1404, 1240, 1022, 935, 935, 704 cm^{-1} .

HRMS (FTMS + p NSI): $[\text{C}_{15}\text{H}_{19}\text{O}_2\text{N}_2]^+$ Calcd. 259.1447, Found 259.1449.

(S)-4-((1,2,3,4-tetrahydrocyclopenta[b]indol-7-yl)methyl)oxazolidin-2-one (138)

Following the general procedure, compound **138** was obtained from cyclopentanone (1 mmol, 0.084 g) to yield an off-white solid (41%, 0.105 g, 0.41 mmol).

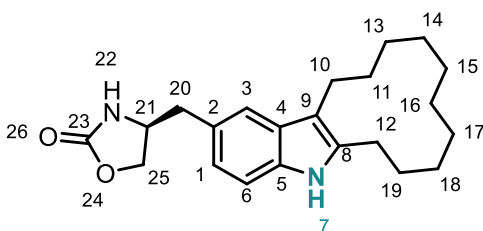
^1H NMR (500 MHz, CDCl_3) δ 7.93 (s, 1H, NH^{14}), 7.28 – 7.19 (m, 2H, ArH), 6.87 (dd, $J = 8.2, 1.5$ Hz, 1H, ArH^2), 5.10 (s, 1H, NH^9), 4.47 (t, $J = 8.4$ Hz, 1H, CH^8), 4.28 – 4.14 (m, 1H, CH_2^{12}), 4.14 – 4.03 (m, 1H, CH_2^{12}), 3.00 – 2.89 (m, 2H, CH_2^7), 2.84 (dt, $J = 26.0, 6.9$ Hz, 4H, $\text{CH}_2^{17,19}$), 2.62 – 2.47 (m, 2H, CH_2^{18}) ppm.

^{13}C NMR (126 MHz, CDCl_3) δ 159.0 (CO^9), 145.0 (ArC), 140.0 (ArC), 127.0 (ArC), 125.5 (ArC), 121.5 (ArC), 119.5 (ArC), 119.0 (ArC), 112.0 (ArC), 70.0 (CH_2^{12}), 54.5 (CH^8), 42.0 (CH_2^7), 29.0 (CH_2), 26.0 (CH_2), 24.5 (CH_2) ppm.

mp (DCM): 180 - 182 °C.

IR: 3385, 3277, 2980, 2947, 2857, 1755, 1713, 1225, 1022, 1005, 488 cm^{-1} .

HRMS (FTMS + p NSI): $[\text{C}_{15}\text{H}_{17}\text{O}_2\text{N}_2]^+$ Calcd. 257.1290, Found 257.1293.

(S)-4-((6,7,8,9,10,11,12,13,14,15-decahydro-5H-cyclododeca[b]indol-2-yl)methyl)oxazolidin-2-one (139)

Following the general procedure, compound **139** was obtained from cyclododecanone (1 mmol, 0.182 g) to yield a white solid (55%, 0.196 g, 0.55 mmol).

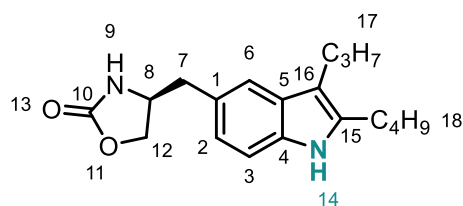
^1H NMR (500 MHz, CDCl_3) δ 7.75 (s, 1H, NH^7), 7.32 (s, 1H, ArH^3), 7.23 (d, $J = 8.2$ Hz, 1H, ArH^6), 6.90 (dd, $J = 8.2, 1.6$ Hz, 1H, ArH^1), 5.00 (s, 1H, NH^{22}), 4.48 (t, $J = 8.3$ Hz, 1H, CH^{21}), 4.25 – 4.17 (m, 1H, CH_2^{25}), 4.14 – 4.06 (m, 1H, CH_2^{25}), 3.00 – 2.87 (m, 2H, CH_2), 2.78 – 2.67 (m, 4H, CH_2), 1.86 – 1.72 (m, 4H, CH_2), 1.54 – 1.40 (m, 4H, CH_2), 1.34 (dd, $J = 6.2, 3.2$ Hz, 6H, CH_2), 1.29 – 1.19 (m, 2H, CH_2) ppm.

^{13}C NMR (126 MHz, CDCl_3) δ 159.0 (CO^{23}), 137.0 (ArC), 135.0 (ArC), 129.0 (ArC), 126.5 (ArC), 122.0 (ArC), 119.0 (ArC), 112.5 (ArC), 111.0 (ArC), 70.0 (CH_2^{25}), 54.5 (CH^{21}), 42.0 (CH_2^{20}), 28.0 (CH_2), 27.5 (CH_2), 25.0 (3 CH_2), 24.0 (CH_2), 22.5 (2 CH_2), 22.0 (CH_2), 21.5 (CH_2) ppm.

mp (DCM): 96 - 100 cm^{-1} .

IR: 3393, 3285, 2922, 2851, 2361, 1732, 1614, 1323, 1111, 1067, 702 cm^{-1} .

HRMS (FTMS + p NSI): $[\text{C}_{22}\text{H}_{31}\text{O}_2\text{N}_2]^+$ Calcd. 355.2380, Found 355.2382.

(S)-4-((2-butyl-3-propyl-1H-indol-5-yl)methyl)oxazolidin-2-one (140)

Following the general procedure, compound **140** was obtained from 5-nonanone (1 mmol, 0.142 g) to yield a light brown oil (52%, 0.164 g, 0.52 mmol).

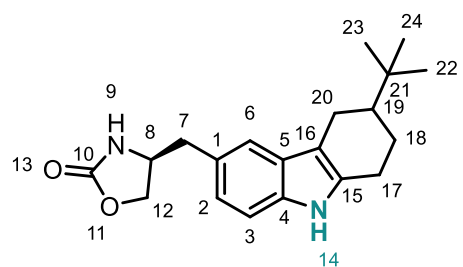
^1H NMR (500 MHz, CDCl_3) δ 7.77 (s, 1H, NH^{14}), 7.31 – 7.20 (m, 2H, ArH), 6.89 (dd, $J = 8.2, 1.6$ Hz, 1H, ArH^2), 5.03 (s, 1H, NH^9), 4.48 (t, $J = 8.3$ Hz, 1H, CH^8), 4.23 – 4.18 (m, 1H, CH_2^{12}), 4.14 – 4.06 (m, 1H, CH_2^{12}), 3.00 – 2.87 (m, 2H, CH_2^7), 2.76 – 2.68 (m, 2H, CH_2), 2.68 – 2.61 (m, 2H, CH_2), 1.68 – 1.60 (m, 4H, CH_2), 1.46 – 1.33 (m, 2H, CH_2), 0.97 (t, $J = 5.5$ Hz, 3H, CH_3), 0.94 (t, $J = 5.5$ Hz, 3H, CH_3) ppm.

^{13}C NMR (126 MHz, CDCl_3) δ 159.0 (CO^{10}), 136.5 (ArC), 134.5 (ArC), 129.5 (ArC), 126.5 (ArC), 121.5 (ArC), 118.5 (ArC), 112.0 (ArC), 111.0 (ArC), 70.0 (CH_2^{12}), 54.5 (CH^8), 42.0 (CH_2^7), 32.0 (CH_2), 26.5 (CH_2), 26.0 (CH_2), 24.5 (CH_2), 22.5 (CH_2), 14.5 (CH_3), 14.0 (CH_3) ppm.

mp (DCM): 64 - 68 °C.

IR: 3395, 3308, 2955, 2928, 2868, 1736, 1479, 1454, 1404, 1240, 1022 cm^{-1} .

HRMS (FTMS + p NSI): $[\text{C}_{19}\text{H}_{27}\text{N}_2\text{O}_2]^+$ Calcd. for 315.2068, Found 315.2067.

(S)-4-((3-(tert-butyl)-2,3,4,9-tetrahydro-1H-carbazol-6-yl)methyl)oxazolidin-2-one (141)

Following the general procedure, compound **141** was obtained from 4-tertbutyl cyclohexanone (1 mmol, 0.154 g) to yield a mixture of the diastereomers as an off-white solid (73%, 0.238 g, 0.73 mmol).

^1H NMR (500 MHz, CDCl_3) δ 7.75 (s, 1H, NH^{14}), 7.29 – 7.20 (m, 2H, ArH), 6.89 (dd, $J = 8.2, 1.6$ Hz, 1H, ArH^2), 5.04 (s, 1H, NH^9), 4.47 (t, $J = 8.4$ Hz, 1H, CH^8), 4.25 – 4.16 (m, 1H, CH_2^{12}), 4.15 – 4.04 (m, 1H, CH_2^{12}), 3.03 – 2.86 (m, 2H, CH_2^7), 2.85 – 2.66 (m, 3H, CH_2), 2.48 – 2.31 (m, 1H, CH_2), 2.16 – 2.03 (m, 1H, CH^{19}), 1.58 – 1.47 (m, 2H, CH_2), 1.01 (s, 9H, $\text{CH}_3^{22,23,24}$) ppm.

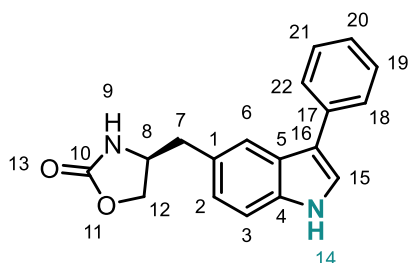
^{13}C NMR (126 MHz, CDCl_3) δ 159.5 (CO^{10}), 135.5 (2ArC), 129.0 (2ArC), 128.5 (ArC), 126.5 (ArC), 122.0 (ArC), 118.0 (ArC), 111.0 (ArC), 110.5 (ArC), 70.0 (CH_2^{12}), 54.5 (2 CH^8), 42.0 (CH_2^7), 27.5 (3 CH_2), 25.0 (CH^{19}), 22.5 ($\text{CH}_3^{22,23,24}$, C^{21}) ppm.

mp (DCM): 94 - 98 °C.

IR: 3387, 3283, 2947, 2909, 2843, 1736, 1476, 1242, 1022, 750 cm^{-1} .

HRMS (FTMS + p NSI): [C₂₀H₂₇N₂O₂]⁺ Calcd. 327.2070, Found 327.2067.

(S)-4-((3-phenyl-1H-indol-5-yl)methyl)oxazolidin-2-one (142)



Following the general procedure, compound **142** was obtained from phenylacetaldehyde dimethylacetal (1 mmol, 0.166 g) to yield a slightly yellow solid (68%, 0.198 g, 0.68 mmol).

¹H NMR (400 MHz, CDCl₃) δ 8.37 (s, 1H, NH¹⁴), 7.71 (s, 1H, ArH¹⁵), 7.64 (d, *J* = 7.5 Hz, 2H, ArH^{18,22}), 7.47

(t, *J* = 7.6 Hz, 2H, ArH^{19,21}), 7.40 (d, *J* = 8.4 Hz, 2H, ArH), 7.31 (t, *J* = 7.3 Hz, 1H, ArH²⁰), 7.04 (d, *J* = 8.3 Hz, 1H, ArH), 5.15 (s, 1H, NH⁹), 4.47 (t, *J* = 8.3 Hz, 1H, CH⁸), 4.23 – 4.07 (m, 2H, CH₂¹²), 3.06 – 2.90 (m, 2H, CH₂⁷) ppm.

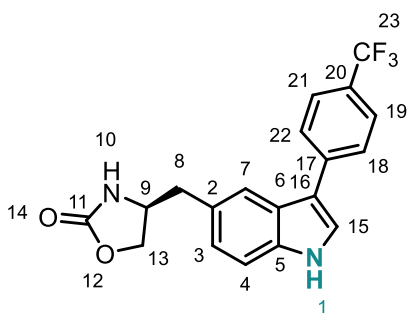
¹³C NMR (126 MHz, CDCl₃) δ 159.5 (CO¹⁰), 136.0 (ArC), 135.5 (ArC), 129.0 (ArC), 127.5 (2ArC), 126.5 (ArC), 126.0 (ArC), 123.5 (ArC), 123.0 (ArC), 120.0 (ArC), 118.0 (ArC), 112.0 (ArC), 70.0 (CH₂¹²), 54.5 (CH⁸), 42.0 (CH₂⁷) ppm.

mp (DCM): 72 - 77 °C.

IR: 3401, 3275, 2911, 1732, 1601, 1541, 1475, 1414, 1242, 1024, 939, 768, 752, 698 cm⁻¹.

HRMS (FTMS + p NSI): [C₁₈H₁₇O₂N₂]⁺ Calcd. 293.1285, Found 293.1288.

(S)-4-((3-(4-(trifluoromethyl)phenyl)-1H-indol-5-yl)methyl)oxazolidin-2-one (143)



Following the general procedure, compound **143** was obtained from 4-methoxy phenylacetaldehyde dimethylacetal (1 mmol, 0.196 g) to yield a yellow solid (67%, 0.241 g, 0.67 mmol).

¹H NMR (500 MHz, CDCl₃) δ 8.44 (s, 1H, NH¹), 7.77 – 7.66 (m, 5H, ArH), 7.48 – 7.40 (m, 2H, ArH), 7.08 (d, *J* = 8.2 Hz, 1H, ArH), 5.03 (s, 1H, NH¹⁰), 4.49 (t, *J* = 8.5

Hz, 1H, CH⁹), 4.25 – 4.18 (m, 1H, CH₂¹³), 4.18 – 4.10 (m, 1H, CH₂¹³), 3.08 – 2.91 (m, 2H, CH₂⁸) ppm.

¹³C NMR (126 MHz, CDCl₃) δ 159.5 (CO¹¹), 139.0 (ArC), 136.0 (ArC), 128.5 (ArC), 128.0 (q, *J* = 32.5 Hz, ArC²⁰), 127.5 (ArC), 126.0 (ArC), 126.0 (q, *J* = 3.7 Hz, ArC^{19,21}), 124.5 (q, *J* = 271.5 Hz, CF₃²³), 124.0 (ArC), 123.5 (ArC), 119.5 (ArC), 117.0 (ArC), 112.5 (ArC), 70.0 (CH₂¹³), 54.5 (CH⁹), 42.0 (CH₂⁸) ppm.

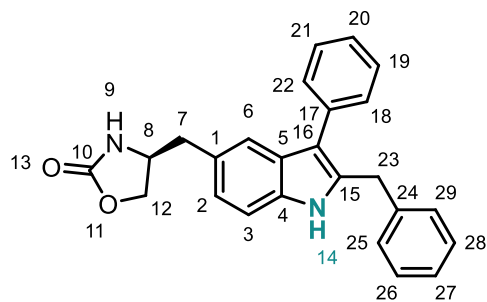
¹⁹F NMR (376 MHz, CDCl₃) δ -62.25 (CF₃²³) ppm.

mp (DCM): 182 - 186 °C.

IR: 3431, 3265, 2320, 2853, 1745, 1730, 1612, 1325, 1096, 1065, 800, 442 cm^{-1} .

HRMS (FTMS + p NSI): $[\text{C}_{25}\text{H}_{23}\text{O}_2\text{N}_2]^+$ Calcd. 361.1158, Found 361.1164.

(S)-4-((2-benzyl-3-phenyl-1H-indol-5-yl)methyl)oxazolidin-2-one (144)



Following the general procedure, compound **144** was obtained from 1,3-diphenylacetone (1 mmol, 0.210 g) to yield an off-white solid (49%, 0.187 g, 0.49 mmol).

^1H NMR (500 MHz, CDCl_3) δ 7.87 (s, 1H, NH^{14}), 7.56 – 7.42 (m, 5H, ArH), 7.41 – 7.29 (m, 3H, ArH), 7.29 – 7.16 (m, 4H, ArH), 6.96 (d, $J = 8.1$ Hz, 1H, ArH), 4.96 (s, 1H, NH^9), 4.45 (t, $J = 8.1$ Hz, 1H, CH^8), 4.24 (s, 2H, CH_2^{23}), 4.17 (t, $J = 6.9$ Hz, 1H, CH_2^{12}), 4.14 – 4.04 (m, 1H, CH^{12}), 3.00 – 2.85 (m, 2H, CH^7) ppm.

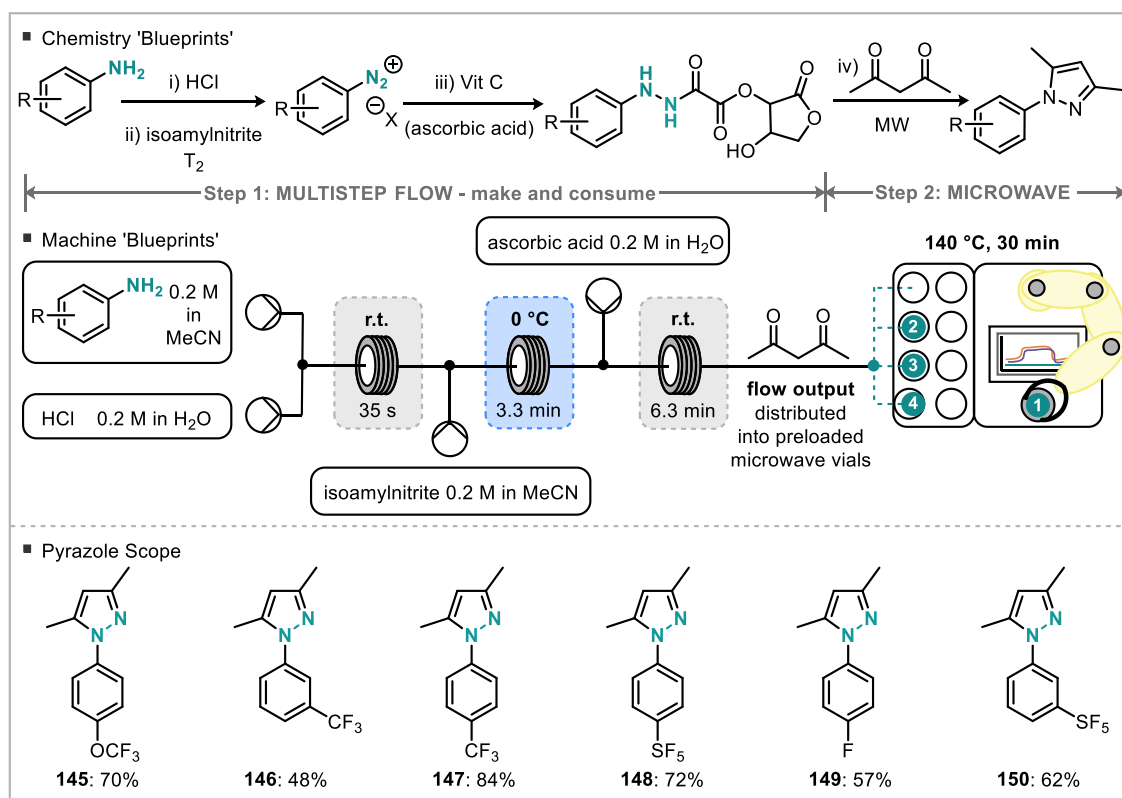
^{13}C NMR (126 MHz, CDCl_3) δ 159.0 (CO^{10}), 138.5 (ArC), 135.0 (ArC), 134.5 (ArC), 129.5 (ArC), 129.0 (4ArC), 128.5 (ArC), 127.5 (ArC), 127.0 (ArC), 126.5 (ArC), 123.0 (ArC), 119.5 (ArC), 115.5 (ArC), 111.5 (ArC), 70.0 (CH_2^{12}), 54.5 (CH^8), 42.0 (CH_2^7), 33.0 (CH_2^{23}) ppm.

mp (DCM): 166 - 168 °C.

IR: 3393, 3238, 2922, 1755, 1730, 1601, 1493, 1404, 1026, 705 cm^{-1} .

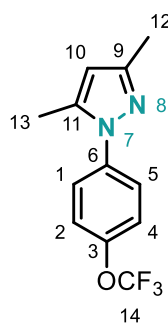
HRMS (FTMS + p NSI): $[\text{C}_{25}\text{H}_{23}\text{O}_2\text{N}_2]^+$ Calcd. 383.1755, Found 383.1754.

3.6 General Method for the Preparation of Pyrazoles



Scheme 6.9: Pyrazole Synthesis

Solutions of the aniline (0.2 M in acetonitrile), HCl (0.2 M in water), isoamyl nitrite (0.2 M in acetonitrile) and ascorbic acid (0.2 M in acetonitrile) were prepared. The solutions were then pumped through the flow system (see Scheme 6.9) at a flow rate of 0.2 mL min⁻¹. After 20 min steady state was reached and 20 mL (1 mmol, 25 min) of the resulting reaction mixture was collected and transferred into a microwave vial equipped with a stirrer bar and 2,4-pentadione (0.200 g, 2 mmol, 2 equiv). The mixture was heated to 140 °C for 30 min in the microwave. After cooling to room temperature, the reaction mixture was quenched with 10 mL NaHCO₃, extracted with DCM (3 x 20 mL), washed with brine and dried over MgSO₄. After removing the solvent under reduced pressure, the crude product was further purified by column chromatography (EtOAc in petroleum ether, 0 to 20%) to give the desired product.

3,5-dimethyl-1-(4-(trifluoromethoxy)phenyl)-1H-pyrazole (145)

Following the general procedure, the title compound **145** was obtained as a brown oil (70%, 0.180 g, 0.70 mmol).

^1H NMR (400 MHz, CDCl_3) δ 7.46 (d, $J = 7.5$ Hz, 2H, $\text{ArH}^{1,5}$), 7.29 (d, $J = 8.2$ Hz, 2H, $\text{ArH}^{2,4}$), 6.00 (s, 1H, ArH^{10}), 2.31 (s, 3H, CH_3), 2.29 (s, 3H, CH_3) ppm.

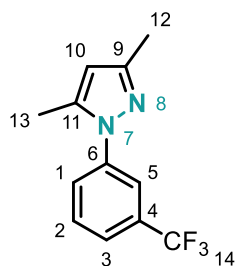
^{13}C NMR (126 MHz, CDCl_3) δ 149.5 (ArC), 147.0 (ArC), 139.5 (ArC), 138.5 (ArC), 126.0 (ArCH), 121.5 (ArCH), 120.5 (q, $J = 258$ Hz, OCF_3^{14}),

107.5 (ArCH), 13.5 (CH_3), 12.5 (CH_3) ppm.

^{19}F NMR (376 MHz, CDCl_3) δ -58.00 ppm.

IR: 2928, 1558, 1514, 1252, 1202, 1155, 853 cm^{-1} .

HRMS (FTMS + p NSI): $[\text{C}_{12}\text{H}_{12}\text{F}_3\text{N}_3\text{O}]^+$ Calcd. 257.0894, Found 257.0896.

1-(3-(trifluoromethyl)phenyl)-3,5-dimethyl-1H-pyrazole (146)

Following the general procedure, the title compound **146** was obtained as a yellow oil (48%, 0.116 g).

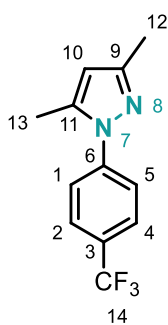
^1H NMR (500 MHz, CDCl_3) δ 7.74 (s, 1H, ArH^5), 7.68 – 7.53 (m, 3H, $\text{ArH}^{1,2,3}$), 6.03 (s, 1H, ArH^{10}), 2.34 (s, 3H, CH_3), 2.30 (s, 3H, CH_3) ppm.

^{13}C NMR (126 MHz, CDCl_3) δ 145.0 (ArC), 140.5 (ArC), 139.5 (ArC), 132.0 (q, $J = 32.8$ Hz, ArCH), 129.5 (ArCH), 127.5 (ArCH), 124.0 (q, $J = 3.6$ Hz, ArC), 123.5 (q, $J = 272.5$ Hz, CF_3^{14}), 121.5 (q, $J = 3.8$ Hz, ArC), 108.0 (ArCH^{10}), 13.5 (CH_3), 12.5 (CH_3) ppm.

^{19}F NMR (376 MHz, CDCl_3) δ -62.68 ppm.

IR: 2978, 1597, 1562, 1497, 1454, 1381, 1366, 1327, 1165, 1123, 1069, 895, 799, 698 cm^{-1} .

HRMS (ASAP+): $[\text{C}_{12}\text{H}_{12}\text{N}_2\text{F}_3]^+$ Calcd. 241.0953, Found 241.0953.

1-(4-(trifluoromethyl)phenyl)-3,5-dimethyl-1H-pyrazole (147)

Following the general procedure, the title compound **147** was obtained as a yellow oil (84%, 0.202 g).

^1H NMR (400 MHz, CDCl_3) δ 7.71 (d, $J = 8.0$ Hz, 2H, ArH), 7.59 (d, $J = 8.1$ Hz, 2H, ArH), 6.04 (s, 1H, ArH¹⁰), 2.36 (s, 3H, CH₃), 2.30 (s, 3H, CH₃) ppm.

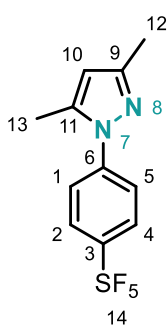
^{13}C NMR (126 MHz, CDCl_3) δ 150.0 (ArC), 143.0 (ArC), 139.5 (ArC), 129.0 (q, $J = 32.8$ Hz, ArC³), 126.5 (q, $J = 3.5$ Hz, ArC), 124.5 (ArCH),

124.0 (q, $J = 272.0$ Hz, CF₃¹⁴), 108.5 (ArCH¹⁰), 13.5 (CH₃), 13.0 (CH₃) ppm.

^{19}F NMR (376 MHz, CDCl_3) δ -62.34 ppm.

IR: 2928, 1614, 1321, 1119, 1067, 843, 457 cm^{-1} .

HRMS (FTMS + p NSI): $[\text{C}_{11}\text{H}_{12}\text{F}_3\text{N}_2]^+$ Calcd. 241.0944, Found 241.0947.

1-(4-pentafluorothio)-3,5-dimethyl-1H-pyrazole (148)

Following the general procedure, the title compound **148** was obtained as a yellow solid (62%, 0.186 g).

^1H NMR (400 MHz, CDCl_3) δ 7.83 (d, $J = 8.4$ Hz, 2H, ArH), 7.57 (d, $J = 8.6$ Hz, 2H, ArH), 6.05 (s, 1H, ArH¹⁰), 2.38 (s, 3H, CH₃), 2.30 (s, 3H, CH₃) ppm.

^{13}C NMR (126 MHz, CDCl_3) δ 151.5 (q, $J = 17.6$ Hz, ArC³), 150.5 (ArC), 142.5 (ArC), 140.0 (ArC), 127.0 (p, $J = 4.3$ Hz, ArC), 123.5 (ArC), 108.5

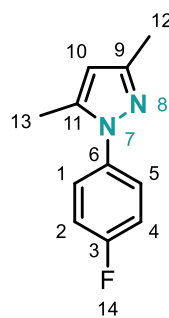
(ArCH¹⁰), 13.5 (CH₃), 13.0 (CH₃) ppm.

^{19}F NMR (376 MHz, CDCl_3) δ 85.17 – 83.13 (m, 1F), 63.68 – 62.92 (m, 4F) ppm.

IR: 2980, 1555, 1503, 1366, 808, 789, 768, 660, 575 cm^{-1} .

mp (DCM): 57 - 58 °C

HRMS (ASAP+): $[\text{C}_{11}\text{H}_{12}\text{F}_5\text{N}_2\text{S}]^+$ Calcd. 299.0641, Found 299.0648.

1-(4-fluorophenyl)-3,5-dimethyl-1H-pyrazole^[18] (149)

Following the general procedure, the title compound **149** was obtained as a yellow oil (57%, 0.566 g).

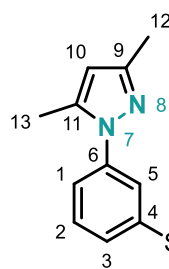
¹H NMR (400 MHz, CDCl₃) δ 7.43 – 7.33 (m, 2H, ArH), 7.18 – 7.07 (m, 2H, ArH), 5.98 (s, 1H, ArH¹⁰), 2.28 (s, 3H, CH₃), 2.26 (s, 3H, CH₃) ppm.

¹³C NMR (126 MHz, CDCl₃) δ 161.5 (d, J = 247.0 Hz, ArC³), 149.0 (ArC), 139.5 (ArC), 136.0 (d, J = 2.8 Hz, ArC⁶), 127.0 (d, J = 8.6 Hz, ArC^{1,5}), 116.0 (d, J = 22.8 Hz, ArC^{2,4}), 107.0 (ArC¹⁰), 13.5 (CH₃), 12.5 (CH₃) ppm.

¹⁹F NMR (471 MHz, CDCl₃) δ -114 ppm.

IR: 2924, 1557, 1510, 1383, 1219, 837, 610 cm⁻¹.

HRMS (FTMS + p NSI): [C₁₁H₁₁FN₂+H]⁺ Calcd. 191.0979, Found 191.0975.

1-(3-pentafluorothio)-3,5-dimethyl-1H-pyrazole (150)

Following the general procedure, the title compound **150** was obtained as a yellow oil (72%, 0.137 g).

¹H NMR (400 MHz, CDCl₃) δ 7.87 (s, 1H, ArH⁵), 7.72 (d, J = 8.1 Hz, 1H, ArH), 7.62 (d, J = 7.9 Hz, 1H, ArH), 7.59 – 7.51 (m, 1H, ArH), 6.04 (s, 1H, ArH¹⁰), 2.34 (s, 3H, CH₃), 2.30 (s, 3H, CH₃) ppm.

¹³C NMR (101 MHz, CDCl₃) δ 150.0 (ArC), 140.5 (ArC), 139.5 (ArC), 129.5 (ArC), 127.5 (ArC), 124.5 – 124.0 (m, ArC), 122.5 – 122.0 (m, ArC), 108.0 (ArCH¹⁰), 13.5 (CH₃), 12.5 (CH₃) ppm.

¹⁹F NMR (376 MHz, CDCl₃) δ 84.42 – 82.41 (m, 1F), 63.24 – 62.43 (m, 4F) ppm.

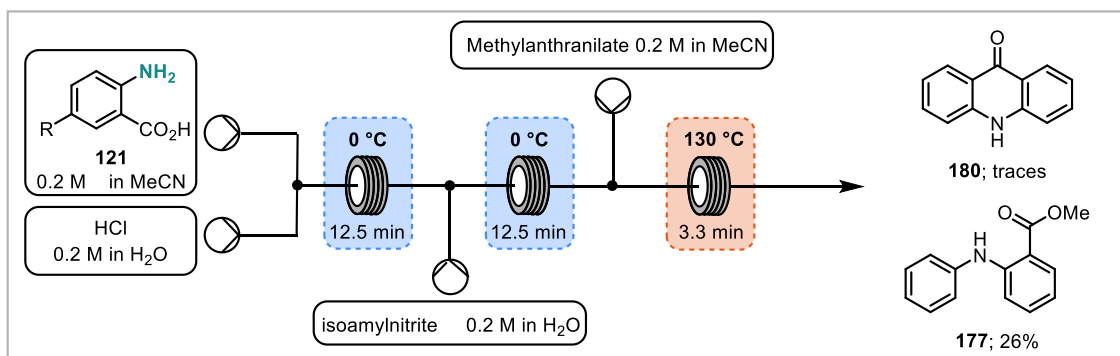
IR: 2980, 1605, 1493, 829, 771, 596 cm⁻¹.

HRMS (ASAP+): [C₁₁H₁₂F₅N₂S]⁺ Calcd. 299.0641, Found 299.0664.

4 Chapter 4 - Benzyne

4.1 Initial Setup

Solutions of anthranilic acid (0.2 M in MeCN), HCl (0.2 M in water), isoamylnitrite (0.2 M in MeCN) and methyl anthranilate (0.2 M in MeCN) were prepared and pumped through the flow system (Scheme 6.10) with a flow rate of 0.2 mL min⁻¹ for each pump. After waiting for steady state (approximately two residence times, 20 min), a fraction from the outlet was collected (20 mL, 1 mmol, 25 min). The crude mixture was diluted with 20 mL water and the product extracted with EtOAc (3 x 20 mL). The combined organic layers were washed with brine (20 mL), dried over MgSO₄, filtered and the solvent was removed under reduced pressure. The crude product was further purified via column chromatography (0 to 50% EtOAc in petroleum ether). Four products were isolated, starting material methyl anthranilate **194** (0.070 g, 0.47 mmol), uncyclized product **177** (26%, 0.060 g, 0.26 mmol), starting material anthranilic acid **121** (0.015 g, 0.11 mmol) and traces of the desired acridone **180**.



Scheme 6.10: Initial Setup for the Formation of Acridones

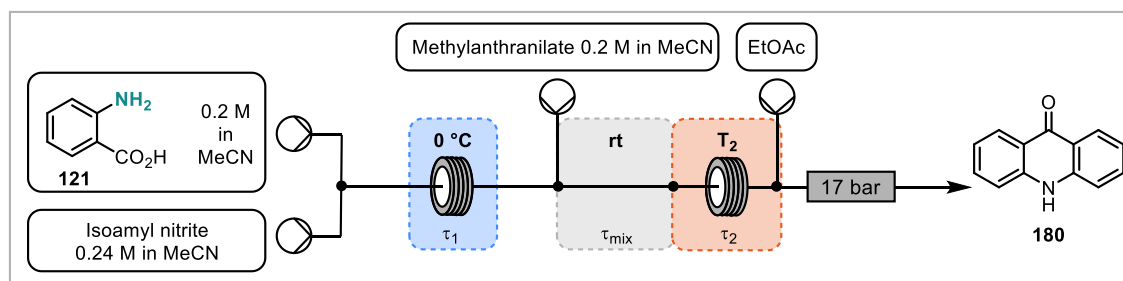
4.2 Optimisation

4.2.1 Optimisation Acridone

Solutions of anthranilic acid (0.2 M in MeCN), isoamylnitrite (0.2 M in MeCN) and methyl anthranilate (0.2 M in MeCN) were prepared and pumped through the flow system at a flow rate of 0.2 mL min⁻¹ each (Table 6.3). The EtOAc stream was pumped through the system at a flow rate of 1 mL min⁻¹. After waiting for steady state (approximately two residence times), a fraction from the outlet was collected (20 mL, 0.5 mmol, 12.5 min). The crude mixture was diluted with 20 mL of saturated NaHCO₃ solution and the product extracted with EtOAc (3 x 20 mL). The combined organic layers were washed with brine (20 mL), dried over MgSO₄, filtered and the solvent was removed under reduced

pressure. The crude product was further purified via column chromatography (20 to 50% EtOAc in petroleum ether) to yield the acridone product **180**.

Table 6.3: Optimisation of the Formation of Acridones

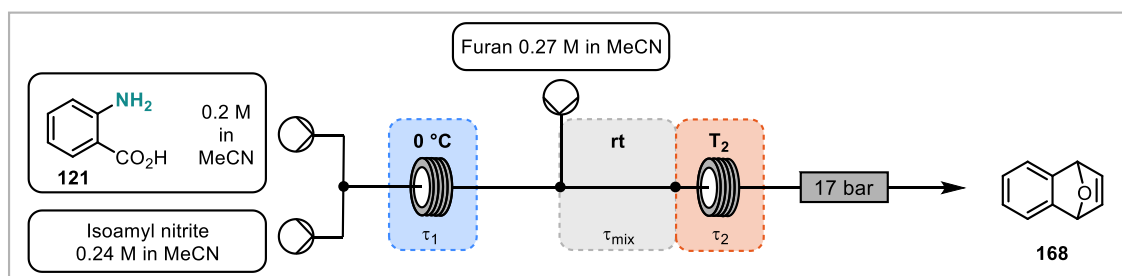


entry	V ₁	T ₁ [min]	V ₂	T ₂ [min]	T [°C]	yield ^a %
1	2	5	1	1.67	90	29
2	7.5	18.75	1	1.67	90	27
3	5	12.5	1	1.67	90	32
4 ^b	5	12.5	2	3.33	90	36
5 ^c	5	12.5	2	3.33	90	43
6	5	12.5	2	3.33	90	41
7	7.5	18.75	2	3.33	90	43
8	5	12.5	3	5	90	37
9	5	12.5	4	6.67	90	41
10	5	12.5	5	8.33	90	40
11	5	12.5	3	5	70	34
12	7.5	18.75	3	5	90	37
13	5	12.5	2	3	110	39
14 ^d	5	12.5	2	3.33	90	39
15 ^e	5	12.5	2	3.33	90	41
16 ^f	5	12.5	2	3.33	90	37
17 ^{f,g}	5	12.5	2	3.33	90	46
18 ^{d,g}	5	12.5	2	3.33	90	31
19^{d,h}	5	12.5	2	3.33	90	51
20 ^{d,h,i}	5	12.5	2	3.33	90	36

a: isolated yields; b: collection stirred for another 30 min; c: collection into NaHCO₃ quench; d: mixing time before elevated temperature range 20 cm; e: mixing time before elevated temperature range 40 cm; f: mixing time before elevated temperature range 60 cm; g: 0.4 M methylantranilate; h: 0.24 M isoamyl nitrite; i: anthranilic acid instead of methylantranilate

4.2.2 Optimisation Dihydroepoxynaphthalene 168

Solutions of anthranilic acid (0.2 M in MeCN), isoamyl nitrite (0.2 M in MeCN) and furan (0.27 M in MeCN) were prepared and pumped through the flow system at a flow rate of 0.2 mL min⁻¹ each as (Table 6.4). After waiting for steady state (approximately two residence times), a fraction from the outlet was collected (7.5 mL, 0.5 mmol, 12.5 min). To that solution mesitylene (0.5 mmol, 60 mg, 70 µL) was added and the solution was mixed. From that approximately 0.7 mL was filtered through a plug of silica into a GC vial. The plug was washed through twice with DCM (0.7 mL) and the resulting solution analysed by GC and the yield determined from the response.

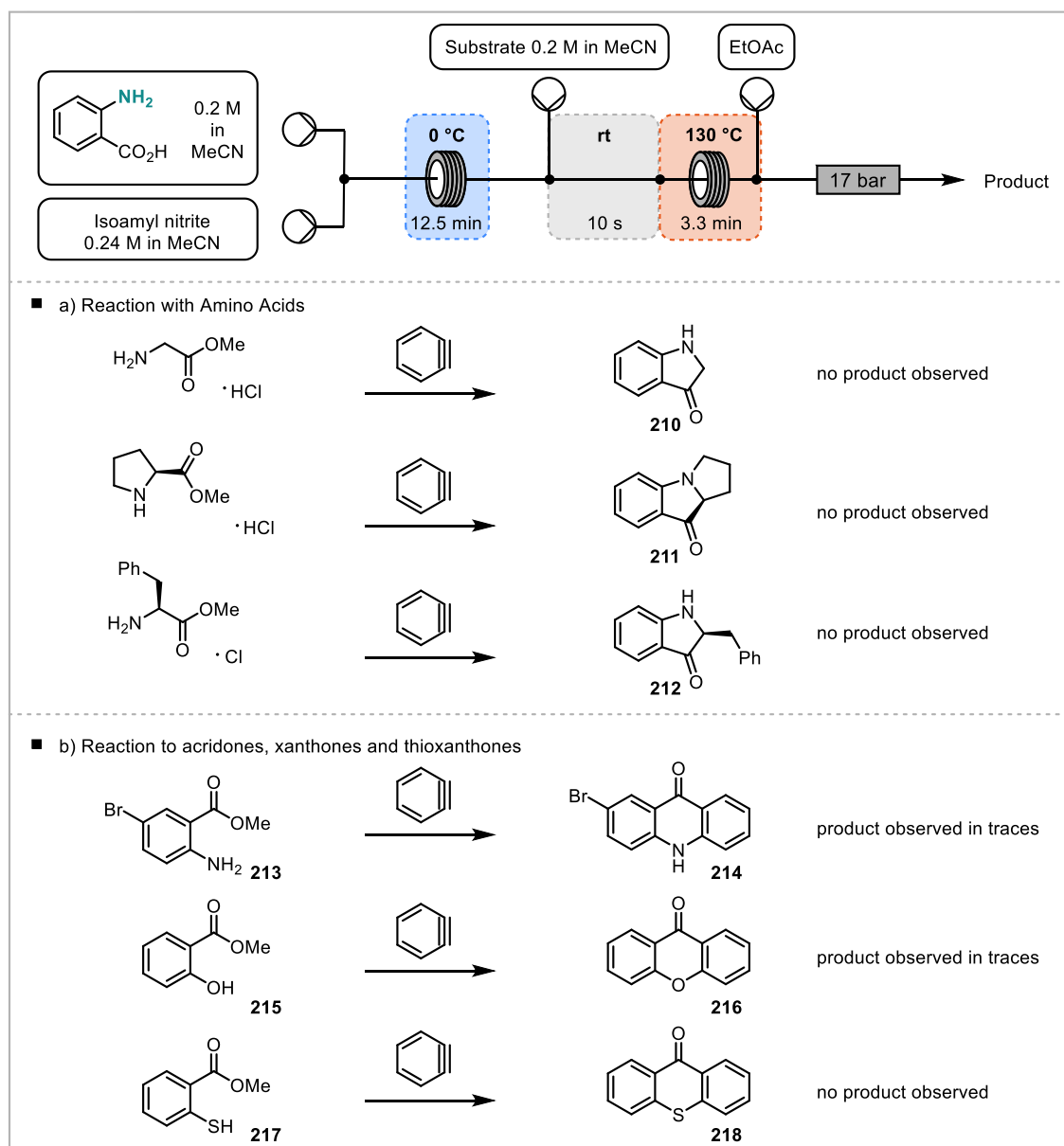
Table 6.4: Optimisation for the Diels Alder Reaction of Benzyne and Furan to Form Dihydroepoxynaphthalene

entry	T ₁ min	T ₂ min	T ₂ °C	GC yield [%]
1	12.5	3.3	90	69
2 ^a	12.5	3.3	90	66
3 ^b	12.5	3.3	90	64
4	7.5	3.3	90	63
5	18.8	3.3	90	66
6	12.5	1.7	90	66
7	12.5	5	90	64
8	12.5	3.3	70	67
9	12.5	3.3	110	69
10	7.5	1.7	110	67
11	12.5	1.7	110	64
12	7.5	1.7	90	61
13	12.5	3.3	50	41
14	7.5	3.3	50	41
15	7.5	1.7	50	30
16 ^c	12.5	3.3	70	52
17 ^d	12.5	3.3	70	46
18 ^d	12.5	3.3	90	48
19 ^d	12.5	3.3	110	54
20 ^d	12.5	3.3	130	57
21 ^d	7.5	3.3	90	53
22 ^d	18.8	3.3	90	51

T_{mix} = 10 s; a: T_{mix} = 20 s; b: T_{mix} = 30 s; c: anthranilic acid in acetone; d: anthranilic acid in THF

4.3 Substrate Investigation

Solutions of anthranilic acid (0.2 M in MeCN), isoamylnitrite (0.2 M in MeCN) and the substrate (0.2 M in MeCN) were prepared and pumped through the flow system at a flow rate of 0.2 mL min⁻¹ each (Scheme 6.11). The EtOAc stream was pumped through the system at a flow rate of 1 mL min⁻¹. After waiting for steady state (approximately two residence times), a fraction from the outlet was collected for GCMS analysis (0.7 mL), filtered through a plug of silica and washed twice with EtOAc (0.7 mL). Another fraction was collected for isolation (20 mL, 0.5 mmol, 12.5 min). The crude mixture was diluted with 20 mL of saturated NaHCO₃ solution and the product extracted with EtOAc (3 x 20 mL). The combined organic layers were washed with brine (20 mL), dried over MgSO₄, filtered and the solvent was removed under reduced pressure. The crude product was analysed by TLC, ¹H and ¹³C NMR.

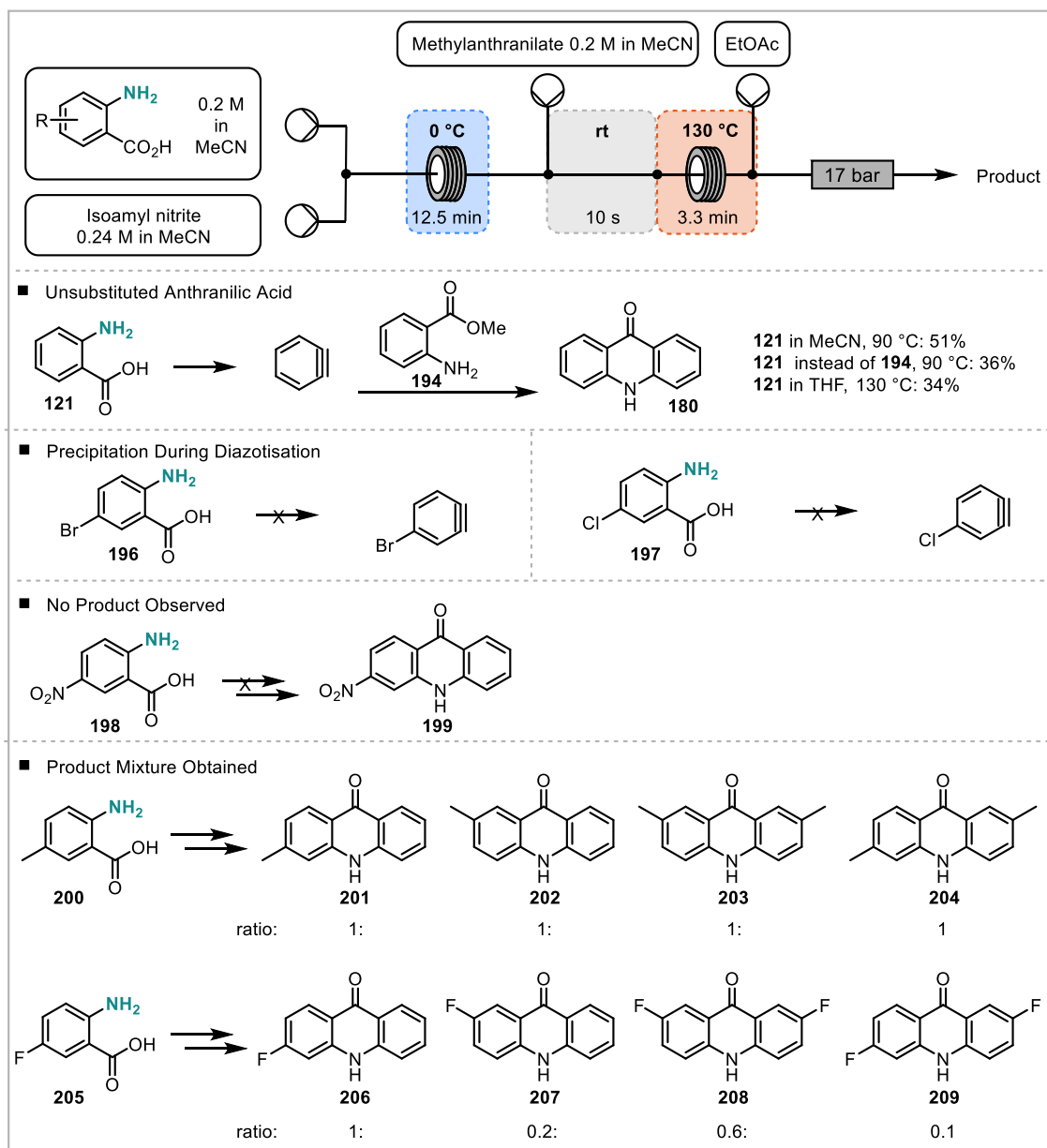


Scheme 6.11: Substrate Investigation with Amino Acids to Form Indolinones (a, left) and with Substituted Methyl Anthranilate, Methyl Salicylate and Methyl Thiosalicylate to Form a Substituted Acridone, Xanthone and Thioxanthone (b, right)

4.3.1 Substituted Anthranilic Acids

Solutions of the anthranilic acid (0.2 M in MeCN), isoamyl nitrite (0.2 M in MeCN) and the methyl anthranilate (0.2 M in MeCN) were prepared and pumped through the flow system at a flow rate of 0.2 mL min⁻¹ each (Scheme 6.12). The EtOAc stream was pumped through the system at a flow rate of 1 mL min⁻¹. After waiting for steady state (approximately two residence times), a fraction from the outlet was collected for GCMS analysis (0.7 mL), filtered through a plug of silica and washed twice with EtOAc (0.7 mL). Another fraction was collected for isolation (20 mL, 0.5 mmol, 12.5 min). The crude

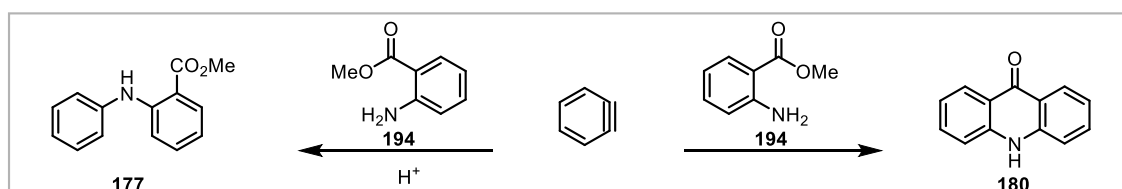
mixture was diluted with 20 mL of saturated NaHCO₃ solution and the product extracted with EtOAc (3 x 20 mL). The combined organic layers were washed with brine (20 mL), dried over MgSO₄, filtered and the solvent was removed under reduced pressure. The crude product was analysed by TLC, ¹H and ¹³C NMR. The crude product was then further purified via column chromatography (20% EtOAc in petroleum ether) to yield the acridone product.



Scheme 6.12: Substrate Scope with Substituted Anthranilic Acids to Form Substituted Acridones

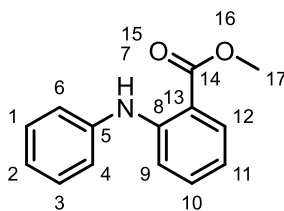
4.4 Switch to Uncyclised Product **177** with Acid

Solutions of anthranilic acid (0.2 M in MeCN: HCl (1 M) 1:1 (v/v)), isoamyl nitrite (0.2 M in MeCN) and methyl anthranilate (0.2 M in MeCN) were prepared and pumped through the flow system at a flow rate of 0.2 mL min⁻¹ each. The EtOAc stream was pumped through the system at a flow rate of 1 mL min⁻¹. After waiting for steady state (approximately two residence times), a fraction from the outlet was collected (20 mL, 0.5 mmol, 12.5 min). The crude mixture was diluted with 20 mL of saturated NaHCO₃ solution and the product extracted with EtOAc (3 x 20 mL). The combined organic layers were washed with brine (20 mL), dried over MgSO₄, filtered and the solvent was removed under reduced pressure. The crude product was analysed by TLC and ¹H and no evidence could be found for the formation of the desired product **177**. In addition, the reaction was performed with the elevated reaction coil at 50 °C, but again, the desired product was not observed.



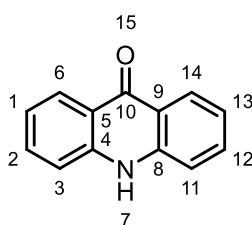
Scheme 6.13: Switch to Uncyclised, N-arylated Product **177 with Acid**

4.5 Product Characterisation

methyl 2-(phenylamino)benzoate 177^[19]

¹H NMR (400 MHz, CDCl₃) δ 9.46 (s, 1H, NH⁷), 7.96 (dd, *J* = 8.0, 1.3 Hz, 1H, ArH), 7.38 – 7.28 (m, 3H, ArH), 7.28 – 7.22 (m, 3H, ArH), 7.09 (t, *J* = 7.3 Hz, 1H, ArH), 6.76 – 6.70 (m, 1H, ArH), 3.90 (s, 3H, CH₃) ppm.

¹³C NMR (101 MHz, CDCl₃) δ 169.0 (CO¹⁵), 148.0 (ArC), 140.5 (ArC), 134.0 (ArCH), 131.5 (ArCH), 129.0 (ArCH), 123.5 (ArCH), 122.5 (ArCH), 117.0 (ArCH), 114.0 (ArCH), 111.5 (ArC), 52.0 (CH₃¹⁷) ppm.

acridin-9(10H)-one 180^[20]

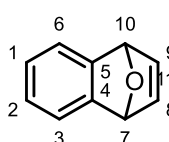
¹H NMR (400 MHz, DMSO) δ 11.73 (s, 1H, NH), 8.23 (d, *J* = 7.9 Hz, 2H, ArH), 7.74 (t, *J* = 7.6 Hz, 2H, ArH), 7.55 (d, *J* = 8.2 Hz, 2H, ArH), 7.26 (t, *J* = 7.3 Hz, 2H, ArH) ppm.

¹³C NMR (126 MHz, DMSO) δ 176.5 (CO), 141.0 (ArC), 133.5 (ArCH), 126.0 (ArCH), 121.0 (ArCH), 120.5 (ArC), 117.5 (ArCH).

mp (DCM): < 300 °C.

IR: 2943, 1632, 1593, 1528, 1480, 1341, 746, 669, 548 cm⁻¹.

HRMS (FTMS + p NSI): [C₁₃H₁₀NO]⁺ Calcd. 196.0757; Found 196.0757.

1,4-dihydro-1,4-epoxynaphthalene 168^[21]

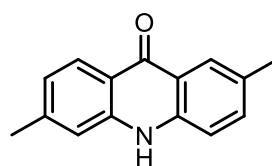
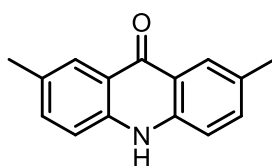
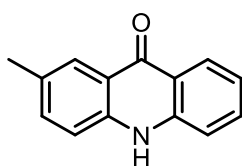
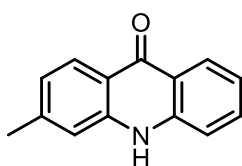
¹H NMR (500 MHz, CDCl₃) δ 7.28 – 7.22 (m, 2H), 7.05 – 7.01 (m, 2H), 7.00 – 6.94 (m, 2H), 5.72 (s, 2H, CH^{7,10}) ppm.

¹³C NMR (126 MHz, CDCl₃) δ 149.0 (Ar-C^{5,4}), 143.0(Ar-C), 125.0(Ar-C), 120.5(Ar-C), 82.5 (C^{7,10}H) ppm.

mp (DCM): 61 - 64 °C.

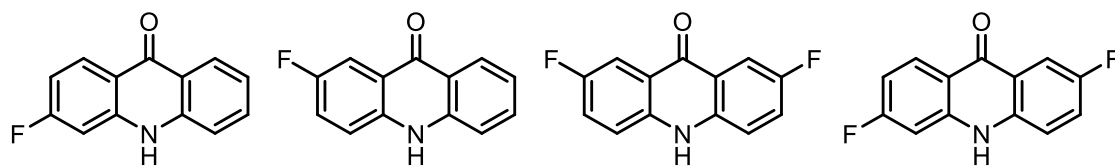
IR: 2980, 2359, 1763, 1717, 1458, 845, 154 cm⁻¹.

HRMS (CI⁺): [C₁₀H₈O+NH₄⁺] Calcd. 145.0648; Found 145.0650.

3/2-methylacridin-9(10H)-one, 2/3,7-dimethylacridine-9(10H)-one 201 – 204

HRMS (TOF MS ES⁺): [C₁₄H₁₂ON]⁺ Calcd. 210.0919; Found 210.0923.

HRMS (TOF MS ES⁺): [C₁₅H₁₄ON]⁺ Calcd. 224.1080; Found 224.1075.

3/2-fluoroacridin-9(10H)-one, 2/3,7-difluoroacridine-9(10H)-one 206-209

HRMS (TOF MS ES⁺): [C₁₃H₉ONF]⁺ Calcd. 214.0668; Found 214.0664.

HRMS (TOF MS ES⁺): [C₁₃H₈ONF₂]⁺ Calcd. 232.0574; Found 232.0575.

5 Chapter 5 – Exotherm Monitoring

5.1 General Methods

Trifluoromethyl trimethyl silane (TMSCF₃) and diethylene glycol dimethyl ether (diglyme) were purchased from Fluorochem (007685 and 075235). Sodium borohydride was purchased from Acros Organics (44850). TMSCF₃ and sodium borohydride were used without further purification. Diglyme was dried over CaH₂ and distilled prior to use.

NMR measurements were conducted on a Bruker Ascend™500 (500 MHz) using the InsightMR software.

The flow setup consisted of perfluoroalkoxy (PFA) tubing of an 0.8 mm ID, 1.2 mm OD supplied by Polyflon and two pumps. The residence coil was made from the tubing by taking the appropriate length (4 m) for the desired volume (2 mL). Fittings were supplied by Kinesis and part numbers given where appropriate.

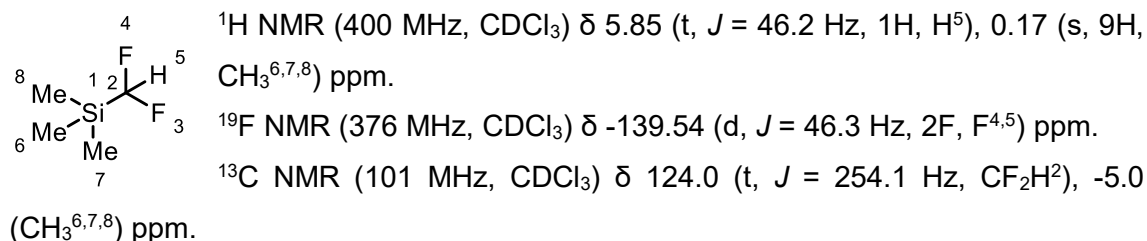
The thermocouples are xlogger (itec) parts with a temperature sensor, a reading panel and a USB adapter.

In all cases solutions of the two reactants were prepared separately before and pumping them into the flow system where they were combined at a T-piece and passed through the reactor coil.

5.2 Batch Reaction

Following a known procedure^[22] trimethylsilanetrifluoromethane (24.0 g, 169 mmol) was added slowly over 20 min to an ice cold solution of sodium borohydride (2.22 g, 59 mmol, 0.43 equiv) in dry diglyme (50 mL). After 2 h the ice bath was removed and the reaction stirred for another 18 h. The reaction mixture was distilled twice at atmospheric pressure (set temperature 170 °C and 90 °C) to yield 13.1 g (62%, 105.4 mmol) of TMSCF₂H.

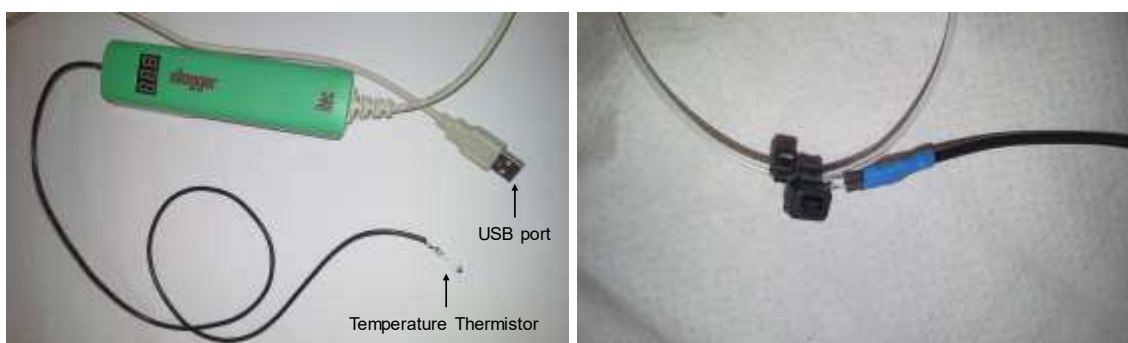
Difluoromethyltrimethylsilane (TMSCF₂H)^[23]



IR: 2963, 2903, 1321, 1256, 1078, 989, 858 cm⁻¹.

5.3 Temperature Measurements

The temperature measurements were conducted using xlogger temperature sensors (itec) with the software being built-in to excel. The setup consists of a thermistor, temperature reading and a USB cable (Picture 6.1). The sensors of each thermocouple were attached to the surface of the flow tubing with a cable tie at the inlet (about 1 cm), 1.3 m (1/3 of the length), 2.6 m (2/3 of the length) and at the outlet (4 m). They were insulated with cotton wool. Prior to use the room temperature reading was taken for calibration. The room was thermostatically controlled, and the temperature was 19 °C during all measurements. The room temperature value of the thermocouples was corrected to that value.

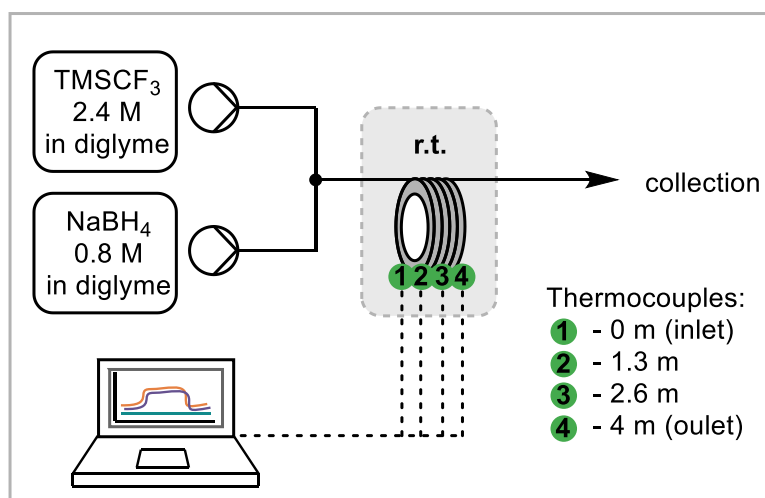


Picture 6.1: xlogger Thermocouples with Temperature Thermistor Attached to Flow Tubing

Solutions of TMSCF_3 (2.4 M in diglyme) and of sodium borohydride (0.8 M in diglyme) were pumped through the setup equipped with the thermocouples according to Scheme 6.14 using syringe pumps (Picture 6.2). The temperature measurement was started when the flow was started. The temperature reading was taken after 8 residence times to ensure steady state. For 4 mL/min and 1 mL/min the measurement was repeated three times, the average taken and the standard error in the mean calculated to be a maximum of 2 °C (Table 6.4, Figure 6.24).



Picture 6.2: Picture of Flow Setup for Temperature Measurements



Scheme 6.14: Modified Flow Setup for Temperature Measurements

Table 6.4: Temperature Measurements Results

entry	flowrate [mL/min]	residence time [min]	T1 [°C]	T2 [°C]	T3 [°C]	T4 [°C]
1	4	0.5	20	58	46	39
2	3	0.7	20	55	41	33
3	2	1	20	45	33	29
4	1	2	19	25	25	22
5	0.5	4	21	21	21	20

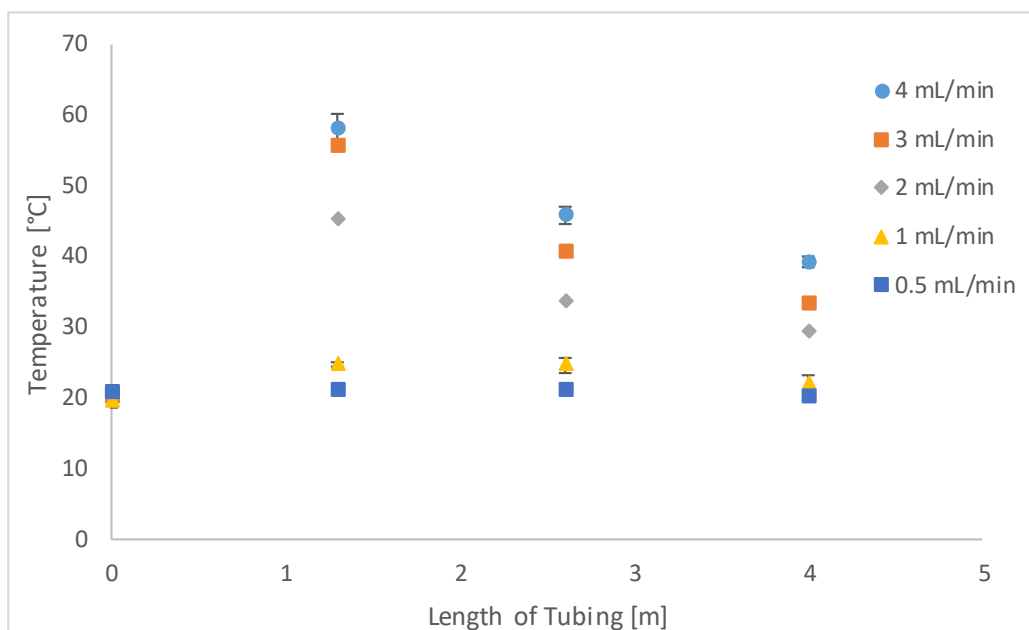


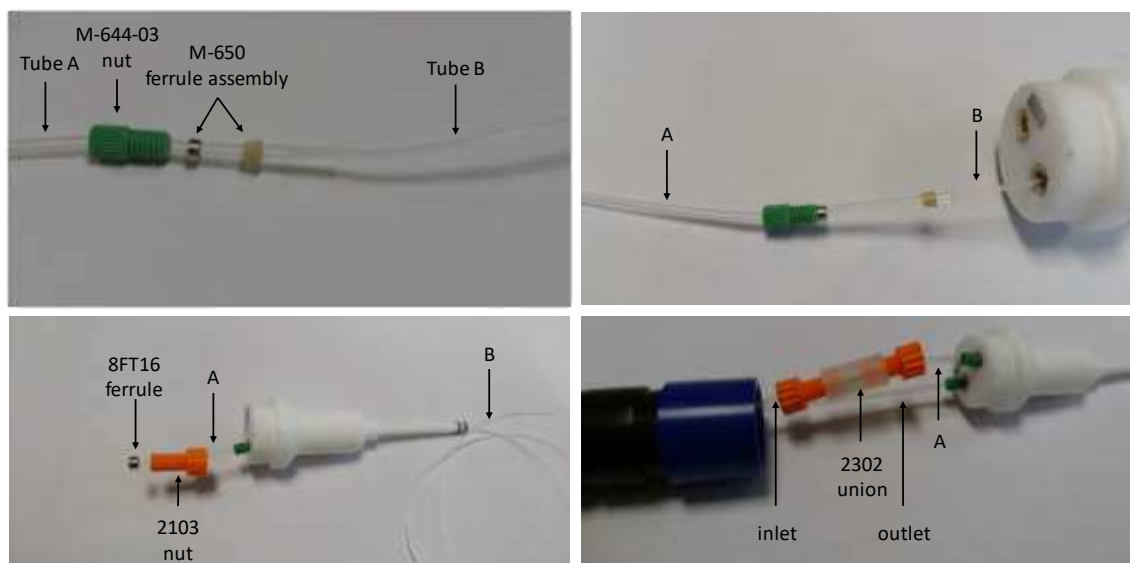
Figure 6.24: Temperature Profile Along the Length of the Tubing

5.4 Flow NMR Modifications

The NMR yield was determined using the Bruker InsightMR flow tube (Picture 6.3). The original setup provided by Bruker consisted of thermostatically controlled inlet and an outlet 0.8 mm OD tubing. This was modified to connect the standard 1.2 mm OD tubing to the flow tube (Picture 6.4). The inlet standard sized tubing (tube A) had to be connected to the 0.8 mm OD tubing leading into the NMR tube (tube B). For that the 0.8 mm OD tubing was inserted into the standard sized tubing fitted with nut (M-644-03) and ferrule assembly (M-650) and the standard sized tubing used as a sleeve. After connecting that to the sample holder, a standard sized fitting (nut: 2103, ferrule: 8FT16) was fitted to the other end to then connect a union (2302) and the reaction coil of standard sized tubing. The outlet from the NMR tube was directly connected to the standard sized tubing using the nut (M-644-03) and ferrule assembly (M-650) used before.



Picture 6.3: InsightMR Flow Tube

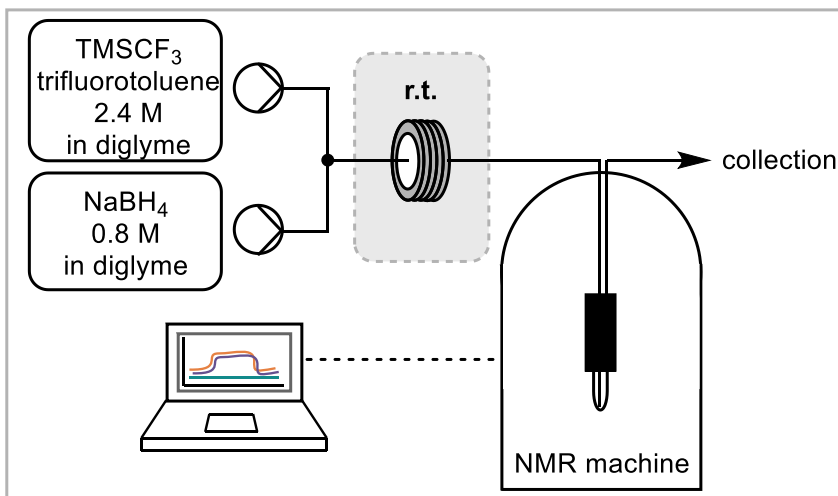


Picture 6.4: Modifications to the InsightMR Flow Cell

5.5 Flow NMR Measurements

The modified setup was employed to measure yields at different flow rates and residence times acquiring ^{19}F NMR spectra using the Bruker InsightMR software. The flow cell was inserted into the NMR machine and the system flushed with a solution of trifluorotoluene (1.6 M) in diglyme. After stopping the pumps, the spectrometer was set to optimise the shim settings in respect to the ^1H spectrum of the solution and then tune back to ^{19}F . After that the reaction measurements were started by pumping a solution of TMSCF_3 (2.4 M) and trifluorotoluene (1.6 M) in diglyme and a solution of sodium borohydride (0.8 M in diglyme) through the setup according to Scheme 6.15 using a dual syringe pump. At each flow rate, the system was stabilised for three residence times and then integrals of TMSCF_2H were measured in comparison to the trifluorotoluene standard for one residence time. Each spectrum was acquired using only one scan and the frequency of spectra acquisition adjusted depending on the flow rate. For fast flow rates the frequency was high (highest frequency possible approximately every 7 s) and for flow

rates the frequency was lower (e.g. 0.66 mL/min flow rate, 30 min residence time, 2 min frequency of spectra acquired).



Scheme 6.15: Flow Setup for the NMR Measurements

The acquired spectra were integrated using the InsightMR software, the data exported into Excel and converted into a diagram showing the integration over time (Figure 6.25, example for 0.67 mL/min flow rate, 3 min residence time).

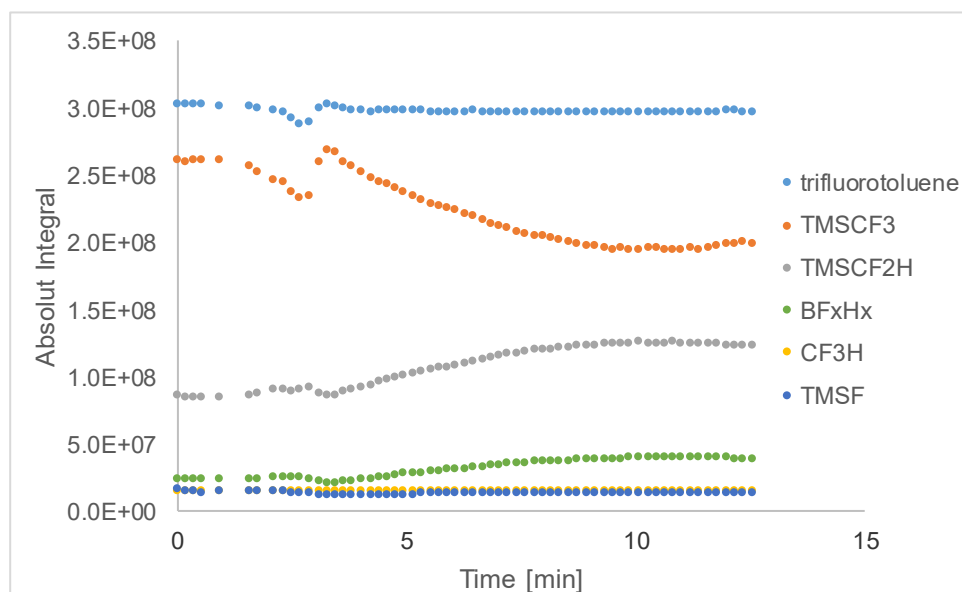


Figure 6.25: Integration over Time, Example for 0.67 mL/min Flow Rate, 3 min Residence Time

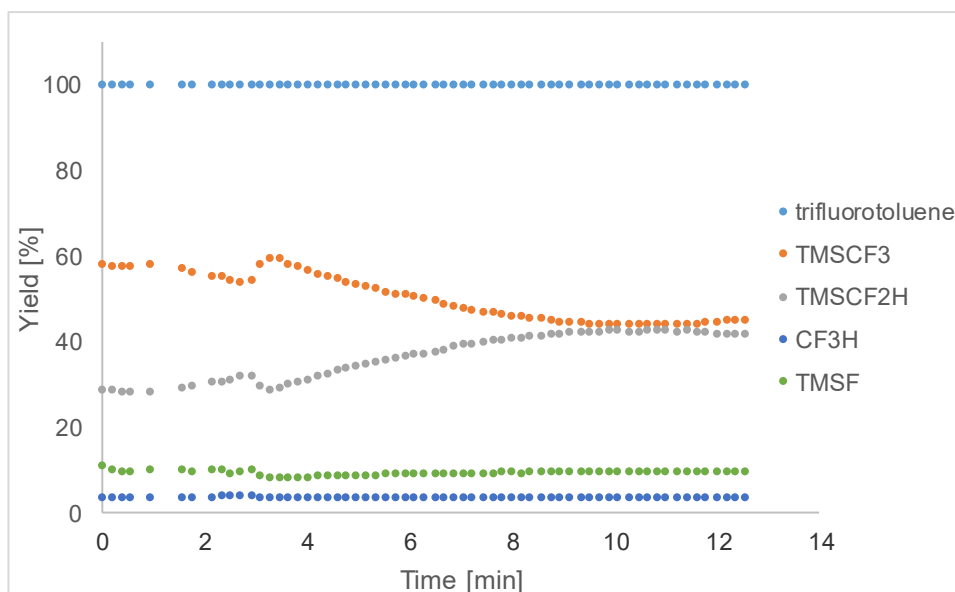


Figure 6.26: Yields over Time, Example for 0.67 mL/min Flow Rate, 3 min Residence Time

The yields (Y) were calculated from the integral of the trifluorotoluene standard and the integral of the compound (Figure 6.26) after stabilisation (after 3 residence times), averaged and the standard error in the mean calculated, which proved to be a maximum of 0.3% for all measurements.

$$Y = \frac{I_{TMSCF_2H}}{I_{trifluorotoluene}} \cdot 100\%$$

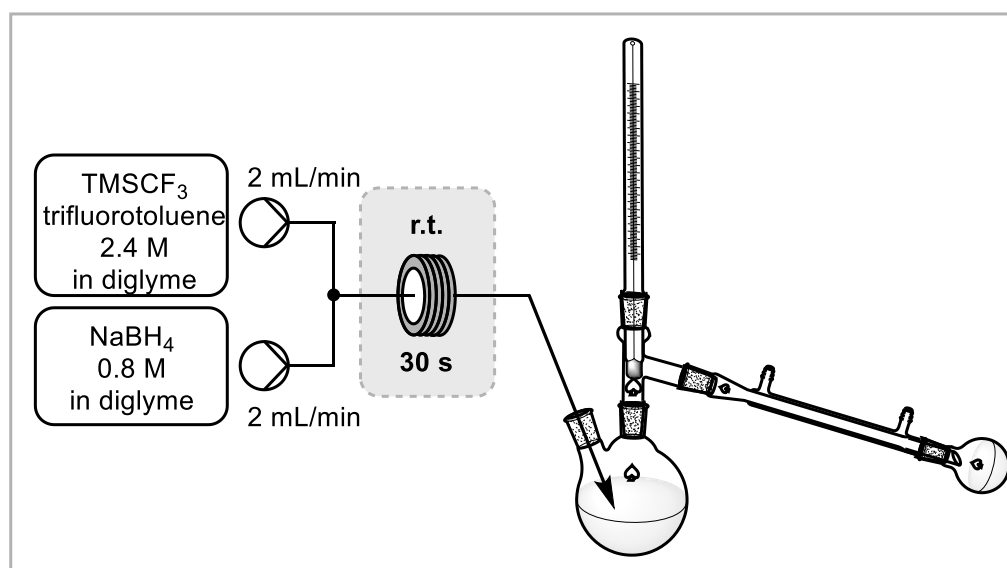
Applying this method for all residence times/ flow rates gave the $TMSCF_2H$ yield for different residence times resulting from the change in flow rates (Table 6.6). Notably, the reaction continued in the collection flask.

Table 6.6: Results *in line* NMR measurements

entry	flow rate [mL/min]	residence time [min]	yield [%]	error [%]
1	0.066	30	52	0.3
2	0.1	20	53	0.3
3	0.2	10	50	0.1
4	0.4	5	46	0.1
5	0.50	4	45	0.1
6	0.67	3	42	0.1
7	1	2	36	0.1
8	2	1	30	0.2
9	4	0.5	27	0.2

5.6 Telescoped Large Scale Reaction

Solutions of sodium borohydride (0.8 M) and trifluoromethyltrimethylsilane (2.4 M) in diglyme were prepared and pumped through the flow system according to Scheme 6.16 using HPLC pumps at 2 mL/min each (residence time 30 s). After 1 minute (allowing the system to reach steady state), the output was fed directly into a flask and stirred at 50 °C. After 75 minutes (51 g, 360 mmol starting material processed), the pumps were stopped and the flask stirred at 50 °C for another 30 minutes. The temperature was increased to 180 °C and crude product collected by distillation. Further distillation (b.p. 65 - 70 °C) yielded difluoromethyltrimethylsilane (25.04 g, 202 mmol, 56%) as a colourless liquid.

**Scheme 6.16: Scheme of Telescoped Reaction Process**

6 References

- [1] C. Wang, H. Chen, Z. Wang, J. Chen, Y. Huang, *Angew. Chem. Int. Ed.* **2012**, *51*, 7242-7245.
- [2] W. Li, M. Beller, X.-F. Wu, *Chem. Commun.* **2014**, *50*, 9513-9516.
- [3] A. Zarei, L. Khazdooz, H. Aghaei, G. Azizi, A. N. Chermahini, A. R. Hajipour, *Dyes Pigm.* **2014**, *101*, 295-302.
- [4] aY. Zhang, Y. Li, X. Zhang, X. Jiang, *Chem. Commun.* **2015**, *51*, 941-944; bM. L. Gross, D. H. Blank, W. M. Welch, *J. Org. Chem.* **1993**, *58*, 2104-2109.
- [5] S. Sengupta, S. K. Sadhukhan, *Org. Synth.* **2002**, *79*, 52.
- [6] A. Hafner, C. Hussal, S. Bräse, *Synthesis* **2014**, *46*, 1448-1454.
- [7] D. Farquhar, J. Benvenuto, *J. Med. Chem.* **1984**, *27*, 1723-1727.
- [8] W. Erb, A. Hellal, M. Albini, J. Rouden, J. Blanchet, *Chem. Eur. J.* **2014**, *20*, 6608-6612.
- [9] Z. Gonda, F. Béke, O. Tischler, M. Petró, Z. Novák, B. L. Tóth, *Eur. J. Org. Chem.* **2017**, *2017*, 2112-2117.
- [10] M. Peña-López, H. Neumann, M. Beller, *Chem. Eur. J.* **2014**, *20*, 1818-1824.
- [11] S. Chandrasekhar, S. Mukherjee, *Synth. Commun.* **2015**, *45*, 1018-1022.
- [12] S. Tong, Z. Xu, M. Mamboury, Q. Wang, J. Zhu, *Angew. Chem. Int. Ed.* **2015**, *54*, 11809-11812.
- [13] C. S. Yeung, R. E. Ziegler, J. A. Porco, E. N. Jacobsen, *J. Am. Chem. Soc.* **2014**, *136*, 13614-13617.
- [14] D.-Q. Xu, J. Wu, S.-P. Luo, J.-X. Zhang, J.-Y. Wu, X.-H. Du, Z.-Y. Xu, *Green Chem.* **2009**, *11*, 1239-1246.
- [15] S. Chen, Y. Liao, F. Zhao, H. Qi, S. Liu, G.-J. Deng, *Org. Lett.* **2014**, *16*, 1618-1621.
- [16] P. J. Murray, S. T. Onions, J. G. Williams, K. Joly, Google Patents, **2015**.
- [17] S. K. Vujjini, V. R. Mothukuri, A. Islam, R. Bandichhor, M. Kagga, G. C. Malakondaiah, *Synth. Commun.* **2013**, *43*, 3294-3306.
- [18] J.-S. Poh, D. L. Browne, S. V. Ley, *React. Chem. Eng.* **2016**, *1*, 101-105.
- [19] H. Rao, H. Fu, Y. Jiang, Y. Zhao, *J. Org. Chem.* **2005**, *70*, 8107-8109.
- [20] C. Pal, M. K. Kundu, U. Bandyopadhyay, S. Adhikari, *Bioorg. Med. Chem. Lett.* **2011**, *21*, 3563-3567.
- [21] T. Nishimura, T. Kawamoto, K. Sasaki, E. Tsurumaki, T. Hayashi, *J. Am. Chem. Soc.* **2007**, *129*, 1492-1493.
- [22] A. Tyutyunov, V. Boyko, S. Igoumnov, *Fluorine notes* **2011**, *1*, 74.

- [23] B. Bayarmagnai, C. Matheis, K. Jouvin, L. J. Goossen, *Angew. Chem. Int. Ed.* **2015**, *54*, 5753-5756.